DEVELOPMENT AND ASSESSMENT OF GASTRORETENTIVE SUSTAINED RELEASE CAPTOPRIL TABLETS

A Thesis Submitted to Rhodes University in Fulfilment of the

Requirements for the Degree of

MASTER OF SCIENCE (PHARMACY)

By

Samantha Yolanda Mukozhiwa

February 2014

Faculty of Pharmacy

Rhodes University

Grahamstown

South Africa

ABSTRACT

Cardiovascular diseases (CVD) are the leading cause of death worldwide and global projections predict that the number of deaths due to CVD will continue to increase over the next 17 years [1]. With the growing burden of CVD the design and development of formulations that optimise the delivery of existing therapeutic molecules may be an approach to improving the management of patients with CVD. Captopril (CPT) is an angiotensin converting enzyme (ACE) inhibitor used for the routine management of hypertension, cardiac failure and diabetic nephropathy [2-4]. However it has a relatively short half-life and typical therapeutic dosing regimens require multiple dosing [2]. CPT is a potential candidate for sustained oral drug delivery, however its poor stability profile and high water solubility present significant formulation challenges. CPT exhibits optimal stability at pH < 4 and is unstable in the alkaline environment of intestinal fluids [5]. A sustained release gastroretentive formulation is therefore proposed as an approach that may improve the *in vivo* stability of CPT in addition to slowly releasing the molecule at a desired rate that may also minimize the occurrence of drug-related adverse effects.

A Capillary Zone Electrophoresis (CZE) method for the quantitation of CPT in pharmaceutical dosage forms was developed and optimised using a Central Composite Design (CCD) approach. The CZE method was found to have the necessary linearity, accuracy, precision, sensitivity and specificity for the analysis of CPT in pharmaceutical formulations.

Preformulation studies were conducted as part of the preparative work required to manufacture high quality, stable gastroretentive sustained release CPT tablets. The experiments conducted were tailored for the development of CPT sustained release tablets using direct compression manufacture and included an analysis of particle size and shape, powder flow properties and CPT-excipient compatibility studies. The results revealed that there was no definite evidence of interactions between CPT and the excipients to be used to manufacture CPT tablets, and CPT formulations were developed using these excipients.

A direct compression procedure was selected for tablet manufacture due to apparent simplicity and to avoid unnecessary exposure of CPT to the heat and moisture that would be encountered if a wet granulation manufacturing process was used. A numerical optimisation

approach was used to predict a formulation composition that would produce minimal CPT release initially, a short floating lag time (FLT) and maximum CPT release after 12 hours of dissolution testing. The effect of increasing the agitation speed of USP Apparatus 2 on the release of CPT from the optimised formulation was also investigated. The results revealed that changing the speed of the paddle had only a relatively small impact on the *in vitro* release behaviour of CPT from the tablets. The optimised formulation was subjected to additional testing in an attempt to investigate the effects of pH and osmolarity on the swelling and erosion characteristics of the dosage form. It was important to evaluate the effects of pH and osmolarity from the perspective of the solubility and stability of CPT. The results generated from swelling studies revealed that the swelling characteristics of the proposed formulation were not significantly altered by a change in pH and osmolarity of the test medium and this is probably due to the non-ionic nature of HPMC. In addition, the results revealed that the solubility and/or stability of CPT in different dissolution media did not affect the water uptake and swelling of the tablet matrices. The results revealed the erosion rate constants were low and suggest that although polymer erosion does occur, the role of this phenomenon in the release of CPT may not be as significant as that of diffusion.

The release kinetics of CPT from the tablets was established by fitting *in vitro* release data to several mathematical models. The *in vitro* release data were best described using the Korsmeyer-Peppas model and values of release exponent (*n*) suggest that the majority of the tablets exhibited an anomalous CPT transport mechanism. The short-term stability of the optimised formulation was established by undertaking stability studies at 25°/60% RH and 40°/75% RH. The results revealed that there was no significant change in appearance and physicochemical properties of the tablets over 60 days. In conclusion, gastroretentive sustained release CPT tablets with the potential for further development and optimisation have been successfully developed and assessed in these studies. A basis is thus provided for further development of this technology.

ACKNOWLEDGEMENTS

I would like to extend my heartfelt gratitude to the following people:

My supervisor, Dr S.M.M. Khamanga for providing valuable advice and meticulous guidance which helped shape my thinking throughout the course of my studies. I am deeply grateful for his patience, enthusiasm and continuous optimism.

My co-supervisor, Professor R.B. Walker, for providing valuable guidance and expertise. I sincerely appreciate his patience and continuous encouragement throughout the duration of my studies. I would also like to thank him for his valuable contribution as my tutor during my academic internship.

Professor R.B. Walker, in his capacity as the Head and Dean of the Faculty of Pharmacy, for allowing me to use the resources and facilities in the Faculty.

The Henderson Scholarship Programme and the Rhodes University Research Committee for the generous financial support, without which, these studies could not have been completed. I am sincerely grateful.

Protea Chemicals (Midrand, Johannesburg, South Africa) for donating captopril and Aspen Pharmacare (Port Elizabeth, South Africa) for donating excipients.

Dr K. Wa Kasongo for his support and encouragement.

Mr T. Samkange and Mr C. Nontyi for the technical assistance during my studies. Special thanks to Mr L. Purdon and Mrs T. Kent their assistance and warm encouragement.

Dr D. Grooff from the Department of Physical and Polymer Chemistry, Nelson Mandela Metropolitan University, for allowing me use the DSC instrumentation.

My colleagues in the Biopharmaceutical Research Laboratory: Chiluba Mwila, Farai Mhaka, Chiedza Zindove, Tendai Chanakira and Tawanda Dube. Special thanks to Ashmita

Ramanah, Ayeshah Fauzee and Pedzisai Makoni for the friendship, support and willingness to help.

My dear friends, Chikomborero Chakaingesu, Byron Mubaiwa, Mandilakhe Sidzumo and Yandiswa Maqodwana for the never-ending support and warm encouragement. Special thanks to Olukemi Owolabi for the support, good advice and friendship.

My parents, Ruth and Wilfred Mukozhiwa for their support and for believing in me. My sisters, Olivia, Amanda and Tatenda Mukozhiwa for the prayers, love and support. My grandfather, Mr George Tambo and my aunt, Mrs Priscilla Dhlamini, for their love and support.

The Lord Almighty, for giving me the courage and strength to pursue postgraduate studies.

STUDY OBJECTIVES

Cardiovascular diseases (CVD) are the leading cause of death in developed and developing countries and global projections predict that the number of deaths due to CVD will continue to increase over the next 17 years [1]. With the growing burden of CVD the design and development of formulations that optimise the delivery of existing compounds such as captopril (CPT) may be an approach to improving the management of patients with CVD. CPT is used alone or in combination with other agents to manage hypertension, congestive heart failure and diabetic nephropathy [2-4]. CPT has a relatively short half-life and typical dosing requires multiple dose administration. CPT is therefore a potential candidate for sustained oral delivery, however the poor stability profile and high water solubility of the molecule present significant formulation challenges. CPT exhibits optimal stability at pH < 4 and is unstable in the alkaline environment of intestinal fluids [5]. The rationale for developing a sustained release gastroretentive formulation was to provide an approach that may improve the *in vivo* stability of CPT in addition to releasing the molecule at a desired rate that may minimize the occurrence of drug-related adverse effects.

The objectives of the study were:

i. To collect, analyse and interpret information relating to the physicochemical, pharmacological and biopharmaceutical properties of CPT
ii. To develop and validate a Capillary Zone Electrophoresis (CZE) method for the quantitation of CPT in pharmaceutical dosage forms
iii. To characterise powder blends for direct compression
iv. To use Differential Scanning Calorimetry (DSC) and Fourier Transform-Infrared (FT-IR) analysis to identify excipients that may be incompatible with CPT
v. To develop and manufacture sustained release gastroretentive CPT tablets using direct compression
vi. To investigate the effects of formulation variables on CPT release and the floating properties of the tablets
vii. To use Response Surface Methodology (RSM) to optimise the formulation
viii. To use model-dependent approaches to establish the kinetics of CPT release from the tablets
ix. To identify key aspects of the formulation that require further investigation

TABLE OF CONTENTS

ABSTRACT		**i**
ACKNOWLEDGEMENTS		**iii**
STUDY OBJECTIVES		**v**
LIST OF TABLES		**xiii**
LIST OF FIGURES		**xv**
LIST OF ABBREVIATIONS		**xviii**
CHAPTER 1		**1**
CAPTOPRIL		**1**
1.1	**INTRODUCTION**	**1**
1.2	**PHYSICOCHEMICAL PROPERTIES**	**2**
1.2.1	Description	2
1.2.2	Isomerism	2
1.2.3	Solubility	3
1.2.4	Dissociation constant (pK_a)	3
1.2.5	Biopharmaceutics Classification system	4
1.2.6	Partition coefficient	4
1.2.7	Hygroscopicity	4
1.2.8	Polymorphism	4
1.2.9	Melting range	5
1.2.10	Ultraviolet (UV) spectrum	5
1.2.11	Infrared (IR) spectrum	6
1.3	**SYNTHESIS**	**7**
1.3.1	Synthetic pathway	7
1.3.2	Structure activity relationship	8
1.4	**STABILITY**	**8**
1.4.1	Stability in aqueous solution	8
1.4.2	Stability in the solid state	9
1.4.3	Solution pH	9
1.5	**CLINICAL PHARMACOLOGY**	**9**
1.5.1	Mechanism of action	9
1.5.2	Clinical indications	10
1.5.3	Off-label or investigational use	10
1.5.4	Contraindications	10
1.5.5	Precautions and high risk groups	11
1.5.5.1	*Paediatric use*	11
1.5.5.2	*Geriatric use*	11
1.5.5.3	*Use in pregnancy*	11
1.5.5.4	*Use in lactation*	12

1.5.5.5 *Renal impairment* 12
1.5.6 Drug interactions 12
1.5.7 Adverse effects 13
1.5.7.1 *Respiratory* 13
1.5.7.2 *Taste disturbances* 13
1.5.7.3 *Cardiovascular* 13
1.5.7.4 *Dermatological* 14
1.5.7.5 *Renal* 14
1.5.7.6 *Haematological* 14
1.5.7.7 *Miscellaneous* 14
1.6 CLINICAL PHARMACOKINETICS 15
1.6.1 Dosage and administration 15
1.6.2 Overdose 15
1.6.3 Absorption 16
1.6.4 Distribution 16
1.6.5 Metabolism 16
1.6.6 Elimination 17
1.7 CONCLUSIONS 17

CHAPTER 2 18

DEVELOPMENT OF A CAPILLARY ZONE ELECTROPHORESIS METHOD FOR THE QUANTITATION OF CAPTOPRIL IN PHARMACEUTICALS 18

2.1 INTRODUCTION 18
2.1.1 Principles of capillary electrophoresis 18
2.1.2 Electro-osmotic flow 19
2.1.3 CE instrumentation 20
2.1.4 Modes of CE 21
2.1.4.1 *Capillary zone electrophoresis (CZE)* 21
2.1.4.2 *Capillary isotachophoresis (CITP)* 21
2.1.4.3 *Capillary gel electrophoresis (CGE)* 22
2.1.4.4 *Capillary isoelectric focussing (CIEF)* 22
2.1.4.5 *Capillary electrochromatography (CEC)* 23
2.1.4.6 *Micellar electrokinetic chromatography (MECK)* 23
2.2 METHOD DEVELOPMENT AND OPTIMISATION 24
2.2.1 Capillary selection 24
2.2.2 Method of detection 25
2.2.3 Running buffer selection 25
2.3 RESPONSE SURFACE METHODOLOGY 28
2.3.1 Overview 28
2.3.2 Central composite design 30
2.4 CAPTOPRIL ANALYSIS 31

2.5 EXPERIMENTAL 33
2.5.1 Instrumentation 33
2.5.2 Chemical reagents 33
2.5.3 Preparation of stock solutions 34
2.5.4 Preparation of running buffer 34
2.5.5 Capillary conditioning 34
2.5.6 Selection of internal standard 35
2.5.7 System suitability testing 35
2.5.8 Experimental design 36
2.6 METHOD VALIDATION 38
2.6.1 Overview 38
2.6.2 Calibration, linearity and range 38
2.6.3 Precision 39
2.6.3.1 Repeatability 40
2.6.3.2 Intermediate precision 40
2.6.3.3 Reproducibility 40
2.6.4 Accuracy 41
2.6.5 Limits of detection (LOD) and quantitation (LOQ) 41
2.6.6 Stability in running buffer 42
2.6.7 Specificity 43
2.6.8 Assay 43
2.7 RESULTS AND DISCUSSION 44
2.7.1 System suitability testing 44
2.7.2 Verification and evaluation of the model for the migration time of CPT 44
2.7.3 Diagnostic plots 46
2.7.4 Visual presentation of the model equation 49
2.7.4.1 Voltage 49
2.7.4.2 Buffer molarity 50
2.7.4.3 Buffer pH 51
2.7.4.4 Capillary length 52
2.7.5 Establishment of optimal conditions 53
2.7.6 Validation of the CZE method 54
2.7.6.1 Calibration, linearity and range 54
2.7.6.2 Precision 55
2.7.6.3 Accuracy 57
2.7.6.4 LOD and LOQ 57
2.7.6.5 Solution stability 57
2.7.6.6 Specificity 58
2.7.6.7 Assay 58
2.8 CONCLUSIONS 59

CHAPTER 3 **60**

PREFORMULATION CONSIDERATIONS FOR MANUFACTURING CAPTOPRIL SUSTAINED RELEASE TABLETS **60**

3.1 INTRODUCTION **60**
3.2 SELECTION OF PHARMACEUTICAL EXCIPIENTS **60**
3.2.1 Overview 60
3.2.2 Materials 61
3.2.2.1 Hydroxypropyl methylcellulose (HPMC) 63
3.2.2.2 Microcrystalline cellulose 63
3.2.2.3 Ethylcellulose 64
3.2.2.4 Carbomers 64
3.2.2.5 Sodium bicarbonate 64
3.2.2.6 Magnesium stearate 65
3.2.2.7 Talc 65
3.2.2.8 Colloidal silicon dioxide 65
3.3 PARTICULATE AND MECHANICAL PROPERTIES **66**
3.3.1 Particle size analysis 66
3.3.2 Characterisation of powder blend 66
3.3.2.1 Powder density 67
3.3.2.2 Angle of repose 67
3.4 API-EXCIPIENT COMPATIBILITY **68**
3.4.1 Types of interactions 68
3.5 EXPERIMENTAL **71**
3.5.1 Particle shape and size 71
3.5.2 Powder density 71
3.5.3 Angle of repose 71
3.5.4 Thermogravimetric analysis (TGA) 72
3.5.5 Differential Scanning Calorimetry (DSC) 72
3.5.6 FT-IR spectroscopy 72
3.6 RESULTS AND DISCUSSION **73**
3.6.1 Particle shape and size 73
3.6.2 Characterisation of powder blend 77
3.6.3 Thermogravimetric analysis 78
3.6.4 Differential Scanning Calorimetry 79
3.6.5 FT-IR spectroscopy 87
3.7 CONCLUSIONS **92**

CHAPTER 4 **94**

DEVELOPMENT, MANUFACTURE AND ASSESSMENT OF CAPTOPRIL SUSTAINED RELEASE TABLETS **94**

4.1 INTRODUCTION **94**
4.2 MECHANISMS OF DRUG RELEASE FROM ORAL CONTROLLED RELEASE SYSTEMS **95**
4.2.1 Dissolution-controlled systems 95
4.2.2 Diffusion-controlled systems 95
4.2.3 Erosion-controlled systems 98
4.2.4 Osmotic-controlled systems 99
4.2.5 Ion exchange resins 100
4.3 PROPOSED FORMULATION **101**
4.3.1 Background 101
4.3.2 Rationale 102
4.4 EXPERIMENTAL **102**
4.4.1 Method of manufacture 102
4.4.2 Evaluation of tablets 106
4.4.2.1 Content uniformity 106
4.4.2.2 Weight uniformity 106
4.4.2.3 Assay 106
4.4.2.4 Crushing strength and tensile strength 107
4.4.2.5 Friability 107
4.4.2.6 In vitro buoyancy testing 107
4.4.2.7 In vitro release studies 107
4.5 RESULTS AND DISCUSSION **108**
4.5.1 Physical appearance 108
4.5.2 Content uniformity 108
4.5.3 Weight uniformity 109
4.5.4 Assay 109
4.5.5 Crushing strength and tensile strength 109
4.5.6 Friability 110
4.5.7 *In vitro* buoyancy testing 112
4.5.8 *In vitro* release studies 112
4.6 CONCLUSIONS **122**

CHAPTER 5 **124**

FORMULATION OPTIMISATION AND MATHEMATICAL MODELLING OF CAPTOPRIL RELEASE **124**

5.1 INTRODUCTION **124**
5.2 EXPERIMENTAL **124**
5.2.1 Materials and methods 124
5.2.2 Experimental design 124
5.2.3 Evaluation of CPT sustained release tablets 126
5.2.4 Effect of agitation rate 127
5.2.5 Swelling studies 127
5.2.6 Matrix erosion studies 127
5.2.7 Stability testing 128
5.3 MATHEMATICAL MODELLING OF CPT RELEASE **129**
5.3.1 Overview 129
5.3.2 Zero-order model 129
5.3.3 First-order model 129
5.3.4 Higuchi model 130
5.3.5 Hixson-Crowell model 130
5.3.6 Korsmeyer-Peppas model 131
5.3.7 Approaches for selecting the best-fit mathematical model 132
5.4 RESULTS AND DISCUSSION **133**
5.4.1 Central composite design 133
5.4.2 Verification and evaluation of the model for response Y_3 135
5.4.3 Diagnostic plots for the model for response Y_3 137
5.4.4 Response surface plots for response Y_3 140
5.4.5 Evaluation of sustained release CPT tablets 145
5.4.6 Mathematical modelling 149
5.4.7 Formulation optimisation 152
5.4.8 Effect of agitation speed on *in vitro* CPT release 154
5.4.9 Swelling studies 156
5.4.10 Matrix erosion studies 158
5.4.11 Stability testing 160
5.5 CONCLUSIONS **165**

CHAPTER 6 **167**

CONCLUSIONS **167**

REFERENCES **172**

APPENDIX I: SAMPLE BATCH PRODUCTION RECORD **192**
APPENDIX II: BATCH SUMMARIES **197**
APPENDIX III: DIAGNOSTIC, TWO-DIMENSIONAL AND THREE-DIMENSIONAL RESPONSE SURFACE PLOTS MONITORED IN THE CCD OPTIMISATION PROCESS **231**

LIST OF TABLES

Table 1.1 Solubility of CPT in different solvents (Adapted from [5]) 3
Table 1.2 Infrared characteristic band assignment of CPT 6

Table 2.1 A list of commonly used buffers and their respective pK_a values (Adapted from [86, 94]) 27
Table 2.2 Analysis of CPT 32
Table 2.3 Translation of the coded levels used in CCD 36
Table 2.4 Experimental conditions for CCD 37
Table 2.5 Recommended minimum ranges for determining linearity (Adapted from [149] 39
Table 2.6 ANOVA for Response Surface Quadratic Model for migration time 45
Table 2.7 Migration time analysis following data transformation 46
Table 2.8 Optimum electrophoretic conditions 53
Table 2.9 Linearity of CPT analysis 54
Table 2.10 Precision of CPT analysis 56
Table 2.11 Accuracy of CPT analysis 57
Table 2.12 CPT stability 58
Table 2.13 Assay results for commercially available products containing CPT 59

Table 3.1 Excipients used to manufacture sustained release CPT tablets 62
Table 3.2 Interpretation of Carr's index (Adapted from [188]) 67
Table 3.3 Interpretation of the angle of repose (Adapted from [13]) 68
Table 3.4 Techniques used in API-excipient compatibility testing (Adapted from [151, 167]) 70
Table 3.5 Particle size distribution of CPT and excipients 76
Table 3.6 Characterization of powder blends used to manufacture preliminary formulations 77
Table 3.7 Thermal parameters of CPT and CPT-excipient mixtures 79

Table 4.1 Tablet composition for preliminary formulations 103
Table 4.2 Content uniformity data of CPT sustained release tablets 109
Table 4.3 Physicochemical assessment of CPT sustained release tablets 111

Table 5.1 Translation of the coded levels used in CCD 125
Table 5.2 Actual experimental conditions for CCD 126
Table 5.3 Interpretation of release exponents for systems of different geometries (Adapted from 247) 132

Table 5.4 Summary of the model selection process for response Y_3 136
Table 5.5 ANOVA for the quadratic model for Y_3 137
Table 5.6 Physicochemical assessment of CPT sustained release tablets 146
Table 5.7 Summary of mathematical model and release kinetic parameters 151

Table 5.8 Formulation composition for the optimised formulation 152
Table 5.9 Predicted and average experimental responses (n=3) for the optimised formulation 152
Table 5.10 Summary of mathematical model paramters for the optimised formulation 154
Table 5.11 Difference and similarity factors for dissolution profiles obtained using different agitation speeds 156
Table 5.12 Summary of the kinetic parameters for tablet erosion in different dissolution media 160
Table 5.13 Results from stability testing for the optimised formulation stored at 25°C/60% RH 162
Table 5.14 Results from stability testing for the optimised formulation stored at 40°C/75% RH 162
Table 5.15 Results from the Timm *et al.* test for the effect of stability test conditions on the physicochemical properties of CPT tablets after storage at 25°C/60% RH for 60 days 164
Table 5.16 Results from the Timm *et al.* test for the effect of stability test conditions on the physicochemical properties of CPT tablets after storage at 40°C/75% RH for 60 days 164

LIST OF FIGURES

Figure 1.1 Chemical structure of CPT [$C_9H_{15}NO_3S$] MW = 217.29 (Adapted from [5]) 2
Figure 1.2 Isomers of CPT (a) *cis* isomer (b) *trans* isomer (Adapted from [18]) 3
Figure 1.3 Dissociation constants of CPT 4
Figure 1.4 UV absorption spectrum of CPT in water 5
Figure 1.5 Infrared absorption spectrum of CPT 6
Figure 1.6 Synthetic pathway of CPT (Adapted from [5]) 7

Figure 2.1 Simplified CE instrumentation (Adapted from [86]) 20
Figure 2.2 Theoretical separation of a mixture of ions (Adapted from [86]) 21
Figure 2.3 Normal plot of residuals for migration time 47
Figure 2.4 Plot of residuals versus predicted for migration time 48
Figure 2.5 Box-Cox plot for power transformation 49
Figure 2.6 Contour plot for migration time as a function of buffer molarity and voltage 50
Figure 2.7 Contour plot for migration time as a function of buffer molarity and capillary length 51
Figure 2.8 Contour plot for migration time as a function of buffer pH and buffer molarity 52
Figure 2.9 Contour plot for migration time as a function of buffer pH and capillary length 53

Figure 2.10 Typical electropherogram of a standard solution of IS (1), CPT (2) and sodium metabisulphite (3). CZE conditions: 20 mM phosphate buffer, pH 7.0; applied voltage 23.9 kV; capillary length 67.5 cm (57.5 cm effective length) x 75 µm I.D; detection wavelength 214 nm 54
Figure 2.11 Typical electropherogram obtained from the analysis of Mylan Captopril 50. IS (1) and CPT (2). CZE conditions: 20 mM phosphate buffer, pH 7.0; applied voltage 23.9 kV; capillary length 67.5 cm (57.5 cm effective length) x 75 µm I.D; detection wavelength 214 nm 58

Figure 3.1 Particle size and shape of excipients 74
Figure 3.1 (cont) Particle size and shape of excipients 75
Figure 3.2 TG curve of CPT degradation 78
Figure 3.3 DSC curve for CPT 80
Figure 3.5 DSC curve for a 1:1 mixture of CPT and Avicel® PH-102 81
Figure 3.5 DSC curve for a 1:1 mixture of CPT and Methocel® K100M 82
Figure 3.6 DSC curve for a 1:1 mixture of CPT and Talc 82
Figure 3.7 DSC curve for a 1:1 mixture of CPT and colloidal silicon dioxide 83
Figure 3.8 DSC curve for a 1:1 mixture of CPT and magnesium stearate 84
Figure 3.9 DSC curve for a 1:1 mixture of CPT and sodium bicarbonate 85
Figure 3.10 DSC curve for a mixture of CPT and all excipients 86
Figure 3.11 FT-IR spectrum for CPT 88

Figure 3.12 FT-IR spectrum for a 1:1 mixture of CPT and Methocel® K100M 88
Figure 3.13 FT-IR spectrum for a 1:1 mixture of CPT and Avicel® PH-102 89
Figure 3.14 FT-IR spectrum for a 1:1 mixture of CPT and Carbopol® 974 NF 89
Figure 3.15 FT-IR spectrum for a 1:1 mixture of CPT and ethylcellulose 90
Figure 3.16 FT-IR spectrum for a 1:1 mixture of CPT and talc 90
Figure 3.17 FT-IR spectrum for a 1:1 mixture of CPT and magnesium stearate 91
Figure 3.18 FT-IR specturm for a 1: mixture of CPT and colloidal silicon dioxide 91
Figure 3.19 FT-IR spectrum for a 1:1 mixture of CPT and sodium bicarbonate 92

Figure 4.1 Schematic representation of API release from a diffusion-based reservoir tablet (Adapted from [188]) 97
Figure 4.2 Schematic representation of API release from diffusion-based matrix tablet (Adapted from [188]) 98
Figure 4.3 Schematic representation of API release from an erosion-based release tablet (Adapted from [188]) 98
Figure 4.4 Osmotic-controlled release 99
Figure 4.5 Schematic illustrations of approaches that may be used to achieve gastro-retention 102
Figure 4.6 Schematic representation of the manufacturing process 105
Figure 4.7 CPT release from formulation C1 113
Figure 4.8 CPT release from formulation C2 114
Figure 4.9 CPT release from formulation C3 115
Figure 4.10 CPT release from formulation C4 116
Figure 4.11 CPT release from formulation C5 117
Figure 4.12 CPT release from formulation C6 118
Figure 4.13 CPT release from formulation C7 119
Figure 4.14 CPT release from formulation C8 120
Figure 4.15 CPT release from formulation C9 121
Figure 4.16 CPT release from formulation C10 122

Figure 5.1 Normal plot of residuals for response Y_3 138
Figure 5.2 Plot of residuals vs. predicted for response Y_3 139
Figure 5.3 Box-Cox plot for response Y_3 139
Figure 5.4a Contour plot of the effect of Methocel® K100M and Avicel® PH-102 on CPT release at 6 hours 140
Figure 5.4b Three-dimensional contour plot of the effect of Methocel® K100M and Avicel® PH-102 on CPT release at 6 hours 141
Figure 5.5a Contour plot of the effect of Methocel® K100M and sodium bicarbonate on CPT release at 6 hours 142
Figure 5.5b Three-dimensional contour plot of the effect of Methocel® K100M and sodium bicarbonate on CPT release at 6 hours 143
Figure 5.6a Contour plot of the effect of Avicel® PH-102 and sodium bicarbonate on CPT release at 6 hours 144

Figure 5.6b Three-dimensional contour plot of the effect of Avicel® PH-102 and sodium bicarbonate on CPT release at6 hours 144
Figure 5.7 Photographs of a typical sustained release CPT floating matrix tablet at 1 min (A), 10 min (B), 4 hours (C) and 12 hours (D) 148
Figure 5.8 CPT release from the optimised formulation 153
Figure 5.9 Effect of stirring rate on CPT release 154
Figure 5.10 Effect of pH on the SI 157
Figure 5.11 Effect of osmolarity on the SI 158
Figure 5.12 Effect of pH on the % erosion 159
Figure 5.13 Effect of osmolarity on the % erosion 159

LIST OF ABBREVIATIONS

ACE	Angiotensin Converting Enzyme
ANOVA	Analysis of Variance
AOR	Angle of Repose
API	Active Pharmaceutical Ingredient
BCS	Biopharmaceutics Classification System
BD	Bulk Density
CCD	Central Composite Design
CE	Capillary Electrophoresis
CEC	Capillary electrochromatography
CGE	Capillary Gel Electrophoresis
cGMP	Current Good Manufacturing Practices
CI	Carr's Index
CIEF	Capillary isoelectric focussing
CITP	Capillary isotachophoresis
cont	Continued
CPT	Captopril
CVD	Cardiovascular Diseases
CZE	Capillary Zone Electrophoresis
DOE	Design of Experiments
DSC	Differential Scanning Calorimetry
EDL	Electric Double Layer
EOF	Electro-osmotic flow
FDA	Food and Drug Administration
FLT	Floating lag time
FT-IR	Fourier Transform-Infrared
GC	Gas chromatography
GRAS	Generally Regarded as Safe
HPLC	High Performance Liquid Chromatography
HPMC	Hydroxypropyl methylcellulose
HR	Hausner Ratio
ID	Internal diameter
IR	Infrared
IS	Internal standard
LC-MS	Liquid Chromatography-Mass Spectroscopy
LOD	Limit of detection
log P	Partition coefficient
LOQ	Limit of quantitation
MCC	Microcrystalline cellulose

MECK	Micellar electrokinetic chromatography
pK_a	Dissociation constant
RSD	Relative standard deviation
RSM	Response Surface Methodology
SEM	Scanning Electron Microscopy
SI	Swelling index
SMBS	Sodium metabisulphite
TBD	Tapped Bulk Density
TFT	Total floating time
TGA	Thermogravimetric Analysis
UV	Ultraviolet

CHAPTER 1

CAPTOPRIL

1.1 INTRODUCTION

Cardiovascular diseases (CVD) are a leading cause of death worldwide [6]. In 2008 approximately 17.3 million people died of CVD, accounting for 30% of the total number of deaths recorded worldwide that year [1]. More than 80% of these deaths occurred in low- and middle-income countries [1]. Mortality due to CVD has declined in the majority of high-income countries, however the number of CVD-related deaths occurring in low- and middle-income countries has increased rapidly over the last 20 years [6,7]. Global projections indicate that the number of deaths due to CVD will continue to increase over the next 16 years, and 23.3 million people will die from CVD annually by 2030 [1]. Strategies to address the global burden of CVD include surveillance, monitoring, prevention, reduction of risk factors and improved management of healthcare through early detection and timely treatment [6]. The development of new drugs to combat CVD may be time consuming and expensive, therefore improving and optimising the delivery of existing compounds with established pharmacokinetics, efficacy and safety profiles may be a strategic approach to improve community health-related outcomes.

Captopril (CPT) is an angiotensin converting enzyme (ACE) inhibitor, and was the first agent from this class to be approved for clinical use and commercially marketed [8,9]. CPT is used alone or in combination to manage conditions such as hypertension, cardiac failure and diabetic nephropathy [2,4]. CPT has a short half-life and is normally administered 8-12 hourly [2]. The development of a controlled release formulation requiring less frequent administration would be more convenient and acceptable to patients and may improve patient adherence [10, 11]. There are a number of therapeutic advantages of controlled release formulations, including reduced fluctuation of plasma drug concentration, maintenance of an optimal plasma concentration and a reduced incidence of drug-related adverse effects [10].

CPT is commercially available in South Africa as CaptoHexal®, Adco-Captomax®, Mylan-Captopril®, Sandoz Captopril®, Zapto®, Bio-Captopril® and Capace®. These formulations are supplied as immediate release tablets containing 12.5, 25 or 50 mg CPT [2].

1.2 PHYSICOCHEMICAL PROPERTIES

1.2.1 Description

CPT is a white or almost white crystalline powder that may have a slight yet characteristic mercaptan odour [4,5,12]. Chemically CPT is known as (2S)-1-[(2S)-2-methyl-3-sulfanylpropanoyl] pyrrolidine-2-carboxylic acid [12]. The chemical content of $C_9H_{15}NO_3S$ in CPT must be greater than or equal to 97.5% and not more than 102.0%, calculated on an anhydrous basis [13]. The chemical structure of the CPT molecule is shown in Figure 1.1.

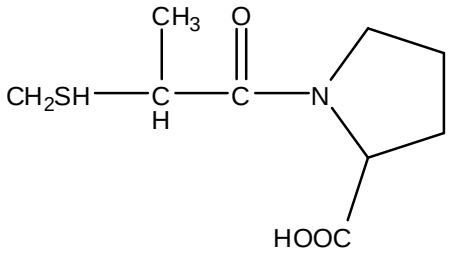

Figure 1.1 Chemical structure of CPT [$C_9H_{15}NO_3S$] MW = 217.29 (Adapted from [5])

1.2.2 Isomerism

CPT exhibits *cis-trans* isomerism across the proline amide bond (Figure 1.2) [14-16]. The *cis* and *trans* isomers of CPT exist in a state of equilibrium in aqueous solution. The *trans* isomer of CPT is reported to be six times more abundant than the *cis* isomer, binds to and inhibits ACE and is the biologically active isomer [14,17].

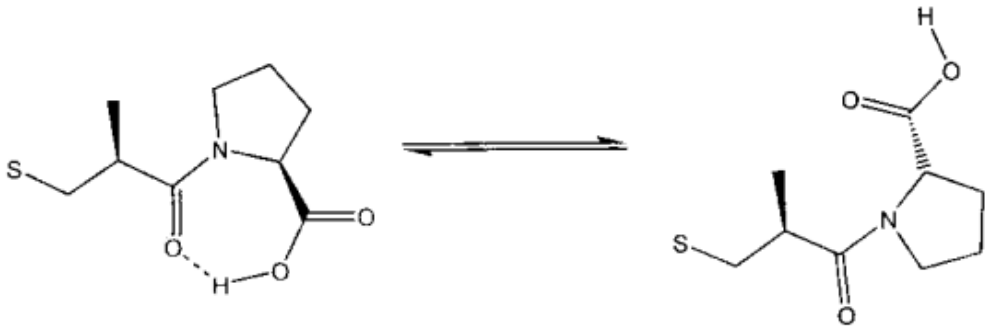

Figure 1.2 Isomers of CPT (a) *cis* isomer (b) *trans* isomer (Adapted from [18])

1.2.3 Solubility

CPT is freely soluble in water, isopropanol, chloroform, methanol, ethanol, methylene chloride and ethyl acetate at 25°C [5,19-22]. A summary of the solubility of CPT in additional solvents is listed in Table 1.1.

Table 1.1 Solubility of CPT in different solvents (Adapted from [5])

Solvent	Solubility (mg/mL)
Water	160
Sesame oil	< 1
Corn oil	< 1
Glyceryl triacetate	> 20

1.2.4 Dissociation constant (pK_a)

The pK_a of the carboxyl group of CPT is 3.7 and the pK_a of the sulfhydryl group is 9.8 [5,21,23]. The functional groups associated with the dissociation constants and their corresponding pK_a values of CPT are shown in Figure 1.3.

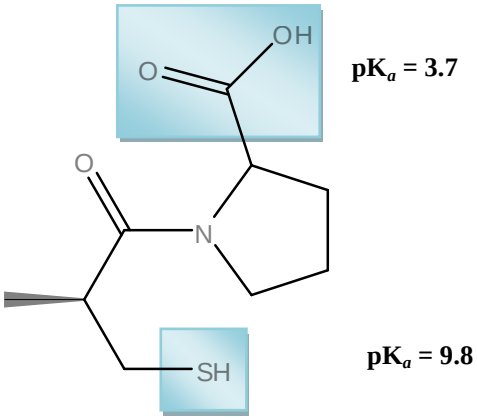

Figure1.3 Dissociation constants of CPT

1.2.5 Biopharmaceutics Classification System (BCS)

CPT is highly soluble in water and exhibits poor gastrointestinal permeability and is therefore classified as a BCS Class III compound [24,25].

1.2.6 Partition coefficient

The partition coefficient (log P) of CPT provides an indication of the relative affinity of a solute for an aqueous or organic phase [26]. High values for log P indicate a high degree of lipid solubility [26]. CPT is weakly lipophilic and has a log P of 0.24 [27].

1.2.7 Hygroscopicity

CPT is not hygroscopic when stored under conditions where the relative humidity is ≤ 50% [5]. If the relative humidity is > 50%, caking may occur after 24 to 48 hours[5].

1.2.8 Polymorphism

CPT can exist in one of two polymorphic forms, distinguished by their melting point [5,28]. The stable polymorph has a melting point of approximately 106°C and the unstable polymorph has a lower melting point of 86°C [5]. The two polymorphs display similar optical rotation, bioassay and solution state infrared spectra, however they exhibit different solid state infrared spectra, powder and single crystal X-ray diffraction patterns [5].

1.2.9 Melting range

CPT polymorphs melt over extremely narrow temperature ranges with the stable polymorph melting in the range 105.2 to 105.9°C and the unstable polymorph between 87.0 and 88.0°C [5].

1.2.10 Ultraviolet (UV) Absorption spectrum

The ultraviolet (UV) absorption spectrum of a 25 µg/mL solution of CPT in water is shown in Figure 1.4. The spectrum was generated using a Model GBC 916 UV VIS double beam spectrophotometer (GBC Scientific Equipment Pty Ltd, Melbourne, Victoria, Australia). The spectrum yielded maximal or an absorption peak at 198.45 nm. Identifying the wavelength of maximal absorption is important for selecting the optimum detection conditions when using UV detection.

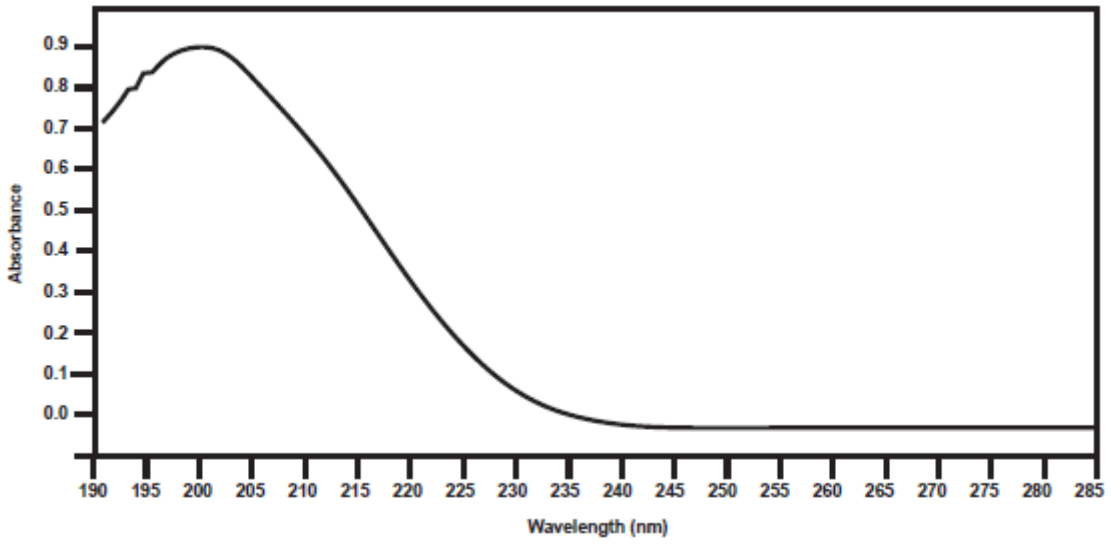

Figure 1.4 UV absorption spectrum of CPT in water

1.2.11 Infrared (IR) absorption spectrum

Infrared (IR) spectroscopy is widely used for the identification of compounds [29-31]. The interpretation of infrared spectra provides information regarding the presence or absence of functional groups which may be characteristic of a certain class of compounds [29,30]. The IR spectrum of CPT powder was generated using a Spectrum 100 FT-IR ATR spectrophotometer (Perkin Elmer® Ltd Beaconsfield, England) and is shown in Figure 1.5. The spectrum is similar to previously reported spectra [32], and the characteristic absorption bands and the relevant structural assignments of CPT are listed in Table 1.2. The bands in the region 1640 cm^{-1} and 2560 cm^{-1} correspond to the presence of the amide moiety [5]. The presence of the S-H moiety is indicated by the vibration in the 2650 cm^{-1} region [5].

Table 1.2 Infrared characteristic band assignment of CPT

Frequency (cm^{-1})	Structural assignment
1640	C=O (amide moiety)
1750	C=O (carboxyl moiety)
2560	S-H

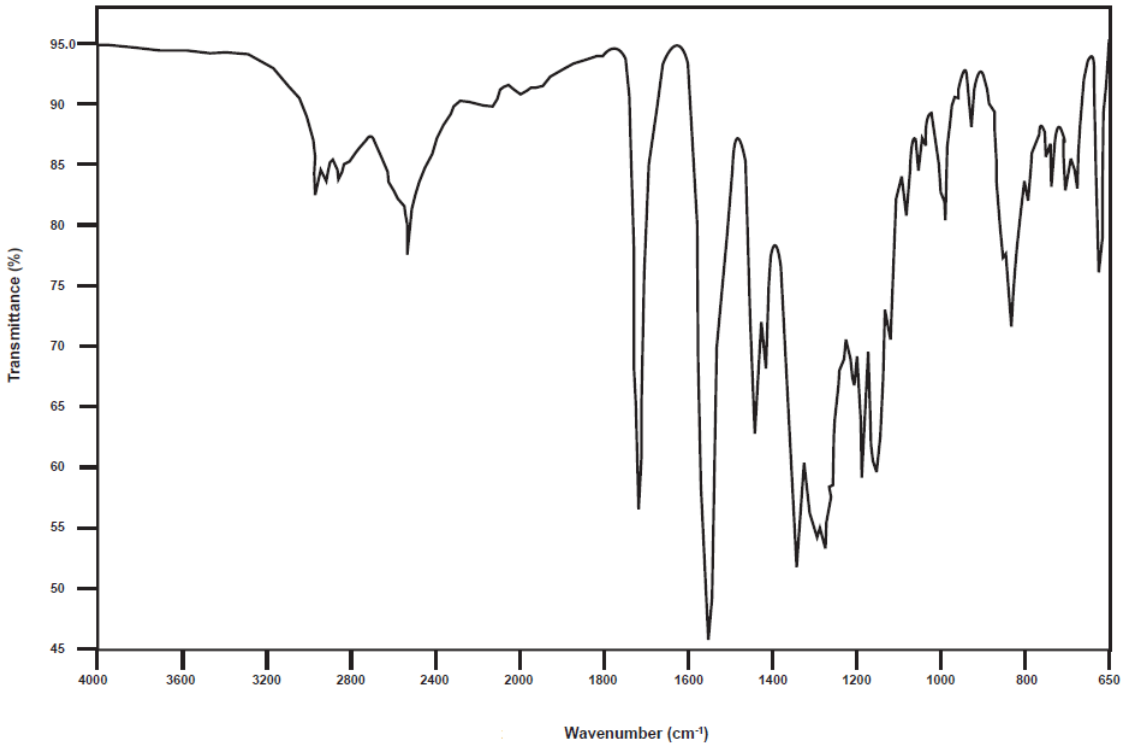

Figure 1.5 Infrared absorption spectrum of CPT

1.3 SYNTHESIS

1.3.1 Synthetic pathway

The synthetic pathway of CPT may be summarized in four main steps and is illustrated in Figure 1.6.

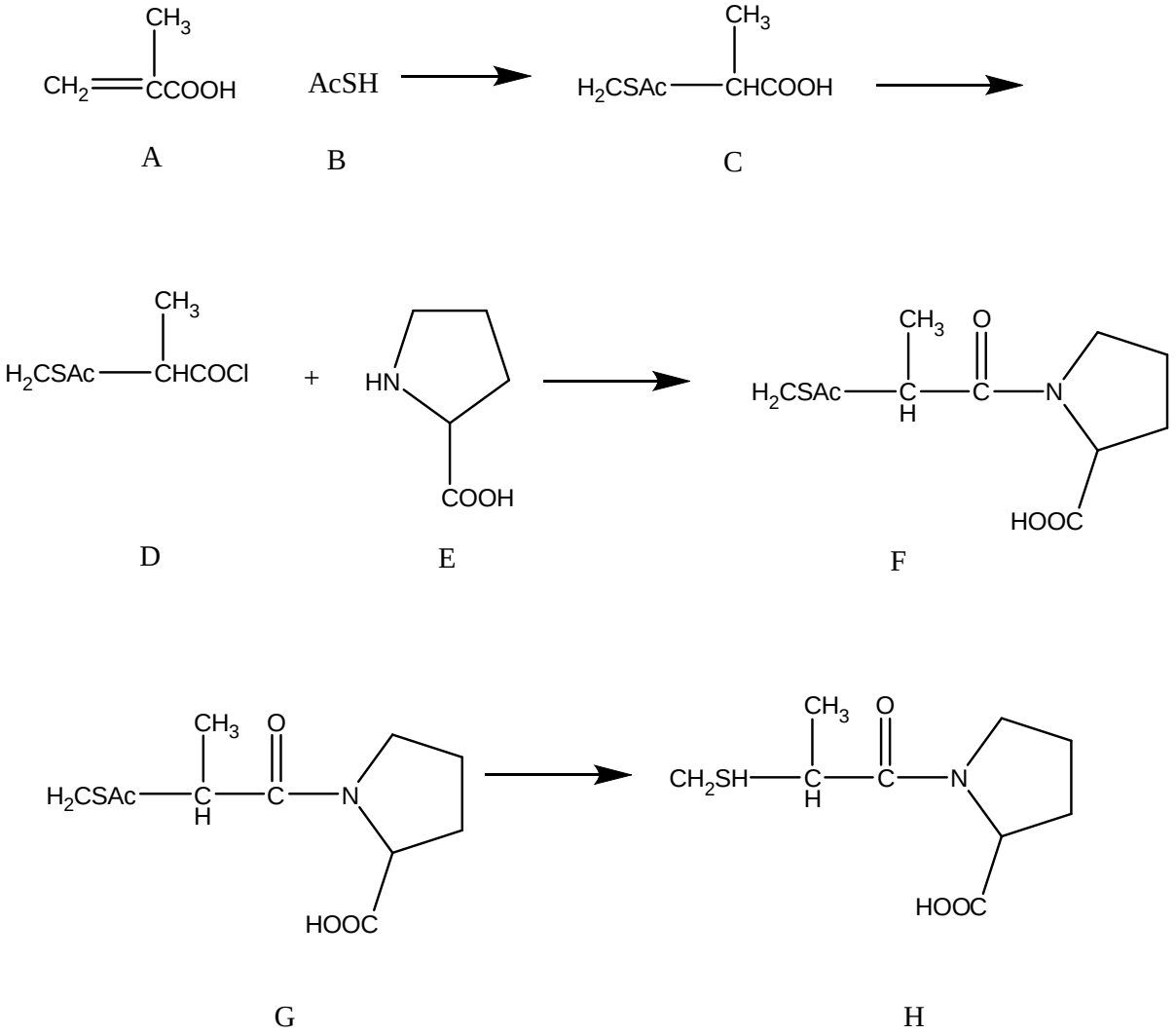

Figure 1.6 Synthetic pathway of CPT (Adapted from [5])

Initially a condensation reaction of methacrylic acid (A) and thiolacetic acid (B) is undertaken to yield a racemic mixture of 2-methyl-3-acetylthiopropionic acid (C) [5]. Chlorination of C followed by reaction of the resultant acid chloride (D) with L-proline (E) via an acetylation reaction yields a proline thioester (F) [5]. Recrystallization from an aqueous solvent resolves product F from the R,S isomer [5]. Saponification of the proline thioester (F) using sodium hydroxide yields the sodium salt of CPT which may be easily converted to CPT (H) via an acidification reaction [5].

1.3.2 Structure activity relationship

On the basis of structural differences, ACE inhibitors are subdivided into three subclasses: sulfhydryl-, carboxyalkyl dipeptide and phosphorus-containing compounds [33]. CPT is characterised by the presence of a sulfhydryl moiety responsible for the ability of the molecule to chelate the zinc atom that is bound to ACE [26]. All ACE inhibitors available for clinical use act as either di- or tri-peptide substrate analogues [26]. ACE is a stereo-selective target; therefore in order to achieve optimum *in vivo* activity ACE inhibitors must display stereochemistry similar to that of L-amino acids found in natural substrates of the enzyme. [26]. The presence of a large heterocyclic N-containing ring enhances the potency of ACE inhibitors and results in changes to the pharmacokinetic properties of these compounds [26]. A carboxylic acid functional group on the pyrrolidine is essential for mimicking the C-terminal carboxylate present in natural substrates of ACE [26].

1.4 STABILITY

1.4.1 Stability in aqueous solution

CPT undergoes first order, free radical oxidative degradation in aqueous solution at the thiol moeity to yield the dimer, captopril-disulphide. The use of a low oxygen headspace or nitrogen gas and increasing the concentration of CPT in solution have been shown to significantly delay the oxidative degradation of CPT [5]. The addition of anti-oxidants or chelating agents to CPT solutions is an effective stabilization approach to delay oxidation of the molecule [5,34,35]. In a study conducted by Brustugun *et al* [36] the incorporation of 0.1 mg/mL of sodium edetate to extemporaneously prepared solutions of CPT was shown to stabilize solutions for up to one year provided the solutions were stored at 22°C. The

presence of 0.2% w/v sodium metabisulphite in CPT solutions was found to be sufficient to delay oxidation and offer protection from oxidative degradation over a 24 hour period (Chapter 2).

Degradation of CPT due to hydrolysis of the amide moiety is highly unlikely and is considered to be insignificant since it occurs only on exposure to extreme degradation conditions [5].

1.4.2 Stability in the solid state

CPT exhibits good solid state stability. Solid samples of CPT stored at temperatures of 5, 30 and 50 °C for six months did not show signs of significant degradation [5]. Direct exposure of solid samples of CPT to visible light of 900 foot candles for a 30-day period did not result in significant degradation of the samples [5].

1.4.3 Solution pH

A study conducted to determine the oxidation rate constants of CPT in solutions of different pH indicated that solutions of CPT in citrate-phosphate buffers maintained at 50°C exhibited optimal stability in acidic solutions at pH < 3.5 [5].

1.5 CLINICAL PHARMACOLOGY

1.5.1 Mechanism of action

The renin-aldosterone pathway plays an essential role in regulating mammalian blood pressure, in addition to controlling *in vivo* sodium and water balance [37,38]. Decreased renal perfusion and reduced arterial pressure trigger the release of renin from the juxtaglomerular cells of the kidneys. The release of renin results in the conversion of angiotensinogen to the inactive compound angiotensin I [39-42]. ACE is responsible for the conversion of angiotensin I to angiotensin II, a potent vasoconstrictor which stimulates the release of aldesterone from the adrenal cortex [39,43,44]. Inhibition of ACE also leads to the accumulation of bradykinin, a vasodilator which further contributes to the antihypertensive effects produced by ACE inhibitors [45,46].

Similar to other ACE inhibitors, CPT interferes with the renin-aldosterone pathway [47] and is a competitive inhibitor of ACE, exhibiting haemodynamic effects on the cardiac system that include decreased blood pressure, preload and afterload which occurs as a consequence of reduced systemic vascular resistance [45,47,48]. The effects of CPT on the renal system are beneficial and may be regarded as reno-protective and include increased renal blood flow [45,49]. The effect(s) of CPT on the sympathetic nervous system include decreased synthesis of norepinephrine and the inhibition of the reuptake of epinephrine [45].

1.5.2 Clinical indications

CPT is used alone or in combination with other antihypertensive agents to manage hypertension [2,44,45]. In addition to the role in the management of hypertension, CPT is also indicated for the treatment of Type 1 diabetic nephropathy and for cardiac therapy [3,45]. Subsequent to a myocardial infarction with symptomatic or asymptomatic left ventricular dysfunction, CPT prophylaxis is provided to clinically stable patients in order to reduce overt heart failure and recurring infarction with an improvement in patient survival rate [2,4,47]. CPT is also used as adjunctive therapy for the treatment of patients with congestive heart failure [3,45].

1.5.3 Off-label or Investigational uses

Although it is considered to be off-label use, CPT delivered sublingually and orally has been shown to be effective in the management of patients presenting with hypertensive crises [50,51]. CPT may also be used for the diagnosis of anatomic renal artery stenosis and primary aldosteronism [3,47]. Other off-label use of CPT includes treatment of rheumatoid arthritis, idiopathic oedema, Bartter's syndrome and hypertension in patients with pre-existing scleroderma renal crisis or Takayasu's disease [3,47].

1.5.4 Contraindications

CPT is contraindicated in patients who may experience hypersensitivity reactions to CPT, to other ACE inhibitors or to any excipients in a formulation [2,3]. CPT should not be administered to patients with idiopathic or hereditary angioedema or those who have previously presented with angioedema which occurred as result of ACE inhibitor therapy

[2,3,47]. CPT is also contraindicated in patients with single and bilateral kidney artery stenosis [2,3].

1.5.5 Precautions and high risk groups

Hypotension may occur subsequent to an initial dose of CPT and is most likely to occur in patients with depleted sodium and blood volume levels and those who are at risk must remain under careful supervision following initiation of therapy [3,47]. Anaphylactic reactions may also occur as a result of treatment with CPT [3,47]. Patients on CPT therapy may present with angioedema in the intestinal or head and neck regions [2,3,47]. The risk of angioedema appears to be greater in black patients than those in other racial groups [47]. Caution must be taken when administering CPT to patients prior to, directly after or when using anaesthetics [3,47]. CPT must be used with caution in cases where patients have been diagnosed with hyperkalemia, valvular stenosis or vascular collagen disease [3].

1.5.5.1 Paediatric use

Clinical experience with the use of CPT in paediatric patients is limited, and for that reason CPT has not yet been registered for use in paediatric patients [2,3,52]. The use of CPT in patients in this age group is reserved for cases where conventional therapy is unsuccessful and if used, doses must be carefully titrated against the clinical response of individual patients [2].

1.5.5.2 Geriatric use

The administration of CPT to geriatric patients is considered to be safe and effective [52]. Dosage adjustments are not necessary except in cases where patients have impaired kidney function [52].

1.5.5.3 Use in pregnancy

CPT is contraindicated in pregnancy [2]. The United States Food and Drug Administration (FDA) considers CPT as a pregnancy category D compound and it should therefore not be used for the entire duration of pregnancy [3,52]. CPT is able to cross the placenta and has

been associated with still birth, neonatal hypotension, oligo hydramnios, anuria, cranial defects and pulmonary hypoplasia [2,47,52,53].

1.5.5.4 Use in lactation

CPT may be safely administered to breastfeeding women [2,54]. Small amounts of CPT may be transferred from maternal blood into breast milk, however the concentration in breast milk is much lower than that measured in the blood and has been reported to be approximately 1% that of blood concentrations [2,3,55].

1.5.5.5 Renal impairment

Administration of CPT to patients with impaired renal function increases the risk of haematological disorders such as neutropenia and agranulocytosis [52,53]. It is therefore imperative for white blood cell counts to be monitored in these patients for the first three months of therapy [52]. The risk of proteinuria is also higher in patients with impaired renal function, and for that reason urinary protein estimates must be determined periodically for at least one year following initiation of therapy in these patients [52,53].

1.5.6 Drug interactions

The antihypertensive effects of CPT are increased by concomitant administration with monoamine oxidase inhibitors, oestrogen, antipsychotics, anxiolytics, hypnotics, sedatives, alcohol and other cardio active agents [56]. Aldesleukin, alprostadil, baclofen, carbenoxolone and levodopa are examples of drugs that enhance the antihypertensive effects of CPT [56]. In addition to increasing the hypotensive effects of CPT, alpha blockers such as terazosin may give rise to severe first-dose hypotension when administered concomitantly with CPT [56]. Inhibitors of the CYP2D6 enzyme such as fluoxetine, miconazole, quinine, ritonavir, chlorpromazine, quinidine pergolide, paroxetine, ropinirole and delavirdine may increase the antihypertensive effects of CPT [3,56]. Probenecid and phenothiazines are other examples of drugs that may enhance the antihypertensive effects of CPT. Concomitant administration of CPT and diuretics results in increased antihypertensive effects [3].

The antihypertensive effects of CPT are diminished when CPT is administered with rifampicin [3,56]. Concurrent administration of corticosteroids or of aspirin in doses exceeding 300 mg counteracts the antihypertensive effects of CPT [3,56]. The concurrent administration of CPT and antacids is not recommended as it results in decreased absorption and bioavailability of CPT [56,56]. Non-steroidal anti-inflammatory agents, particularly indomethacin, may negate the antihypertensive activity of CPT [52,56].

Concurrent administration of CPT with potassium sparing diuretics, high doses of co-trimoxazole, angiotensin receptor blockers, tacrolimus, erythropoietin, heparin, ciclosporin or potassium supplements is not recommended as hyperkalaemia may occur [3,52,56].

Similar to other ACE inhibitors, CPT may increase the levels and pharmacological effects of the sulphonylureas, digoxin and lithium, and potentially cause toxicity [3,56]. Concomitant administration of CPT and allopurinol, azathioprine, potassium supplements or digoxin is considered to be a risk in patients with impaired renal function [56].

1.5.7 Adverse effects

1.5.7.1 Respiratory

A dry hacking cough that may present within the first week of therapy and in some cases up to a year following the commencement of therapy is a common adverse effect of CPT [57-60]. Other less common respiratory adverse effects include rhinitis, bronchospasm and eosinophilic pneumonitis [3].

1.5.7.2 Taste disturbances

CPT has been associated with the occurrence of taste disturbance, in particular the lack of perception of basic taste, ageusia and misinterpretation of taste, dysgeusia [22,61-67].

1.5.7.3 Cardiovascular

The occurrence of hypotension in otherwise healthy patients taking CPT is infrequent, yet is commonly observed in patients with renal artery stenosis, on sodium-restricted diets, taking

diuretic or vasodilator medication concurrently and in cases where it is used to treat cardiac failure [2,4,47]. Other undesirable cardiovascular effects of CPT include angina, myocardial infarction, palpitations, pericarditis, Raynaud's Syndrome, tachyarrhythmia, syncope, flushing and pallor [2-4,47].

1.5.7.4 Dermatological

Dermatological reactions to CPT are uncommon and normally present as a maculopapular or urticarial rash which is normally mild and self-limiting and disappears on discontinuation of therapy [2,3,47,68]. CPT has also been associated with the appearance of eruptions resembling pityriasis rosea [69]. Life-threatening dermatological reactions such as Stevens-Johnson syndrome have also been reported [3,47].

1.5.7.5 Renal

Proteinuria has been reported to occur in approximately 1% of patients receiving CPT within 3 to 9 months of initiation of therapy [70]. Cases of renal failure, nephritic syndrome, oliguria and polyuria have also been reported [3].

1.5.7.6 Haematological

Although haematological side effects are rare, severe haematological effects such as neutropenia, agranulocytosis, thrombocytopenia, pancytopenia and anemia have been reported [3,47,71-74].

1.5.7.7 Miscellaneous

In rare case, patients have presented with alopecia and impotence [2,3,75]. Angioedema is an uncommon but serious adverse effect of CPT [9,47,76]. Cases of blurred vision, jaundice and pancreatitis have been reported as adverse effects of CPT [3]. Hypersensitivity and anaphylactoid reactions are additional adverse effects associated with CPT use [3].

1.6 CLINICAL PHARMACOKINETICS

1.6.1 Dosage and administration

The usual initial adult dose of CPT is 12.5 mg administered orally 8–12 hourly [2]. Following 7–14 days of therapy, the dose may be increased to 25 mg administered 8–12 hourly if necessary [2]. The prescribing guidelines published in the South African Medicines Formulary advise that the maximum total daily dose of CPT must not exceed 150 mg [2]. When treating hypertension the total daily dose of CPT is divided into two equal doses and is administered 12 hourly, whereas for the treatment of cardiac failure the total daily dose is administered in three equally divided doses [2]. In cases where hypotension is expected as an adverse effect a trial dose of 6.25 mg of CPT is administered prior to the initiation of maintenance therapy [2]. The recommended dose for the management of diabetic nephropathy is 25 mg every 8 hours [3].

The elimination half-life of CPT is increased in patients with impaired renal function and therefore it is appropriate to reduce the dose and frequency of dosing [2]. In cases where the glomerular filtration rate (GFR) of a patient is < 10 mL/min, 50% of the usual dose of CPT must be administered every 24 hours [2]. In cases where the GFR is between 10-50 mL/min 75% of the usual dose must be administered every 12-18 hours [2].

The safety and efficacy profile of CPT in paediatric patients is unknown and therefore CPT is not registered for use in paediatric patients [47]. The recommended dose in paediatric patients is 0.1–1.0 mg/kg/dose administered every 8–12 hours and doses must be individualized and cautiously titrated against the clinical response for each patient [2].

1.6.2 Overdose

Cases of overdose may be managed by haemodialysis to remove excess drug from the circulation and hypotension may be rectified by use of blood volume expanders [53].

1.6.3 Absorption

Subsequent to oral administration of CPT between 60 and75% of the administered dose is rapidly absorbed from the gastro-intestinal tract (GIT) [3,53,77]. The bioavailability of the CPT is reported to be approximately 65% [77]. Peak plasma concentrations of CPT are observed within 45-60 min of oral administration [4,47,77]. The antihypertensive effects are observed 15–60 min following oral administration and may last for up to 6 hours [2]. Pharmacokinetic studies conducted by Endoh *et al.* revealed that the degree of inhibition of ACE is proportional to the plasma concentration of CPT [78]. A decline in bioavailability and peak plasma concentrations are observed when CPT is administered with food, however the clinical effects of the decrease are not significant as the antihypertensive activity of CPT is not affected [4,77,79-81].

1.6.4 Distribution

Approximately 25–30% of CPT circulating in plasma is bound to plasma proteins [52,53]. Data obtained from a pharmacokinetic study conducted by Duchin *et al.* [82] in healthy participants revealed that the volume of distribution (Vd) of CPT at steady-state was 0.7 L/kg. In the same study, the average Vd for CPT in the central compartment was 0.2 L/kg, and that for the elimination phase was 2 L/kg [82]. This suggests that CPT is distributed in deep tissue [82].

1.6.5 Metabolism

CPT is a substrate for human cytochrome P450 enzymes, specifically CYP2D6 [83]. *In vivo* metabolic reactions of CPT are reported to occur at the sulfhydryl functional moiety and yield 35% polar metabolites, 3% captopril-disulphide and trace amounts of S-methyl CPT. The remaining proportion of CPT is excreted unchanged in the urine. The metabolite, captopril-disulphide is a biologically inactive dimer which may be converted back to CPT *in vivo* [52]. Captopril-disulphide from this reaction acts as a reservoir for CPT and provides an explanation for the extended duration of action observed, which is longer than expected when evaluating the pharmacokinetics of the compound [52].

1.6.6 Elimination

In comparison to the other agents in its class, CPT is reported to have a relatively short elimination half-life of between 1.9 and 3 hours in healthy individuals [2]. The elimination half-life of the drug may increase to 32 hours in patients with renal failure [53]. More than 95% of the administered active drug undergoes renal elimination within 24 hours of the administration of an oral dose [2,3]. Between 40-50% of CPT is excreted unchanged in the urine [2,53] and the remaining proportion is excreted as metabolites [53].

1.7 CONCLUSIONS

CPT was the first commercially available ACE inhibitor for clinical use and is still widely used for the treatment of hypertension, cardiac failure and diabetic nephropathy. In comparison to other ACE inhibitors CPT exhibits a relatively short elimination half-life of 1.9 to 3 hours and is normally administered 8–12 hourly. CPT is a BCS Class III drug exhibiting high water solubility of 160 mg/mL and low GIT permeability. CPT contains a sulfhydryl moiety which has been associated with the development of skin rashes and taste disturbances. It exhibits instability in aqueous solution and is most stable at pH < 4. Careful consideration of the stability profile of the drug molecule during formulation development and manufacture is essential in order to ensure that the integrity of CPT is not altered.

With the growing burden of CVD the design and development of formulations which optimise the delivery of existing drugs such as CPT may be an approach to improving the management of patients with CVD. The short half-life of CPT and the need for multiple daily dosing make CPT a potential candidate for delivery using oral controlled release technologies. However the poor stability profile and high water solubility of the molecule present a formulation challenge. The development of a sustained release formulation of CPT may be beneficial in reducing the incidence of drug-related adverse effects, such as the dry hacking cough associated with the molecule, and possibly improve therapeutic outcomes particularly for patients on long-term therapy. Consequently, the objective of this study was to develop, manufacture and assess sustained release tablets of CPT.

CHAPTER 2

DEVELOPMENT OF A CAPILLARY ZONE ELECTROPHORESIS METHOD FOR THE QUANTITATION OF CAPTOPRIL IN PHARMACEUTICALS

2.1. INTRODUCTION

2.1.1. Principles of capillary electrophoresis

Capillary electrophoresis (CE) is a separation technique based on the differential migration of ions through a solution or gel medium under the influence of an applied electric field [84,85]. During a CE separation a narrow zone of a mixture of analytes, typically 1-20 nL, is introduced into the anodic end of a buffer-filled capillary and is swept towards the cathode through a detection system by electroendo-osmotic and electrophoretic movements [86]. The size and the ionic charge carried by each ion determine the migration rate and electrophoretic mobility of each ion. Ions with small radii exhibit high mobility and therefore reach the detector prior to larger ions carrying the same charge [86]. Similarly, highly charged ions will reach the detector before similarly sized ions carrying a lower charge [86]. The charge/mass ratio of an ion therefore governs the electrophoretic mobility of the ion, as shown in Equation 2.1 [86].

$$\mu E = \left(\frac{q}{6\prod}\right)\eta r \qquad \textbf{(Equation 2.1)}$$

Where

μE = Electrophoretic mobility
q = Number of charges
η =Solution viscosity
r = Radius of an ion

Different analytes exhibit different electrophoretic mobility and consequently they migrate at different velocities [87,88]. Migration velocity is proportional to the strength of the electric field and to the electrophoretic mobility as shown in Equation 2.2 [86].

$$v = \mu E\,(E) \qquad \textbf{(Equation 2.2)}$$

Where

v = Velocity of an ion
μE = Electrophoretic mobility
E = Electric field strength

2.1.2. Electro-osmotic flow

Electro-osmosis, a key phenomenon in CE, occurs under the application of an electric field and is used to describe the relative movement of the electrophoretic medium through the interior surface of a capillary [89]. The interior surface of fused silica capillaries is layered with silanol (SiOH) groups which are deprotonated on exposure to buffers of pH > 2 to yield negatively charged SiO^- groups [89]. Any counter-ions (in this case cations) present in the buffer are attracted to the SiO^- groups and the difference in electric potential across the capillary-buffer interface is described by the electric double layer (EDL) model [88]. On application of an electric field across the length of the capillary, the solvated cations present in the diffuse layer of the EDL are hydrated and the bulk buffer solution migrates towards the cathode, thereby generating electro-osmotic flow (EOF) [89]. The mobility of EOF relates to the Zeta potential on the surface of the capillary, dielectric constant and viscosity of the buffer (Equation 2.3) [86].

$$\mu EOF = \left(\frac{\varepsilon\zeta}{\eta}\right) \qquad \textbf{(Equation 2.3)}$$

Where

μEOF = Mobility of EOF
ε = Dielectric constant of buffer
ζ = Zeta potential on capillary surface
η = Viscosity of the buffer

EOF is largely dependent on pH and the sum of EOF and electrophoretic mobility yields apparent mobility that is dependent on the migration time, applied voltage and capillary length (Equation 2.4) [86].

$$\mu A = \mu E + \mu EOF = \frac{lL}{tV} \qquad \textbf{(Equation 2.4)}$$

Where

μA = Apparent mobility
μE = Electrophoretic mobility
μEOF = Mobility of electro-osmotic flow
l = Effective length of the capillary
L = Total capillary length
t = Migration time
V = Voltage

2.1.3. CE instrumentation

The instrumentation required to perform CE is relatively simple and typically consists of a high-voltage power supply delivering between -30 and +30 kV, two buffer reservoirs, a capillary which passes through a detector and a data collection system (Figure 2.1) [86,88]. The basic CE setup may be enhanced by addition of features such as automation, temperature control of the sample and capillary, use of multiple detectors and computer interfacing [87]. A standard CE instrument is not limited to performing one mode of CE but may be used to perform more than one of the six modes of CE [87].

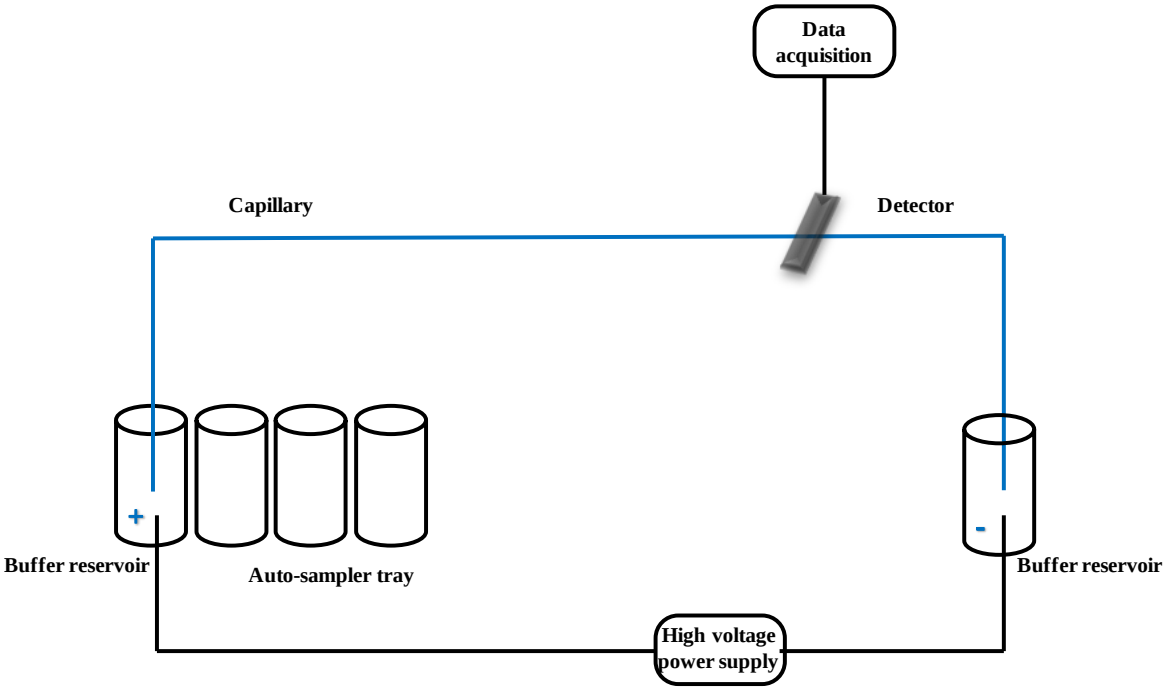

Figure 2.1 Simplified CE instrumentation (Adapted from [86])

2.1.4. Modes of CE

2.1.4.1. Capillary zone electrophoresis (CZE)

CZE, also known as free solution capillary electrophoresis, is the most commonly used mode of CE [86,87]. CZE has been successfully used in different fields for the analysis and separation of various compounds including Active Pharmaceutical Ingredient (API) molecules, peptides, proteins and inorganic molecules [90-93]. CZE has gained popularity due to its versatility and ease of operation [88]. During a CZE separation, a narrow zone of analytes is introduced into a buffer-filled capillary and the application of an electric field results in separation of the sample into spatially discrete zones of the individual analyte [89]. Separation occurs since the analytes exhibit different charge/mass ratios and therefore different apparent mobilities at any specific pH [87]. Simultaneous separation and detection of anions and cations is possible when using CZE due to the presence of EOF [86]. Anions would naturally migrate towards the anode, however EOF sweeps them towards the cathode allowing them to pass through the detector [86]. Given that neutral molecules cannot be separated on the basis of charge, they migrate with EOF and cannot be resolved using CZE [89]. The order in which a theoretical mixture of anions, cations and neutral species would migrate is shown in Figure 2.2.

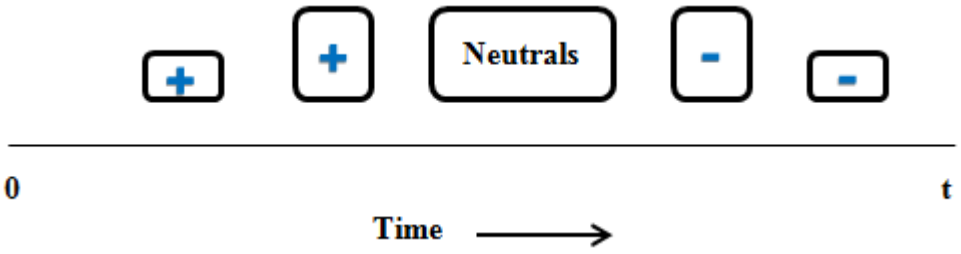

Figure 2.2 Theoretical separation of a mixture of ions (Adapted from [86])

2.1.4.2. Capillary isotachophoresis (CITP)

CITP is a moving boundary technique which is operated using a combination of two buffer systems [88]. The first buffer system is known as the leading buffer and exhibits a higher mobility than that of the analytes and the second buffer [88]. The second buffer is known as the terminating buffer and exhibits the lowest mobility in the system [89]. Various differences between CITP and the other modes of CE such as CZE exist, for example CZE is

performed using a single homogenous buffer whereas CITP is performed using a discontinuous buffer system [87]. Subsequent to a CZE separation the detector signal is recorded as an electropherogram where the peak heights or peak areas may be used for quantitative purposes, whereas following CITP separation an isotachopherogram is generated and consists of a series of steps instead of peaks where each step represents the presence of a specific analyte zone [87,94]. The length of each zone is proportional to the amount of analyte present in the sample of interest. A limitation of CITP is that it may not be used for the simultaneous separation of cations and anions [89].

2.1.4.3. Capillary gel electrophoresis (CGE)

CGE is a separation technique that was adapted from conventional slab or tube gel electrophoresis [88,89]. CGE separations are performed in gel-filled capillaries where the gel acts as a molecular sieve and separates molecules based on their different molecular sizes [88,89]. Large molecules exhibit longer migration times than smaller molecules as they are hindered as they migrate across the polymer network [89]. Linear polymers such as polyethylene glycol or cross-linked polymers such as agarose and polyacrylamides may be used as separation media [88,89]. CGE is mainly used for the separation of biological macromolecules such as nucleic acids and proteins [88,89,95,96].

2.1.4.4. Capillary isoelectric focussing (CIEF)

CIEF is a high-resolution separation technique widely used for the separation of zwitterionic analytes such as amino acids, peptides and proteins [88,97-99]. In contrast to other CE modes, separation using CIEF is based on differences in the iso-electric point as opposed to differences in apparent mobilities of analytes [94]. During a CIEF separation a capillary is filled with the sample of interest and a mixture ampholytes (zwitterions) which is used to create a continuous pH gradient within the capillary [88]. The cathodic end of the capillary is immersed in an alkaline solution such as sodium hydroxide and the anodic end of the capillary is immersed in an acidic solution such as phosphoric acid [88]. The application of an electric field causes the charged ampholytes to migrate towards a region where they will be converted into uncharged species *viz.*, negatively charged ampholytes are attracted towards the anode and *vice versa*, resulting in the generation of a continuous pH gradient inside the capillary [88]. Within this pH gradient analytes are focussed into narrow zones

(volume elements) where they are no longer charged *viz.* where pH is equal to the isoelectric point. At this point a steady state is reached and the analytes stop migrating [88,94,100]. During a CIEF separation, isoelectric focussing is monitored by measuring the current generated and a current reading of zero indicates that analyte migration has ceased and that isoelectric focussing is complete [88]. The application of external pressure or the substitution of one of the buffer reservoirs with a salt solution induces the movement of the analytes towards the detector, thereby allowing the analyte to be detected and electropherograms to be generated [88,94].

2.1.4.5. Capillary electrochromatography (CEC)

CEC is a separation technique based on a combination of the principles of high performance liquid chromatography (HPLC) and CE [101,102]. Silica-packed columns with diameters ranging from 50 to 100 µm are frequently used for CEC separation and these typically consist of both open and packed portions [101,103]. Upon the application of an electric field, analytes and the running buffer are mobilized across the column by EOF rather than by pressure application, as observed when using HPLC [101-103]. Uncharged species are separated as they partition differently between the column (stationary phase) and running buffer (mobile phase) [101]. The mechanism of separation of charged species involves a combination of differential electro-migration and differential interaction with the column [101].

2.1.4.6. Micellar electrokinetic chromatography (MECK)

MECK is commonly used for the separation of small neutral molecules as well as charged species [104,105]. The separation medium used in MECK separations consists of an ionic surfactant solution in which the surfactant concentration is above the critical micellar concentration [104]. MECK separation is based on the differential migration of charged species and differential distribution of the solutes between micelles and the bulk surfactant solution [104]. Either cationic or anionic surfactants may be used for separation and the micelles formed will migrate towards the oppositely charged electrode or with EOF [88]. Anionic surfactants such as sodium dodecyl sulfate are propelled towards the anode, however if the pH of the surfactant solution is basic or neutral EOF will be greater than the

electrophoretic migration of the micelle and will cause the negatively charged micelle to migrate towards the cathode [88].

2.2. METHOD DEVELOPEMENT AND OPTIMISATION

2.2.1. Capillary selection

The dimensions (length and internal diameter) of the capillaries used for CZE separations are essential parameters of CZE systems as they contribute to the total run time, resolution and efficiency of separation [94,106]. Fused silica capillaries are commonly used for CZE separations however, due to the fragility of this material, manufacturers commonly coat the capillaries with a protective polyimide coat [86]. The polyimide layer protects the outer surface of the capillary from abrasion and increases the mechanical strength and flexibility of the capillary [107]. Teflon and borosilicate have been used as alternative materials for manufacturing capillaries, however due to drawbacks experienced when using these materials fused silica continues to be the preferred and most widely used material [86]. The desirable intrinsic properties of fused silica capillaries include chemical inertness, UV transparency, the ability to generate EOF, high thermal conductivity, the ability to withstand high pressure and electrical resistance [94,107]. Limitations associated with the use of fused silica capillaries include an additional capillary preparation step to remove the UV-absorbing polyimide coating from a portion of the capillary in order to create a detection window on the capillary [86]. The uncovered portion of the capillary becomes extremely fragile and must be handled with care when the capillary is installed, removed and stored [107].

Capillaries used for separations have extremely narrow bores, and the most commonly used capillaries have internal diameters ranging between 25 and 100 µm [86]. High separation efficiencies can be achieved using narrow-bore capillaries as they provide an optimum surface area to volume ratio to dissipate heat and minimize the undesirable effects of Joule heating that are observed when capillaries of large diameter are used [104,108]. In addition, the use of narrow-bore capillaries makes it possible to operate at high separation voltages of up to 30 kV, whilst generating relatively low current in the microampere range [88]. Although the use of narrow-bore capillaries presents a number advantages, one major disadvantage is reduced sensitivity due to the extremely short optical path length for UV absorption [109]. The use of rectangular-shaped capillaries, bubble cells and Z-shaped flow

cells are variations that have been investigated in an attempt to enhance the sensitivity of this technique by increasing the optical path length without altering the total capillary volume [109-111].

The total length of a capillary influences the electric field and typically ranges from 10 to 100 cm [94,112]. The effective capillary length is usually 5-10 cm shorter than the total capillary length and is recorded as the distance from the point of injection to the point of detection [94,112]. The effective length affects the mobility, migration time and peak resolution of the technique [86,94].

2.2.2. Methods of detection

On-column detection systems are frequently used in CE analysis and provide a preferable approach as minimal peak broadening is observed [107]. Detection systems that have been used in combination with CE systems include UV, photodiode array, fluorescence, laser-induced fluorescence and mass spectrometric systems [86,107]. The physicochemical properties of an analyte such as the presence of UV-absorbing chromophores and system sensitivity are key factors to consider when selecting a detection system for CE separations [113]. UV detectors are commonly supplied with commercial CE instruments and capillaries can be easily aligned with these detectors [86].

The sensitivity is a function of absorbed light when using UV detection and it is proportional to the concentration of absorbing species, molar absorptivity and the optical path length as described by the Beer-Lambert law [114]. The studies for this project were performed using UV detection at a wavelength of 214 nm.

2.2.3. Running buffer selection

Several factors must be taken into consideration when selecting a running buffer for CE analysis. Such factors include the solubility and stability of solutes in the buffer, the buffer capacity at the desired pH and the UV absorbance at the detection wavelength [86]. Ideally solutes should be soluble in the selected buffer and must not precipitate [86]. In addition the selected buffer should not absorb UV light at the wavelength of detection [86]. During the method development process it is critical to optimise buffer pH and concentration. Changes

in buffer concentration affect EOF whereas changes in buffer pH influence the charge of the analyte, EOF, electrophoretic mobility, characteristics of the inner capillary wall and peak resolution [86,115].

During analysis the concentration of inorganic buffer such as phosphate and borate buffers is generally held between 10 and 50 mM [86]. Higher buffer concentrations may result in an improved peak shape however the challenge of Joule heating may arise and therefore high buffer concentrations are generally avoided [86]. "Good buffers" or biological buffers such as Tris (Tris-[hydroxymethyl]-aminomethane) may be used at high concentrations as they exhibit low conductivity and generate minimal heat, however a major limitation of using these buffers is that they have the ability to strongly absorb UV light [86]. A list of buffers commonly used for CE analysis and their respective pK_a values is shown in Table 2.1.

Table 2.1 A list of commonly used buffers and their respective pK_a values (Adapted from [86, 94])

Buffer	pK_a value(s)
Phosphate	pK_a 1 = 2.12; pK_a 2 = 7.21; pK_a 3 = 12.32
Citrate	pK_a 1 = 3.06; pK_a 2 = 5.40
Acetate	4.75
2-(N-Morpholino)ethanesulfonic [MES]	6.15
Piperazine-1,4-bis(2-ethanesulfonic acid) [PIPES]	6.80
N-(2-acetamido)-2-aminoethanesulfonic acid [ACES]	6.90
3-Morpholino-2-hydroxypropanesulfonic acid MOPSO	6.90
3-(N-Morpholino)propanesulphonic acid [MOPS]	7.20
4-(2-Hydroxyethyl)piperazine-1-ethanesulfonic acid [HEPES]	7.55
Tris-(hydroxymethyl)-aminomethane [Tris]	8.30
Borate	9.24
3-(Cyclohexylamino)ethanesulfonic acid [CHES]	9.50
3-(Cyclohexylamino)propanesulphonic acid [CAPS]	10.40

2.3. RESPONSE SURFACE METHODOLGY (RSM)

2.3.1. Overview

The use of experimental design is a strategic approach for the optimisation of processes, analytical procedures, products and formulations [116]. Compared to conventional experimental approaches of manipulating one variable at a time whilst maintaining constant levels of the other variables, the use of statistical experimental designs offers numerous advantages [116,117]. The Design of Experiments (DOE) approach permits a researcher to study the interactive relationships between input (independent) variables and responses (dependent variables) [116-119]. Through this approach the researcher can quickly identify significant independent variables and use mathematical models to predict respective responses to variations of the independent variables over an entire experimental domain [116]. In addition the total number of experiments that must be performed is reduced, thereby decreasing the overall cost and time spent during the development and optimisation phases of a project [116,117].

RSM is an optimisation technique consisting of a set of statistical and mathematical methods relating independent variables to responses [117,119]. Some of the objectives of RSM include understanding the individual and combined of effects of independent variables using statistical modelling to predict the relationships between independent variables and responses, and determining the values of independent experimental variables that produce an optimal response(s) [116].

Optimisation of the performance of a system, process or product using RSM consists of five main steps. The initial step is a screening process that permits the identification of independent variables that have the most influence on a system [116,119]. At this stage the researcher conducts preliminary experiments with the aim of determining the levels at which the independent variables should be studied [116,119]. Full factorial or fractional factorial screening designs such as D-optimum or Plackett-Burman designs may be used for this purpose [116,117,120].

The second step in RSM involves selecting the most appropriate response surface design, the selection of which depends on the nature of the data set [117]. At this stage it is important to

establish if the responses exhibit linearity or curvature [117,119]. If the data can be precisely described using linear functions then the experimental data can be fitted to Equation 2.5 [117].

$$y = \beta 0 \sum_{i=1}^{k} \beta i x i + \varepsilon \quad \textbf{(Equation 2.5)}$$

Where

y = Experimental response
k = Total number of independent variables
β_0 = A constant term
β_i = Regression coefficient of the linear parameters
x_i = Independent variable
ε = Residual associated with the experiments

The use of second-order models is appropriate when the responses are non-linear and exhibit curvature [117]. First-order effects may be approximated using two-level factorial designs, however in cases where second-order effects are significant, additional terms are added to the polynomial model used to describe the data set [117]. The inclusion of a quadratic term allows for the determination of critical points that are present in the experimental domain such as maximum, minimum or saddle points (Equation 2.6) [117]. Examples of commonly used second-order symmetrical designs include central composite design (CCD), Box-Behnken design and Doehlert designs [117,121]. The main differences between these designs relates to the selection of experimental points, the number of levels at which the variables are investigated, the number of runs and blocks [117].

$$y = \beta 0 + \sum_{i=1}^{k} \beta i x i + \sum_{i=1}^{k} \beta i i x i x^2 + \sum_{1 \le i \le j}^{k} \beta i j x i j + \varepsilon \quad \textbf{(Equation 2.6)}$$

Where

β_{ij} = Regression coefficient of the interaction parameter
β_{ii} = Regression coefficient of the quadratic parameter

The third step of the optimisation process is characterised by mathematical and statistical analysis of experimental data [117]. Once a suitable design has been selected in step two and the appropriate experiments have been conducted the method of least squares analysis is used to define the equation of the model that best describes experimental data [117,119]. The coefficients of the equation are also predicted at this stage [119]. Step four involves

evaluation of the fitted mathematical model using analysis of variance (ANOVA) with the aim of determining whether or not the mathematical model adequately describes the experimental domain under investigation [117]. The fifth and final step involves determining the combination(s) of input variables that generate an optimum response. Numerical predictions or visual inspection of graphical representations of the model equation in the form of three-dimensional response surface plots or two-dimensional contour plots may be used to define the optimum conditions [117,119].

2.3.2. Central composite designs

Following the introduction of CCD by Box and Wilson in 1951 [122] the RSM approach has been successfully applied in the development and optimisation of analytical methods using techniques such as HPLC, gas chromatography (GC) and CE [121,123-126]. CCD consist of three main components, a two-level full or fractional factorial, a central point and additional star points that are positioned at a distance (α) from the centre of the design[121]. Using a CCD approach for optimisation permits the determination of linear and quadratic models [121]. Consider a design consisting of a total of *k* coded independent variables *viz.* x_1, x_2....x_k, a CCD for such factors would be characterised as follows:

i. A factorial or cubic design consisting of n_{fact} points with coordinates $x_i = -1$ or $x_i = +1$, for $i = 1$ up to $i = k$ [121].
ii. The star component of the design would comprise of $n_{ax} = 2k$ points where one coordinate is set at a specified value of α and the remaining coordinates are kept null (0). The value of α would vary depending on the total number of independent variables under investigation [121].
iii. Replicate experiments would be conducted at the central point *viz.* all coded factor levels for these experiments would be set at 0 [121].

The use of RSM with a CCD for the optimisation of a CZE method would be a rapid and effective approach to establishing the interactive effects between the parameters affecting the performance of a separation using CZE [119]. This approach would require relatively few experiments, thereby reducing the overall time and resources required during the method development process [117,119]. A CCD approach would also simplify the process of identifying the optimal conditions required for the determination of CPT in pharmaceutical

products developed in these studies using CZE. A CCD approach was therefore used as an optimisation strategy for the analysis of CPT.

2.4. CAPTOPRIL ANALYSIS

Several methods have been reported for the determination of CPT in pharmaceutical formulations and biological matrices. These include GC [127,128], GC-mass spectroscopy (GC-MS) [129,130] and HPLC using photometric [131-134], fluorimetric [135] and electrochemical detection [136]. CZE is an alternate method for the analysis of CPT due to the short analysis time, high separation efficiency, relatively low cost of operation and tedious derivatization procedures and use of toxic organic modifiers can be avoided [137-140]. A summary of analytical methods that have been used for the determination and quantitation of CPT is given in Table 2.2.

Table 2.2 Analysis of CPT

Matrix analysed	Analytical technique	Experimental conditions	Detection	Total run time (min)	Reference
Blood and urine	GC	Column: coiled glass column (1 m x 2 mm I.D.); carrier gas: helium (30 mL/min); column temperature: 195°C; temperature of injection port and ion source: 270°C; accelerating voltage, ionization voltage and trap current were 3.5 kV, 70 eV and 60 µA respectively	Flame photometric	-	[141]
Human blood	GC-MS	Column: DB-5 fused-silica capillary column (15 m X 0.25 mm I.D., 0.25 µm film thickness); carrier gas: helium. The splitless Grob-injector was kept at 290° C; The capillary column was kept at 180°C for 12 s, and then the temperature was raised to 320° C at 40 °C/min	Mass spectrometer	-	[142]
Human plasma	RP-HPLC	CPT stabilized using p-bromophenacyl bromide; column: Spherisorb C18 and mobile phase: water:acetonitrile:acetic acid mixture (44:55:0.2, v/v/v)	UV (258 nm)	< 5	[143]
Human plasma	HPLC	Column: Inertsil 5 ODS-2 (Chrompack, Varian (150 mm L X 4,6 mm i.d. X 5 µm d.p)); mobile phase: 0.1% aqueous trifluoracetic acid (TFA)/ACN=85/15	Fluorescence	< 13	[135]
Pharmaceuticals	HPLC	Column: Phenomenex® Luna 5 µm (C(18)) column; mobile phase: phosphate buffer (pH 3.0): acetonitrile (70:30 v/v)	ECD	< 8	[136]
Human urine and pharmaceuticals	CZE	Derivatization with 5-IAF; running buffer:20 mM phosphate buffer (pH 12); applied voltage: 10 kV; fused silica capillary, total length-57 cm, i.d.: 75 µm and pressure injection: 5s at 0.5 psi	Laser-induced fluorescence	< 15	[144]
Pharmaceuticals	CZE	Running buffer: CTAB and 100 mM phosphate buffer (pH 5.5); applied voltage: -15 kV; fused silica capillary, total length-60 cm, i.d.: 75 µm and hydrodynamic injection 10cm above buffer vial for l0 s.	UV (214nm)	< 8	[35]
Mixture of 6 ACE inhibitors	MECK	Running buffer: 100 mM SDS in 50 mM borate buffer (pH 8.2); applied voltage: +25 kV; fused silica capillary, total length: 57 cm, i.d.: 75 µm and pressure injection for 5 or l0 s.	UV (200 nm)	< 13	[145]

The objectives of this section of the study were to develop a CZE method for the quantitation of CPT in pharmaceutical dosage forms and optimise the method using an experimental design approach with a CCD. On the basis of a study of the influence of electrolyte and system variables on the electrophoretic procedure, the buffer pH and molarity, applied voltage and capillary length were considered key factors for the optimisation of the method.

2.5. EXPERIMENTAL

2.5.1. Instrumentation

CZE was performed using a PrinCE (4 tray) Electrophoresis System Model 0500-002/CR (Prince Technologies, Emmen, Netherlands). The analyses were undertaken at an ambient temperature of 22°C and detection achieved using a Linear UV/Vis-200 Variable Wavelength Detector, Model 0200-9060 (Linear Instruments Corporation, Reno, Nevada, USA) set at 214 nm. The detector output was interfaced via a SATIN® box to Waters Empower™ 3 chromatography data software (Waters Chromatography Division, Milford, MA, USA) that was used to collect and evaluate all chromatographic data. To avoid siphoning effects a flexible fused silica capillary with a small internal diameter (I.D.) of 75µm and an outer diameter (O.D.) 363µm was used (Polymicro Technologies, Phoenix, AZ, USA). The pH of solutions was measured using a Crison GLP21 pH-meter (Barcelona, Spain).

2.5.2. Chemicals and reagents

All chemicals and reagents were at least of analytical grade and were used without further purification. CPT was donated by Protea Chemicals (Midrand, South Africa). Anhydrous theophylline was used as an internal standard (IS) and was donated by Aspen Pharmacare (Port Elizabeth, South Africa). HPLC grade water used for the preparation of buffer solutions was purified using a Milli-Q® Academic A10 water purification system (Millipore®, Bedford, MA, USA) that consisted of an Ion-X® ion-exchange cartridge and a Quantum® EX-Ultrapore Organex cartridge that was fitted with a 0.22 µm Millipak® 40 sterile filter (Millipore®). All sample solutions were filtered using 0.45 µm hydrophilic PVDF filters membranes purchased from the same source. Sodium hydroxide pellets and 85% v/v o-phosphoric acid were purchased from Merck Laboratories (Merck, Wadeville, South Africa). Zapto®-50 (Aspen Pharmacare), Sandoz Captopril 50 (Sandoz (Pty) Ltd), Adco-Captomax 50

(Adcock Ingram Limited) and Mylan Captopril 50 (Mylan (Pty) Ltd) tablets containing 50 mg of CPT were purchased from a local pharmacy.

2.5.3. Preparation of stock solutions

Standard stock solutions of CPT (100 µg/mL) and IS (100 µg/mL) in buffer solution were prepared on a daily basis. Approximately 10mg of CPT and the IS were accurately weighed and transferred into separate 100 mL A-grade volumetric flasks and made up to volume with buffer solution. To aid dissolution the stock solutions were sonicated for 10 min using a Branson B12 sonicator (Shelton, CN, USA). Serial dilution of the stock solution with buffer yielded CPT solutions of 10, 20, 40, 50 and 70 µg/mL concentration. All samples were protected from light using aluminium foil and were stored at 4°C for a maximum period of 24 hours.

2.5.4. Preparation of running buffer

20 mM phosphate buffer solutions (pH 7.0) were freshly prepared on the day of analysis by pipetting 1.36 mL of 85% v/v ortho-phosphoric acid into a 1L A-grade volumetric flask and making up to volume with HPLC grade water. A 0.1 M NaOH solution was prepared by dissolving 0.4 g sodium hydroxide in 100 mL of HPLC grade water and was used to adjust the pH of the buffer solutions to pH 7.0. The running buffer was filtered through a 0.45 µm Millex HV® Hydrophilic filter membrane prior to transfer into the inlet and outlet vials in the CZE instrument.

2.5.5. Capillary conditioning

Prior to analysis a small portion of the polyimide coating of the capillary used for the separation was removed by exposing it to a low heat flame so as to create a detection window. The charred coating on the capillary was then removed with a soft tissue which had been soaked in ethanol. The clear uncovered portion of the capillary was aligned to the UV source on the detector block. Prior to use each new capillary was conditioned by flushing with 0.1 M NaOH for 30 min, 1 M NaOH for 60 min and HPLC grade water for 15 min. To ensure the presence of an optimal charge density on the capillary wall at the beginning of each day of analysis and between consecutive runs the capillary was conditioned and

regenerated by rinsing with HPLC grade water for 1 min, followed by 0.1 M NaOH for 2 min and with running buffer for 4 min. Capillary conditioning was facilitated by application of a constant external pressure of 300 kPa using nitrogen.

2.5.6. Selection of an internal standard

The volume of sample injected may fluctuate during analysis, resulting in poor precision of an analytical method [86,89]. It is therefore necessary to consider using internal calibration when developing analytical methods for quantitative purposes [86,146]. The addition of an internal standard (IS) to each test and calibration solution is an effective way of reducing error and improving precision [86]. Several factors must be considered when selecting an internal standard. The internal standard should not interfere with or exhibit the same migration time as the analyte of interest [86]. An ideal IS should exhibit a migration similar to that of the analyte and demonstrate good solubility and stability in the solvent used for analysis. The IS must be affordable, readily available, non-toxic and exhibit good UV absorbance at the wavelength of detection. Anhydrous theophylline, cyclizine, hydrochlorothiazide, salicylic acid and imipramine were considered as possible compounds to use as an IS. Anhydrous theophylline was selected as the IS in these studies as it demonstrated the desired characteristics for an IS for this separation

2.5.7. System suitability testing

The parameters investigated in order to establish system suitability include selectivity, precision and separation performance [86,147]. Linearity and the limit of detection may also be assessed, however this approach is less common [86,147].System suitability was established by performing ten replicate injections of a calibration solution containing 50 µg/mL CPT. The % relative standard deviation (% RSD) of the peak resolution and the migration time of CPT were documented. Peak resolution was calculated using Equation 2.7 [148]. Precision < 5% for the migration time and peak height of CPT and resolution of > 2 for all the analytes were considered as acceptable limits for these parameters.

$$R_s = \frac{2(t_2 - t_1)}{(w_{1-w_2})} \quad \textbf{(Equation 2.7)}$$

Where

R_s = Resolution
t_1 and t_2 = Migration times of peak 1 and peak 2
w_1 and w_2 = Peak widths measured at the baseline between tangents drawn to the sides of the peak

2.5.8. Experimental design

A CCD approach was used to optimise the method, and the levels at which the independent variables were studied were based on a preliminary study of the influence of electrolyte and system variables on CZE separation of CPT. The independent variables optimised in the CZE separation were buffer pH (X_1) and molarity (X_2), applied voltage (X_3) and capillary length (X_4). Migration time (Y_1) and peak resolution (Y_2) of CPT were selected as the dependent responses or variables to be monitored. After establishing the range of values of independent variables to be studied the factors were coded to lie at factorial, centre or axial points. A randomized full factorial design was used, in which the four factors were evaluated at five levels ($-\alpha$, $+\alpha$, -1, 0 and +1) with six replicates at the centre point to estimate the experimental error. Design Expert® (Version 7.0.1, Stat-Ease Inc., Minneapolis, MN, USA) statistical software was used to analyse the data generated from thirty experiments. ANOVA was used to analyse the data and calculate the significance and relevance of the critical factors in the model. The upper and lower limits selected for the independent factors are summarized in Table 2.3. Although investigating the use of buffers with pH values ranging from 6-8 compromised the stability of test solutions, the use of low pH values was undesirable and is discussed in Chapter 2, §2.7.4.3. Thirty experiments were performed using the experimental conditions listed in Table 2.4 and these experiments were performed in triplicate and random order to avoid systematic error and the introduction of bias.

Table 2.3 Translation of the coded levels used in CCD

Independent factors	High value (-1)	Centre (0)	Low value (+1)
Buffer pH	6.0	7.0	8.0
Buffer molarity (mM)	20.0	32.5	45.0
Applied voltage (kV)	12.0	18.0	24.0
Capillary length (cm)	60.0	67.5	75.0

Table 2.4 Experimental conditions for CCD

Experiment (Run)	Type	x_1	x_2	x_3	x_4
1	Axial	7	57.5	18	67.5
2	Axial	7	7.5	18	67.5
3	Centre	7	32.5	18	67.5
4	Centre	7	32.5	18	67.5
5	Fact	8	45	24	60
6	Fact	6	20	24	60
7	Fact	8	45	24	75
8	Fact	8	20	12	75
9	Axial	7	32.5	30	67.5
10	Fact	8	20	12	60
11	Centre	7	32.5	18	67.5
12	Axial	9	32.5	18	67.5
13	Fact	6	20	24	75
14	Fact	6	45	12	60
15	Fact	6	45	12	75
16	Fact	6	20	12	60
17	Fact	8	45	12	60
18	Fact	6	20	12	75
19	Centre	7	32.5	18	67.5
20	Fact	6	45	24	75
21	Axial	7	32.5	18	52.5
22	Axial	5	32.5	18	67.5
23	Fact	8	45	12	75
24	Fact	7	45	24	60
25	Fact	7	20	24	60
26	Axial	7	32.5	18	82.5
27	Centre	7	32.5	18	67.5
28	Centre	7	32.5	18	67.5
29	Axial	7	32.5	6	67.5
30	Fact	8	20	24	75

2.6. METHOD VALIDATION

2.6.1. Overview

The validation of an analytical method is necessary to ensure that the method is appropriate and suitable for its intended use [149-151]. Method validation provides information regarding the reliability and quality of the results obtained using the proposed method [149]. Generally, in pharmaceutical analysis method validation is performed for analytical methods intended for assay, identification of compounds and for the determination of impurities [149,150]. During the validation process a series of well documented experiments must be conducted to evaluate the linearity, range, precision, accuracy, detection limit, quantitation limit and specificity of a method [149]. The validation characteristics that are analysed and the total number of determinations that are required for each characteristic vary depending on the purpose of the analytical procedure [149,152]. Although method validation is time consuming and tedious it provides critical information about the consistency and quality of the proposed method and must therefore be regarded as an essential component of pharmaceutical analysis [153].

Several guidelines for the validation process have been published by regulatory bodies such as the Food and Drug Administration (FDA) and by the International Conference of Harmonization (ICH) [150,154]. The guidelines for validation approaches that are used for the validation of conventional HPLC methods have been successfully applied to the validation of CE methods [155,156]. The degree to which general validation guidelines are followed differs depending on the area of application and the extent of the intended use of the proposed method [86,157].

2.6.2. Calibration, linearity and range

The linearity of an analytical method refers to the ability of a method to produce test results that are directly or following mathematical transformation, proportional to the concentration of an analyte within a specified concentration range [149,153,154]. The range is defined as the interval between, and including the upper and lower analyte concentration levels within which the analytical method has shown satisfactory levels of precision, accuracy and linearity [149,153,154].

During the method validation process, visual inspection of a plot of the signal versus analyte concentration gives an indication of whether or not a linear relationship exists between two variables [154]. If a linear relationship does exist the data should undergo further analysis using appropriate statistical tests such as the determination of the regression line using the least squares linear regression method [154]. A summary of the recommended minimum ranges (expressed as percentages of the test concentration) for analytical method validation studies is listed Table 2.5.

Table 2.5 Recommended minimum ranges for determining linearity (Adapted from [149])

Type of analysis	Recommended range (%)
Assay of drug substance or finished product	80-120
Impurity determination	Reporting threshold-120
Content uniformity	70-130
Dissolution testing	± 20% over the set range

Calibration curves of the peak height ratio of CPT to IS versus CPT concentration were constructed from five standards prepared on the day of analysis for the validation process and were used to establish the linearity of the analytical method over the concentration range 10-70 µg/mL CPT. The calibration standards were prepared by appropriate dilution of a stock solution with running buffer and included the addition of IS at a concentration of 1 µg/mL. Least squares linear regression analysis was used to determine the regression equation and correlation coefficient, and test sample concentrations were calculated by interpolation. Correlation coefficients of $\geq$ 0.99 and y-intercepts close to the origin were considered acceptable.

2.6.3. Precision

The precision of an analytical method provides an indication of the degree of scatter between a series of individual measurements and, is obtained through multiple sampling from a homogeneous test sample under specific conditions [149,158,159]. Ideally the precision should be determined using homogenous and authentic samples [149].

The precision of an analytical procedure is generally determined at three different levels *viz.* repeatability, intermediate precision and reproducibility [149,158]. For each level the

precision is normally expressed as either the standard deviation or as the relative standard deviation (RSD) of a set of measurements defined within a set confidence interval [149,154].

2.6.3.1. Repeatability

The repeatability (intra-assay) precision of an analytical procedure provides an indication of the precision of the procedure over a short period of time, provided that the method is operated under the same conditions, *viz.* by the same analyst using the same instrumentation in the same laboratory [149,158]. Repeatability may be investigated by performing at least six quantitative determinations at 100% of the test concentration [154,158]. Alternatively the repeatability may be investigated by performing at least nine quantitative determinations covering a specified concentration range [154,158]. The repeatability of the CZE method was established on one day at three different concentrations levels within the specified range, *viz.* low, intermediate and high levels of the expected concentration. All test solutions were analysed in triplicate (n=3) and the repeatability of the method was assessed using % RSD values with an acceptable limit set at ± 5%.

2.6.3.2. Intermediate precision

Intermediate precision is also termed inter-day precision and may provide an initial indication of the long-term variability of an analytical procedure [149,154,158]. Determination of the intermediate precision provides an indication of the influence of random factors such as use of different analysts, instrumentation and/or different days of analysis on the results when the method is used within the same laboratory [149,153,154]. The intermediate precision of this method was determined on three consecutive days at three concentration levels within the specified range, *viz.* low, intermediate and high. The intermediate precision of the CZE method was assessed using % RSD with an acceptable limit set at ± 5%.

2.6.3.3. Reproducibility

The reproducibility of an analytical method is a measure of the precision of a method when it is used in different laboratories and is essential for collaborative studies and the standardization of analytical methods such as those that appear in official compendia

[149,158]. The proposed CZE method was intended for use by one analyst and in the same laboratory and therefore the reproducibility of the method was not determined.

2.6.4. Accuracy

The accuracy of an analytical method refers to the closeness of agreement between a value obtained experimentally and an accepted conventional true or reference value [149,150,154,158]. Accuracy may be established using several different approaches and is documented as the percent recovery of the amount of analyte that is added to a sample or as the difference between the mean and the true value established using confidence intervals [149]. Accuracy should be determined over a specified concentration range with a minimum of nine analyses, using at least three different concentration levels [154,160].

One approach for establishing the accuracy of a method is to compare the results obtained using the proposed method to those obtained using a well-characterised and independent analytical method [150,154]. Alternatively the accuracy (for an API) can be established by applying the proposed method to the analysis of a reference material of known purity [150,154]. The accuracy (for a product) can be established by calculating the recovery of a known amount of API that is added to drug or placebo product [150,154]. Accuracy may be inferred after the linearity, precision and specificity of a method have been established [150,154]. Accuracy can also be determined by spiking products or API with known quantities of impurities [150,154].

2.6.5. Limits of detection (LOD) and quantitation (LOQ)

The limit of detection (LOD) of an analytical method is defined as the minimum concentration of an analyte in a sample that can be detected, but not necessarily quantitatively determined as a correct value [149]. The LOD is a useful parameter for determining the presence of an analyte at a specified level [149]. The limit of quantitation (LOQ) refers to the minimum concentration of analyte that can be determined with adequate precision and requisite accuracy [149].

Several non-instrumental and instrumental methods have been suggested for determining the value for the LOD and LOQ. The analysis of an appropriate number of samples at the

respective limits is essential in order to verify the proposed limits [149]. The first approach involves visual evaluation and may be used for either non-instrumental or instrumental methods of analysis [149,150,154]. In this case test samples with a known concentration of analyte are analysed and used to determine the lowest concentration at which the analyte can be reliably detected or quantitated using the proposed analytical method [149,150,154]. Another approach is based on the calculation of signal to noise ratios and is only appropriate for analytical methods for which baseline noise is evident [149,150,154]. In this case signal ratios that are two or three times greater than the noise level, *viz.* ratios of 2:1 or 3:1, are considered appropriate for the verification of the LOD [149,150,154]. A higher signal to noise ratio of 10:1 is required for the determination and validation of the LOQ [149,150,154]. A third approach that can be used to determine LOD and LOQ values is based on the calculation performed using the standard deviation of a response and the gradient of the calibration curve (Equations 2.8 and 2.9) [149,150,154].The LOQ of the CZE method was determined by establishing the lowest concentration of CPT that produced a % RSD that was ≤5%, and using conventional practice the LOD was taken as one third of the LOQ [150].

$$\mathrm{LOD} = \frac{[3.3(\mathrm{SD})]}{\mathrm{S}} \qquad \textbf{(Equation 2.8)}$$

$$\mathrm{LOQ} = \frac{[10(\mathrm{SD})]}{\mathrm{S}} \qquad \textbf{(Equation 2.9)}$$

Where

S = Slope of the linear regression line
SD = Standard deviation of the y-intercept of the linear regression equation, standard deviation of the blank samples or the residual standard deviation of a regression line

2.6.6. Stability in running buffer

It is essential to determine the stability of calibration standards in the running buffer before proceeding with method validation studies. Stability studies were undertaken to establish the optimal storage conditions for calibration solutions and whether calibration standards and/or running buffer had to be freshly prepared on each day of analysis. The stability of CPT in the running buffer was established by analyzing a freshly prepared stock solution containing 100 µg/mL of CPT diluted to 50 µg/mL using running buffer. 20 mL portions of the stock solution were stored in A-Grade volumetric flasks under different recorded conditions, *viz.* on

a laboratory bench top (22°C), in a refrigerator (4°C), unprotected from light and protected from light using aluminium foil.

CPT exhibits poor stability in solution and maximum stability is generally observed in solutions of pH < 4 [5]. CZE analyses were performed using a phosphate buffer (pH >4) and the influence of the addition of an anti-oxidant, *viz.* sodium metabisulphite (SMBS) on the stability of sample solutions was also studied. Following storage for 3, 6, 9, 12 and 24 hours, the solutions were diluted with IS solution and made up to volume with running buffer to produce a solution of 50 µg/mL CPT. The IS concentration was 1 µg/mL and was added to all test solutions prior to analysis The solutions were analysed and the results generated were compared to those obtained following analysis of freshly prepared samples. All refrigerated solutions were allowed to equilibrate to ambient temperature prior to dilution and analysis. Six replicate injections of each test solution were analysed and the CPT solutions were considered 'fresh' if the difference between the assay results of the fresh and stored samples was < 5%.

2.6.7. Specificity

The specificity of an analytical method is defined as the ability of a method to determine the analyte of interest distinctively and accurately in the presence of other components that may be expected to be present in a typical test sample [149,150,154]. Examples of such components include degradation products, impurities and formulation excipients. The specificity of the CZE method was determined by comparing electropherograms obtained following the analysis of pure CPT in buffer solution with those generated from analysis of commercially available dosage forms dissolved in buffer.

2.6.8. Assay

Four commercially available CPT products were purchased from a local pharmacy and were used to determine the applicability of the method for the quantitation of CPT in pharmaceutical formulations. The products included Zapto®-50, Sandoz Captopril 50, Adco-Captomax 50 and Mylan Captopril 50. For each of the four products the label claim stated that each tablet contained 50 mg CPT. To assay the products, twenty tablets were weighed and pulverized to a fine powder using a mortar and pestle. An amount of powder equivalent

to the weight of one tablet was quantitatively transferred into a 100 mL A-Grade volumetric flask and made up to volume with running buffer. To ensure complete extraction and dissolution of CPT the mixture was sonicated for 15 min prior to filtration using a 0.45 µm hydrophilic PVDF filter membrane. The solution was diluted with running buffer to achieve a final concentration of 50 µg/mL CPT. The IS concentration was 1 µg/mL and was added to all filtered test solutions prior to analysis.

2.7. RESULTS AND DISCUSSION

2.7.1. System suitability testing

The % RSD for the migration time and the peak area of CPT was < 5%, and the resolution was > 2 for all adjacent peaks. The CZE system was therefore deemed suitable for undertaking method validation studies.

2.7.2. Verification and evaluation of the model for the migration time of CPT

The key responses monitored were peak resolution and CPT migration time, of which the latter was considered to be the most important factor as it has an impact on the total experimental run time. The mean of least squares linear regression method was used to establish the mathematical model that was most suitable to describe the data generated from thirty experiments. The quality of the mathematical model, significance and relevance of independent input factors on responses was determined by ANOVA using Design Expert® software (Version 7.0.1, Stat-Ease Inc., Minneapolis, MN, USA).

The null hypothesis was that no factor effects exist and the alternative hypothesis was that a factor effect existed. A value for Prob> F is the probability of obtaining the observed F value if the null hypothesis is true. Conversely if the probability value is small the null hypothesis is rejected. If the two variances are similar then their ratio will be close to one and it is less likely that the independent variables have an effect on the responses.

The Fisher F-ratio was used to determine whether or not the model was significant and was set at p=0.05. The F-value calculated was 10.44, suggesting that the model was significant (Table 2.6). It is unlikely that a Model F-Value this large can be a consequence of noise, as

the probability due to noise was only 0.01%. Values of Prob>F that are < 0.05 indicate that the model terms are significant. The Prob>F for the entire model was < 0.0001, therefore the null hypothesis can be rejected, indicating that the quadratic model was significant and that there is a factor effect with an overall contribution of terms in the model that have a significant impact on the migration time of CPT. A p-value > 0.05 suggested that buffer pH and molarity had no significant effect on the migration time of CPT, whereas the applied voltage and length of the capillary length had a significant effect on the migration time of CPT in the ranges under investigation.

Table 2.6 ANOVA for Response Surface Quadratic Model for migration time

Source	Sum of Squares	df	Mean Square	F-value	p-Value Prob>F
Model	**613.50**	**14**	**43.83**	**10.44**	**<0.0001**
A-pH	12.60	1	12.60	3.00	0.1051
B-Molarity	15.66	1	15.666	3.73	0.0738
C-Voltage	**346.05**	**1**	**346.05**	**82.47**	**<0.0001**
D-Capillary length	**139.69**	**1**	**139.69**	**33.29**	**<0.0001**
AB	4.96	1	4.96	1.18	0.2955
AC	0.98	1	0.98	0.23	0.6359
AD	0.39	1	0.39	0.093	0.7649
BC	13.25	1	13.25	3.16	0.0973
BD	11.34	1	11.34	2.70	0.1225
CD	10.85	1	10.85	2.59	0.1302
A^2	17.55	1	17.55	4.18	0.0601
B^2	1.35	1	1.35	0.32	0.5796
C^2	10.90	1	10.90	2.60	0.1294
D^2	5.50	1	5.50	1.31	0.2716
Residual	58.75	144.20			
Lack of fit	58.66	9	6.52	404.61	<0.0001
Pure error	0.081	5	0.016		
Cor total	672.32	28			

The lack of fit for the quadratic model for migration time of CPT was significant, and this is undesirable as it is ideal for the data to fit the model. Therefore to improve the model it was necessary to consider model reduction, response transformation and outliers. Model transformation was selected in an attempt to improve the model. The ANOVA data for the quadratic model transformed to an inverse square-root model are summarized in Table 2.7. Following model transformation, capillary length and applied voltage were factors that had

statistically significant effects on the migration time of CPT ($p < 0.0001$), and are highlighted in Table 2.7.

Table 2.7 Migration time analysis following data transformation

Source	Sum of Squares	df	Mean Square	F-value	p-Value Prob>F
Model	**0.066**	**4**	**0.017**	**57.15**	**<0.0001**
A-pH	*1.354E-003*	1	1.354E-0003	4.66	0.0411
B-Molarity	*8.509E-004*	1	*8.509E-004*	2.93	0.0998
C-Voltage	**0.049**	**1**	**0.049**	**168.91**	**<0.0001**
D-Capillary length	**0.015**	**1**	**0.015**	**52.11**	**<0.0001**

The R^2 value was 0.9050, and the predicted R^2 value of 0.8487 is in good agreement with the adjusted R^2 value of 0.8892. The value of Adeq Precision was used to measure the signal to noise ratio, and in order to navigate the design space the signal to noise ratio should be > 4. A ratio of 26.521 was observed, indicating that an adequate signal had been produced, thereby suggesting that the model may be used to predict the migration time of CPT within the ranges studied.

The experimental data were fitted to a second-order model relating migration time of CPT to other factors. The final quadratic equation for migration time (Y_1) in terms of coded factors is shown in Equation 2.10. Negative coefficients adjacent to the linear or quadratic contributions are indicative of antagonism, whereas positive coefficients indicate synergism between input factors.

$$Y_1 = 11.76 - 0.72X_1 + 0.81X_2 - 4.49X_3 + 2.41\ X_4 - 0.56\ X_1\ X_2 - 0.25\ X_1\ X_3 + 0.16X_1\ X_4 - 0.91X_2X_3 + 0.84\ X_2\ X_4 - 0.82X_3X_4 + 0.81X_1^{\ 2} - 0.22X_2^{\ 2} + 0.83\ X_3^{\ 2} + 0.45\ X_4^{\ 2} \quad \textbf{(Equation 2.10)}$$

2.7.3. Diagnostic plots

Model adequacy checking was performed using a normal probability plot of residuals, a plot of studentized residuals versus predicted values and a Box-Cox plot for power transformation. The analysis of residuals was used to determine the validity and accuracy of the model used. The normal probability plot of residuals is shown in Figure 2.3. The pattern

of the residuals is a slight S-shaped curve, and consequently the normality assumption is loosely satisfied in this case.

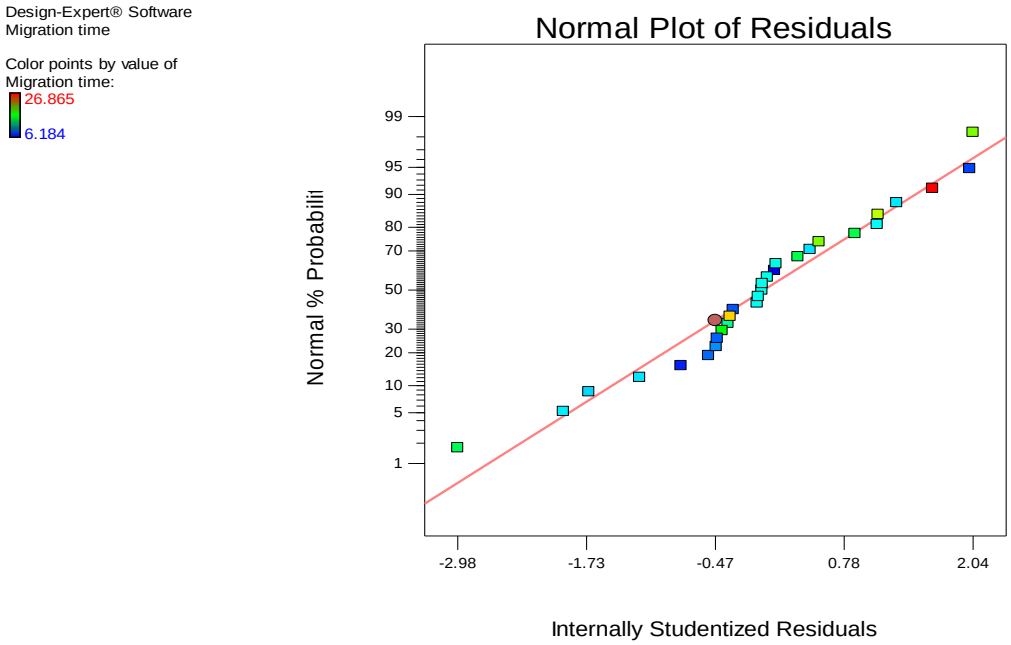

Figure 2.3 Normal plot of residuals for migration time

The plot of the residuals versus the predicted response for the migration time of CPT (Figure 2.4) indicates that no clear scatter pattern is observed and that the residuals are almost uniformly scattered above and below the *y*-axis, further suggesting that the model is adequate. As such, violation of an independence or constant variance assumption was not suspected. Outlier points were verified by identifying any data that were scattered beyond the red limit lines, indicating that the data fit the model well.

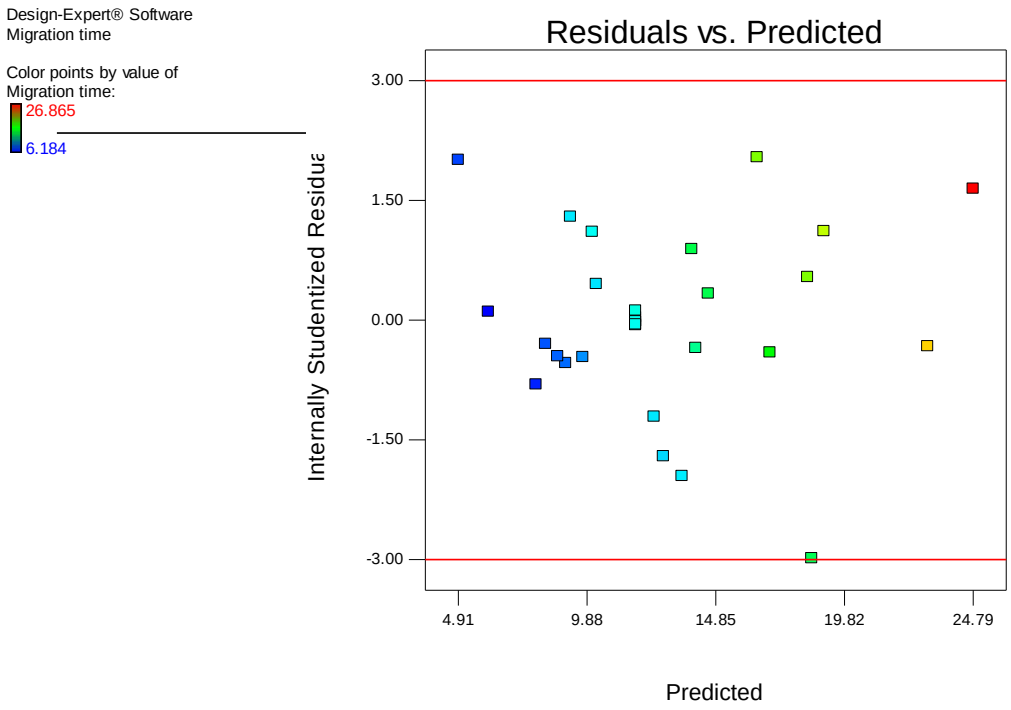

Figure 2.4 Plot of residuals versus predicted for migration time

The Box-Cox plot (Figure 2.5) was used to select the most appropriate power law transformation and the lowest point of the plot (lambda) signifying the power applied to the response values [161]. The green line represents the best lambda value, which is -0.58. The blue line represents the current transformation, and in this case points to a value of lambda = -0.5. The red lines represent the 95% confidence interval surrounding the best lambda value. It is clear that a power transformation was required for the analysis of migration time. The recommended power transformation model is the inverse square of the response values, and these must be satisfied before method development can be completed.

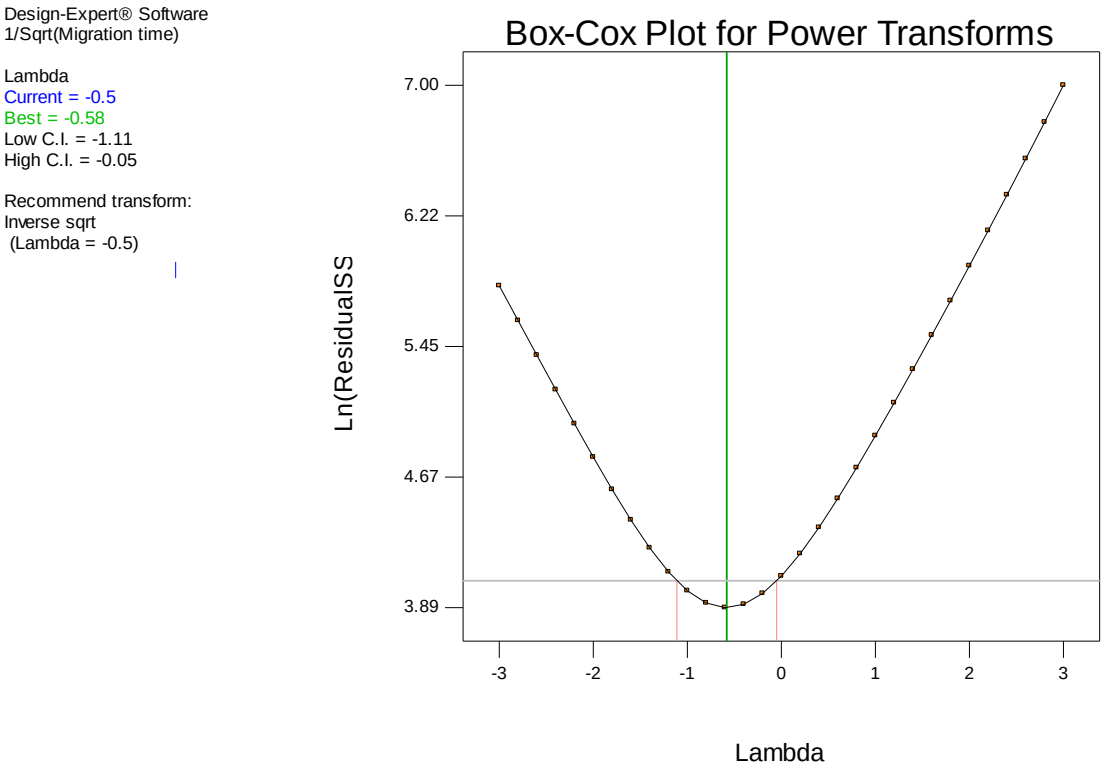

Figure 2.5 Box-Cox plot for power transformation

2.7.4. Visual presentation of the model equation

Two-dimensional contour and three-dimensional plots were used to study the interactive effects of input factors on the responses. These are shown in Figures 2.6 to 2.10.

2.7.4.1. Voltage

$$V_{eo} = \mu E\,(E) \qquad \textbf{(Equation 2.11)}$$

$$E = \frac{\text{Voltage}}{\text{Capillary Length}} \qquad \textbf{(Equation 2.12)}$$

Where

V_{eo} = Velocity of the EOF
μE = Electrophoretic mobility
E = Applied electric field strength

The velocity of the EOF is directly proportional to electrophoretic mobility and the applied electric field strength, as shown in Equation 2.11. Increasing the applied voltage and

therefore the electric field strength results in an increase in EOF, with a consequent decrease in the migration time of CPT that was observed with an increase in the applied voltage when the length of capillary length, buffer molarity and pH were held constant (Figures 2.6). The use of extremely high voltages during analysis is undesirable as Joule heating occurs, and the generation of a high current negatively impacts peak resolution as a result of band broadening [89,162]. It is therefore necessary to select an applied voltage sufficiently high to produce a rapid separation but that does not result in Joule heating. An applied voltage of 23.9 kV generated a sufficiently low current and was therefore selected as the optimum voltage for this separation.

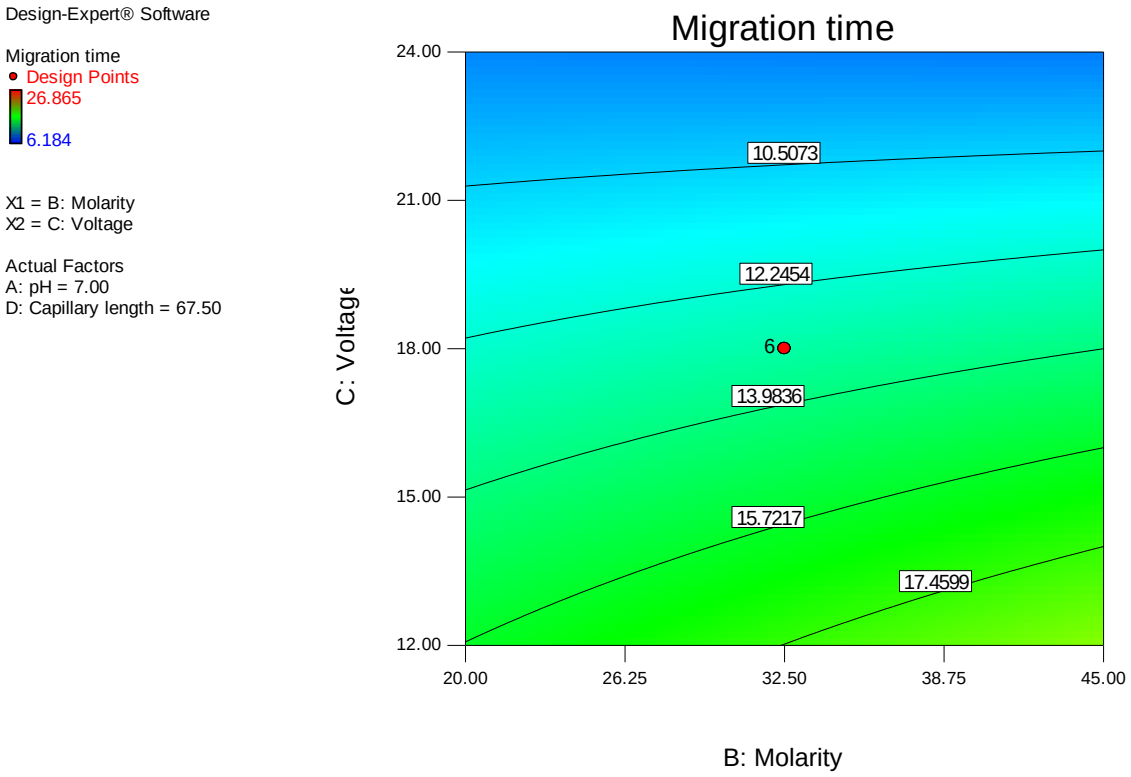

Figure 2.6 Contour plot for migration time as a function of buffer molarity and voltage

2.7.4.2. Buffer molarity

The use of buffers of molarity in the range 20 to 45 mM was investigated. High buffer concentrations were avoided as they tend to induce Joule heating and generate high background current [163]. An increase in buffer molarity with constant buffer pH, applied voltage and capillary length resulted in an increase in the migration time of CPT (Figure 2.7). This is probably due to a decrease in electro-osmosis that occurs as a consequence of the collapse of the electric double layer (EDL) when buffer concentrations are increased [89].

Analyte adsorption onto the capillary wall may occur when low buffer concentrations are used [163], and it was necessary to select a buffer concentration that did not compromise the quality of the separation by causing adsorption or Joule heating.

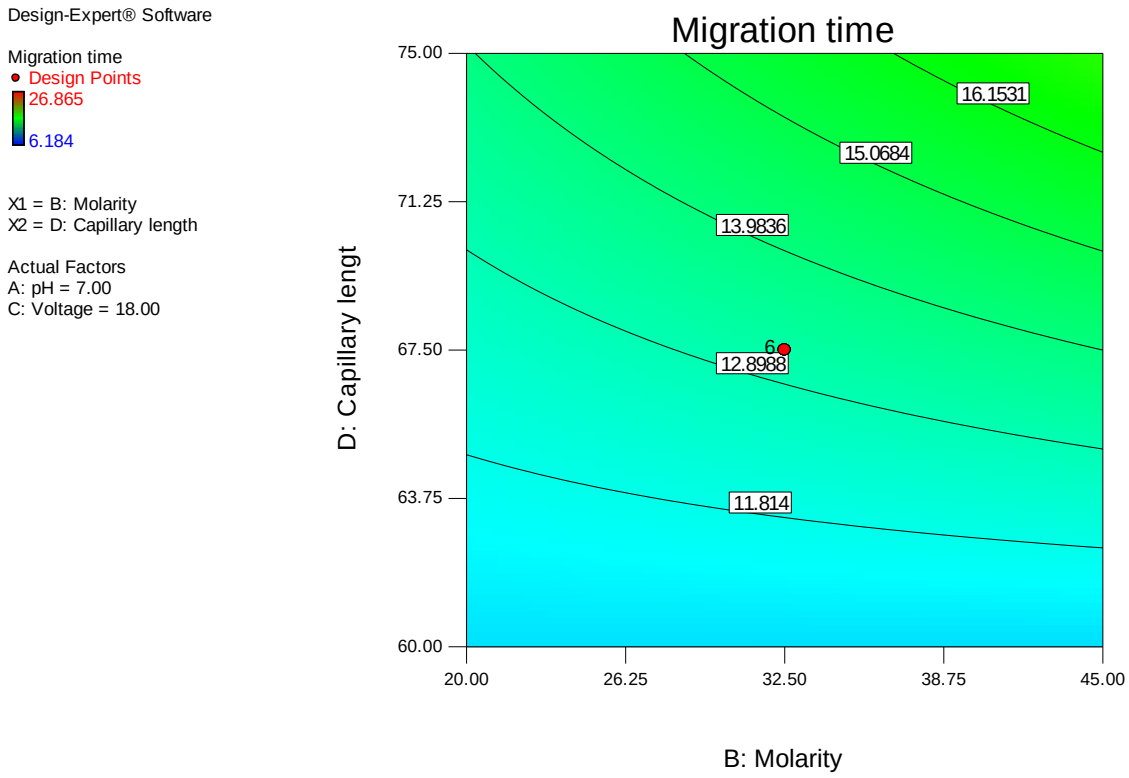

Figure 2.7 Contour plot for migration time as a function of buffer molarity and capillary length

2.7.4.3. Buffer pH

CPT is amphoteric, with an isoelectric point of approximately 6.8. At pH values < 6.8 CPT is positively charged and therefore will migrate towards the cathode, and at pH > 6.8 it is negatively charged. However CPT will still migrate towards the cathode since the EOF is greater than electrophoretic mobility. At a pH of 6.8 CPT possesses no net charge and therefore exhibits no electrophoretic mobility, however the presence of EOF results in CPT migration towards the cathode.

The pH of the surrounding solution also affects the nature of the charge on the walls of the capillary. At low pH values electro-osmosis is reduced as a result of the protonation of SiO^- to form SiOH, which results in a decrease in the Zeta potential at the capillary-buffer interface. The Zeta potential is directly proportional to the electrophoretic mobility (Equation

2.3, § 2.1.2) [89] and therefore the use of buffers of low pH values is undesirable despite the stability of CPT, as this would result in long migration times. Consequently the anti-oxidant SMBS was included in sample solutions to ensure the stability of CPT without compromising migration time. The optimum pH for analysis was in the range pH 6 to 8, and increasing the buffer pH (Figure 2.8) with low molarity resulted in short migration times with the optimum pH for the separation established as pH 7.0. At this pH good peak shape and acceptable resolution were observed, and the migration time for CPT was < 6 min.

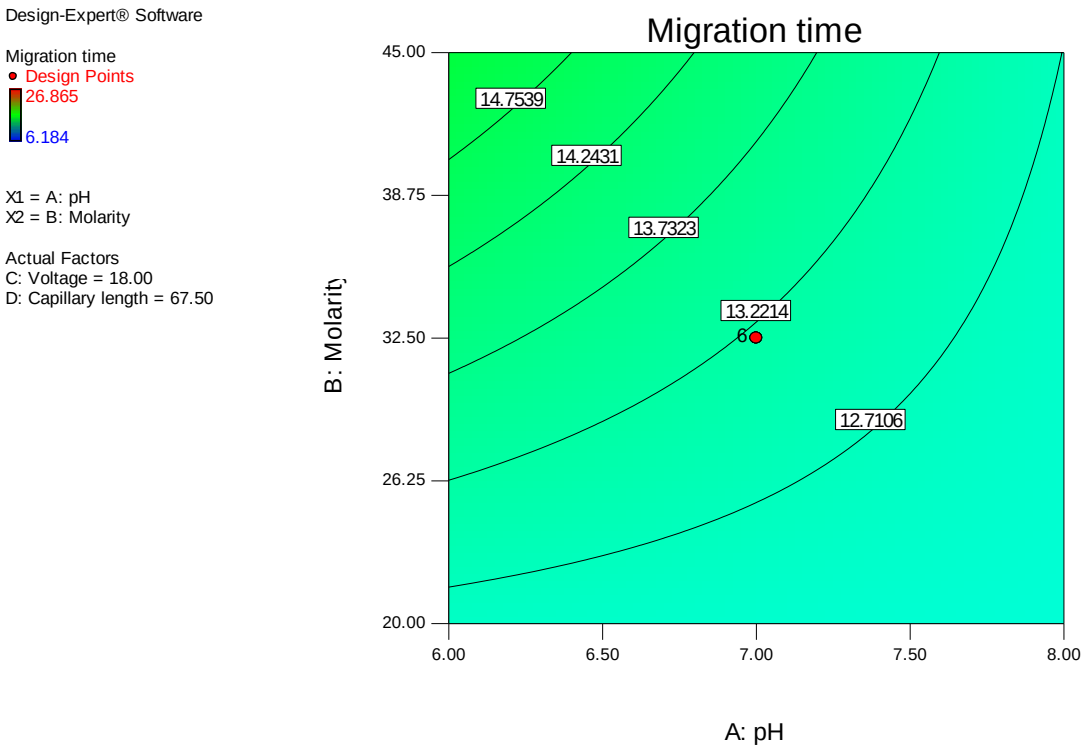

Figure 2.8 Contour plot for migration time as a function of buffer pH and buffer molarity

2.7.4.4. Capillary length

The effect of capillary length on migration time of CPT and peak resolution was evaluated. It was established that increasing the capillary length whilst maintaining constant voltage, buffer pH and buffer molarity resulted in an increase in the migration time of CPT (Figure 2.9), which is a direct result of an increase in the length of the migration path.

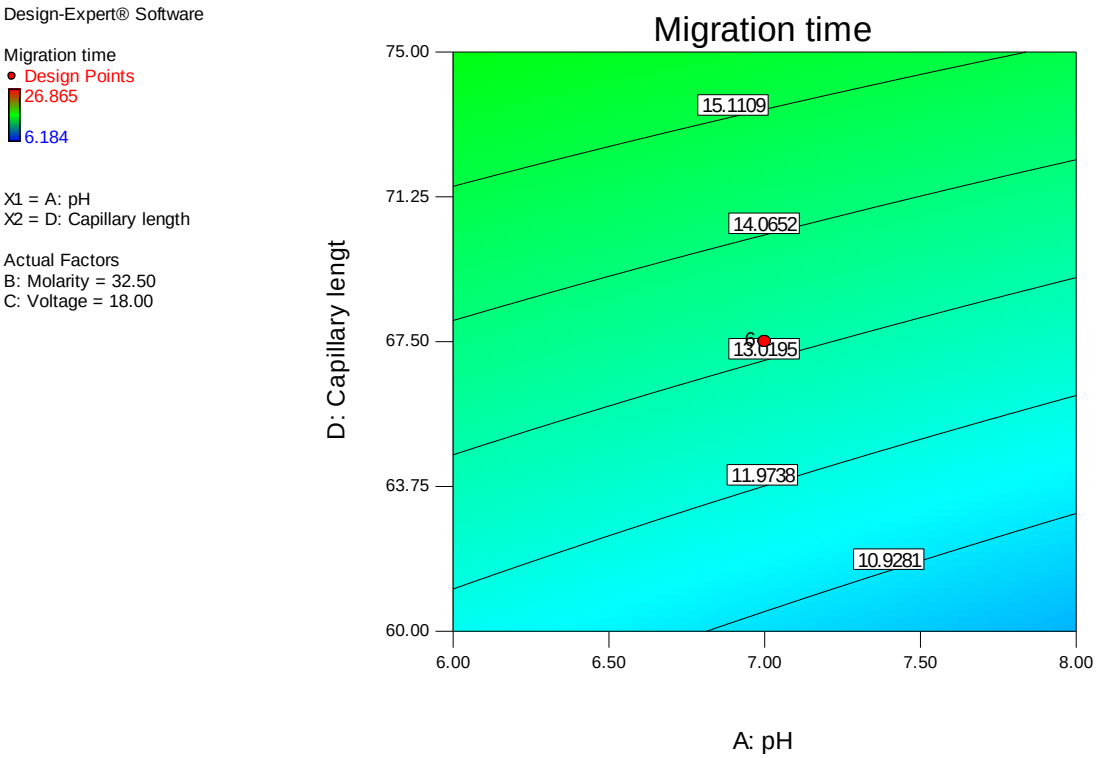

Figure 2.9 Contour plot for migration time as a function of buffer pH and capillary length

2.7.5. Establishment of optimal conditions

The optimum experimental conditions identified for CZE analysis of CPT are summarized in Table 2.8, and were used for all future analyses. This combination of factors produced good separation of CPT, the internal standard and the anti-oxidant (Figure 2.10), and the peak resolution was suitable for the quantitative analysis of CPT.

Table 2.8 Optimum electrophoretic conditions

Factor	Optimum conditions
X_1	pH 7.0
X_2	20 mM freshly prepared phosphate buffer
X_3	23.90 kV (Ramp 6 kV/sec)
X_4	Total length: 67.5 cm and effective length: 57.5 cm

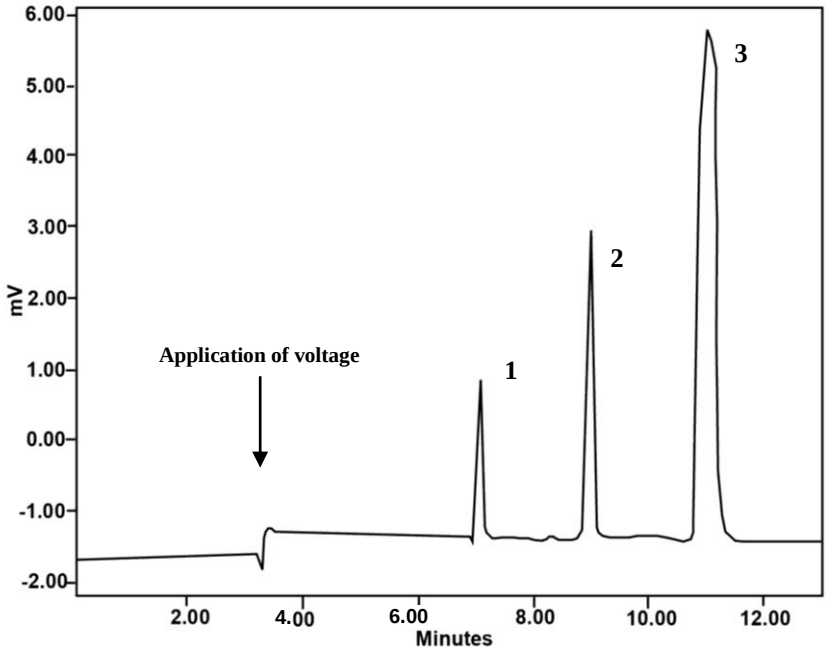

Figure 2.10 Typical electropherogram of a standard solution of IS (1), CPT (2) and sodium metabisulphite (3). CZE conditions: 20 mM phosphate buffer, pH 7.0; applied voltage 23.9 kV; capillary length 67.5 cm (57.5 cm effective length) x 75 µm I.D; detection wavelength 214 nm

2.7.6. VALIDATION OF THE CZE METHOD

2.7.6.1. Calibration, linearity and range

Calibration curves constructed on each day of validation were found to be linear over the range 10-70 µg/mL CPT, with correlation coefficients > 0.99 observed on all three days of validation (Table 2.9).

Table 2.9 Linearity of CPT analysis

Day of analysis	Slope	*y* - intercept	Correlation coefficient (R^2)
Day 1	0.0267	- 0.0345	0.9969
Day 2	0.0292	- 0.0346	0.9972
Day 3	0.0268	- 0.0221	0.9973

2.7.6.2. Precision

The method was validated with respect to repeatability and inter-day precision. Nine replicate samples of concentration 15.50 µg/mL, 45.50 µg/mL and 65.50 µg/mL were prepared and analysed on the same day (intra-day precision). The same three sample concentrations were also analysed on three consecutive days, and the data obtained were used to establish the inter-day precision of the method. The experimental results were expressed as % RSD of the peak height ratios, which were < 5% for all determinations (Table 2.10), clearly indicating that the method is precise.

Table 2.10 Precision of CPT analysis

	Day 1 (n=3)			Day 2 (n=3)			Day 3 (n=3)		
Theoretical concentration (µg/mL)	15.53	45.59	65.63	15.50	45.50	65.50	15.51	45.54	65.56
Concentration obtained (µg/mL)	15.23	46.19	63.05	14.76	43.16	65.09	15.99	44.66	67.08
% RSD	2.61	3.49	0.75	0.98	0.65	2.05	1.08	2.12	4.04
% RE	+1.93	-1.31	+3.93	+4.77	+5.14	+0.62	- 3.06	+1.93	- 2.31

2.7.6.3. Accuracy

Interpolation of peak height ratios generated from accuracy samples using the relevant calibration curve was undertaken to establish the accuracy of the method. The results summarized in Table 2.11 demonstrate the accuracy of the method, as all data are within the limits specified of < 5% Relative error (RE).

Table 2.11 Accuracy of CPT analysis

Theoretical CPT Concentration (µg/mL)	Actual CPT concentration (µg/mL) (n=3)	Accuracy ±SD	% RE
15.50	15.46	99.74 ±1.30	+0.26
45.50	44.67	98.18±1.51	+1.81
65.50	67.09	102.43±2.00	-2.42

2.7.6.4. LOD and LOQ

The LOQ was determined by establishing the lowest concentration of CPT that produced a value of % RSD ≤5%. The LOQ was found to be 10µg/mL, and using conventional practice [160] the LOD was taken as one third of the LOQ and was set at 3.0 µg/mL.

2.7.6.5. Solution stability

A decrease in peak height ratio of CPT/IS was observed for the test samples stored without SMBS, irrespective of whether the solutions were protected from light, stored on a laboratory bench top or in a refrigerator. The presence of 0.2% w/v sodium metabisulphite in sample solutions was found to be sufficient to delay oxidative degradation over 24 hours. Acceptable solution stability was indicated by the absence of unknown peaks and adequate precision as indicated by the peak height ratios and % RSD values presented in Table 2.12. For that reason calibration solutions were freshly prepared on each day of analysis and SMBS was added to each solution during these studies.

Table 2.12 CPT stability

	Time (hours)				
Storage	**0**	**3**	**6**	**12**	**24**
	Peak height ratio (% RSD)				
Bench top	2.53 (0.93%)	2.43 (1.06%)	2.05 (0.67%)	1.62 (0.91%)	0.83 (1.25%)
0.2 %w/v SMBS	2.53 (0.93%)	2.54 (0.97%)	2.55 (1.17%)	2.54 (0.72%)	2.53 (0.85%)

2.7.6.6. Specificity

Comparison of the electropherograms generated from the analysis of pure CPT in buffer solutions, and those generated following the analysis of commercially available formulations (Figure 2.11) revealed no interference with the CPT peak. The CZE method was therefore deemed specific.

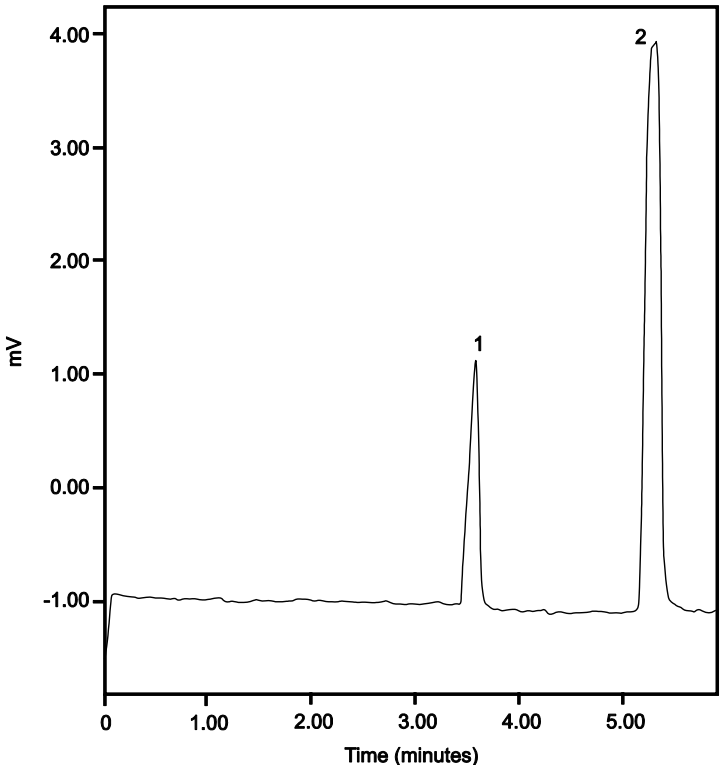

Figure 2.11 Typical electropherogram obtained from the analysis of Mylan Captopril 50. IS (1) and CPT (2). CZE conditions: 20 mM phosphate buffer, pH 7.0; applied voltage 23.9 kV; capillary length 67.5 cm (57.5 cm effective length) x 75 µm I.D; detection wavelength 214 nm.

2.7.6.7. Assay

The analytical method was applied to the analysis of commercial products containing CPT. The data collected and summarized in Table 2.13 reveal that the average CPT content for all

products was between 96.19 and 101.77% of label claim declared by the pharmaceutical companies. There was no interference from tablet excipients, running buffer or impurities as, no interfering peaks were observed on the electropherograms when monitored at 214 nm.

Table 2.13 Assay results for commercially available products containing CPT

Product	CPT found (mg)	% Recovery	% RSD
Zapto® - 50	48.10	96.19	2.46
Sandoz Captopril 50	50.89	101.77	0.75
Adco-Captomax 50	49.65	99.29	2.58
Mylan Captopril 50	49.61	99.23	2.19

2.8. CONCLUSIONS

The CZE method developed, validated and reported in this Chapter has the necessary linearity, accuracy, precision, and sensitivity for the analysis of CPT in pharmaceutical formulations. The LOQ and LOD were in the µg/mL range. Through the use of CCD and RSM the time required to develop the analytical method was reduced. CCD and RSM have been successfully applied to the experimental data and optimisation of the method. The influence of buffer pH and molarity, applied voltage and capillary length on peak resolution, and the migration time of CPT were evaluated. CZE offers several advantages over conventional HPLC methods, including, a short analysis time and low cost of operation, as the capillaries used for CZE are significantly cheaper than HPLC columns. In addition the proposed method avoids the inclusion of tedious and lengthy derivatization procedures and the use of relatively toxic and expensive organic solvents. The method developed is rapid and has been successfully used to analyse CPT in dosage forms, and may be suitable for routine analysis of CPT in dosage forms for quality control purposes.

CHAPTER 3

PREFORMULATION CONSIDERATIONS FOR MANUFACTURING CAPTOPRIL SUSTAINED RELEASE TABLETS

3.1 INTRODUCTION

Preformulation testing is an essential step in the development of pharmaceutical dosage forms [164]. It refers to the process of conducting experiments to establish the physicochemical and biopharmaceutical properties of an API, alone or in combination with pharmaceutical excipients [164,165]. In order to make rational decisions during product development it is essential for a formulation scientist to have sufficient and relevant preformulation data [164]. The nature of the data collected during preformulation studies depends on the type of dosage form to be developed [164]. Thorough preformulation studies are key for the design, development and manufacture of a stable and robust formulation [164,165]. The available pharmacological, physicochemical and biopharmaceutical properties of CPT have been reported (§ Chapter 1) and in this chapter preformulation data required for the development and manufacture of CPT sustained release tablets will be discussed.

3.2 SELECTION OF PHARMACEUTICAL EXCIPIENTS

3.2.1 Overview

APIs are commonly combined with excipients in order to aid the manufacturing process, facilitate delivery to the systemic circulation and improve the ease of administration [166]. Solid oral dosage forms such as tablets include excipients that may constitute the bulk of a formulation. Careful selection of excipients is therefore an integral part of the preformulation process [167]. The selection of an excipient is based on a number of factors including physical and chemical compatibility, which is particularly important for compressed solids where there is a potential for interfacial interactions due to intimate contact between the API and excipients [164].

Furthermore, the choice of an excipient is based on safety, thus the FDA recommends the use of excipients that are generally regarded as safe (GRAS) [168,169]. The supplier of

excipients also influences the selection process and the formulator must therefore consider whether the material from a proposed supplier complies with current Good Manufacturing Practices (cGMP) [167]. The formulator must also consider whether a supplier can reliably supply the required quantity of excipients, as changes in source may influence the quality, performance and regulatory status of a formulation [170]. The type and quantities of excipients used must also be considered in the selection process, and the choice is largely dependent on the design and desired release profile of the proposed formulation [164].

3.2.2 Materials

All the excipients used in this study are listed in Table 3.1, and appear on the GRAS list and/or are included in the FDA inactive ingredients database and/or are accepted for use as food additives in Europe.

Table 3.1 Excipients used to manufacture sustained release CPT tablets

Excipient	Trade name	Supplier/Donor
Captopril	Captopril	Protea Chemicals, RSA
Hydroxypropyl methylcellulose	Methocel® (K100M, K15M, K100LV Premium)	Dow Chemical Company, USA
Microcrystalline cellulose	Avicel® PH-102	Aspen Pharmacare, RSA
Ethylcellulose NF	Ethocel® 90M	Dow Chemical Company, USA
Carbomer	Carbopol® 974P NF	Noveon, Inc., UK
Sodium bicarbonate	Sodium bicarbonate	Aspen Pharmacare, RSA
Magnesium stearate	Magnesium stearate	Aspen Pharmacare, RSA
Talc	Talc	Aspen Pharmacare, RSA
Colloidal silicon dioxide	Cab-O-Sil® TS610	Cabot Corporation, USA

3.2.2.1 Hydroxypropyl methylcellulose (HPMC)

Hydroxypropyl methylcellulose (HPMC), or hypromellose, is partly *O*-methylated and *O*-(2-hydroxypropylated) cellulose [171]. It occurs as a white or creamy-white fibrous or granular powder [171]. HPMC is a tasteless, odourless, non-ionic, water-soluble and swellable polymer commercially available in several grades [164,171,172]. The different grades of HPMC vary in respect of viscosity and the degree of substitution [171].

HPMC has a wide range of application in the pharmaceutical, cosmetic and food industries [171]. It has been successfully used for the manufacture of various pharmaceutical formulations including oral, topical, nasal and ophthalmic delivery systems [171]. The primary and secondary role of HPMC in these formulations depends on the concentration of polymer used in the formulation. HPMC may be used as an emulsifier, suspending or thickening agent in semi-solid dosage forms [171]. In solid oral dosage forms HPMC may be used as a coating agent, binder, granulating aid or modulator of API release [164,171]. High viscosity grades of HPMC may be used to form hydrophilic matrices in capsules and tablets. The concentration levels at which it is used in this role typically range from 10 to 80% [171].

HPMC forms a gel layer when in contact with aqueous fluids and the thickness, strength and speed at which this layer forms is dependent on the polymer concentration used [172]. The release of water-soluble API such as CPT from hydrophilic matrices is controlled by diffusion of the molecule through the gel layer [172].

HPMC is extensively used as a hydrophilic matrix former and offers numerous advantages over other water-soluble and water-swellable polymers, including an excellent stability profile, compatibility and synergism with release-retarding excipients [173]. HPMC is suitable for manufacturing tablets using either wet granulation or direct compression processes [173].

3.2.2.2 Microcrystalline cellulose (MCC)

Microcrystalline cellulose (MCC) is a purified, partially depolymerised cellulose derivative that is insoluble in water [171]. It occurs as a white, odourless, tasteless crystalline powder consisting of porous particles [171]. Several grades of MCC are commercially available,

differing in respect of particle size, moisture content and intended use [173]. MCC can be used as a diluent or binder to manufacture tablets using either wet-granulation or direct compression approaches. It compresses readily and has a high dilution potential and capacity [164]. It also exhibits adsorbent, disintegrant and anti-adherent properties, thus making it extremely useful in tablet manufacture [173-175].

3.2.2.3 Ethylcellulose

Ethylcellulose is a non-toxic and inert polymer with a wide range of application in pharmaceutical formulations [171,176]. It occurs as a white to light tan coloured, tasteless, free-flowing powder [171]. It is used in formulations as a coating agent, flavouring agent and as a viscosity modifier [171]. Ethylcellulose is also used as a matrix-forming material, binder or filler in tablet formulations [171,176-178].

3.2.2.4 Carbomers

Carbomers are non-toxic, stable and water-swellable synthetic high-molecular-weight polymers of acrylic acid [171]. Carbomers may be cross-linked with allyl sucrose or allyl ethers of pentaerythritol, and contain between 52 and 68% carboxylic acid functional groups, calculated on an anhydrous basis [171]. Carbomers are commercially available in several grades that vary in terms of viscosity, degree of cross-linking and chemical structure [171]. In formulations they are used as emulsifying, gelling or suspending agents, and in tablet formulations are binders and/or controlled release agents at concentrations of 0.75-3% and 5-30% respectively [171].

3.2.2.5 Sodium bicarbonate

Sodium bicarbonate is a white, crystalline, odourless powder with a salty and/or alkaline taste [171]. Its crystal structure is monoclinic prism [171]. Sodium bicarbonate is widely used as an alkalinizing agent in pharmaceutical formulations, and is used alone or in combination with citric acid and/or tartaric acid to produce effervescent systems [171]. Sodium bicarbonate has been successfully used in the development of buoyant controlled release pellets and tablets based on effervescence [179-182].

3.2.2.6 Magnesium stearate

Magnesium stearate is a hydrophobic lubricant widely used in tablet and capsule formulations at levels of 0.5 to 5% w/w [171]. Magnesium stearate occurs as a very fine, light white impalpable powder with a slight stearic acid odour and a characteristic taste [171]. The use of high concentrations of magnesium stearate should be avoided as its hydrophobic nature may retard drug release [171]. Magnesium stearate should be added at the final stage of a manufacturing process, and the blending time with bulk powder blend should be tightly controlled as over-mixing may lead to poor performance of the dosage form [164,171]. A major limitation associated with magnesium stearate use is that it disrupts cohesive bonds within tablets, resulting in a negative effect on the tensile strength of the dosage form [183,184]. Although there are disadvantages associated with the use of magnesium stearate, it remains an efficient and widely used lubricant.

3.2.2.7 Talc

Hydrated magnesium silicate is commonly known as talc and is a naturally occurring compound used as a lubricant and glidant in tablet and capsule formulations at concentrations from 1 to10% w/w [171]. Talc occurs as a very fine white to greyish-white odourless, impalpable crystalline powder that is practically insoluble in water [171,185]. Following oral ingestion talc is not absorbed into the systemic circulation, and is thus considered to be a non-toxic material [171].

3.2.2.8 Colloidal silicon dioxide

Colloidal silicon dioxide is a sub-microscopic fused silica that occurs as a light, loose, bluish-white odourless amorphous powder [171]. It is used at concentrations of 0.1 to 1% w/w as a glidant in tableting and for capsule filling [171]. Several grades of colloidal silicon dioxide are commercially available, varying in respect of density, particle size and surface area [171].

3.3 PARTICULATE AND MECHANICAL PROPERTIES

3.3.1 Particle size analysis

Content uniformity is essential in pharmaceutical formulations, particularly for low-dose API and those with a narrow therapeutic index [10]. Tablets containing too little API may not exhibit any efficacy, whereas those with too much may cause toxicity [10]. It is therefore important to achieve content uniformity in order to ensure efficacy of a formulation and patient safety [10]. The particle shape and size distribution of excipients used for tablet manufacture may influence content uniformity. Particles of materials used in tablet manufacture must be small enough to permit uniform mixing of the bulk powder blend and allow even distribution of the API in each tablet [10]. Inclusion of a micronization step in a manufacturing process is an effective way of reducing the particle size of materials and improving content uniformity [10]. This approach is often accompanied by a deagglomeration step, since micronized particles tend to agglomerate [10,164]. It is important for a manufacturer to specify a particle size range narrow enough to achieve content uniformity but wide enough to minimize cohesive agglomeration [10]. Methods commonly used to determine particle size distribution include microscopic image examination, laser light scattering and sieve analysis [10].

3.3.2 Characterisation of powder blend

The flow properties of powders can and often do affect the manufacturing process, and it is important for a manufacturer to determine the flow properties of powder blends during preformulation studies [164]. Flowability is particularly important in tableting, where a powder is constantly in motion as it is transferred from a hopper into the die cavity during the compaction process [186]. During manufacturing the tablet weight is determined by the volume fill of the powder in the die cavity [186]. Consistent powder flow is therefore critical in order to achieve uniformity in the final tablet [186]. Measurements of powder density and angle of repose (AOR) are commonly used as indicators of flowability [10].

3.3.2.1 Powder density

The flowability of a material may be determined by comparing the bulk density and tapped density of the powder [10,187]. The determination of Carr's index and the Hausner ratio are quick and simple methods that require the use of only a small amount of powder, and can be used to characterise powder flow [187]. Excellent flow is indicated by values of Carr's index (CI) and a Hausner ratio (HR) that is < 10% and between 1.00 and 1.11, respectively. The equations used to calculate Carr's index and the Hausner ratio are shown in Equations 3.1 and 3.2 [187]. An interpretation of values of Carr's index and the Hausner ratio is listed in Table 3.2.

$$\text{Carr's index} = \left[\frac{(\text{Tapped density} - \text{Bulk density})}{\text{Tapped density}}\right] \text{x } 100 \qquad \textbf{(Equation 3.1)}$$

$$\text{Hausner ratio} = \left[\frac{\text{Tapped density}}{\text{Bulk density}}\right] \qquad \textbf{(Equation 3.2)}$$

Table 3.2 Interpretation of Carr's index (Adapted from [188])

Carr's index (%)	Type of flow	Hausner ratio
≤ 10	Excellent	1.00-1.11
11-15	Good	1.12-1.18
16-20	Fair	1.19-1.25
21-25	Passable	1.26-1.34
26-31	Poor	1.35-1.45
32-37	Very poor	1.46-1.59
>38	Very, very poor	> 1.60

3.3.2.2 Angle of repose

Measurement of the AOR is another approach to evaluating the flow properties of a powder [10]. Values of the AOR that are between 25 and 30° indicate excellent flow, and values that are > 66° indicate extremely poor flow. An interpretation of the flow properties of a powder and corresponding AOR is summarized in Table 3.3.

Table 3.3 Interpretation of the angle of repose (Adapted from [13])

Angle of repose (°)	Type of flow
25-30	Excellent
31-35	Good
36-40	Fair
41-45	Passable
46-55	Poor
56-65	Very poor
>66	Very, very poor

3.4 API-EXCIPIENT COMPATIBILITY

Investigating the inherent stability of an API is a critical consideration during preformulation studies, and includes gaining an understanding of the solid and solution-state stability of an API alone and in the presence of potential excipients [164]. Any incompatibility between an API and an excipient may compromise the stability and bioavailability of the API and ultimately decrease the safety and efficacy of the resultant formulation [189]. More specifically, incompatibilities may lead to changes in the organoleptic and mechanical properties of the formulation, dissolution performance, product degradation and potency [190]. Careful selection and consideration of excipients based on their functionality and compatibility is therefore essential for the formulation and manufacture of stable dosage forms [187]. The information pertaining to the solid-state and solution-state stability of CPT has been discussed (§ 1.4), and the following text will therefore focus on drug-excipient compatibility.

3.4.1 Types of interactions

Interactions between API and other materials can manifest in a number of ways. Physical interactions refer to alterations in a formulation that do not involve the breakage or formation of chemical bonds in the structure of an API molecule [191]. Changes in the organoleptic properties of a formulation, such as alteration in taste, odour and/or colour on storage may be indicators of physical instability [191]. Physical interactions may also lead to changes in drug release and may affect the bioavailability of an API significantly [191,192]. Additional

examples of physical instability include crystallization into amorphous systems, segregation, physical attrition and adsorption [191].

Chemical interactions involve changes in the structure of an API molecule and may lead to the formation of degradation products and result in decreased potency [191,192]. Examples of common chemical reactions observed in pharmaceutical materials include hydrolysis, dehydration, oxidation, cyclization, elimination, isomerisation, photo-degradation and charge interactions [191,192].

The degradation rate of a material in a solid oral dosage form may be influenced by the micro-environment pH of the formulation [191]. Excipients with ionisable functional groups act as pH-modifying agents and may result in accelerated degradation [191]. Despite the potential detrimental effects of modifying pH, the pH-altering properties exhibited by certain excipients may be useful for optimising the dissolution rate of an API or for modulating the pH of a formulation [191]. Any impurities or residues present in an excipient may also catalyse instability, particularly if the ratio of drug to excipient is high [192].

Although the majority of drug-excipient interactions are detrimental, several interactions have been shown to be beneficial [190]. For example, antioxidants may be incorporated into formulations to stabilize drugs that are susceptible to oxidation, or complexation of an API with cyclodextrin may enhance resistance to hydrolysis, oxidation and photo-degradation [190].

Regardless of the importance of drug-excipient compatibility testing, there is no globally accepted protocol for conducting such tests [10]. Several methods have been suggested for this purpose and include thermal, non-thermal and chromatographic techniques [193,194]. A tabular summation of the analytical technique commonly used in compatibility testing, and the relevance of the information provided, is summarized in Table 3.4.

Table 3.4 Techniques used in API-excipient compatibility testing (Adapted from [151, 167])

Technique	Measurement	Utility of data
DSC	Absorption or release of energy by a sample as it is heated, cooled or maintained at a constant temperature	Physicochemical compatibility of API and excipients
TGA	Weight changes in a sample as it is heated, cooled or maintained at a constant temperature	Physicochemical compatibility of API and excipients
FT-IR	Absorption of different IR frequencies by a sample	Determination of functional groups; compound identification and structural elucidation
Chromatography	Chemical interaction of the sample with the stationary phase and mobile phase	Chemical compatibility of API and excipients; purity of API and excipients
Micro-calorimetry	Heat absorbed or released by solution sample	Physicochemical compatibility of API and excipients; solution applications
X-ray diffraction	Scattering of x-ray radiation by a solid sample	Characterisation of polymorphs
LC-MS/MS	Chromatographic separation and fragmentation of molecular species	Identification of impurities and degradation products
Microscopy	Magnified visualization of sample	Particle size, shape and morphology

DSC = Differential Scanning Calorimetry, TGA = Thermo-gravimetric Analysis, FT-IR = Fourier Transform-Infrared Analysis and LC-MS = Liquid Chromatography-Mass Spectroscopy

3.5 EXPERIMENTAL

3.5.1 Particle shape and size

The particle shape and size of the excipients used in these studies was assessed using a Vega® Scanning Electron Microscope (Tescan, Vega LMU, Czechoslovakia Republic). A small amount of the powder to be analysed was mounted onto double-sided adhesive carbon tape and placed onto a sample disc carrier (3 mm height and 10 mm diameter). The powders were sputter coated with gold under vacuum (0.25 Torr) for 20 minutes (Balzers Union Ltd, Lichtenstein) and a 20 kV electron beam was used to generate images of the material.

3.5.2 Powder density

The bulk volume of the powder blends used in these studies was determined by measuring the volume occupied by 20 g of powder in a 100 mL A-Grade graduated glass measuring cylinder. The tapped volume of the powders was determined using a Model SVM Erweka® tapped density tester (Erweka, GmbH, Heusenstamm, Germany) after tapping the cylinder for 2 minutes at a rate of 220 taps per minute. The bulk volume and tapped volume measurements were used to calculate the bulk and tapped density of the material. Carr's index and the Hausner ratio were calculated using the bulk and tapped densities as described in § 3.3.21.

3.5.3 Angle of repose

The AOR was measured (n=3) by pouring approximately 20 g of powder though a glass funnel which was held 2 cm above a fixed glass plate. The exact amount of powder used was a function of the bulk density of the material. The height of the cone and the diameter of the base were measured and Equation 3.3 was used to calculate the AOR [13].

$$\tan(\alpha) = \frac{h}{(0.5)d} \qquad \textbf{(Equation 3.3)}$$

Where

α = Angle of repose

h = Height of the cone of powder

d = Diameter of the base of the cone of powder

3.5.4 Thermogravimetric analysis (TGA)

A Model TGA 7 Perkin Elmer Thermogravimetric Analyser (Perkin Elmer® Norwalk, Connecticut, USA) fitted with a platinum sample holder was used to generate a TGA curve for CPT. Approximately 1.3 mg of CPT was added to an open platinum crucible and heated from 25 to 500°C at a rate of 20°C/min in a high purity flow nitrogen atmosphere at a flow rate of 20 mL/min. The data were analysed using Pyris™ Manager Software (Perkin Elmer® Norwalk, Connecticut, USA).

3.5.5 Differential Scanning Calorimetry (DSC)

A Model Q100 Differential Scanning Calorimeter (TA Instruments, New Castle, DE, USA) coupled with a RCS(90) Refrigerated Cooling System (TA Instruments, New Castle, DE, USA) was used for thermal analysis of CPT and 1:1 mixtures of CPT and excipients. Approximately 2-3 mg of each sample was weighed directly onto an aluminium pan and spread evenly across the base of the pan. All samples were analysed in open (uncovered) pans in order to improve heat dissipation and optimise atmospheric interaction. Each pan and an empty reference pan was placed on a raised platform on a constantan disc inside a DSC Standard Cell FC. The samples were heated from 22 to 250°C at a heating rate of 10°C/min and under inert nitrogen atmosphere (flow rate 100 mL/min). The DSC curves generated were analysed using TA Universal Analysis software (TA Instruments, New Castle, DE, USA).

3.5.6 FT-IR spectroscopy

Potential interactions between CPT and excipients were investigated using a Spectrum 100 FT-IR ATR Spectrophotometer (Perkin Elmer® Ltd Beaconsfield, England). Binary mixtures in a ratio of 1:1 of excipient and CPT were prepared by gently mixing the powders using a mortar and pestle. A small amount of each powder was placed on a diamond crystal and a force of approximately 100 N was applied prior to analysis. The scanning range used was 4000-650 $cm^{-1}$and the resolution was 4 cm^{-1}.

3.6 RESULTS AND DISCUSSION

3.6.1 Particle shape and size

The characterisation of particle shape and size is an essential component of preformulation studies [195]. The shape and size of particles may influence physical properties of solid materials such as blending efficiency, tendency for segregation and powder flowability [196]. Particle shape and size also affect the dissolution rate, release rate and the bioavailability of drug molecules [164,196]. The homogeneity of a final tablet is influenced by the particle size of powders therefore it is important to determine, specify and maintain a target particle size range in order to ensure the manufacture of high quality tablets with acceptable content uniformity [164]. An evaluation of the particle size distribution allows a manufacturer to decide if there is a need to include sieving and particle size reduction steps in the manufacturing process [164].

SEM was a suitable method to study particle morphology of the excipients used in these studies since it is a fairly rapid way of observing and measuring the shape and size of individual particles concurrently. The SEM photomicrographs presented in Figure 3.1 reveal the particle shape and size distribution of the excipients used in these studies.

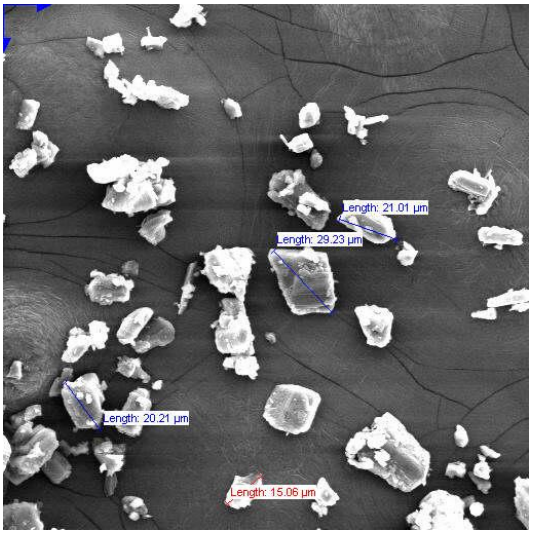

I (CPT)

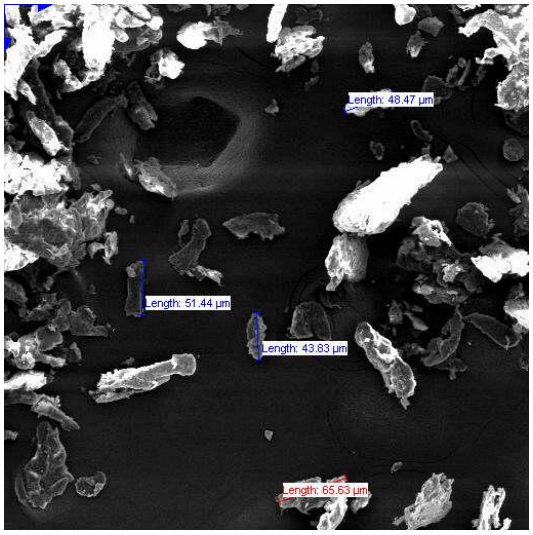

II (Methocel® K100M)

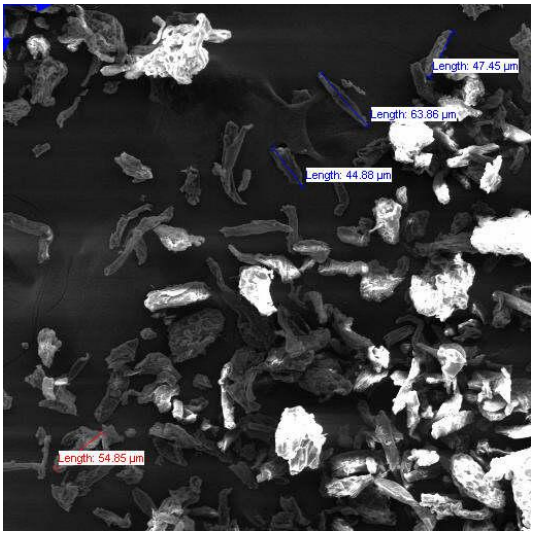

III (Avicel® PH-102)

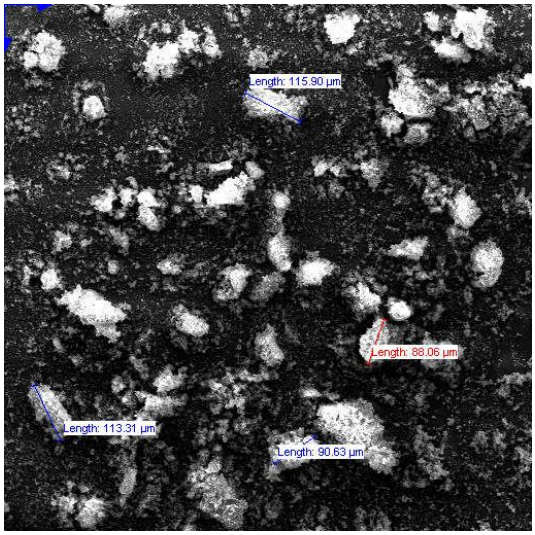

IV (Carbopol® 974P NF)

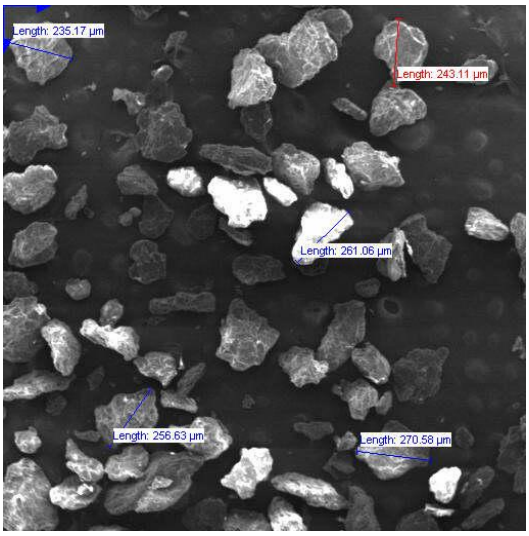

V (Ethylcellulose)

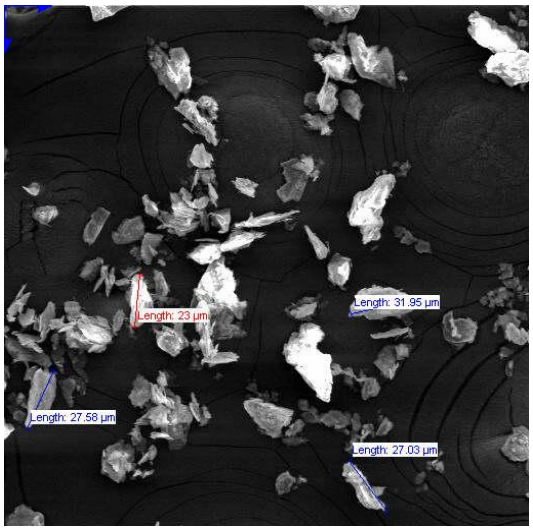

VI (Talc)

Figure 3.1 Particle size and shape of excipients

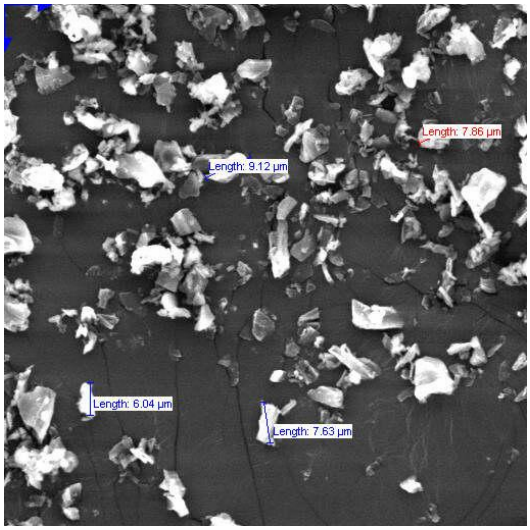

VII (Magnesium stearate)

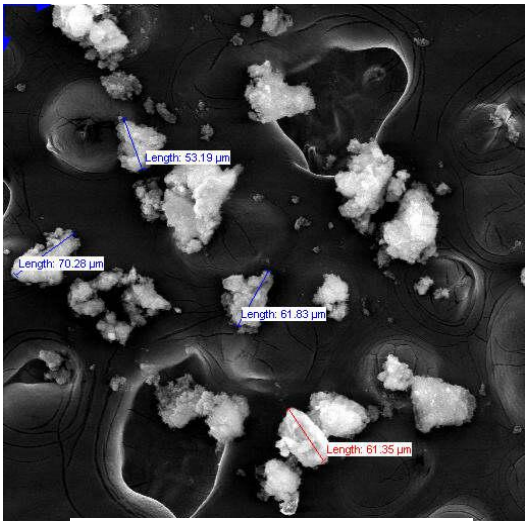

VIII (Colloidal silicon dioxide)

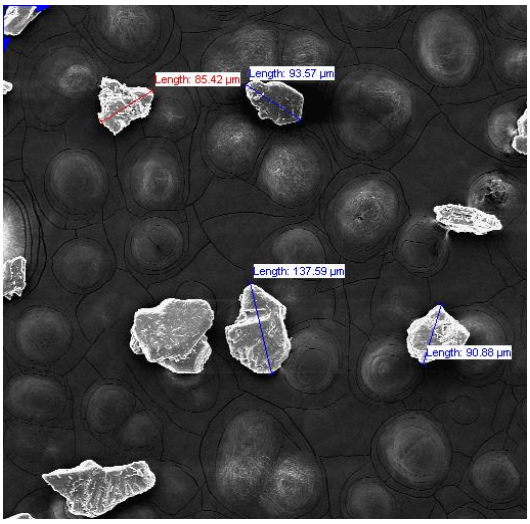

IX (Sodium bicarbonate)

Figure 3.1 (cont) Particle size and shape of excipients

The photomicrographs indicate that CPT (I) particles are sub-angular with medium sphericity. Methocel® K100M (II) particles are angular with low sphericity and Avicel® PH-102 (III) occurs as plate-shaped angular particles with low sphericity. Carbopol® 974 NF (IV) particles are sub-rounded with low sphericity. SEM images of ethylcellulose (V) reveal sub-rounded particles with medium sphericity, whereas Talc (VI) and magnesium stearate (VII) particles are sub-angular with low sphericity. Colloidal silicon dioxide (VIII) particles are sub-rounded with low sphericity and occur in aggregates. SEM photomicrographs of sodium bicarbonate (IX) reveal particles that are angular with medium sphericity.

A summary of the particle size distribution of the excipients used in these studies is listed in Table 3.5. Analysis of size distribution reveals that some of the excipients exhibited particle sizes that are suitable for tablet manufacture using direct compression (100-200 µm) [196]. Powder particles in this size range tend to posses the required flowability and compaction behaviour for tableting by direct compression [196]. In general, as the particle size of a material increases, flowability also increases [197]. Powder particles with diameters > 250 µm are normally free-flowing, whereas particles < 100 µm are cohesive and may exhibit poor flow [197]. If the particle size is < 10 µm cohesive forces between the individual particles increase and the powder is likely to resist flow under gravity [197].

The data revealed a wide particle size range, which when combined with the variation in particle shape, could lead to poor bulk powder flowability. To develop an appropriate manufacturing process, two sieving steps were included in an attempt to achieve a uniform particle size distribution and ultimately improve the flowability of the bulk powder.

Table 3.5 Particle size distribution of CPT and excipients

Excipient	**Particle size range (µm)**
CPT	15-29
Methocel® K100M	44-66
Avicel® PH-102	45-65
Carbopol® 974 NF	88-116
Ethylcellulose	235-270
Talc	23-32
Magnesium stearate	6-9
Colloidal silicon dioxide	53-70
Sodium bicarbonate	85-138

3.6.2 Characterisation of powder blend

The flowability data for the powder blends used to manufacture preliminary formulations (Chapter 4), expressed as the mean and relative standard deviation of three determinations are listed in Table 3.6.

Table 3.6 Characterisation of powder blends used to manufacture preliminary formulations

Formulation	AOR (°)	BD (g/cm^3)	TBD (g/cm^3)	CI (%)	HR
C1	23.27 ± 1.46	0.469 ± 2.00	0.564 ± 1.39	18.64 ± 1.23	1.20 ± 2.43
C2	33.42 ± 1.67	0.342 ± 1.79	0.503 ± 2.58	30.61 ± 1.79	1.44 ± 0.79
C3	26.38 ± 2.03	0.421 ± 2.25	0.514 ± 1.35	16.43 ± 4.59	1.19 ± 0.91
C4	30.11 ± 1.57	0.376 ± 1.04	0.525 ± 0.58	28.37 ± 3.59	1.39 ± 1.42
C5	34.30 ± 1.85	0.367 ± 1.01	0.572 ± 2.70	35.84 ± 3.41	1.56 ± 1.89
C6	31.71 ± 1.66	0.41 ± 0.98	0.603 ± 1.47	31.99 ± 2.75	1.47 ± 1.29
C7	29.83 ± 1.29	0.379 ± 1.79	0.451 ± 2.58	30.62 ± 1.79	1.44 ± 0.79
C8	38.60 ± 2.45	0.295 ± 1.51	0.398 ± 2.31	25.87 ± 1.51	1.35 ± 0.52
C9	28.31 ± 1.18	0.356 ± 1.51	0.488 ± 1.02	27.15 ± 3.55	1.37 ± 1.33

AOR = Angle of repose, BD = Bulk density, TBD = Tapped bulk density, CI = Carr's index and HR = Hausner ratio

The values for AOR ranged between 23.27° ± 1.46 and 38.60° ± 2.45, suggesting that the powder blends exhibit excellent-fair flow properties. The values for BD and TBD were used to determine CI and HR. The results show that the CI ranged between16.43% ± 4.59 and 34.84% ± 3.41, indicating fair to very, very poor flow. The HR ranged between 1.19 ± 0.91 and 1.56 ± 1.89, indicating fair to very poor flow properties. The results from the characterisation of the powder blends indicated that there is a need to add anti-frictional agents to the powder blends to facilitate material flow and achieve acceptable flow properties for tablet manufacture using a direct compression approach. The addition of glidants such as colloidal silicon dioxide or talc to the powder blends may improve powder flow and facilitate the movement of the powder from the hopper feed to the die punch [164]. Addition of a lubricant such as magnesium stearate facilitates the ejection of tablets from the die walls of the tableting press [164].

3.6.3 Thermogravimetric analysis

Thermal decomposition of CPT was determined by measuring the weight loss of CPT as a function of externally applied heat. The TG curve of CPT (Figure 3.2) indicates that CPT is stable up to approximately 150°C, after which mass loss is observed between 150 and 500°C (Δm = > 95%). The mass loss does not occur during the melting process (107.84°C) but rather degradation commences beyond the melting point of CPT. The results are within reasonable agreement with previously reported values and suggest that the degradation of CPT is unlikely under normal tableting conditions, which rarely exceed 100°C [32].

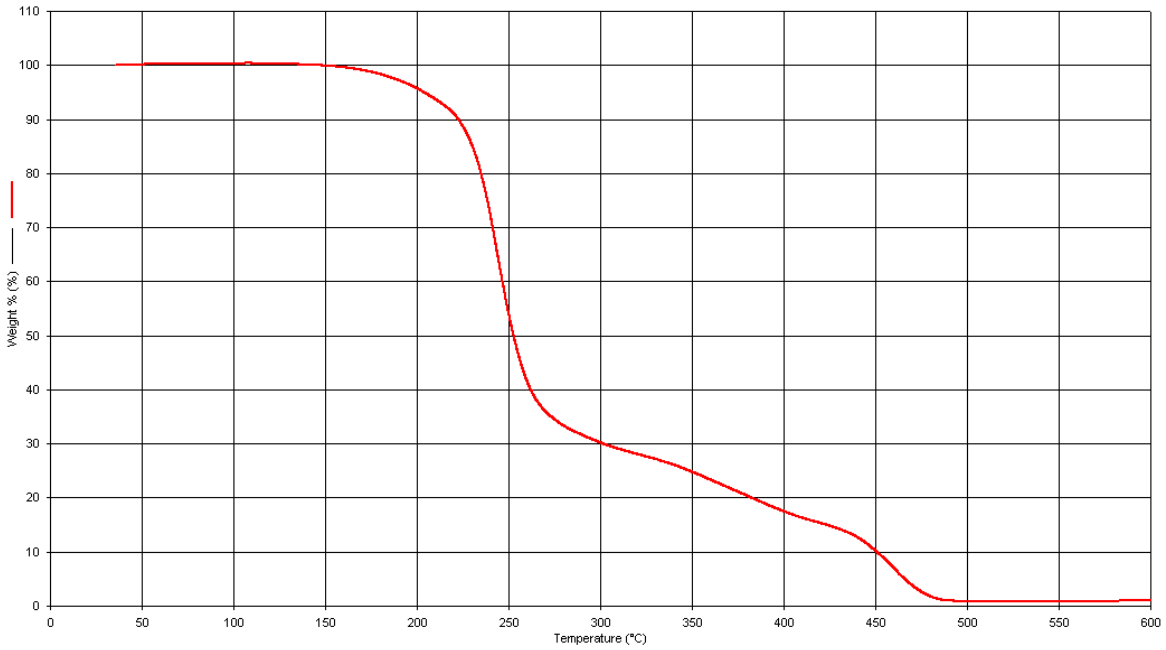

Figure 3.2 TG curve of CPT degradation

3.6.4 Differential Scanning Calorimetry

DSC is a measure of the heat flow required to maintain equality between a reference material and a test sample [195]. DSC thermograms were generated by plotting values of differential heat flow (W/g) against temperature (°C), and the heat absorbed during thermal events was calculated by integrating the respective DSC peaks observed. A tabular summation of the peak transition temperature (T_{peak}) and heat of fusion (enthalpy) (ΔH_{fusion}) for CPT in the different mixtures is summarized in Table 3.7. DSC thermograms were generated once for each CPT-excipient mixture. Although, it is a limitation to use n=1, previous studies focussing on CPT-excipient compatibility using DSC reported similar findings to those obtained in these studies [198, 199].

Table 3.7 Thermal parameters of CPT and CPT-excipient mixtures

Sample composition	T_{peak} **(°C)**	T_{onset} **(°C)**	ΔH_{fusion} **(J/g)**
CPT	107.84	105.83	112.80
CPT + Avicel® PH-102	107.80	104.87	54.59
CPT + Methocel® K100M	107.49	104.56	46.66
CPT + Talc	107.91	105.07	54.05
CPT + Colloidal silicon dioxide	107.40	105.04	19.47
CPT + Magnesium stearate	*	*	*
CPT + Sodium bicarbonate	105.76	102.62	39.16
CPT + all excipients	106.18	102.09	16.09

* Could not be calculated due to the absence of the CPT peak

The DSC curve for CPT (Figure 3.3) shows a sharp endothermic melting peak at 107.84 °C, with a ΔH_{fusion} of 112.8 J/g. These results are within reasonable agreement with the values reported in the literature [32,198,199].

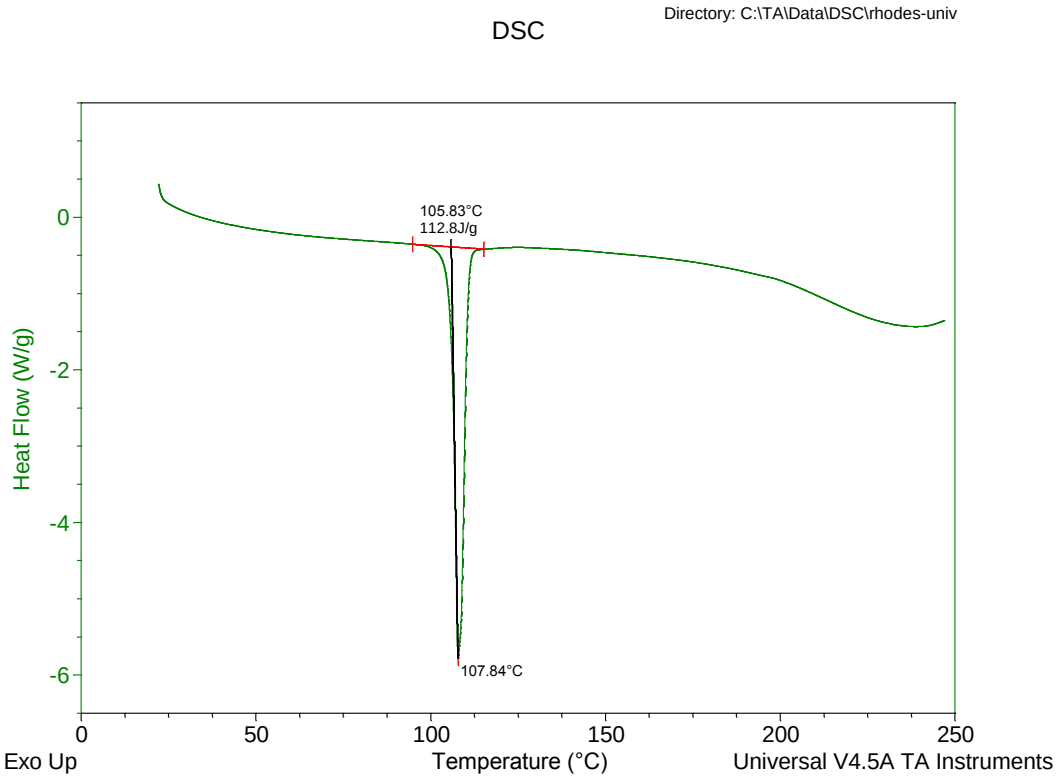

Figure 3.3 DSC curve for CPT

The melting endotherm of CPT was well preserved in the majority of the CPT-excipient mixtures, however in some cases slight broadening of the endotherm and a shift towards lower melting points was observed. Reports from previous DSC work reveal that the presence of impurities in a sample will result in changes in enthalpy and the shape of a DSC curve [200]. Therefore slight changes in the endotherm of CPT were not considered to be an indication of incompatibility but rather a result of lower purity due to the mixture of CPT and excipients [189,200]. The thermogram of a mixture of CPT and Avicel® PH-102 shown in Figure 3.4 shows the melting endothermic peak of CPT at 107.80°C, suggesting that there was no interaction between CPT and Avicel® PH-102.

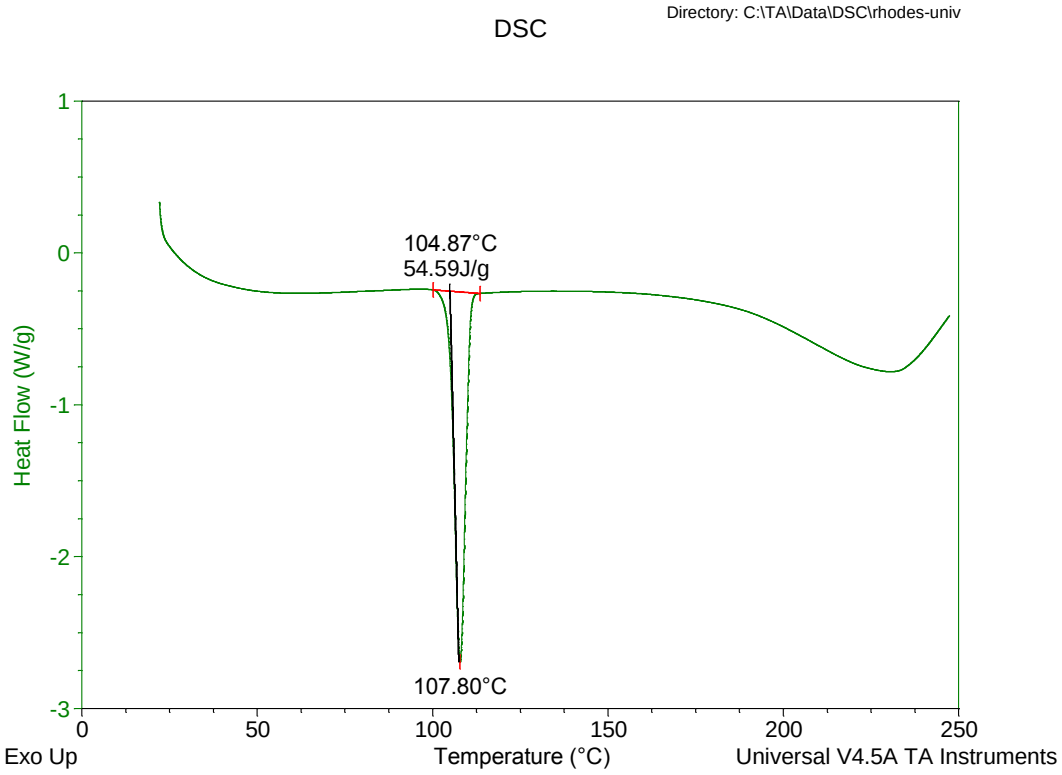

Figure 3.4 DSC curve for a 1:1 mixture of CPT and Avicel® PH-102

The DSC curve of a binary mixture of CPT and Methocel® K100M reveals an endothermic peak of CPT at 107.49°C, indicating that CPT is likely to be compatible with Methocel® K100M (Figure 3.5). The DSC thermogram of a binary mixture of CPT and talc shows a well preserved CPT peak at 107.91°C, signifying that CPT is also likely to be compatible with talc (Figure 3.6).

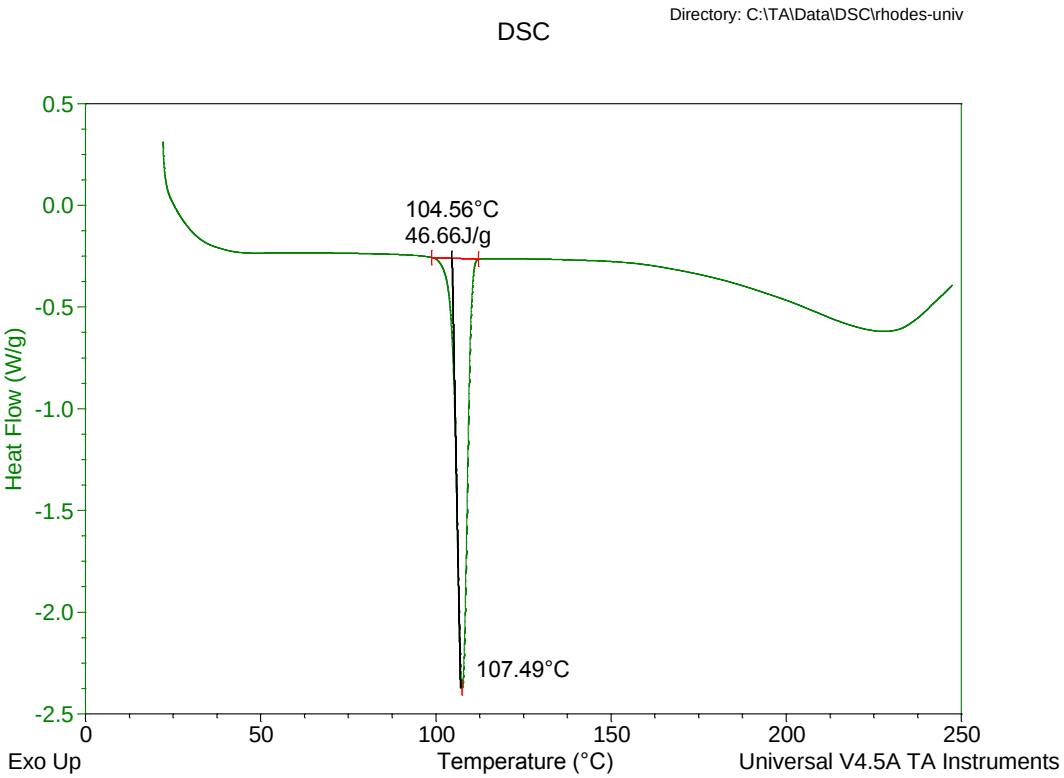

Figure 3.5 DSC curve for a 1:1 mixture of CPT and Methocel® K100M

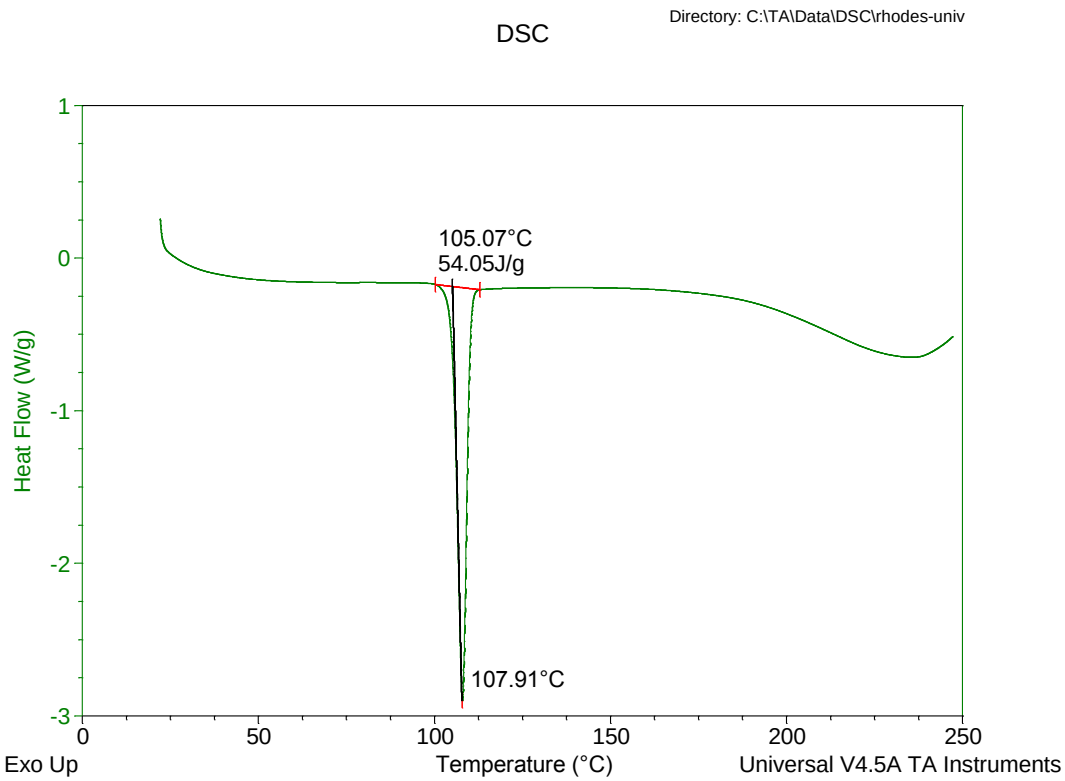

Figure 3.6 DSC curve for a 1:1 mixture of CPT and Talc

Similar results were observed for the mixture of CPT and colloidal silicon dioxide (Figure 3.7), where the CPT endotherm observed at 107.40°C indicates no potential interaction between CPT and colloidal silicon dioxide**.**

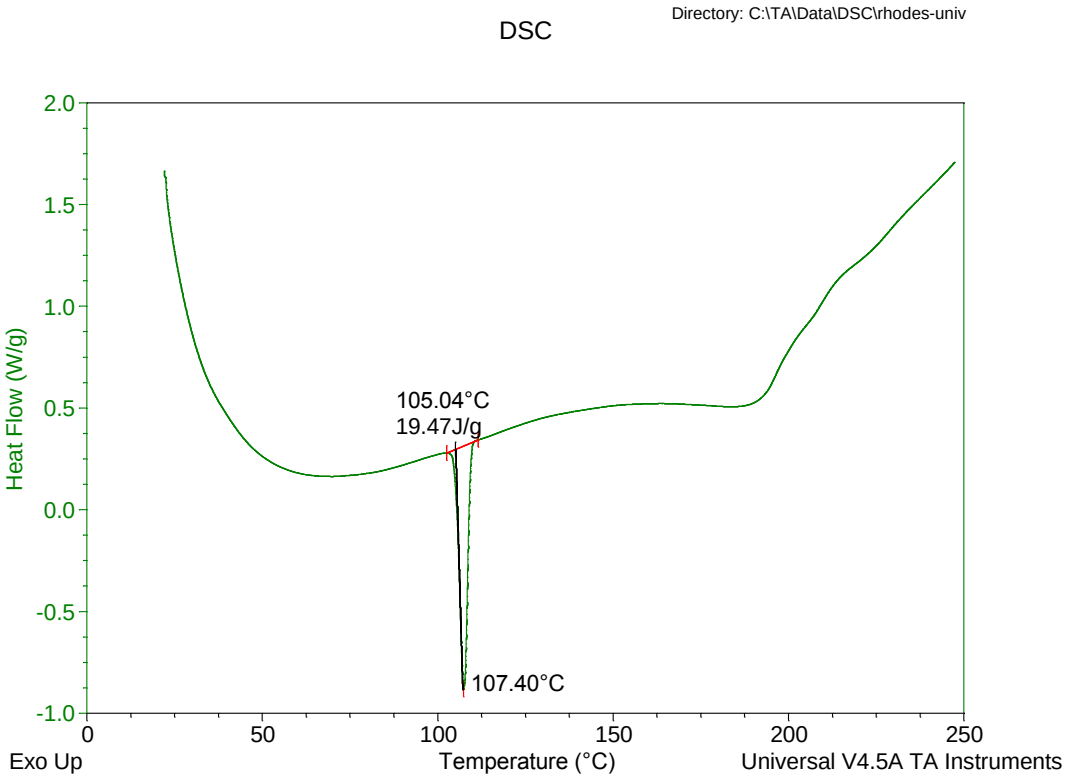

Figure 3.7 DSC curve for a 1:1 mixture of CPT and colloidal silicon dioxide

The DSC thermogram for CPT and magnesium stearate (Figure 3.8) reveals an irregular curve, with endothermic events occurring in the temperature range of 85.01 to 109°C and a shouldered endothermic peak presenting at 90.04°C. These observations are characteristic of the dehydration of magnesium stearate, which typically occurs between 69.85 and 109.85°C [32,201]. The disappearance of the CPT peak for this mixture suggests that there may be some physical incompatibility between the two compounds. To confirm any potential incompatibility FT-IR studies were performed on the mixture of CPT and magnesium stearate.

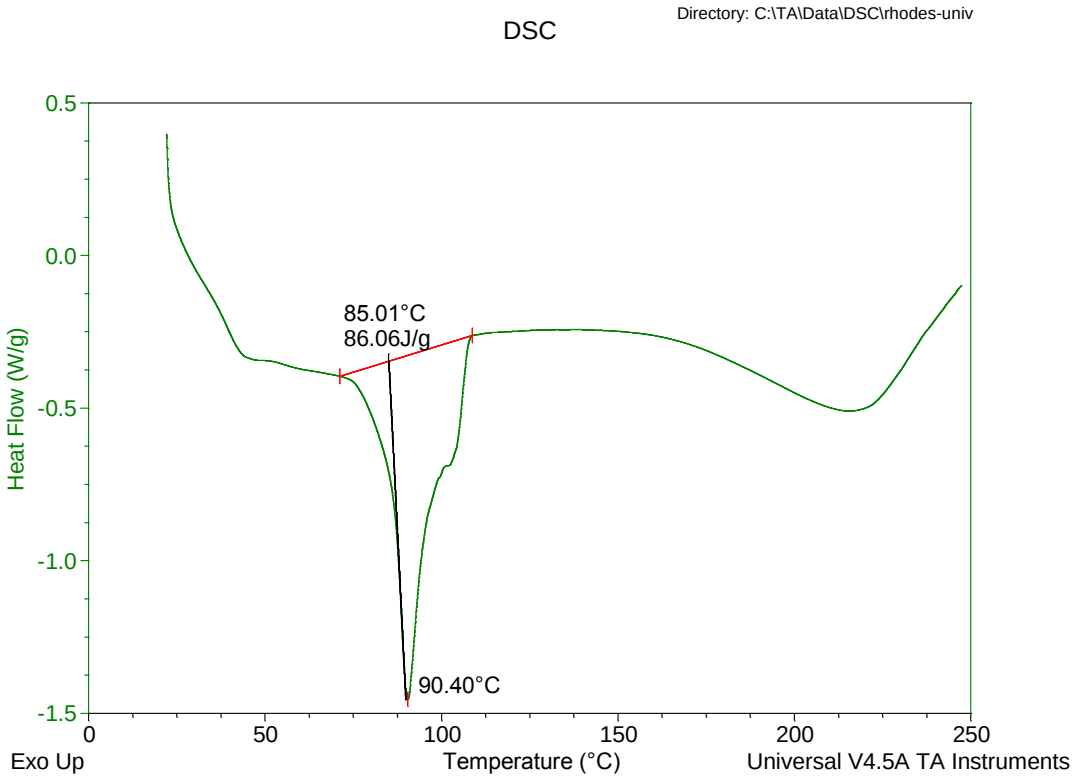

Figure 3.8 DSC curve for a 1:1 mixture of CPT and magnesium stearate

The thermogram of a mixture of CPT and sodium bicarbonate shown in Figure 3.9 reveals a slight shift in the melting endothermic peak of CPT to 105.76°C. FT-IR studies were performed to confirm the presence or absence of an interaction between CPT and sodium bicarbonate.

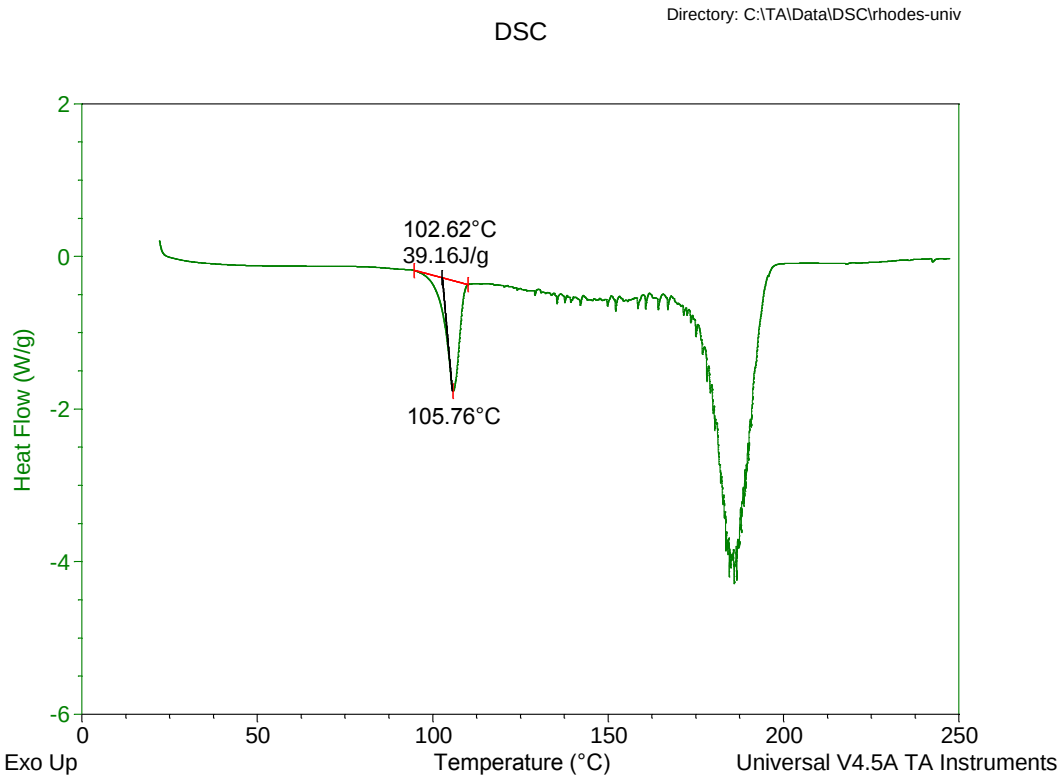

Figure 3.9 DSC curve for a 1:1 mixture of CPT and sodium bicarbonate

The DSC thermogram of a mixture of all excipients reveals an endothermic CPT peak at 106.18°C (Figure 3.10), which is similar to that obtained by analysing pure CPT, suggesting that CPT was present in a characteristic physical and chemical form. CPT was considered to be compatible with all the excipients as there was no definite evidence of interaction. However long-term stability studies would be required to prove this categorically.

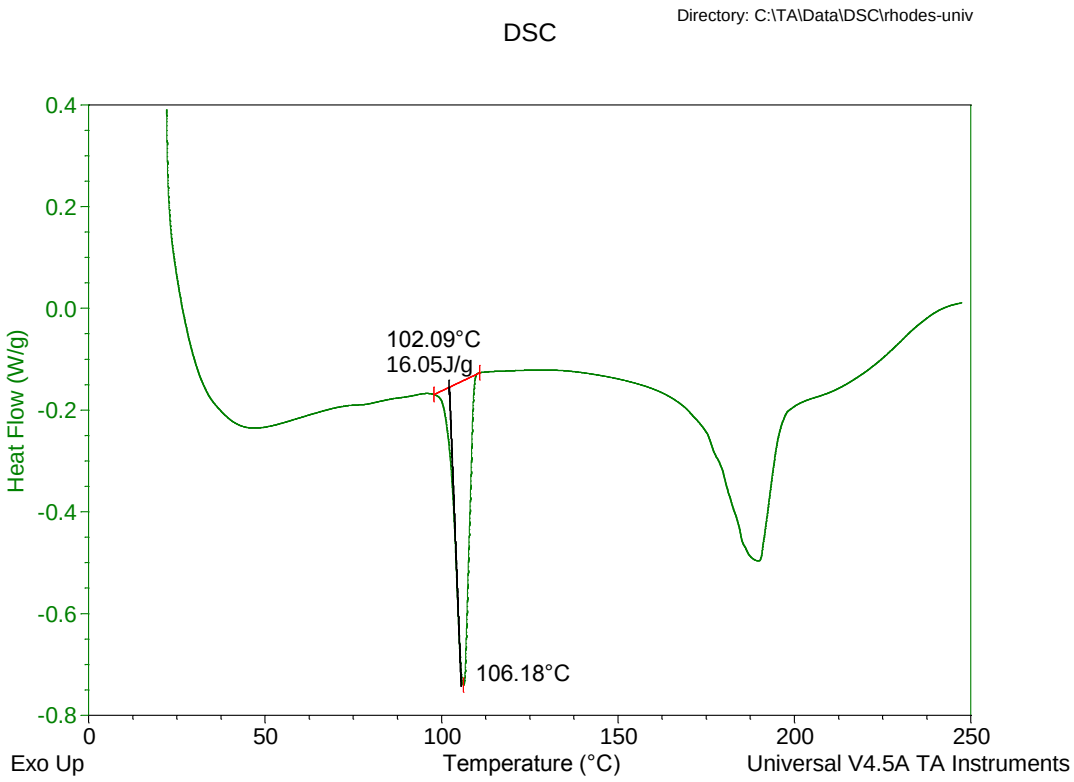

Figure 3.10 DSC curve for a mixture of CPT and all excipients

3.6.5 FT-IR spectroscopy

FT-IR studies were undertaken to provide supplementary data in order to confirm the results generated from thermal analysis and to identify if any chemical interactions between CPT- and excipients in binary mixtures may occur. A collection of the FT-IR spectra generated is shown in Figures 3.11-3.19. The FT-IR spectrum of pure CPT has three characteristic bands in the 2978 and 2870 cm^{-1} region corresponding to the $–CH_2$ and $–CH_3$ groups in the molecule. The characteristic bands of CPT were observed at 2565.92 cm^{-1} (–SH), 1744.04 cm^{-1} (–COOH) and 1583.88 cm^{-1} (amide). The FT-IR spectra generated from binary mixtures of CPT did not suggest potential solid-state interactions as there were no major shifts, changes or disappearance of the characteristic bands for CPT. Slight shifts in the characteristic bands for CPT that were observed during analysis of the binary mixtures may be a result of hydrogen bonding between CPT and the excipients.

The FT-IR spectrum of CPT and magnesium stearate is shown in Figure 3.17. The characteristic bands for CPT were observed at 2572.15 cm^{-1} (–SH), 1745.90 cm^{-1} (–COOH) and 1574.83 cm^{-1} (amide), and correspond to the bands observed when analysing pure CPT. There were no major shifts or absences of vibrations for CPT in the binary mixture, and thus the FT-IR spectrum of the CPT-magnesium stearate mixture may be superimposed on that of the pure CPT spectrum and no major differences will be observed. Although results from DSC studies suggest that a potential interaction between CPT and magnesium stearate may occur, the results from the FT-IR study failed to confirm potential chemical incompatibility between the two compounds. The observations made from the DSC study are possibly a result of the physical interaction between CPT and magnesium stearate.

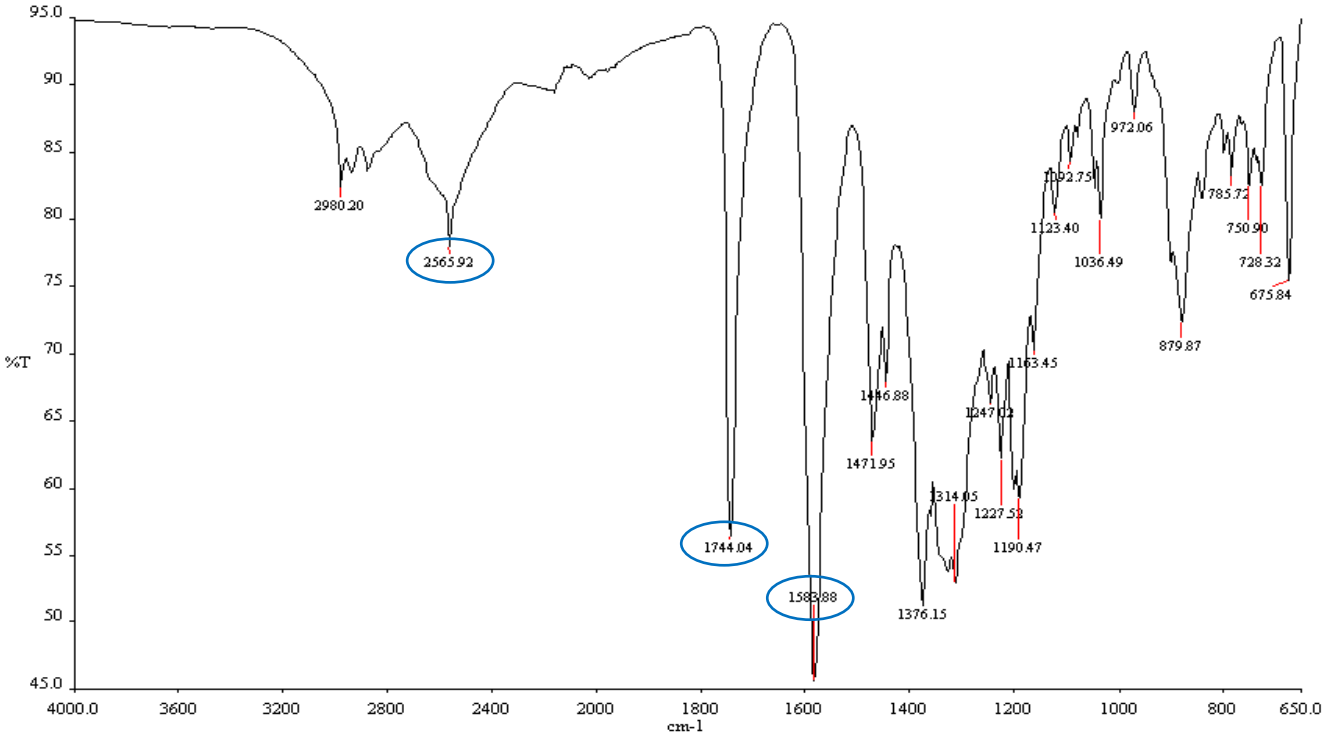

Figure 3.11 FT-IR spectrum for CPT

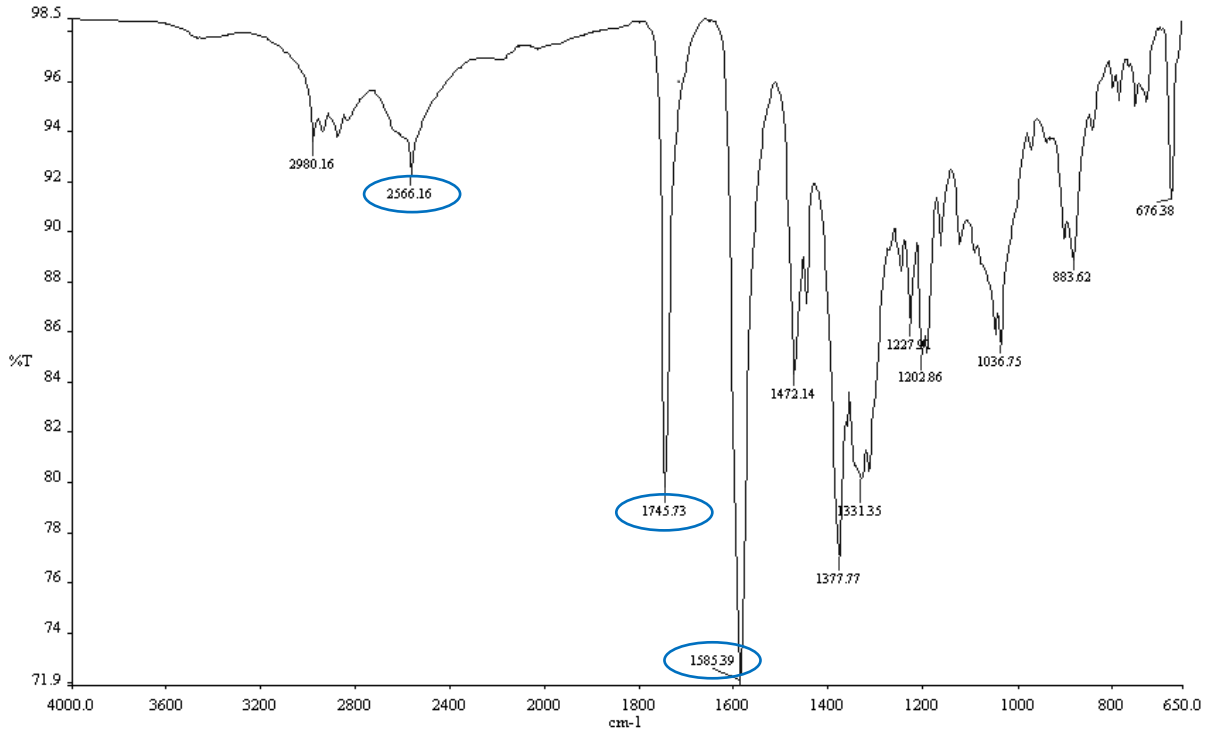

Figure 3.12 FT-IR spectrum for a 1:1 mixture of CPT and Methocel® K100M

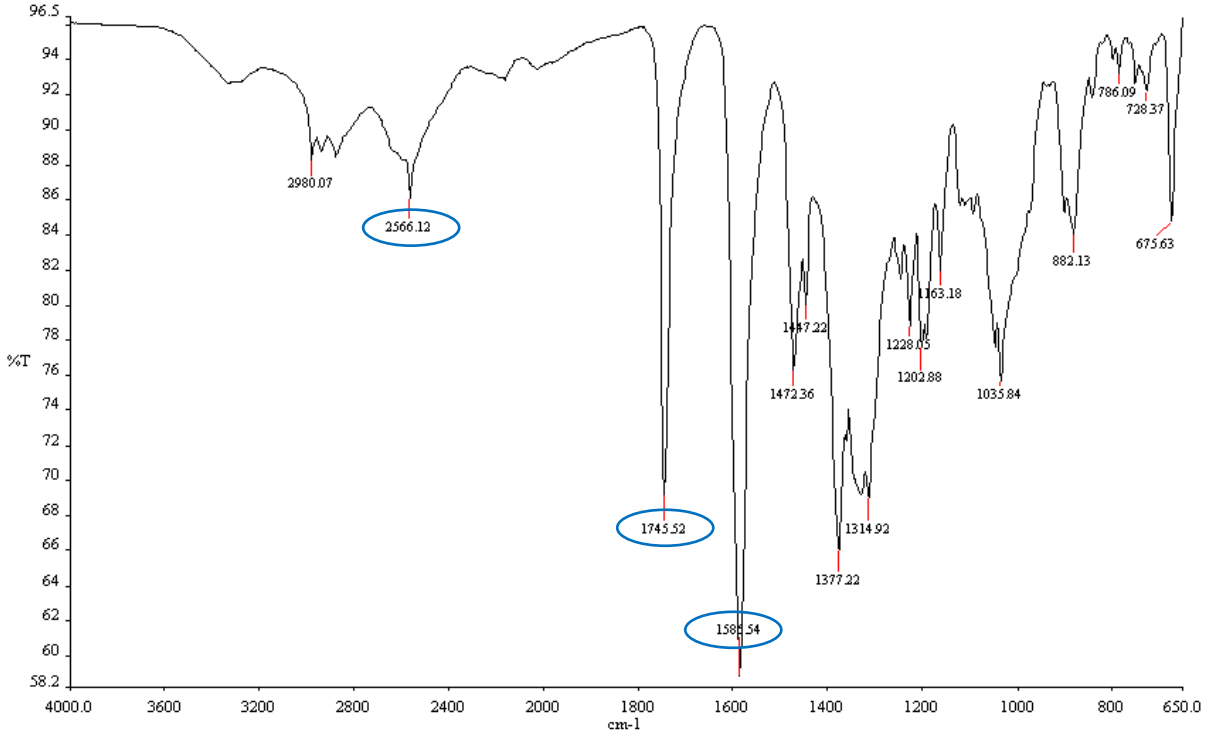

Figure 3.13 FT-IR spectrum for a 1:1 mixture of CPT and Avicel® PH-102

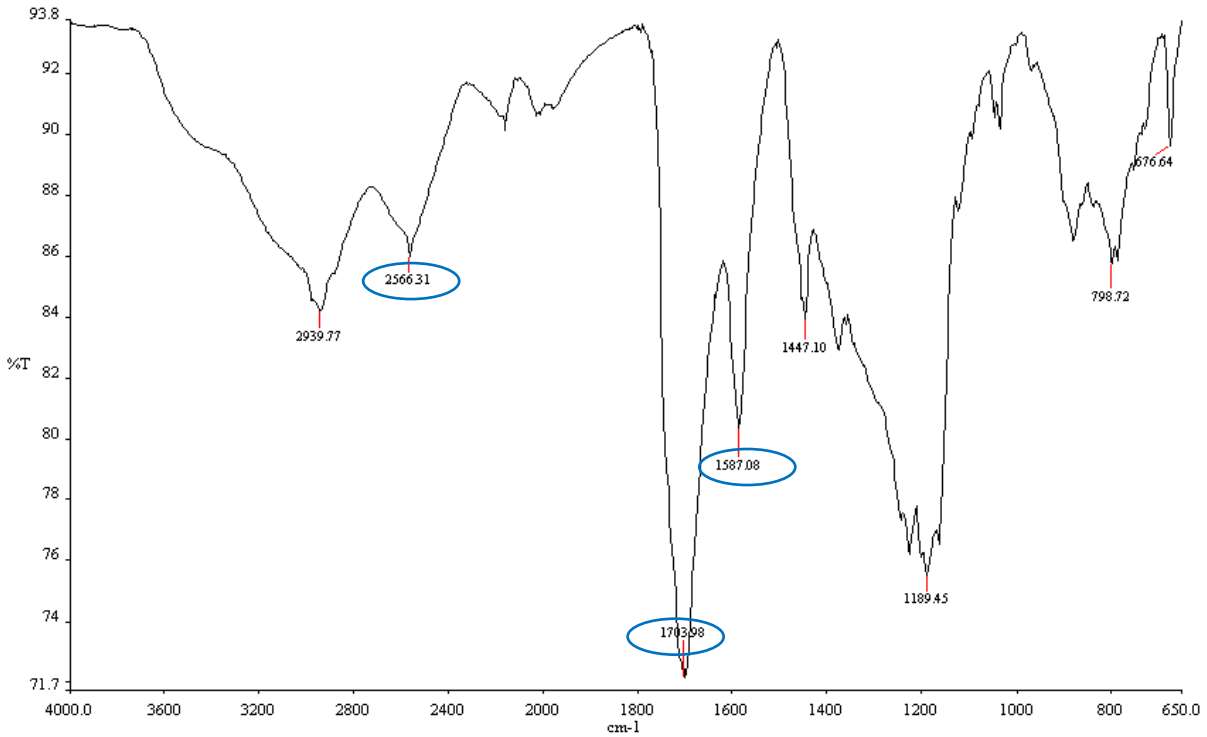

Figure 3.14 FT-IR spectrum for a 1:1 mixture of CPT and Carbopol® 974 NF

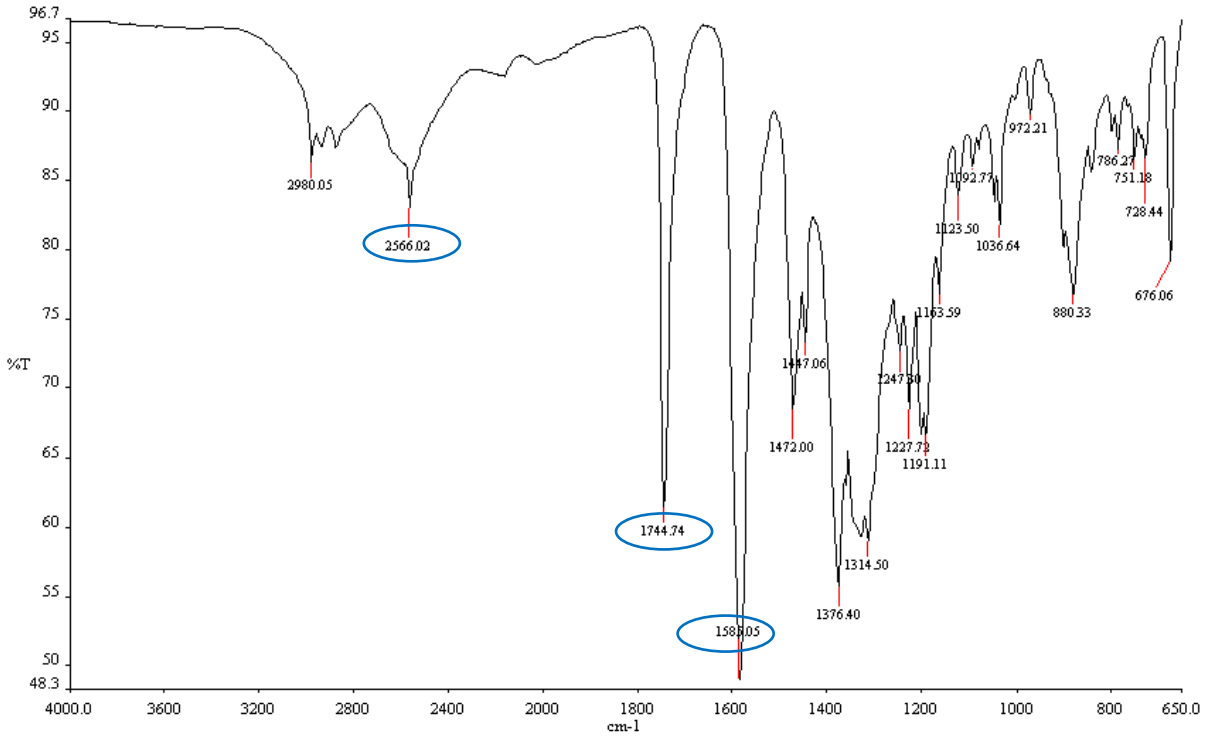

Figure 3.15 FT-IR spectrum for a 1:1 mixture of CPT and ethylcellulose

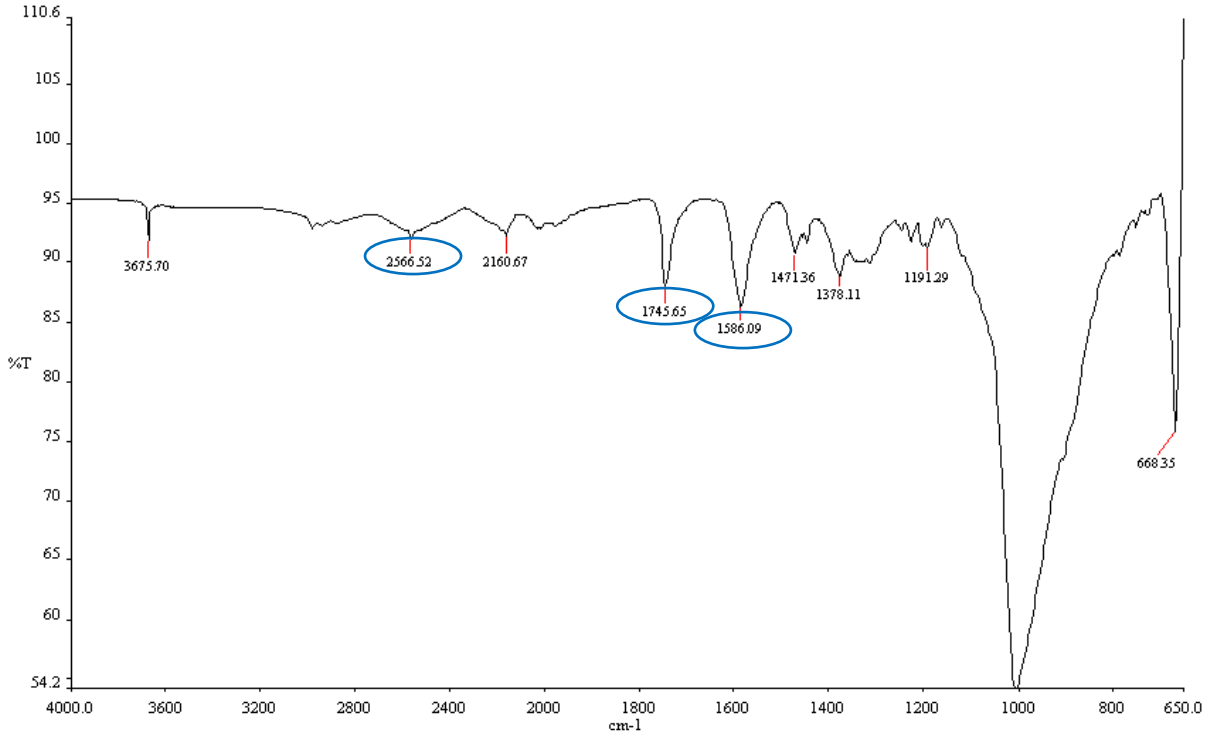

Figure 3.16 FT-IR spectrum for a 1:1 mixture of CPT and talc

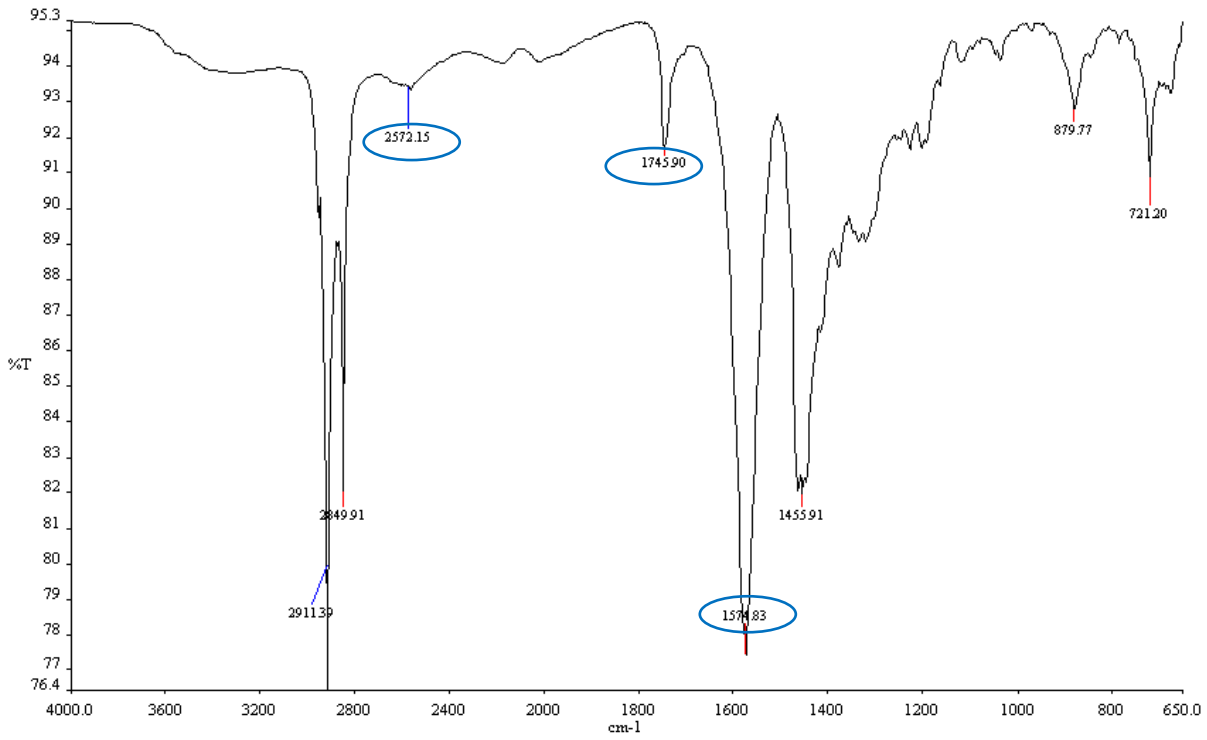

Figure 3.17 FT-IR spectrum for a 1:1 mixture of CPT and magnesium stearate

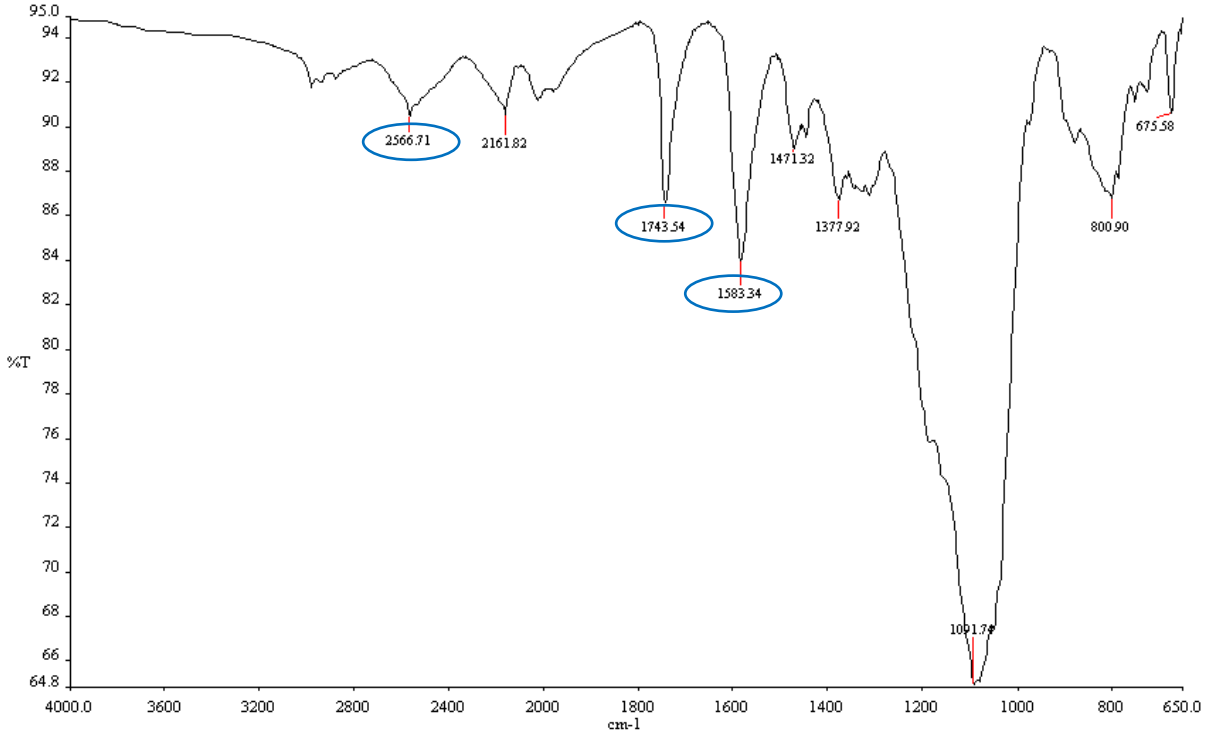

Figure 3.18 FT-IR spectrum for a 1:1 mixture of CPT and colloidal silicon dioxide

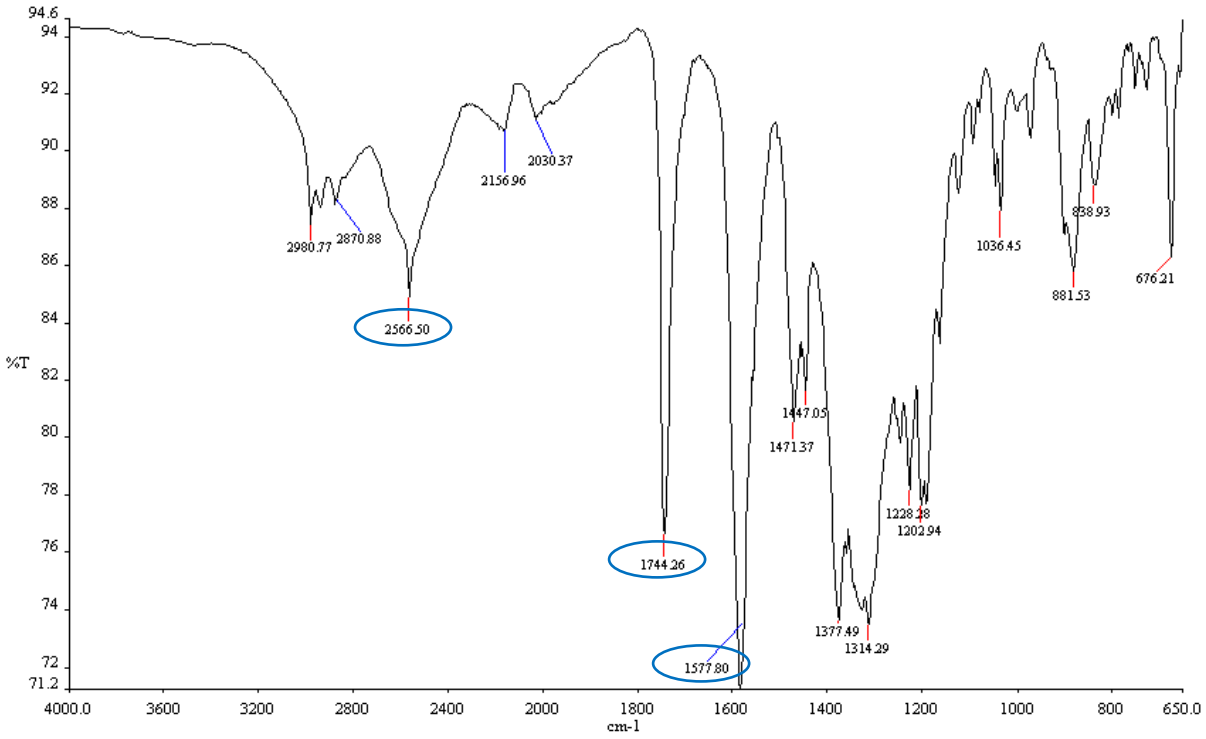

Figure 3.19 FT-IR spectrum for a 1:1 mixture of CPT and sodium bicarbonate

3.7 CONCLUSIONS

Preformulation studies were conducted as part of the preparative work required to manufacture a high quality stable sustained release formulation of CPT. The experiments conducted in these studies were tailored for the development of CPT sustained release tablets using direct compression manufacture and include an analysis of particle shape and size, flow properties of powder blends and drug-excipient compatibility studies.

The particle shape and size of the materials used for tableting affect the flowability, blending efficiency and the overall uniformity of tablets [164]. Results of microscopic analyses of the excipients indicate differences in shape and size of particles. Sieving steps must therefore be included in the manufacturing process to achieve uniform size distribution and improve flowability of powder blends.

Good flowability in tablet manufacture is necessary to ensure powder blend uniformity during mixing and weight and content uniformity of tablets. The flowability of powder blends used to manufacture preliminary formulations was characterised in terms of CI, HR and the

AOR. These studies indicated that the powder blends exhibited excellent to very, very poor flow properties and emphasized the need to add lubricants and glidants to reduce friction, improve powder flow and ensure that the powder blend is suitable for manufacturing tablets using direct compression.

Drug-excipient compatibility studies were conducted to identify excipients that may be incompatible with CPT. Thermal analytical techniques were used to gain an understanding of any physical or chemical changes that may occur when heat is applied to blends of CPT and the excipients. The results reveal that DSC is a quick and valuable technique for identifying drug-excipient incompatibilities during preformulation studies. However successful interpretation of DSC data requires careful thought and consideration, and in some cases supplementary techniques such as FT-IR may be required in order to draw definite conclusions. The DSC results for the binary mixture of CPT and magnesium stearate suggested a possible interaction between the two compounds. However chemical incompatibility between CPT and magnesium stearate was not confirmed by results of FT-IR studies. To ensure that such an incompatibility does not exist, long-term stability studies would be necessary.

FT-IR studies were conducted to identify any potential chemical interactions between CPT and potential excipients by analysis of 1:1 binary mixtures. The spectra obtained did not show evidence of such interactions. The slight shifts observed in the characteristic bands for CPT may be a result of hydrogen bonding in the powder mixtures.

In conclusion there was no definite evidence to support interactions between CPT and the excipients to be used to manufacture sustained release CPT tablets, therefore CPT formulations were developed using these excipients.

CHAPTER 4

DEVELOPMENT, MANUFACTURE AND ASSESSMENT OF CAPTOPRIL SUSTAINED RELEASE TABLETS

4.1 INTRODUCTION

The process of developing products for new chemical entities can be challenging, time consuming and expensive [10,202]. With this in mind increasing emphasis has been placed on developing and improving drug delivery systems for well-known currently available therapeutic compounds. This approach is cheaper and requires a shorter developmental time [10,202].

The use of controlled release formulations has been extensively studied in an effort to enhance the clinical benefits of well known compounds [203-208]. Controlled release formulations offer a number of therapeutic advantages over conventional compounds, including maintenance of optimal plasma concentration levels and increased duration of therapeutic activity [10]. In addition the use of controlled release formulations may also reduce the occurrence of drug-related adverse effects [10,202,209]. Controlled release formulations are a more convenient alternative to immediate release formulations as they require less frequent administration, which in turn simplifies dosing schedules and may thus benefit patients on chronic medication [10,202,209].

Despite the numerous advantages of using controlled release formulations there are a few disadvantages associated with these technologies. Firstly, if the integrity of the dosage form is compromised the entire contents may be released (dose dumping), and expose the patient to toxic drug levels [10]. In addition it is extremely difficult to stop API release from the dosage form once it has been administered such as in cases of drug-related poisoning or if a patient experiences severe adverse effects [10,210]. Finally the total cost of manufacturing controlled release formulations is generally higher than that of manufacturing conventional dosage forms [10,210].

Two commonly used examples of modified release formulations are sustained release and delayed release formulations [10]. Sustained release formulations are designed to release part

of a total dose immediately following administration and the remaining portion of the dose is then released gradually over an extended period of time [10]. In contrast delayed release formulations such as enteric-coated or colonic-specific tablets are designed to delay drug release until the dosage form reaches a specific area in the GIT [10,211].

4.2 MECHANISMS OF DRUG RELEASE FROM ORAL CONTROLLED RELEASE SYSTEMS

Oral controlled release formulations can be classified based on the mechanism through which an API is released from these systems. The most common mechanisms of drug release from oral controlled released systems include dissolution-controlled, diffusion-controlled, erosion-controlled, osmosis-controlled and ion exchange resin systems.

4.2.1 Dissolution-controlled systems

Dissolution-controlled systems may be sub-classified as either reservoir (encapsulated) or matrix systems. The dissolution rate of the API is the rate-controlling step in both types of system [10,212]. For reservoir-type dissolution systems a drug core is encapsulated with a polymeric membrane and the API is released in a controlled manner until the membrane completely dissolves, after which release will be similar to that observed for immediate release formulations [10,212]. The rate at which an API is released from reservoir type systems is therefore determined by the thickness and dissolution rate of the polymeric membrane [10,212]. In addition the presence of solid or solution on the interior of the dosage form also influences the rate at which the API is released from the system. An example of a commercially available reservoir-type dissolution system is the Spansule® range of products manufactured by GlaxoSmithKline [21,212]. The basic design of Spansule® products consists of drug-loaded beads encapsulated by a rate-controlling membrane [212]. Some examples of API that have been successfully incorporated into Spansule® products include detroxamphetamine sulphate, diphenylpyraline HCl and chlorpromazine HCl [21].

For matrix-type dissolution systems an API is uniformly distributed throughout a hydrophilic or hydrophobic polymeric matrix, and drug release may occur through a combination of diffusion and dissolution mechanisms depending on the properties of the API and polymer matrix [10,212]. Drug release does not follow zero-order kinetics in this type of system since

the total surface area of the matrix changes over time [10,212]. Some examples of commercially marketed matrix-type dissolution systems include Diametane® and Quinidex® tablets that contain brompheniramine maleate and quinidine sulphate [21].

4.2.2 Diffusion-controlled systems

Diffusion-controlled systems can be sub-classified as either reservoir or matrix (monolithic) systems [10,212,213]. The rate at which an API is released from a diffusion-controlled system is governed by the rate at which drug molecules diffuse through a polymeric membrane or through the pores of a polymeric matrix [21,188,213,214]. However for matrix systems there may well be a third consideration, and that is that the drug dissolves in the matrix. Thus the rate of solution and diffusion in the matrix is also important. Although a dissolution step is required for drug release to occur the diffusion process is the rate-limiting step for release from these systems [188,212,214].

Exposure of a diffusion-controlled reservoir-type system to gastric fluid commences the drug release process, which occurs via two main steps. Initially the gastric fluid penetrates the dosage form and dissolves the API, resulting in the formation of a concentration gradient across the interior and exterior of the dosage form [10,188,215] . The dissolved API then partitions into an encapsulating membrane (if present) and diffuses through the membrane until it partitions into the gastric fluid (Figure 4.1) [188]. The concentration gradient across the membrane provides the driving force required in order for drug release to occur, and the release rate in reservoir type systems can be estimated using Equation 4.1 [188].

$$\frac{\mathrm{M}}{t} = \frac{(\mathrm{CA}K\mathrm{D})}{l} \qquad \textbf{(Equation 4.1)}$$

Where

$\frac{\mathrm{M}}{t}$ = Release rate
C = Solubility of the drug in the liquid medium
A = Area of the membrane
l = Thickness of the membrane
K = Partition coefficient of the drug between the membrane and fluid at equilibrium
D = Diffusion coefficient of the drug in the membrane

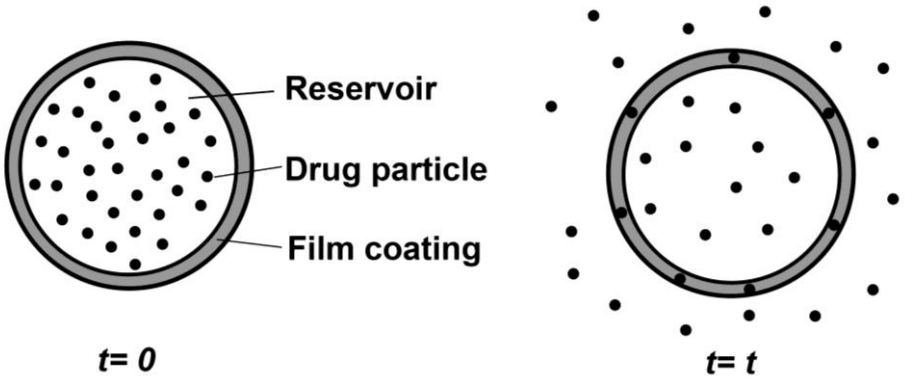

Figure 4.1 Schematic representation of API release from a diffusion-based reservoir tablet (Adapted from [188])

The drug release process is slightly different for diffusion-controlled matrix type systems. Initially when the system is exposed to gastric fluid the API at the surface of the dosage form dissolves and is released [188]. Depending on the nature of the polymers used to form the matrix the remaining drug particles will either diffuse across a gel layer or through liquid-filled pores in the matrix and eventually enter the GIT [188]. The cumulative amount of drug released (M) from a matrix system is proportional to the square root of time (*t*), as shown in Equation 4.2 [188].

$$M = k\sqrt{t} \qquad \textbf{(Equation 4.2)}$$

A schematic representation of the mechanism of drug release observed in diffusion-controlled matrix tablets is shown in Figure 4.2. Some examples of commercially available diffusion-controlled matrix type systems include Desoxyn® and Ferro-Gradumet® tablets which contain methamphetamine and ferrous sulphate respectively [21].

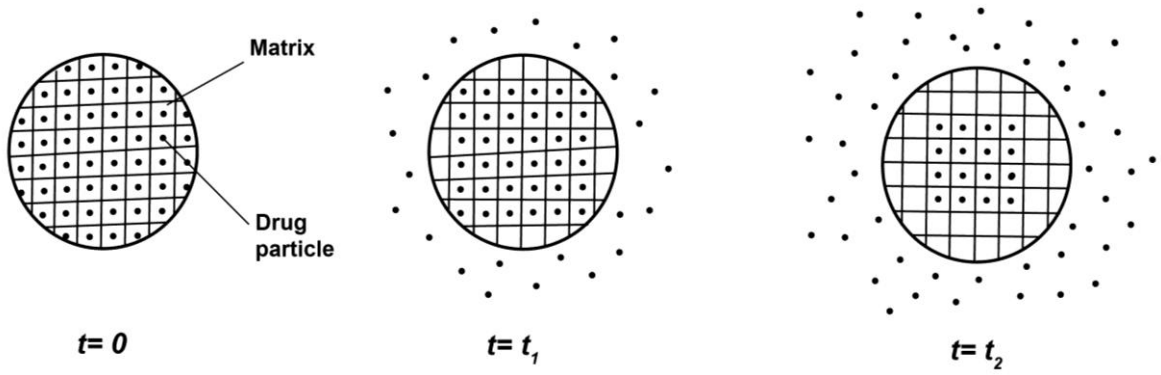

Figure 4.2 Schematic representation of API release from diffusion-based matrix tablet (Adapted from [188])

4.2.3 Erosion-controlled systems

Erosion-controlled systems typically consist of a drug dispersed or dissolved throughout a polymeric matrix [21,188]. The matrix may consist of lipids, waxes or gel-forming polymers such as hydroxyethyl cellulose [188]. The mechanism of drug release for erosion-controlled systems generally follows two steps [188]. Initially the API at the surface of the drug-containing matrix is released into the surrounding fluid. Once the API comes into contact with the gastrointestinal fluid it will either dissolve or mix with the fluid, depending on whether it was dispersed or dissolved in the tablet matrix [188,213]. As these processes continue over time the surface of the tablet continuously erodes, resulting in a decrease in tablet weight as shown in Figure 4.3 [188]. The concept of erosion-controlled drug release has been successfully applied to Egalet® erodible delivery systems that can be designed to achieve zero-order or delayed release profiles [10].

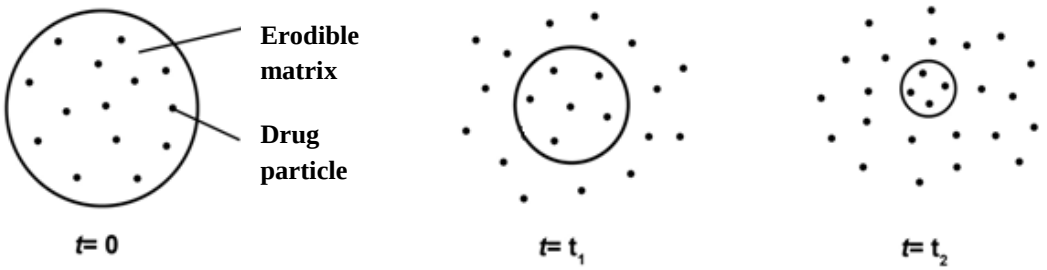

Figure 4.3 Schematic representation of API release from an erosion-based release tablet (Adapted from [188])

4.2.4 Osmotic-controlled systems

Osmosis refers to the movement of water molecules from an area of low solute concentration to an area of high solute concentration through a semi-permeable membrane [10,216] and the process of osmosis has been used as a basis for developing osmotic -driven controlled release systems [21]. The influx of gastric fluid into an osmotic system is propelled by an osmotic pressure gradient between the interior and exterior parts of the dosage form [188,212,215]. Once the gastric fluid has entered the dosage form it dissolves the API, resulting in the formation of a saturated solution on the interior of the dosage form [188]. Thereafter the saturated solution is pumped from the dosage through a single laser-drilled release orifice or through multiple pores located in the semi-permeable membrane surrounding the dosage form [188,212,216].

A schematic illustration of the mechanism of API release from an elementary osmosis-driven system is shown in Figure 4.4. For elementary designs the volume of incoming gastric fluid in the dosage form increases the internal pressure of the entire system and causes the API in solution to be pumped into the bulk gastric fluid [188,212]. However for more advanced systems such as the OROS® push-pull systems developed by ALZA Corporation, a water-swellable polymer is incorporated into the system so as to create an expansion layer that facilitates the pumping process [10,188,212,217]. Once the layer is exposed to water, it swells and occupies a greater volume, pushing the API solution from the dosage form [188,212].

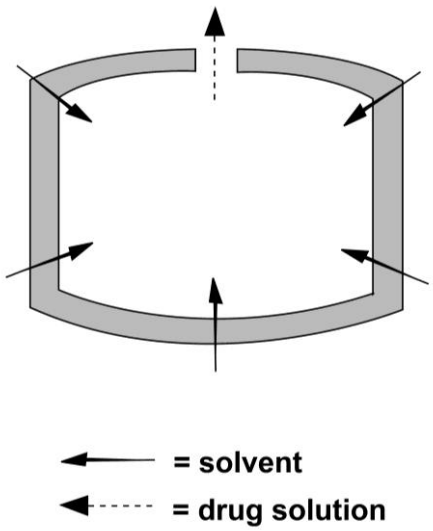

Figure 4.4 Osmotic -controlled release (Adapted from [188])

The concept of osmotic-controlled drug release has been successfully applied to several commercially available products including Tegretol®, Cardura®, Procardia® and Concerta® tablets [10]. Given that the rate-controlling step in these systems is the rate at which the incoming liquid enters the dosage form, the release rate can be approximated using the Lonsdale equation (Equation 4.3) [188]

$$\frac{M}{t} = \frac{CV}{t} \qquad \textbf{(Equation 4.3)}$$

Where

M = Amount of drug
C = Solubility if the drug in the liquid
V = Volume of incoming liquid
t = Time

4.2.5 Ion exchange resins

Ion exchange resins are water-insoluble polymeric materials containing anionic, cationic or sulfonic groups located in repeating positions on a resin chain backbone [10,212]. Ion exchange resin-based formulations consist of drug-resin complexes formed by exposing drug molecules to resins of opposite charge for a prolonged period of time [212]. Drug release occurs when ions such as Na^+ or Cl^- replace similarly charged drug molecules from the drug-resin complex and the release rate depends on the ionic strength of the electrolyte solution amongst, other parameters [10]. API release from these systems can be retarded by adding a rate-limiting barrier to the system, and this can be achieved by coating the resin with a water-insoluble polymer such as ethylcellulose [10,212]. The rate at which drug is released from drug-resin complexes is also influenced by the surface area of the resin particles and the cross-linking density [10].

Sriwongjanya and Bodmeier showed that incorporation of ion exchange resins into HPMC-based matrices can modulate the release of propanolol HCl and sodium diclofenac from such systems [218]. Drug-resin complexes are also an effective way of masking the taste of unpalatable drugs, and the slow release mechanism from these systems can, in some cases, minimize gastric irritation [10]. Ion exchange resin-based formulations also provide an alternative method for delivering individualized doses of a molecule [10].

4.3 PROPOSED FORMULATION

4.3.1 Background

The oral route of administration is convenient and is the most widely used route for drug delivery [10]. However variations in gastric emptying time is of major concern as they may lead, in some cases, to incomplete drug release from a dosage form and ultimately result in reduced therapeutic efficacy [212,219]. It is therefore evident that there is a need for site-specific oral drug delivery systems such as gastroretentive devices to overcome the challenges associated with oral delivery in order to optimise drug delivery [212,220].

Gastroretentive devices are designed to remain in the stomach following oral administration and are particularly useful for delivering compounds, such as CPT, which are unstable in the alkaline environment of the lower parts of the GIT [221]. Gastroretentive devices are also used to deliver compounds that are poorly soluble at intestinal pH and to enhance the absorption of compounds that are primarily absorbed in the stomach or upper part of the small intestine [221]. The use of gastroretentive devices may also enhance the effectiveness of API that are intended to act locally in the proximal regions of the gastrointestinal tract (GIT) [221].

Gastric retention may be achieved via different mechanisms as shown in Figure 4.5. Gastric retention may be achieved by designing devices such as mucoadhesive systems that adhere to the mucous membranes of the walls of the stomach [188,222]. Alternatively, gastric retention may be achieved by designing dosage forms that expand by swelling or unfolding to a size too large to pass through the pyloric sphincter, or by alteration of the density of dosage forms to promote floating on the surface of the gastric fluids, or retention in the lower parts of the stomach [188,222].

(a) Mucoadhesive system **(b) Expandable system** **(c) Floating system**

Figure 4.5 Schematic illustrations of approaches that may be used to achieve gastro-retention (Adapted from [188])

4.3.2 Rationale

The clinical effectiveness of CPT for the treatment of hypertension, congestive heart failure and diabetic nephropathy is well documented [2,3,53]. CPT has a relatively short half-life of 2 to 3 hours, and typical dosage regimens require administration of CPT every 8 to 12 hours [2]. CPT is therefore a potential candidate for oral controlled drug delivery however the poor stability profile of the molecule and high water solubility present formulation challenges. CPT exhibits optimal stability at pH < 4 and is therefore unstable in intestinal fluids (pH 5-7.4) [5,10]. Therefore the development of a gastro-retentive formulation may be an approach to increasing the residence time of CPT in the stomach, where it is most stable [223]. Oral sustained delivery of CPT from a floating matrix tablet could possibly improve the *in vivo* stability of CPT in addition to slowly releasing the molecule at a desired rate, which may minimize the occurrence of drug-related adverse effects. Therefore the objective of this study was to develop, manufacture and assess sustained release floating CPT tablets.

4.4 EXPERIMENTAL

4.4.1 Method of manufacture

Gastroretentive CPT tablets were manufactured using direct compression, and the compositions of the preliminary formulations used are listed in Table 4.1.

Table 4.1 Tablet composition for preliminary formulations

Ingredient (% w/w)	C1	C2	C3	C4	C5	C6	C7	C8	C9	C10
CPT	14.7	14.7	14.7	14.7	14.7	14.7	14.7	14.7	14.7	14.7
Methocel® K100M	-	60.0		-	30.0	50.0	40.0	40.0	50.0	50.0
Methocel® K15M	-	-	60.0	-	-	-	-	-	-	-
Methocel® K100-LV	-	-	-	60.0	30.0	-	-	-	-	-
Ethylcellulose	-	-	-	-	-	-		20.0	10.0	-
Carbopol® 974P NF	-	-	-	-	-	-	-	-	-	10.0
Avicel® PH-102	67.0	7.0	7.0	7.0	7.0	17.0	27.0	7.0	7.0	7.0
Sodium bicarbonate	15.0	15.0	15.0	15.0	15.0	15.0	15.0	15.0	15.0	15.0
Talc	1.3	1.3	1.3	1.3	1.3	1.3	1.3	1.3	1.3	1.3
Magnesium stearate	1.0	1.0	1.0	1.0	1.0	1.0	1.0	1.0	1.0	1.0
Colloidal silicon dioxide	1.0	1.0	1.0	1.0	1.0	1.0	1.0	1.0	1.0	1.0

Direct compression was selected as the method of manufacture due to its simplicity and to avoid unnecessary exposure of CPT to moisture and heat that would be necessary for a wet granulation process. All formulation components were weighed individually using a Model PM top-loading electronic balance (Mettler® Toledo, Zürich, Switzerland). All excipients excluding magnesium stearate, talc and colloidal silicon dioxide were passed through a 20-mesh screen and blended for 20 minutes in a cube blender rotating at a horizontal angle (100 rpm). Magnesium stearate, talc and colloidal silicon dioxide were passed through a 44-mesh screen and blended with the bulk powder for an additional 3 minutes. A schematic representation of the manufacturing process is given in Figure 4.6.

The homogenous powder blend was fed through a feed hopper and compressed into tablets on a 16-station rotary press (Manesty® B3B, Newcastle, England) equipped with sixteen 9.0 mm flat-faced punch and die sets. To facilitate the manufacture of relatively small batches (300 g) of tablets some of the die cavities were blocked with solid Teflon discs. The target crushing strength of the tablets was between 100 and 140 N. The manufactured tablets were de-dusted under vacuum and stored for 24 hours prior to analysis. A typical example of a batch manufacturing record used to record the manufacturing procedure is included in Appendix I. Tablets from each formulation were assessed as per compendial [12] and non-compendial tests and the results and observations for each batch are included in batch summary records that are included in Appendix II.

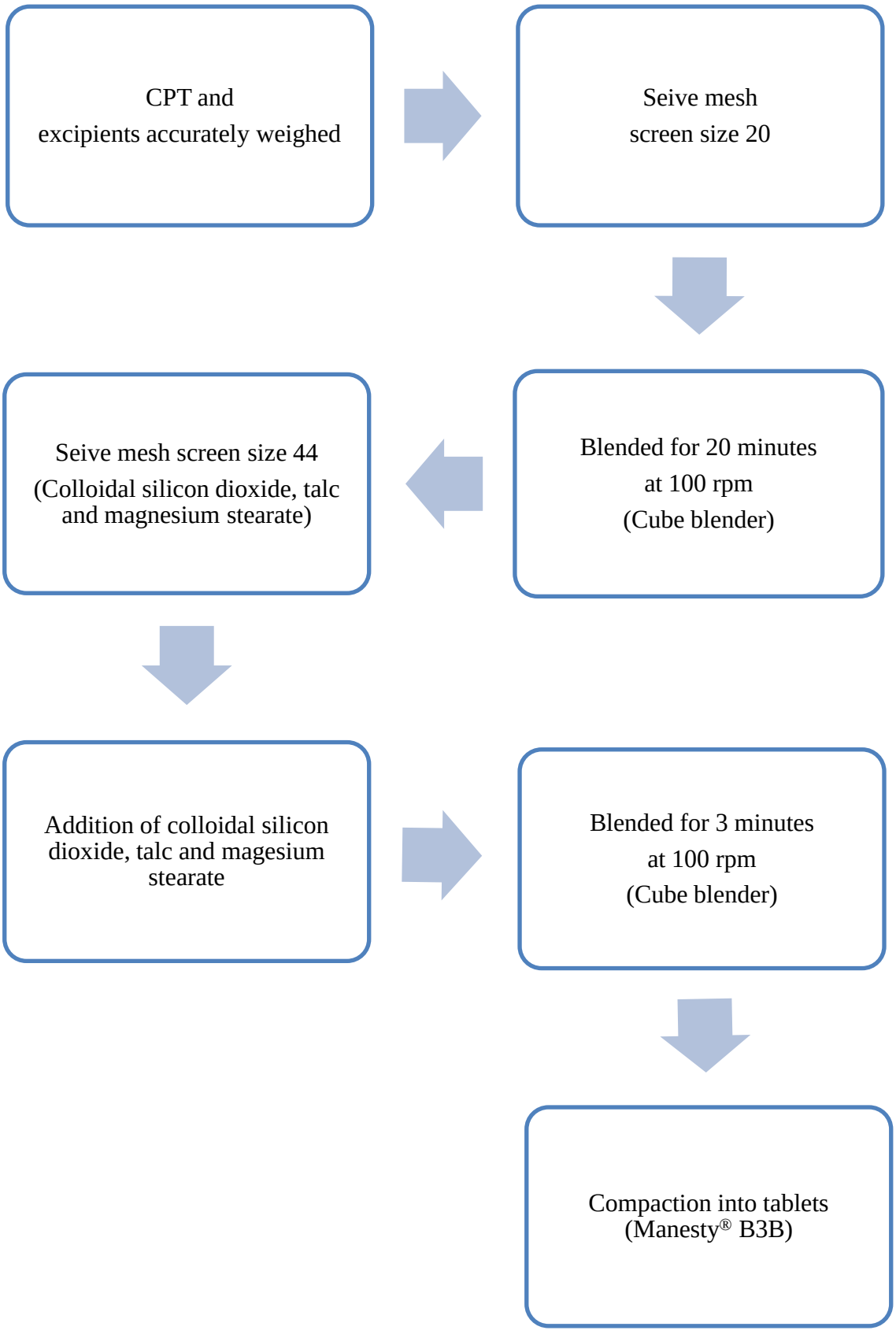

Figure 4.6 Schematic representation of the manufacturing process

4.4.2 Evaluation of tablets

4.4.2.1 Content uniformity

The content uniformity of the tablets was established by determining the amount of CPT in each of 10 randomly selected tablets. Each tablet was individually weighed and pulverized into a fine powder using a mortar and pestle. The powder was quantitatively transferred to a 100 mL A-Grade volumetric flask and made up to volume with phosphate buffer (20 mM, pH 7.0). To ensure complete extraction and dissolution of CPT the mixture was sonicated for 15 min prior to filtration using 0.45 µm hydrophilic PVDF filter membranes. The solution was diluted with running buffer to achieve a final concentration of 50 µg/mL CPT. The IS (1 µg/mL) was added to all test solutions prior to analysis and 0.2% w/v sodium metabisulphite was added to the solutions to offer protection from oxidative degradation.

4.4.2.2 Weight uniformity

The weight uniformity of the tablets was determined by individually weighing 20 randomly selected tablets using a Model AG 135 analytical balance (Mettler® Toledo, Zürich, Switzerland). The average weight of the tablets was recorded and the % deviation from the average mass was calculated.

4.4.2.3 Assay

To estimate the CPT content of the tablets 20 randomly selected tablets were weighed and pulverized to a fine powder using a mortar and pestle. An amount of powder equivalent to the weight of 1 tablet was quantitatively transferred to a 100 mL A-Grade volumetric flask and made up to volume with phosphate buffer (20 mM, pH 7.0). To ensure complete extraction and dissolution of CPT, the mixture was sonicated for 15 min prior to filtration using 0.45 µm hydrophilic PVDF filter membranes. Prior to analysis using the CZE method described in Chapter 2, the solution was diluted with running buffer to achieve a final concentration 50 µg/mL of CPT. The IS was added to all test solutions prior to analysis and 0.2% w/v sodium metabisulphite was added to the solutions to offer protection from oxidative degradation.

4.4.2.4 Crushing strength and tensile strength

The crushing strength of 20 randomly selected tablets was determined using a Model PTB 311 E Hardness Tester (PharmaTest AG®, Hamburg, Germany) and the tensile strength was calculated using Equation 4.4 [224].

$$\sigma = \frac{2F}{\pi dT} \quad \textbf{(Equation 4.4)}$$

Where

σ = Maximum radial tensile strength (N/mm^2)
F = Crushing strength (N)
d = Tablet diameter (mm)
T = Tablet thickness (mm)

4.4.2.5 Friability

The friability of the tablets was determined using an Erweka® TA3R Friability Tester (Erweka®, GmbH, Heuseustamm, Germany) rotating at a rate of 25 revolutions/min for 4 min. Twenty tablets were randomly selected, weighed and placed into the friabilator drum for 100 revolutions, after which the tablets were de-dusted, reweighed and the % weight loss after rotating was calculated .

4.4.2.6 *In vitro* buoyancy testing

The floating behaviour of 6 randomly selected tablets from each formulation was determined using the method described by Rosa *et al.* [225]. Each tablet was placed in a glass beaker containing 100 mL of 0.1 M HCl and the floating lag time (FLT) was recorded as the time required for the tablet to rise to the surface and float. The total floating time (TFT) for each batch was also recorded.

4.4.2.7 *In vitro* release studies

In vitro release studies (n=6) were performed using a Hanson Model No 73-100-104 USP Apparatus 2 (Hanson Research, Chatsworth, CA, USA) coupled with an auto sampler purchased from the same source. The dissolution medium (900 mL, 0.1 M HCl, pH 1.2, enzyme free) was continuously stirred at 50 rpm and the temperature was maintained at 37 ±

0.5°C. Samples (5 mL) were withdrawn and filtered through 10 µm filter membranes at 0.5, 1, 2, 4, 6, 8, 10 and 12 hours after dropping the tablets. The volume of sample withdrawn was replaced with an equivalent volume of fresh dissolution medium. The samples were analysed for CPT content and *in vitro* release profiles of the cumulative % of CPT released over time were plotted. Blank measurements were taken to check the efficiency of cleaning to verify that the system was clean. Since dissolution testing was performed under acidic conditions the degradation of CPT to yield captopril-disulphide was not expected to occur during dissolution testing. The aim of this study was to manufacture CPT tablets that released CPT over a 12 hour period and remained afloat for the duration of the dissolution test. At least 85% of the CPT in the tablets was expected to be released at the end of dissolution testing.

4.5 RESULTS AND DISCUSSION

4.5.1 Physical appearance

The tablets that were manufactured were slightly off-white with flat and smooth surfaces. There was no evidence of capping, lamination, breaking or chipping for any of the formulations tested.

4.5.2 Content uniformity

Each tablet was manufactured to contain 50 mg of CPT and the average CPT content for all test formulations varied between 47.91 and 49.74 mg. The data are summarized in Table 4.2. The amount of CPT in each tablet was within ± 5% of the average amount, thus the results indicate good uniformity and suggest that minimal variability in the CPT content of the final product can be expected.

Table 4.2 Content uniformity data of CPT sustained release tablets

Formulation	Theoretical amount (mg)	Average actual amount for ten tablets (mg)	% RSD
C1	50	48.63	1.25
C2	50	49.74	3.18
C3	50	48.21	2.76
C4	50	48.36	1.49
C5	50	49.39	3.03
C6	50	48.59	2.72
C7	50	49.71	2.84
C8	50	48.57	3.14
C9	50	48.48	4.33
C10	50	47.91	3.84

4.5.3 Weight uniformity

The tablet weight for the different formulations varied between 332 mg ± 3.12 and 345.90 mg ± 1.64 and low values of standard deviation indicated acceptable weight uniformity (Table 4.3). The weight of the tablets met compendial requirements as indicated by the values of weight variation which were within the range of ± 5%.

4.5.4 Assay

The content of CPT for each test formulation expressed as a % of the theoretical amount of CPT following assay are summarized in Table 4.3. The data reveal that the tablets contained between 96.8% ± 3.95 and 101.6% ± 1.17 of the label claim. The results comply with compendial specifications for the analysis of tablets and further confirmed the precision of the manufacturing method.

4.5.5 Crushing strength and tensile strength

The tablet crushing strength ranged between 91.3 N ± 1.93 and 139.9 N ± 1.13 (Table 4.3) and the tensile strength of the tablets ranged from 1.15 N/mm^2 ± 1.87 to 1.75 N/mm^2 ± 1.93 (Table 4.3). Values of tensile strength that are ≥ 1 N/mm^2 may be considered acceptable for small batches of tablets that are not exposed to large mechanical stresses [190,226].

Therefore these findings suggest that a direct compression approach may be used for the manufacture of CPT tablets that would withstand abrasive forces during manufacturing, packaging and transportation.

4.5.6 Friability

Tablets are subjected to various forces during manufacturing, packaging and transportation which may cause them to chip or break and result in reduced quality, dose and aesthetic appeal [187]. Friability testing was therefore performed to establish the combined effects of attrition and shock on the test tablets. The percent weight loss for all tablet formulations was < 1%, indicating good mechanical resistance.

Table 4.3 Physicochemical assessment of CPT sustained release tablets

Formulation	Thickness (mm)	Crushing strength (N)	Tensile strength (N/mm^2)	Weight (mg)	Friability (%)	CPT content (%)	FLT (min)	TFT (hours)
C1	5.67 ± 1.81	112.9 ± 6.86	1.31 ±1.74	338.85 ±1.30	0.143 ± 3.02	100.1 ± 1.12	-	-
C2	5.69 ± 1.42	114.5 ± 6.56	1.42 ± 3.68	345.90 ± 1.64	0.186 ± 1.14	99.3 ± 1.45	16.2 ± 3.63	> 12
C3	5.62 ± 0.57	91.54 ± 2.79	1.18 ± 2.19	342.50 ± 2.27	0.161 ± 2.39	98.7 ± 2.36	15.3 ± 4.08	> 12
C4	5.73 ± 1.48	108.3 ± 4.90	1.40 ± 3.54	332.16 ± 3.12	0.164 ± 1.57	97.5 ± 2.97	15.2 ± 3.27	> 12
C5	5.63 ± 1.79	99.8 ± 3.29	1.28 ± 1.71	339.92 ± 1.02	0.177 ± 2.76	99.6 ± 3.04	8.0 ± 4.53	> 12
C6	5.63 ± 2.29	106.7 ± 4.72	1.39 ± 2.32	336.95 ± 1.94	0.159 ± 1.46	101.6 ± 1.17	11.3 ± 4.68	> 12
C7	5.77 ± 1.36	91.3 ± 1.93	1.15 ± 1.87	340.75 ± 1.24	0.148 ± 2.25	98.1 ± 2.77	11.9 ± 3.96	> 12
C8	5.59 ± 3.12	117.8 ± 2.51	1.52 ± 2.61	337.55 ± 2.28	0.187 ± 1.69	96.8 ± 3.95	4.1 ± 4.78	> 12
C9	5.65 ± 2.46	98.6 ± 4.27	1.26 ± 3.43	339.89 ± 2.11	0.173 ± 3.04	98.2 ± 1.24	1.1 ± 2.05	> 12
C10	5.71 ± 1.79	139.9 ± 1.13	1.75 ± 1.93	338.42 ± 3.43	0.168 ± 2.38	97.8 ± 2.55	24.4 ± 2.71	> 12

* All values are expressed as a mean ± % RSD

4.5.7 *In vitro* buoyancy testing

The proposed design for these tablets was a single unit matrix tablet that achieves *in vitro* buoyancy based on effervescence. The formula for the tablets contained 50 mg CPT, HPMC as a hydrophilic matrix former, MCC as a filler, sodium bicarbonate as an effervescent agent, magnesium stearate as a lubricant and talc and colloidal silicon dioxide as glidants.

On exposure of the tablets to the dissolution medium (0.1 M HCl) the HPMC hydrates to form a gel layer around the tablets. As HCl penetrates the tablets a neutralization reaction occurs between HCl and sodium bicarbonate and CO_2 is released into the HPMC gel layer. The gas entrapped in the gel layer decreases the density of the tablets to < 1 g/mL which promotes an upward motion of the tablets and maintains buoyancy. MCC was selected as the filler since it forms matrices of a highly porous nature and has been reported to retain air and promote floatation [227].

All formulations with the exception of formulation C1 achieved *in vitro* buoyancy within 25 min and remained afloat for up to 12 hours. Formulation C1 did not contain any HPMC, therefore any CO_2 that may have been generated was liberated immediately into the surrounding medium as there was no gel layer to entrap the gas and facilitate flotation.

The effect of different amounts of sodium bicarbonate on the floating behaviour of formulation C2 was investigated by manufacturing batches C2a and C2b, that contained 5% w/w and 10% w/w sodium bicarbonate respectively. Decreasing the concentration of sodium bicarbonate from 15% w/w to 5% w/w resulted in an increase of the FLT from approximately 16 min to >30 min. Consequently, the level of sodium bicarbonate in the formulation was maintained at 15% w/w for all subsequent batches. The effect of different viscosity grades of Methocel® on performance was unclear since formulations manufactured with Methocel® K100M, K15M and K100-LV Premium exhibited similar FLT (Table 4.3).

4.5.8 *In vitro* release studies

All manufactured formulations were subjected to *in vitro* dissolution testing using 0.1 M HCl as the dissolution medium. The studies were conducted over 12 hours and the cumulative % CPT released was recorded as a function of time and used to generate CPT release profiles.

Formulation C1 showed rapid release of CPT, with close to 100% CPT release in < 2 hours of commencing dissolution testing (Figure 4.7). Formulation C1 contained no rate controlling polymers, therefore drug release is rapid. In an effort to retard CPT release from the tablets HPMC was incorporated into subsequently-manufactured formulations.

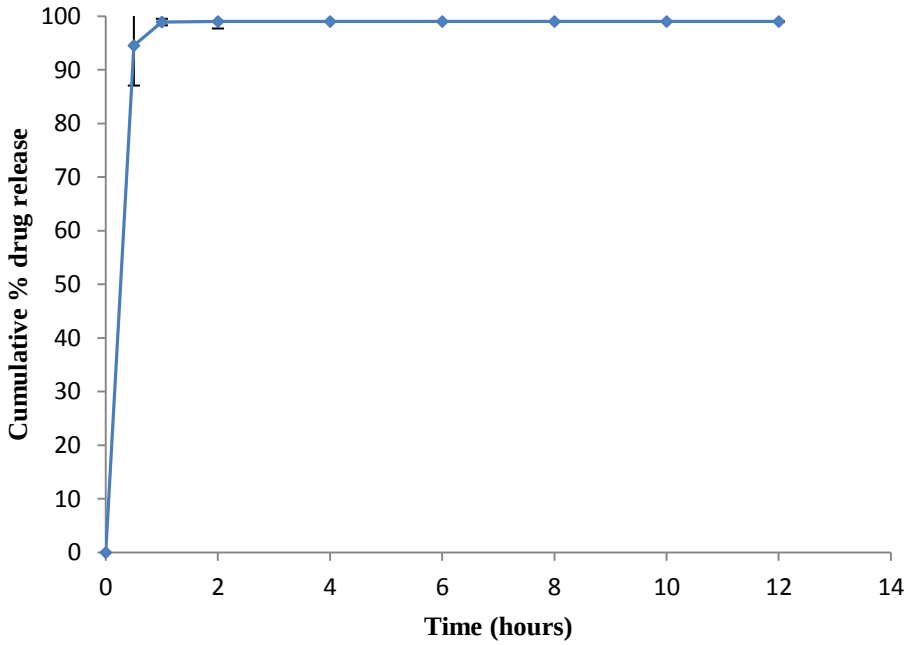

Figure 4.7 CPT release from formulation C1

Methocel® K100M Premium CR was added to formulation C2 as a rate-controlling polymer. The *in vitro* release profile of CPT from formulation C2 is shown in Figure 4.8 and reveals that CPT release after 2 hours of dissolution testing had decreased to 26.8% from the ~100% released in 1 hour from formulation C1. However the total CPT released was incomplete, with only approximately 65.8% released following 12 hours of dissolution testing.

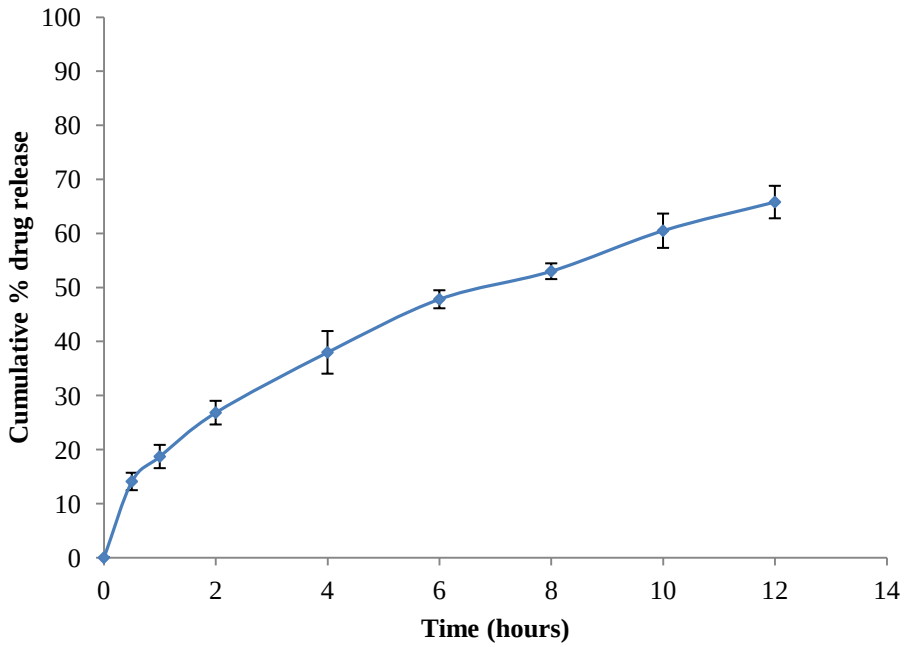

Figure 4.8 CPT release from formulation C2

When tablets manufactured using hydrophilic matrices such as HPMC are exposed to dissolution media the polymer rapidly hydrates and forms a gel layer around the tablet [10,173]. As time elapses the thickness of the gel layer surrounding the tablet increases to form a diffusion barrier to drug release [10,173,228]. The API embedded in the polymer matrix is released into the surrounding fluid by diffusion through the gel layer [10,173]. For water-soluble drugs such as CPT erosion of the HPMC matrix does not impact drug release significantly since the water solubility of the CPT governs release from the matrix [173].

The incomplete CPT release from formulation C2 was below the target of 85% and was therefore not desirable but provided a starting point for developing a more appropriate formulation. Reports from previous work have shown that the type and level of polymer used are key factors influencing drug release [173,229]. Formulations manufactured using high viscosity grades of HPMC have been reported to produce gel layers more resistant to drug release and demonstrate slower release than those manufactured using lower viscosity grades of the polymer [230,231]. Therefore different grades and concentration of Methocel® were approaches used in an attempt to improve the release profile of CPT.

In an attempt to investigate the effect of different grades of Methocel® on the release of CPT, and to increase the extent of CPT release, formulation C3 was manufactured using a lower

viscosity grade of Methocel® (K15M Premium CR). CPT release after 2 hours increased to approximately 29.6% and the extent of CPT release also increased to approximately 73.3% after 12 hours (Figure 4.9).

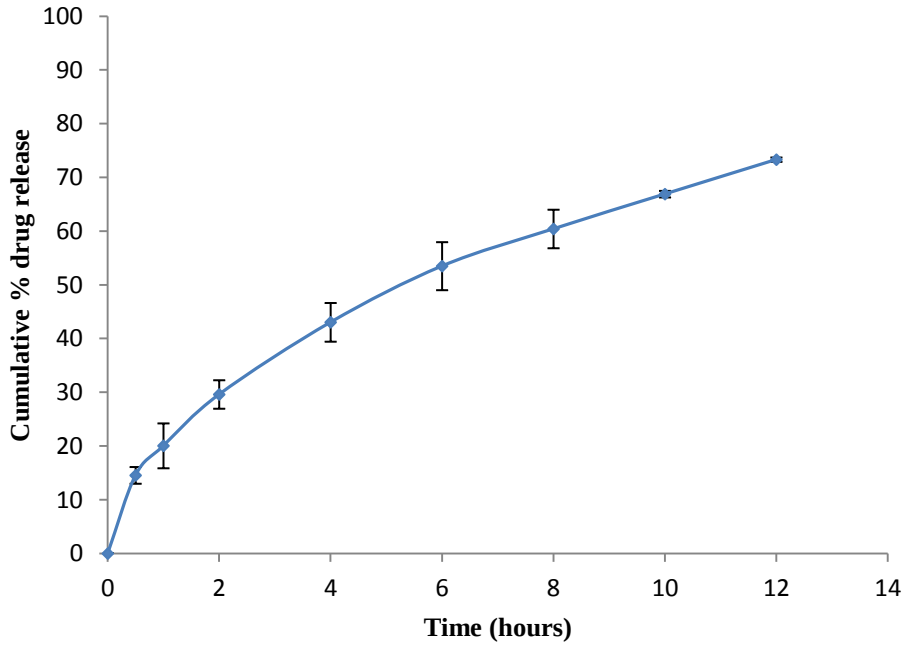

Figure 4.9 CPT release from formulation C3

The CPT release data from formulations C2 and C3 indicated that the use of high viscosity grades of Methocel® (K100M Premium or K15M Premium CR) resulted in slow dissolution of CPT with incomplete drug release after 12 hours. In an effort to increase the % CPT released after 12 hours the effect of using an even lower viscosity grade of Methocel® (K100-LV Premium) was investigated. The release profile for formulation C4 is shown in Figure 4.10 and reveals that the extent of CPT release after 12 hours increased appreciably to approximately 86%. However the % CPT released from the tablets within the first 2 hours of dissolution testing increased to approximately 35.9% compared to < 30% observed for formulations C2 and C3.

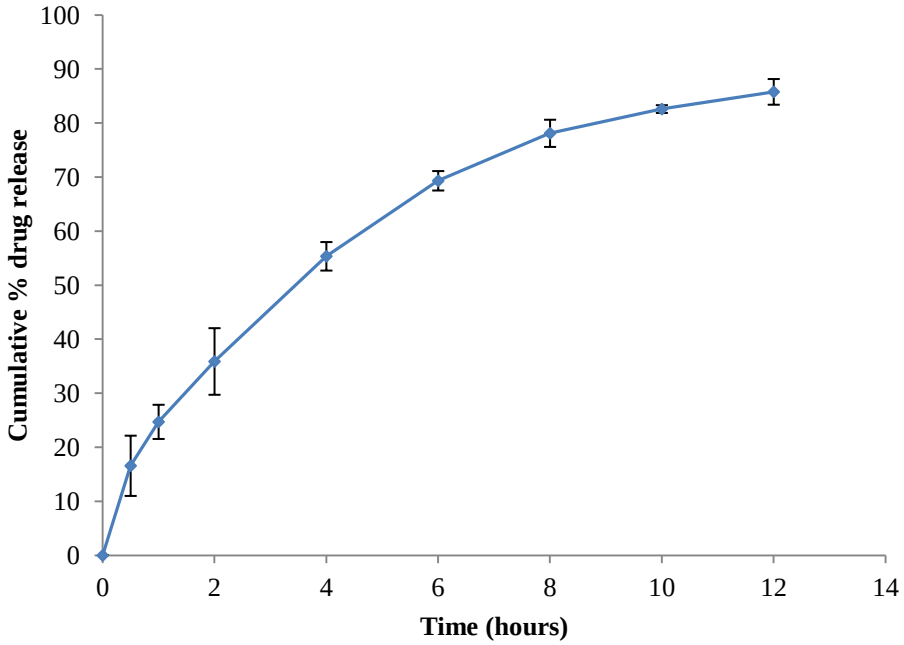

Figure 4.10 CPT release profile from formulation C4

The *in vitro* release behaviour of controlled release formulations can be improved by combining different viscosity grades of Methocel®. Combining high and low viscosity grades of Methocel® has been used as an approach to produce polymer blends with an intermediate viscosity suitable for the modulation of drug release [173,232]. The viscosity of the resultant polymer blend can be calculated using Equation 4.5 [233].

$$V_b^{\frac{1}{8}} = F_1 V_1^{\frac{1}{8}} + F_2 V_2^{\frac{1}{8}} \qquad \textbf{(Equation 4.5)}$$

Where

V_b = Viscosity of the polymer blend (cP)
F_1 = Fraction of polymer 1
V_1 = Viscosity of polymer 1 (cP)
F_2 = Fraction of polymer 2
V_2 = Viscosity of polymer 2 (cP)

In an attempt to modulate the release of CPT a combination of Methocel® K100M Premium CR and K100-LV Premium (1:1 ratio) was investigated. According to the product information supplied by the Dow Chemical company the nominal viscosities of 2% w/v aqueous solutions of Methocel® K100M Premium CR and K100-LV Premium are approximately 100 000 cP and 100 cP at 20°C, respectively [234]. Use of Equation 4.5

suggests that a binary mixture of the two grades of polymer would yield a blend with a viscosity of approximately 6 519.5 cP.

The CPT release profile from formulation C5 is shown in Figure 4.11 and reveals that approximately 30% of CPT was released after 2 hours of dissolution testing and a total of approximately 70% was released in 12 hours. These results indicate that CPT release from a matrix formed using a blend of Methocel® K100M Premium CR and K100-LV Premium was lower than that from a matrix consisting of Methocel® K100-LV Premium only. This is most probably due to an increase in gel strength achieved when low viscosity grade Methocel® K100-LV Premium is combined with a higher viscosity polymer (Methocel® K100M Premium CR).

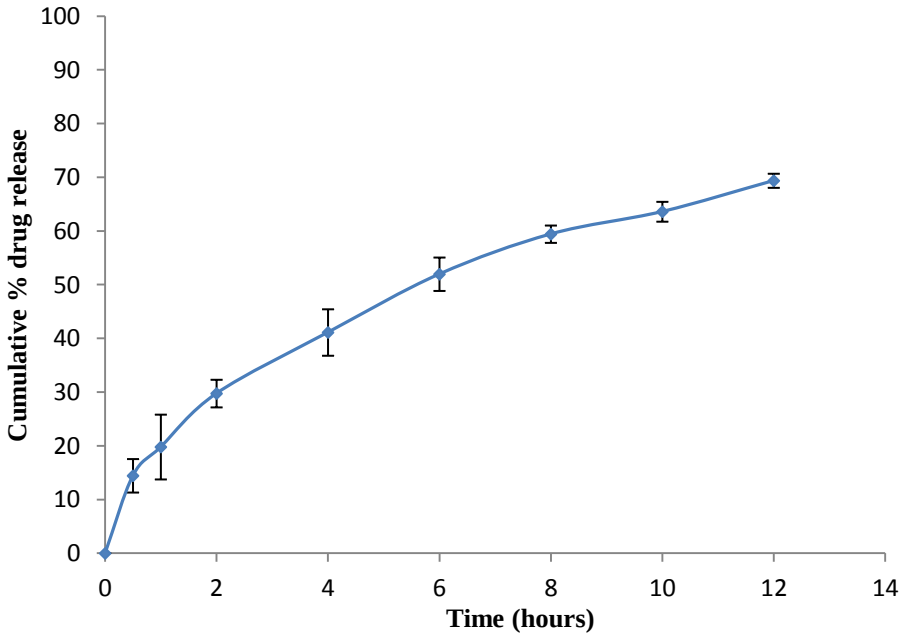

Figure 4.11 CPT release from formulation C5

In an effort to increase the total amount of CPT released after 12 hours of dissolution testing the effect of reducing the concentration of Methocel® K100M in the formulation was investigated. The amount of Methocel® K100M in formulation C6 was reduced to 50% w/w as opposed to the 60% w/w used for formulation C2. The reduction in polymer level resulted in an appreciable increase in the extent of CPT release, to approximately 76.5% after 12 hours of dissolution testing in contrast to the 65.8% observed for formulation C2. However

the reduction in polymer level did not affect CPT release after 2 hours of dissolution testing as it remained at approximately 26.9% (Figure 4.12).

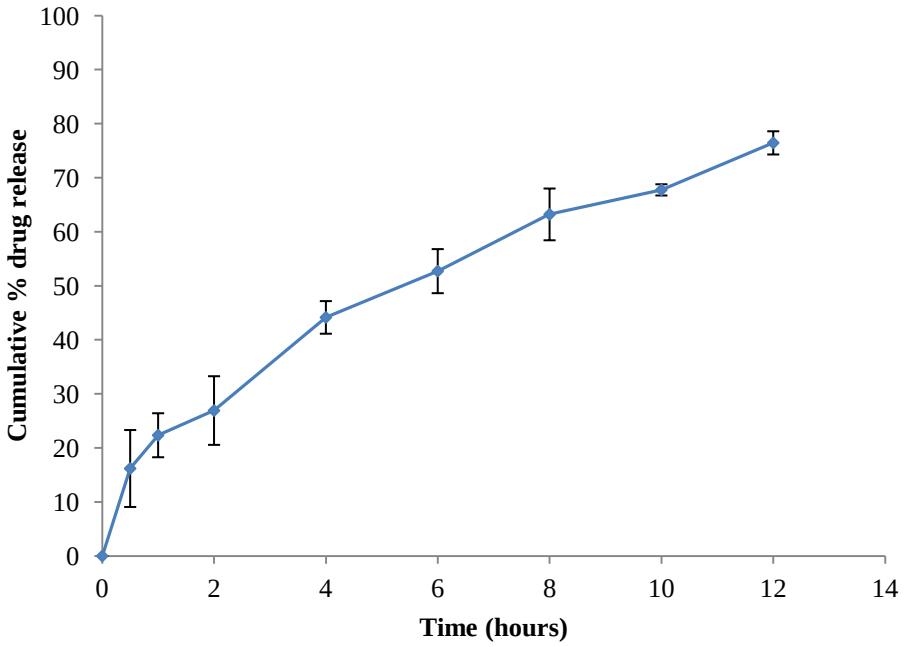

Figure 4.12 CPT release from formulation C6

Although reducing the polymer level in formulation C6 improved the extent of CPT release from the tablets, CPT release after 12 hours of testing was still incomplete. Therefore the concentration of Methocel® K100M was reduced further to 40% w/w in an attempt to increase the extent of CPT release from the tablets. The dissolution profile of CPT from formulation C7 is shown in Figure 4.13 and reveals that the extent of CPT release improved appreciably to approximately 87.5% following 12 hours of dissolution testing. However this was accompanied by a slight increase in CPT release after 2 hours to approximately 32.9%. Formulation C7 produced a sustained release profile for CPT with > 85% of CPT released after 12 hours of dissolution testing and was therefore considered as a starting point for optimisation of the formulation.

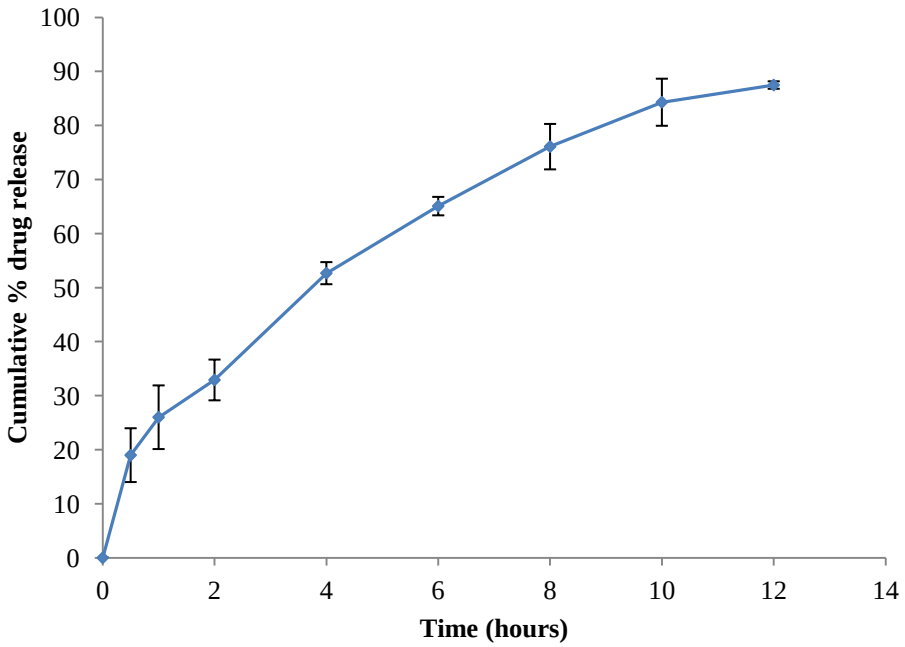

Figure 4.13 CPT release from formulation C7

An initial burst release effect in API release is commonly observed when highly water-soluble drugs such as CPT are incorporated into HPMC-based matrices [173]. The high water solubility of the drug causes the drug molecules at and near the surface of the tablet to rapidly dissolve before a gel layer that is strong enough to create a barrier to release can be formed [232]. Previous studies have shown that inclusion of water-insoluble polymers such as ethylcellulose in HPMC-based matrices can decrease the initial burst release observed for such systems[173]. The presence of a water-insoluble polymer decreases the rate at which the matrix can hydrate and therefore the rate at which the API diffuses from the polymer matrix into the surrounding fluids is decreases [173].

In an effort to reduce the initial release of CPT from the tablets, formulation C8 was manufactured using a combination of Methocel® K100M and 20% w/w ethylcellulose. The *in vitro* release profile of CPT from formulation C8 shown in Figure 4.14 reveals a slight decrease in the amount of CPT released during the first hour of dissolution testing to approximately 21%. However CPT release after 2 hours of dissolution testing was similar to that observed for the formulations which did not contain ethylcellulose. In addition the total amount of CPT released after 12 hours of dissolution testing was incomplete with only 68.7% released in that time.

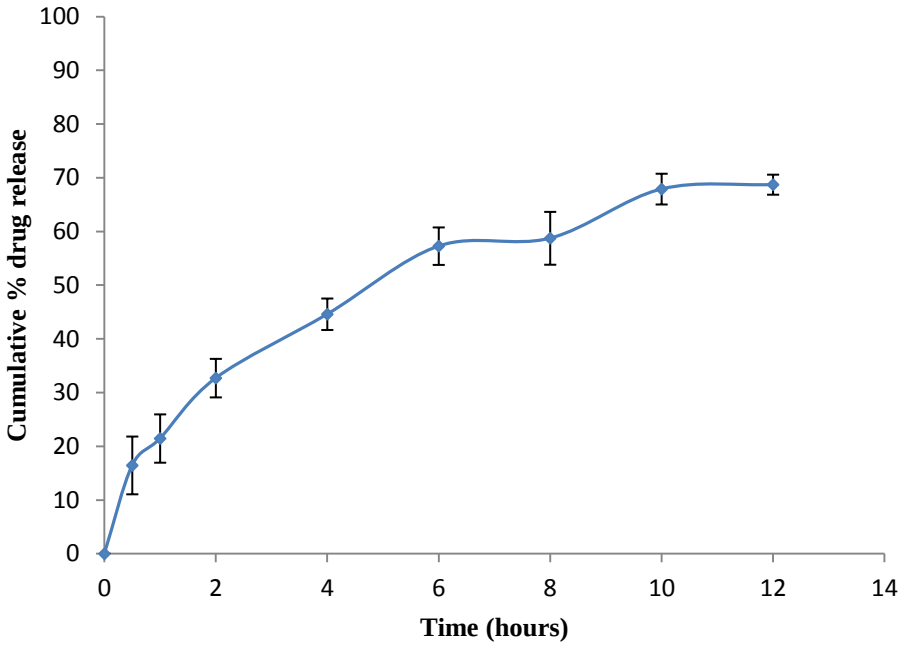

Figure 4.14 CPT release from formulation C8

The concentration of ethylcellulose was reduced to 10% w/ w in an attempt to increase the extent of CPT released from the tablets. An increase in CPT release was observed, with approximately 77.4% CPT released after 12 hours of dissolution testing, as shown in Figure 4.15. However the change in percent CPT released during the first 2 hours was minimal compared to the formulations that did not contain ethylcellulose, therefore this approach to modulate release was not pursued any further.

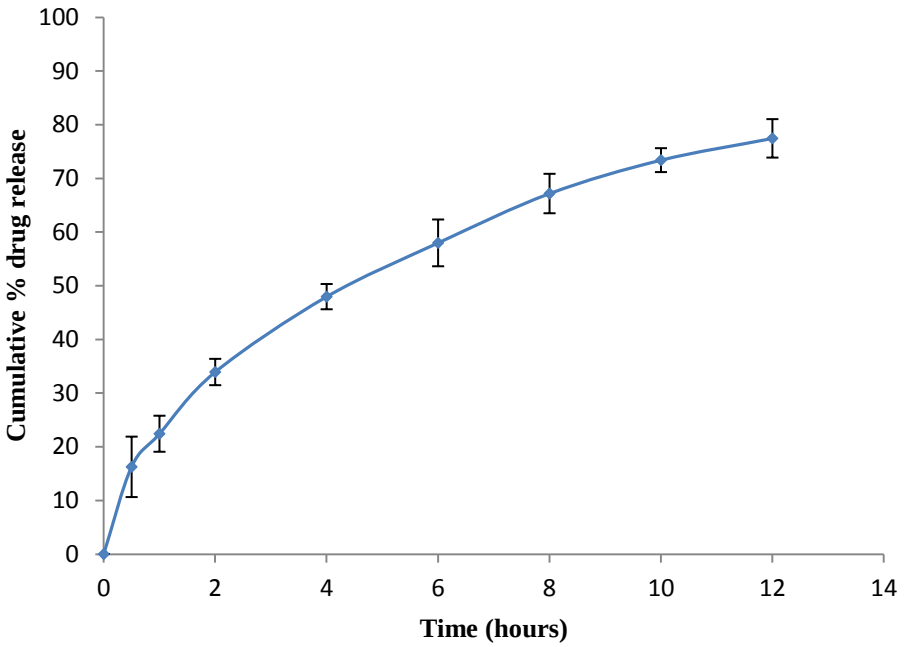

Figure 4.15 CPT release from formulation C9

The addition of ionic polymers such as carbomers to HPMC-based matrices is a well known approach for modulating and optimising drug release in controlled release systems [173]. The polymer is able to modulate drug release and in so doing enhances the function of HPMC as the primary rate-controlling polymer [173]. The augmentation of drug release in these systems may be attributed to the increased strength of the hydrogen bonds between the hydroxyl groups of HPMC and the carboxyl groups of the carbomer used [10,173]. The bonding interaction results in a synergistic increase in the viscosity of the matrix [173]. The presence of a stronger cross-link between HPMC and the carbomer provides a more rigid structure through which the drug must diffuse before liberation into surrounding fluids [173]. Through this approach a more consistent drug release profile can be obtained than when HPMC is used as the only rate controlling polymer in a formulation [173].

The *in vitro* release profile of formulation C10 shown in Figure 4.16 reveals that incorporation of Carbopol® 974P NF at a level of 10% w/w resulted in approximately 26.5% CPT release after 2 hours of dissolution testing, which was similar to what was observed for the formulations containing Methocel® only. In addition, incomplete release of CPT was observed with approximately 66.7% released. The inclusion of Carbopol® 974P NF into the formulation also resulted in considerable fluctuations in the CPT released from individual tablets and in longer FLT, and this approach was therefore not investigated further.

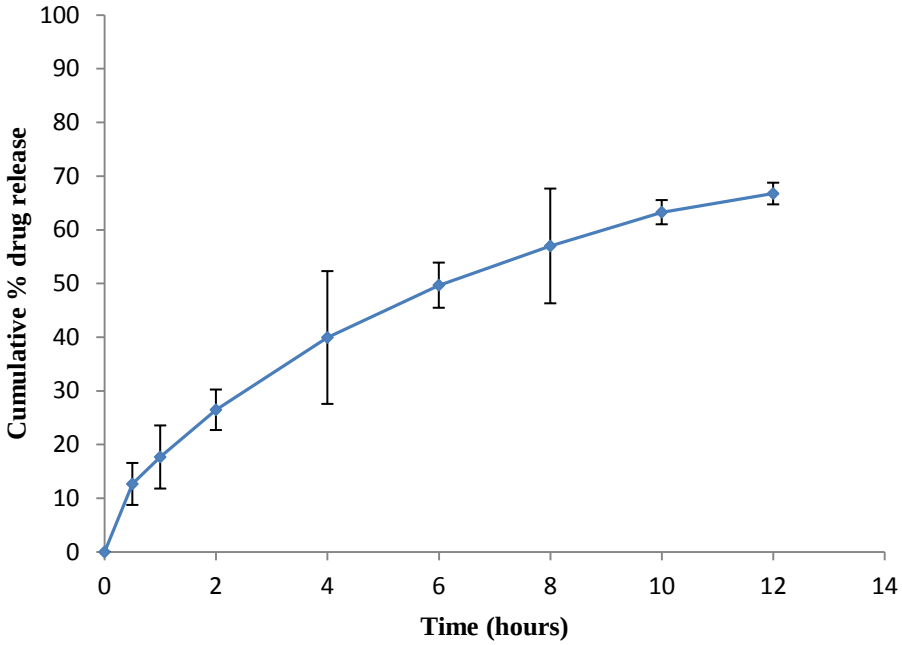

Figure 4.16 CPT release from formulation C10

4.6 CONCLUSIONS

A gastroretentive formulation of CPT was manufactured in an attempt to circumvent the instability of CPT in the alkaline environment of the lower GIT. The direct compression approach was successfully used to manufacture tablets that met compendial specifications with regard to weight uniformity, content uniformity and friability. All formulations were subjected to *in vitro* buoyancy testing, and the results revealed that all the formulations with the exception of formulation C1 achieved *in vitro* buoyancy within 25 minutes and maintained *in vitro* buoyancy for up to 12 hours.

All formulations were manufactured with an HPMC-based matrix and the effect of different grades of HPMC on CPT release was investigated. The results indicate that different HPMC grades influence the *in vitro* release behaviour of CPT from hydrophilic matrices. Formulations manufactured using high viscosity grades of HPMC exhibited lower percent CPT released after 12 hours of dissolution testing when compared to formulations containing lower viscosity grades of the polymer. The effect of varying the HPMC content in formulations was also studied and the results reveal that reducing the HPMC content resulted in an increase in the cumulative % of CPT released after 12 hours of dissolution testing.

The effect of combining water-insoluble and ionic polymers with HPMC was also investigated. Formulations containing a combination of HPMC and ethylcellulose exhibited slower CPT release in the first hour of dissolution testing, however the % of CPT released after 2 hours was similar to that observed for formulations which did not contain ethylcellulose. In addition extent of CPT released from these systems was low, with incomplete release observed after 12 hours of dissolution testing. Combining HPMC with carbomer modulated drug release, however there were considerable fluctuations in CPT release from the individual tablets tested with longer FLT.

Formulation C7 achieved *in vitro* buoyancy rapidly and maintained the buoyant properties for up to 12 hours. Furthermore a sustained release profile with approximately 87.5% of CPT released after 12 hours of dissolution testing was also observed, and this formulation was therefore selected for further optimisation.

CHAPTER 5

FORMULATION OPTIMISATION AND MATHEMATICAL MODELLING OF CAPTOPRIL RELEASE

5.1 INTRODUCTION

RSM has been successfully applied to the development and optimisation of pharmaceutical formulations [235-240]. Some areas of application of RSM include screening of a large number of factors to identify those that have a significant effect on responses and establishing individual and/or the combined influence of input variables on responses [116,241]. In addition RSM can be used to predict a response within a specific experimental domain and identify a combination of input variables that will produce an optimal response [116-118,121]. In comparison to the traditional univariate approach the use of RSM simplifies the experimental process by establishing a mathematical relationship between input variables and resultant responses [116-118,121]. This approach requires fewer experiments to be undertaken and is generally more cost-effective as it minimizes the time and resources required during formulation development and optimisation studies [116,242].

The objective of this study was to use RSM to investigate the effects of formulation variables on the release of CPT from gastroretentive sustained release tablets described in Chapter 4, and to identify the combination of excipient levels required to produce predictable and optimal CPT release.

5.2 EXPERIMENTAL

5.2.1 Materials and Methods

The materials and methods used were described in § 4.4.1.

5.2.2 Experimental design

A RSM approach with CCD was used to study the effect(s) of formulation variables on *in vitro* release of CPT and to optimise the tablet formulation. A CCD normally has several

axial points located outside the cubic design, provided that the axial distance from the centre point (alpha) is not set at $\alpha \leq 1$ [243]. The value of α for a three-factor design was maintained at the default value of $\alpha = 1.68$ set by Design Expert® (Version 7.0.1, Stat-Ease Inc., Minneapolis, MN, USA) statistical software. An α value of 1.68 ensured that the design was rotatable and had the potential to make adequate predictions at points located at the same distance from the centre point [243]. On the basis of a study in which the influence of formulation variables on CPT release was undertaken, Methocel® K100M (X_1), Avicel® PH-102 (X_2) and sodium bicarbonate (X_3) content in the formulations were considered key variables for the optimisation of the tablet formulation. Each factor was studied at five levels *viz.* low (-1), medium (0), high (+1), -α, +α and in replicate (n=5) at the centre point (0,0). The upper and lower limits selected for the independent factors are listed in Table 5.1. All other formulation and processing parameters were kept constant throughout the study. The cumulative % CPT released after 0.5 hours (Y_1), 2 hours (Y_2), 6 hours (Y_3), 12 hours (Y_4) and the FLT (Y_5) were selected as response variables to be studied.

Table 5.1 Translation of the coded levels used in CCD

Independent factors (% w/w)	**Low value (-1)**	**Centre (0)**	**High value (+1)**
Methocel® K100M	32.5	37.5	42.5
Avicel® PH-102	17.5	22.5	27.5
Sodium bicarbonate	10	15	20
Response factors		**Constraints**	
Y_1 = Release after 0.5 hour		Minimal	
Y_2 = Release after 2 hours		Minimal	
Y_3 = Release after 6 hours		50 – 65 %	
Y_4 = Release after 12 hours		> 85 %	
Y_5 = FLT		Minimal	

The experiments were performed in a random order using the conditions listed in Table 5.2 to avoid systematic error and the introduction of bias. The previously described statistical software was used to analyse the data generated from twenty experiments. ANOVA was used to analyse the data and calculate the significance and relevance of the critical factors for each model.

Table 5.2 Actual experimental conditions for the CCD

Formulation	Run	X_1	X_2	X_3
C11	9	29.09	22.50	15.00
C12	15	37.50	22.50	15.00
C13	20	37.50	22.50	15.00
C14	13	37.50	22.50	6.59
C15	18	37.50	22.50	15.00
C16	4	37.50	27.50	10.00
C17	1	42.50	17.50	10.00
C18	14	32.50	22.50	23.41
C19	6	37.50	17.50	20.00
C20	8	42.50	27.50	20.00
C21	17	42.50	22.50	15.00
C22	12	37.50	30.91	15.00
C23	3	32.50	27.50	10.00
C24	2	42.50	17.50	10.00
C25	10	45.91	22.50	15.00
C26	5	32.50	17.50	20.00
C27	16	37.50	22.50	15.00
C28	11	37.50	14.09	15.00
C29	19	37.50	22.50	15.00
C30	7	32.50	27.50	20.00

5.2.3 Evaluation of CPT sustained release tablets

All formulations were subjected to compendial [12] and non-compendial testing, previously described in §4.4.2. Following identification of an optimal formulation composition the product was manufactured and subjected to additional testing.

5.2.4 Effect of agitation rate

The effect of varying agitation rate of USP Apparatus 2 on the *in vitro* release profile of the optimised formulation was determined. The agitation rates investigated were 50, 75, and 100 rpm.

5.2.5 Swelling studies

The swelling characteristics of the tablets manufactured using the optimised formula were determined by individually weighing three randomly selected tablets using a Model AG 135 analytical balance (Mettler® Toledo, Zürich, Switzerland). Swelling studies were conducted using a Hanson Model No 73-100-104 USP Apparatus 2 (Hanson Research, Chatsworth, CA, USA). To assess the swelling behaviour of the tablets each tablet was placed in a dissolution vessel containing 900 mL of 0.1 M HCl maintained at 37 ±0.5°C. The tablets were removed from the vessels at predetermined time intervals (2, 4, 6, 8 and 12 hours) and gently blotted with filter paper to remove excess liquid. The tablets were reweighed and the swelling index (SI) was calculated using Equation 5.1 [244].

$$SI = \left[\frac{(W_t - W_0)}{W_0}\right] \quad \textbf{(Equation 5.1)}$$

Where

SI = Swelling index
W_t = Tablet weight at time *t*
W_0 = Initial tablet weight

To investigate the effect of osmolarity on the SI the experiment was repeated using hypo-osmolar (200 mOsm/L), iso-osmolar (308 mOsm/L) and hyper-osmolar (600 mOsm/L) solutions. The effect of pH on the SI was determined using phosphate buffer adjusted to pH 6.4 and 7.4.

5.2.6 Matrix erosion studies

The erosion characteristics of the tablets manufactured using the optimised formula were determined by individually weighing three randomly selected tablets using a Model AG 135

analytical balance (Mettler® Toledo, Zürich, Switzerland). Erosion studies were conducted using a Hanson Model No 73-100-104 USP Apparatus 2 (Hanson Research, Chatsworth, CA, USA). To assess the erosion behavior of the tablets each tablet was placed in a dissolution vessel containing 900 mL o 0.1 M HCl maintained at 37 ±0.5 °C. The tablets were removed from the dissolution vessel at predetermined time intervals (2, 4, 6, 8 and 12 hours) and tray-dried at 60°C until a constant weight was achieved. The dry tablets were reweighed and the % erosion (E_P) of the matrix tablets was calculated using Equation 5.2 [245].

$$E_P = \left[\frac{(W_i - W_d)}{W_i}\right] x\ 100 \qquad \textbf{(Equation 5.2)}$$

Where

E_P = Matrix erosion (%)
W_i = Initial tablet weight
W_d = Dry weight of a tablet weight at time *t*

To study the effect of osmolarity on the % E_P the experiment was repeated using hypo-osmolar (200 mOsm/L), iso-osmolar (308 mOsm/L) and hyper-osmolar (600 mOsm/L) solutions. The effect of pH on the % E_P was determined using a phosphate buffer adjusted to pH 6.4 and 7.4.

5.2.7 Stability testing

The tablets manufactured using the optimised formula were subjected to short-term stability testing for 60 days. They were stored in high-density polyethylene bottles placed in Model KBF-240 Binder® climatic chambers (Binder GmbH® Ltd, München, Germany) maintained at 25°C/60% RH and 40°C/75% RH. The tablets were visually inspected for changes in color, shape and surface texture after 7, 15, 30 and 60 days. The appearance of crystals on the surfaces of tablets and interior surfaces of storage containers has been reported as a sign of tablet instability [21]. Therefore the surfaces of tablets and interior surfaces of storage containers were also inspected on each day of analysis. The physicochemical properties the tablets *viz.* CPT content, weight uniformity, friability, crushing strength, *in vitro* buoyancy and *in vitro* release were also evaluated.

5.3 MATHEMATICAL MODELLING OF CPT RELEASE

5.3.1 Overview

Mathematical models are commonly used to establish the release kinetics of API from modified-release formulations [246]. The information obtained from mathematical modelling describes how the geometry of pharmaceutical dosage form and/or API dissolution influence the release kinetics of the API [246]. Mathematical models are also used to determine mass transport mechanisms that occur in modified-release dosage forms [247].

5.3.2 Zero-order model

The zero-order model describes the ideal drug release kinetics required to achieve prolonged pharmacological effects [247,248]. The zero-order model is applicable to modified release non-disintegrating dosage forms such as coated, osmotic, some transdermal and matrix tablet systems containing API exhibiting poor water solubility [247,248]. This model describes the dissolution profile for which the same amount of API is released per unit time and can be described using the mathematical relationship shown in Equation 5.3 [247,248].

$$Q_t = Q_0 + K_0 t \qquad \textbf{(Equation 5.3)}$$

Where

Q_t = Amount of drug dissolved at time t
Q_0 = Initial amount of drug in the solution
K_0 = Zero-order release rate constant
t = Time

5.3.3 First-order model

First-order kinetic models can be applied to API dissolution from drug delivery systems such as porous matrix systems containing water-soluble API [246,248]. This model represents a system for which the amount of API released from a matrix is proportional to the amount of API remaining at the matrix core, and therefore assumes that the rate of API release decreases over time [248]. First-order kinetics can be expressed using the mathematical relationship shown in Equation 5.4 [248].

$$\ln Q_t = \ln Q_0 + K_1 t \quad \textbf{(Equation 5.4)}$$

Where

Q_t = Amount of drug released at time t
Q_0 = Initial amount of drug in the solution
K_1 = First-order release rate constant
t = Time

5.3.4 Higuchi model

The Higuchi model can be used to describe diffusional release from solid and/or semi-solid matrices containing water-soluble or poorly water-soluble API [247,248]. The model assumes that the initial concentration of API inside the drug delivery system is considerably higher than the solubility of the API [246-249]. This assumption provides the basis for justifying the pseudo-steady state that is assumed when deriving the Higuchi equation [246-249]. The Higuchi model also hypothesizes that API release occurs only in one dimension, thus. edge effects must be insignificant. The model further assumes that the suspended drug particles are finely divided and are significantly smaller in diameter than the thickness of the system [246-249]. The Higuchi model also assumes that the diffusivity of the API is constant, swelling and dissolution of the polymer matrix is negligible and perfect sink conditions are maintained throughout dissolution testing [246-249]. The mathematical equation describing the Higuchi model is shown in Equation 5.5 [250].

$$Q_t = k\sqrt{t} \quad \textbf{(Equation 5.5)}$$

Where

Q_t = Absolute cumulative amount of drug released at time t
k = A constant reflecting the design variables of the dosage form
t = Time

5.3.5 Hixson-Crowell model

The Hixson-Crowell model describes API release from dosage forms exhibiting changes in diameter and surface area during dissolution testing [246,248]. This model can be used to characterise API dissolution from delivery systems such as tablets in which dissolution occurs in planes parallel to the surface of the tablet [246]. It is assumed that if the tablet dimensions are reduced proportionally over time, the initial geometry of the tablet does not

change [246,248]. The basic equation for the Hixson-Crowell model is shown in Equation 5.6 [248].

$$W_0^{1/3} - W_t^{1/3} = K_S t \quad \textbf{(Equation 5.6)}$$

Where

W_0 = Initial amount of drug in the pharmaceutical dosage form
W_t = Amount of drug remaining in the pharmaceutical dosage form at time *t*
K_s = Constant incorporating the surface-volume relation
t = Time

5.3.6 Korsmeyer-Peppas model

The Korsmeyer-Peppas model describes API release from polymeric systems that may release API by more than one mechanism [250]. This model is normally applied to API dissolution data corresponding to up to 60% release and can be described using Equation 5.7 [247,251].

$$\frac{Q_t}{Q_\infty} = kt^n \quad \textbf{(Equation 5.7)}$$

Where

Q_t = Absolute cumulative amount of drug released at time *t*
Q_∞ = Absolute cumulative amount of drug release at infinite time
k = A constant incorporating the structural and geometrical characteristics of the device
t = Time
n = Release exponent

The model proposes that the release exponent (*n*) can be used to characterise different diffusional release mechanisms from polymeric matrices of different geometry [247-249]. The value of *n* is a function of the swelling behaviour of the polymer matrix and the relaxation rate at the swelling front between the gel layer and glassy core of a hydrophilic matrix [250]. In the case of thin films a value of *n* = 0.5 indicates that API release from the system is governed by Fickian diffusion [247,249]. If *n* = 1, the rate of drug release is controlled by swelling and is independent of time *viz.* Case II transport occurs [247,249]. Values of *n* ranging between 0.5 and 1.0 correspond to anomalous (non-Fickian) transport and suggest that both transport mechanisms occur simultaneously [247,249]. An

interpretation of the diffusional release mechanisms from polymeric systems for the Korsmeyer-Peppas model is shown in Table 5.3.

Table 5.3 Interpretation of release exponents for systems of different geometry (Adapted from [247])

Release exponent (*n*)			Drug transport Mechanism*	Rate as a function of time*
Thin films	**Cylinder**	**Sphere**		
0.5	0.45	0.43	Fickian diffusion	$t^{-0.5}$
$0.5 < n < 1.0$	$0.45 < n < 0.89$	$0.43 < n < 0.85$	Anomalous transport	t^{n-1}
1.0	0.89	0.85	Case II transport	Zero-order release
> 1.0			Super Case II transport	t^{n-1}

*Applies to thin films

5.3.7 Approaches for selecting the best-fit mathematical model

Several approaches can be used to identify the mathematical model that best describes a set of dissolution and release data [248]. One approach to determine the goodness of fit involves comparing the R^2 values obtained when the data are fitted to different mathematical models [248]. The model yielding the highest R^2 value is regarded as the best fit model [248]. Other approaches for selecting the best fit model include performing calculations to determine Akaike's Information Criterion (AIC), sum of squares residues (SSR), mean square error (MSE) and the *F*-ratio probability [248]. The model that best described the *in vitro* release of CPT from the gastroretentive sustained release tablets was established by selecting the model that generated the highest R^2 value.

5.4 RESULTS AND DISCUSSION

5.4.1 Central composite design

Design Expert® (Version 7.0.1, Stat-Ease Inc., Minneapolis, MN, USA) statistical software was used to generate mathematical models that best described the relationships between the independent variables and responses. The individual linear effects of the independent variables on responses were denoted by X_1, X_2 and X_3, whereas interactive effects were denoted by coefficients such as X_1X_2 that contain more than one factor. Quadratic relationships were identified by the presence of coefficients with higher-order terms such as X_1^2. The relative influence of the main and interaction effects of the input variables on the responses was determined by analyzing the sign adjacent to each coefficient. A positive sign indicates synergism whereas a negative sign signifies antagonism. For example the negative coefficients for the individual linear effects of Methocel® K100M (X_1) and sodium bicarbonate (X_3) shown in Equation 5.7a indicate that increasing the amount of these excipients in the formulation had an antagonistic effect on response Y_1 (CPT release after 0.5 hour). In contrast the positive coefficient for the linear contribution of Avicel® PH-102 (X_2) signifies a synergistic effect. The mathematical equations generated for all responses in terms of coded and actual factors are shown in Equations 5.8a - 5.12a and 5.8b - 5.12b respectively.

$$\boldsymbol{Y_1} = 17.47 - 2.02X_1 + 1.04X_2 - 0.68X_3 - 1.71X_1X_2 + 0.47X_1X_3 - 0.83X_2X_3 + 1.70X_1^2 + 0.20X_2^2 + 0.51X_3^2$$ **(Equation 5.8a)**

$$\boldsymbol{Y_1} = 75.98038 - 4.25734X_1 + 2.91138X_2 - 0.69230X_3 - 0.068300X_1X_2 + 0.018600X_1X_3 - 0.033200X_2X_3 + 0.068145X_1^2 + 7.91467^{-3}X_2^2 + 0.020215X_3^2$$ **(Equation 5.8b)**

$$\boldsymbol{Y_2} = 35.92 - 6.65X_1 + 0.96X_2 + 0.047X_3 - 3.13X_1X_2 + 0.42X_1X_3 - 0.97X_2X_3 + 3.69X_1^2 + 0.60X_2^2 + 0.29X_3^2$$ **(Equation 5.9a)**

$$\boldsymbol{Y_2} = 194.76672 - 9.84677X_1 + 4.37576X_2 - 0.10100X_3 - 0.12505X_1X_2 + 0.016812X_1X_3 - 0.038778X_2X_3 + 0.14772X_1^2 - 0.024178X_2^2 + 0.011746X_3^2$$ **(Equation 5.9b)**

$$\boldsymbol{Y_3} = 64.23 - 5.93X_1 + 0.67X_2 - 0.32X_3 - 2.60X_1X_2 - 0.37X_1X_3 - 1.78X_2X_3 + 1.22X_1^2 - 0.31X_2^2 + 1.00X_3^2$$ **(Equation 5.10a)**

$$\boldsymbol{Y_3} = 64.23 - 5.93X_1 + 0.67X_2 - 0.32X_3 - 2.60X_1X_2 - 0.37X_1X_3 - 1.78X_2X_3 + 1.22X_1^2 - 0.31X_2^2 + 1.00X_3^2$$ **(Equation 5.10b)**

$$\boldsymbol{Y_4} = 84.76 - 2.14X_1 + 1.20X_2 + 0.57X_3$$ **(Equation 5.11a)**

$$\boldsymbol{Y_4} = 93.68806 - 0.42804X_1 + 0.24040X_2 + 0.11427X_3$$ **(Equation 5.11b)**

$$\boldsymbol{Y_5} = 11.12 - 0.34X_1 - 0.084X_2 - 2.22X_3$$ **(Equation 5.12a)**

$$\boldsymbol{Y_5} = 20.70060 - 0.067942X_1 + 0.01689X_2 + 0.44328X_3$$ **(Equation 5.12b)**

5.4.2 Verification and evaluation of the model for response Y_3

The mean of least squares linear regression method was used to establish the mathematical model that best described the data for each response. The quality of the mathematical model, significance and relevance of independent variables on the responses was determined by ANOVA. The null hypothesis was that no factor effects exist and the alternative hypothesis was that a factor effect existed. By way of example this discussion will focus on the model for CPT release 6 hours after the commencement of dissolution testing (response Y_3). For completeness the response surface plots for responses Y_1, Y_2, Y_4 and Y_5 are reported in Appendix III.

The experimental data were fitted to linear, two-factor interaction (2FI), quadratic and cubic polynomials for all responses. However the results for all cubic models were regarded as 'aliased' since the CCD did not include enough unique design points to allow for all of the terms for a cubic polynomial to be calculated [252]. A summary of the statistics used to select the most suitable model to describe the data for response Y_3 is given in Table 5.4. The quadratic model highlighted, was selected since it generated a Prob > F value < 0.05 and did not show significant lack of fit. The quadratic model also had a high value for R^2 and low values for standard deviation and "PRESS".

Table 5.4 Summary of the model selection process for response Y_3

Sequential model of sum of squares						
Source	**Sum of squares**	**DF**	**Mean square**	**F value**	***p*-value Prob > F**	**Remarks**
Mean vs Total	85 876	1	85 876.72			
Linear vs Mean	487.49	3	162.50	16.65	< 0.0001	
2FI vs Linear	80.64	3	26.88	4.63	0.0206	
Quadratic vs 2FI	**36.59**	**3**	**12.20**	**3.14**	**0.0741**	**Suggested**
Cubic vs Quadratic	29.01	4	7.25	4.40	0.0531	Aliased
Residual	9.88	6	1.65			
Total	86 520.34	20	4326.02			
Lack of fit tests						
Source	**Sum of squares**	**DF**	**Mean square**	**F value**	***p*-value Prob > F**	**Remarks**
Linear	146.55	11	13.32	6.96	0.0221	
2FI	65.91	8	8.24	4.30	0.0624	
Quadratic	**29.32**	**5**	**5.86**	**3.06**	**0.1224**	**Suggested**
Cubic	0.31	1	0.31	0.16	0.7051	Aliased
Pure error	9.58	5	1.92			
Model summary statistics						
Source	**Standard**	**R^2**	**Adjusted R^2**	**Predicted R^2**	**PRESS**	**Remarks**
Linear	3.12	0.7574	0.7119	0.5723	275.27	
2FI	2.41	0.8827	0.8286	0.6430	299.80	
Quadratic	**1.97**	**0.9396**	**0.8852**	**0.6274**	**239.80**	**Suggested**
Cubic	1.28	0.9846	0.9514	0.8732	81.60	Aliased

Analysis of the quadratic model for response Y_3 revealed that the model was significant as indicated by a model *F*-value of 17.27 (Table 5.5). It is unlikely that a Model *F*-value this large can be a consequence of noise as the probability due to noise was only 0.01%. The data also reveal that the individual linear contribution of X_1 was significant as indicated by a *p*-value < 0.05. The cross-contribution of X_1X_2 and X_2X_3 and the quadratic contribution of X_1^2 also had a significant effect on response Y_3. However a *p*-value > 0.05 indicates that the individual contributions of X_2 and X_3 and the cross-contribution of X_1X_3 and the quadratic contribution of X_2^2 and X_3^2 did not have a significant effect on response Y_3 in the ranges investigated. The Prob>F for the entire model was < 0.0001, therefore the null hypothesis can be rejected, indicating that the quadratic model was significant and that there is a factor effect with an overall contribution of terms in the model that have a significant impact on response Y_3.

Table 5.5 ANOVA for the quadratic model for Y_3

Source	Sum of Squares	df	Mean Square	*F*-value	*p*-Value Prob>*F*	Remarks
Model	**604.72**	**9**	**67.19**	**17.27**	**< 0.0001**	**Significant**
X_1	**479.93**	**1**	**479.93**	**123.38**	**< 0.0001**	**Significant**
X_2	6.18	1	6.18	1.59	0.2360	Not significant
X_3	1.38	1	13.92	0.35	0.5650	Not significant
$X_1 X_2$	**54.14**	**1**	**54.14**	**13.92**	**0.0039**	**Significant**
$X_1 X_3$	1.07	1	1.07	0.28	0.6106	Not significant
$X_2 X_3$	**25.42**	**1**	**25.42**	**6.53**	**0.0286**	**Significant**
X_1^2	**21.35**	**1**	**21.35**	**5.49**	**0.0411**	**Significant**
X_2^2	1.43	1	1.43	0.37	0.5579	Not significant
X_3^2	14.52	1	14.52	3.73	0.0822	Not significant
Residual	38.90	10	3.89	3.89	-	-
Lack of fit	29.32	5	5.86	3.06	0.1224	Not significant
Pure error	9.58	5	1.92	-	-	-
Cor total	643.61	19	-	-	-	-

X_1 = % w/w Methocel® K100M; X_2 = % w/w Avicel® PH-102 and X_3 = % w/w Sodium bicarbonate. The missing values indicate that the parameters were not defined.

5.4.3 Diagnostic plots for the model for response Y_3

Model adequacy was tested using a normal probability plot of residuals, a plot of studentized residuals versus predicted values and a Box-Cox plot for power transformation. The analysis of residuals was used to determine the validity and accuracy of the model used. The normal probability plot of residuals shown in Figure 5.1 reveals that the pattern of the residuals is a slightly S-shaped curve and consequently the normality assumption was loosely satisfied in this case.

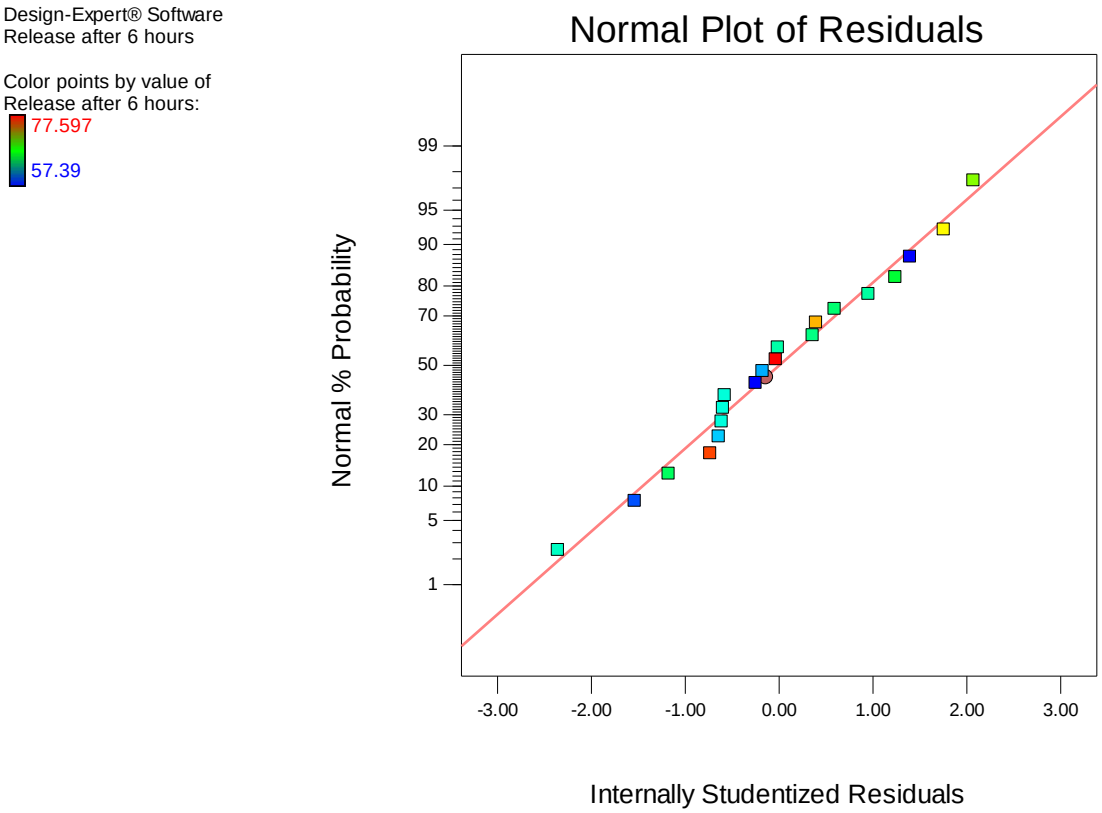

Figure 5.1 Normal plot of residuals for response Y_3

The plot of residuals versus the predicted values for response Y_3 is shown in Figure 5.2. It indicates that no clear pattern exists and that the residuals are almost uniformly scattered above and below the, *y*-axis further suggesting that the model is adequate. As such a violation of independence or a constant variance assumption was not suspected. Outlier points were verified by identifying any data that were scattered beyond the red limit lines indicating that the data fitted the model well. The Box-Cox plot shown in Figure 5.3 has a lambda value of 1, indicating that transformation of the raw data was not necessary.

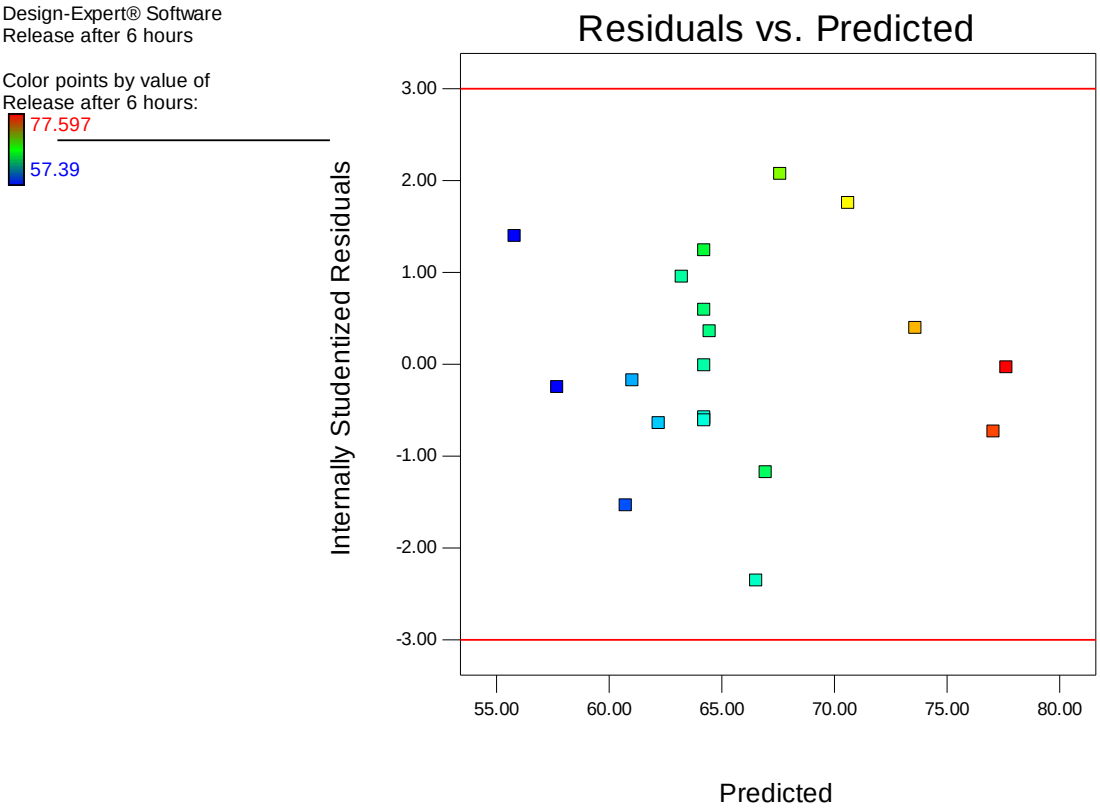

Figure 5.2 Plot of residuals vs. predicted for response Y_3

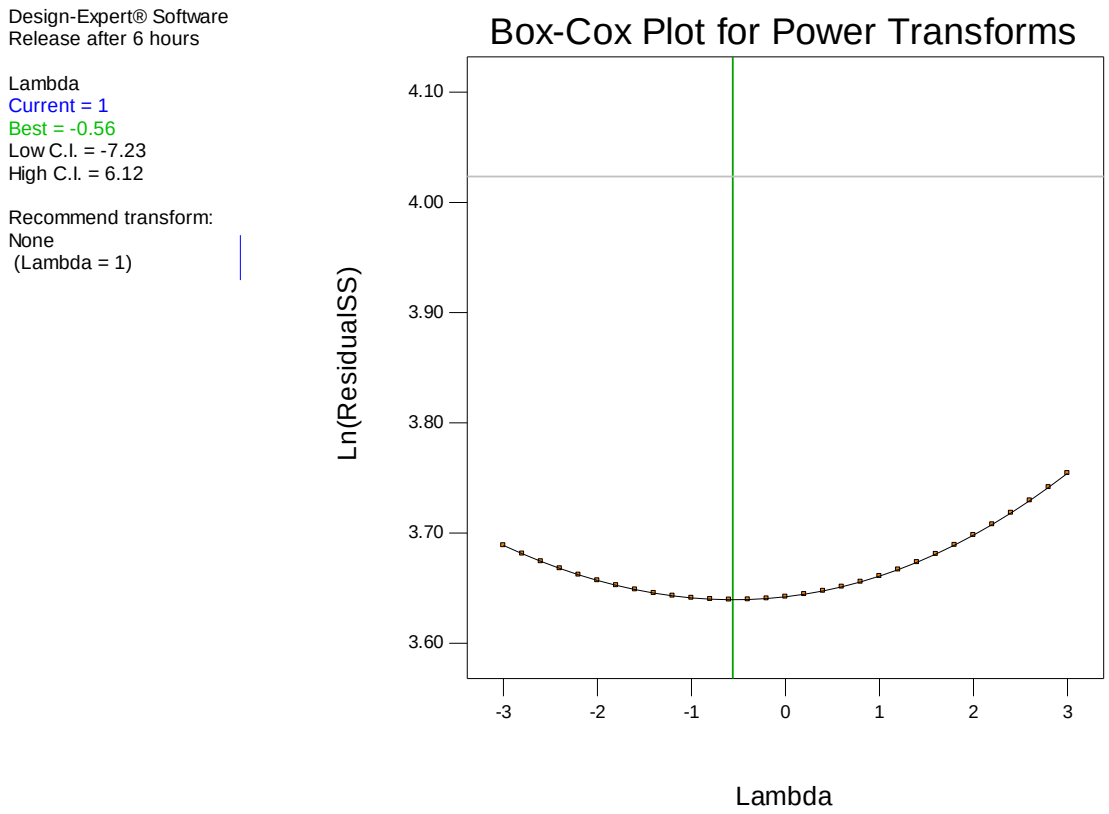

Figure 5.3 Box-Cox plot for response Y_3

5.4.4 Response surface plots for response Y_3

Two-dimensional contour and three-dimensional response surface plots were used to study the interactive effects of input variables on the responses. The contour plot obtained when the concentration of sodium bicarbonate was maintained at 15% w/w reveals that response Y_3 decreases in a non-linear pattern as the Methocel® K100M content in the formulations was increased from 32.5 to 42.5% w/w (Figure 5.4a).

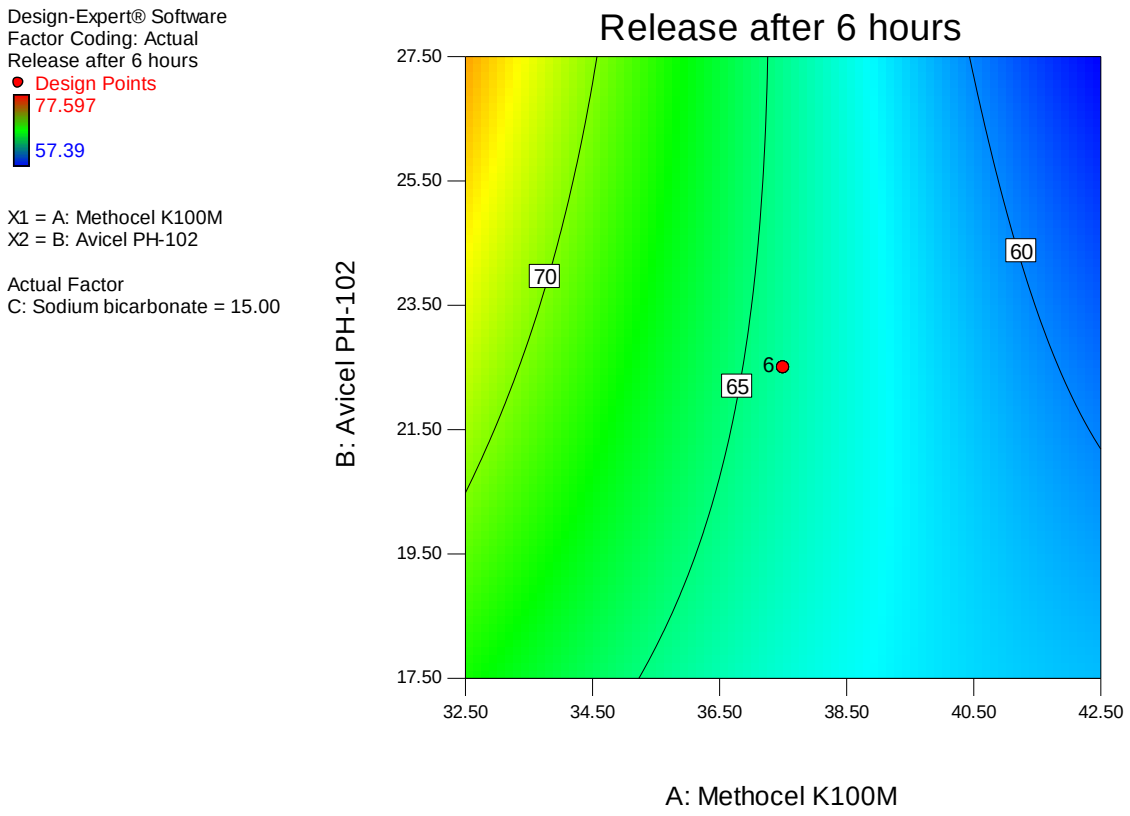

Figure 5.4a Contour plot of the effect of Methocel® K100M and Avicel® PH-102 on CPT release at 6 hours

The corresponding three-dimensional plot shown in Figure 5.4b reveals that CPT release at 6 hours was at its greatest when the content of Methocel® K100M in the formulations was at the lowest level. The effect of Methocel® K100M on response Y_3 appears to be more pronounced than that of Avicel® PH-102. The decrease in % CPT released observed when the content of Methocel® K100M was increased is a result of an increase in the thickness and viscosity of the gel layer that forms around the tablet when hydration occurs, leading to an increase in the diffusional path length that manifests with slow CPT release [253,254]. These observations are in agreement with previous studies reporting that increasing the content of

HPMC in matrix tablets resulted in a decreased rate of API release from hydrophilic matrices [232,255,256].

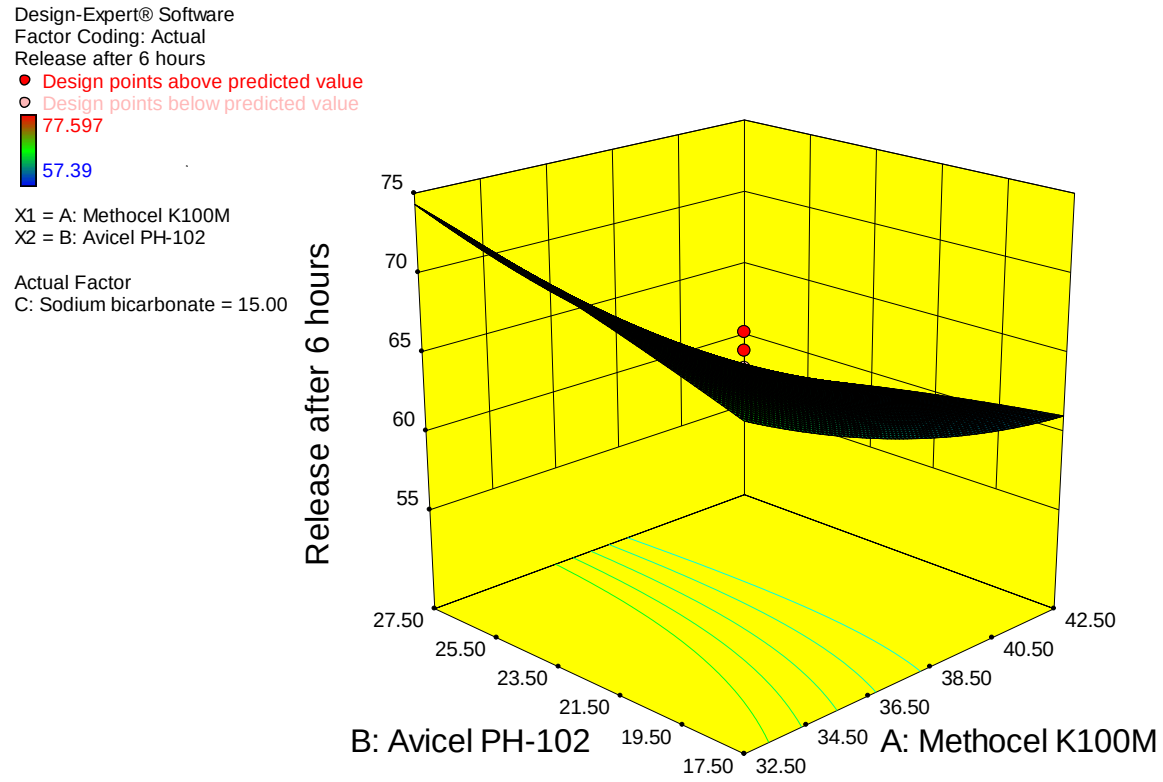

Figure 5.4b Three-dimensional contour plot of the effect of Methocel® K100M and Avicel® PH-102 on CPT release at 6 hours

The contour plot generated when the content of Avicel® PH-102 in the formulations was maintained at 22.5% w/w reveals that response Y_3 increases in a fairly linear manner as the Methocel® K100M content in the formulations was increased (Figure 5.5a).

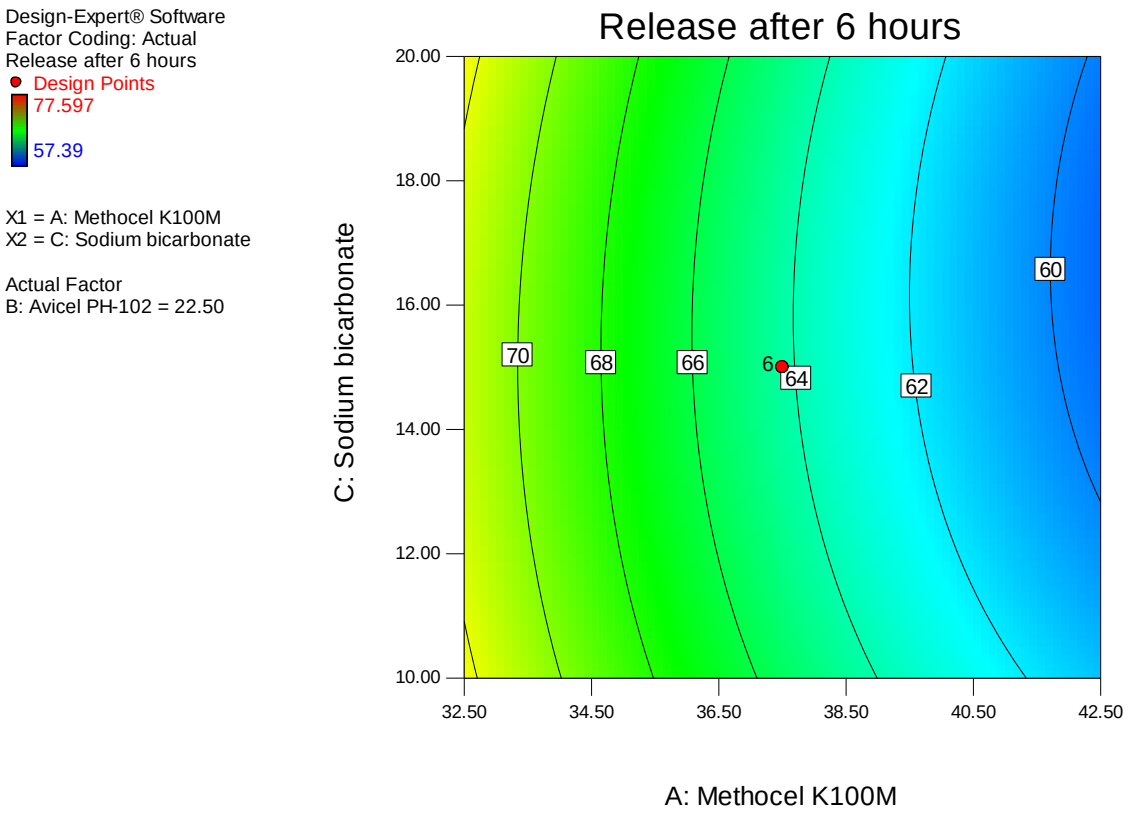

Figure 5.5a Contour plot of the effect of Methocel® K100M and sodium bicarbonate on CPT release at 6 hours

The corresponding three-dimensional plot for Y_3 shown in Figure 5.5b revealed that CPT release at 6 hours was lowest when the Methocel® K100M content in the formulations was at the maximum. The effect of Methocel® K100M on response Y_3 appears to be more pronounced than that observed for sodium bicarbonate. Consequently varying the content of sodium bicarbonate and keeping the Methocel® K100M content constant did not have a significant effect on the release of CPT from the tablets.

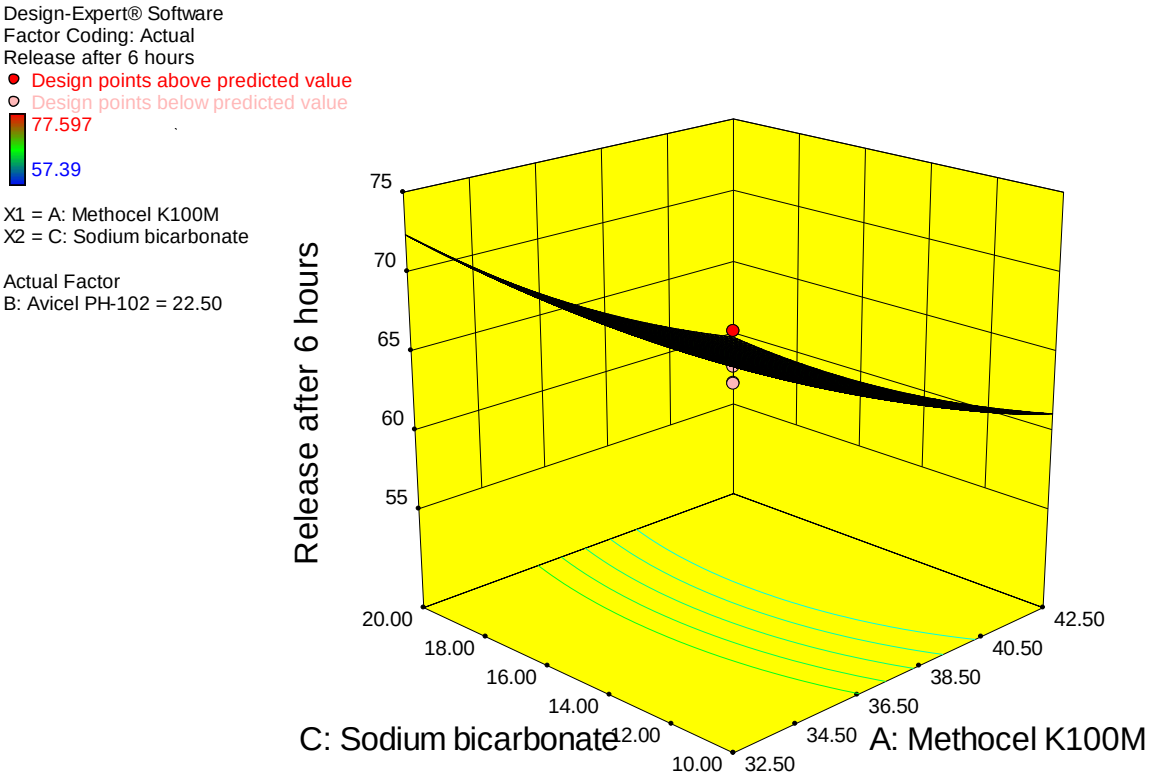

Figure 5.5b Three-dimensional contour plot of the effect of Methocel® K100M and sodium bicarbonate on CPT release at 6 hours

The response surface plots obtained when the concentration of Methocel® K100M was maintained at 37.5% w/w reveals that response Y_3 varied in a horseshoe pattern when the content of Avicel® PH-102 and sodium bicarbonate in the formulations was altered (Figures 5.6a and 5.6b). In addition the effects of Avicel® PH-102 and sodium bicarbonate did not have a statistically significant effect on the release of CPT from the tablets after 6 hours of dissolution testing.

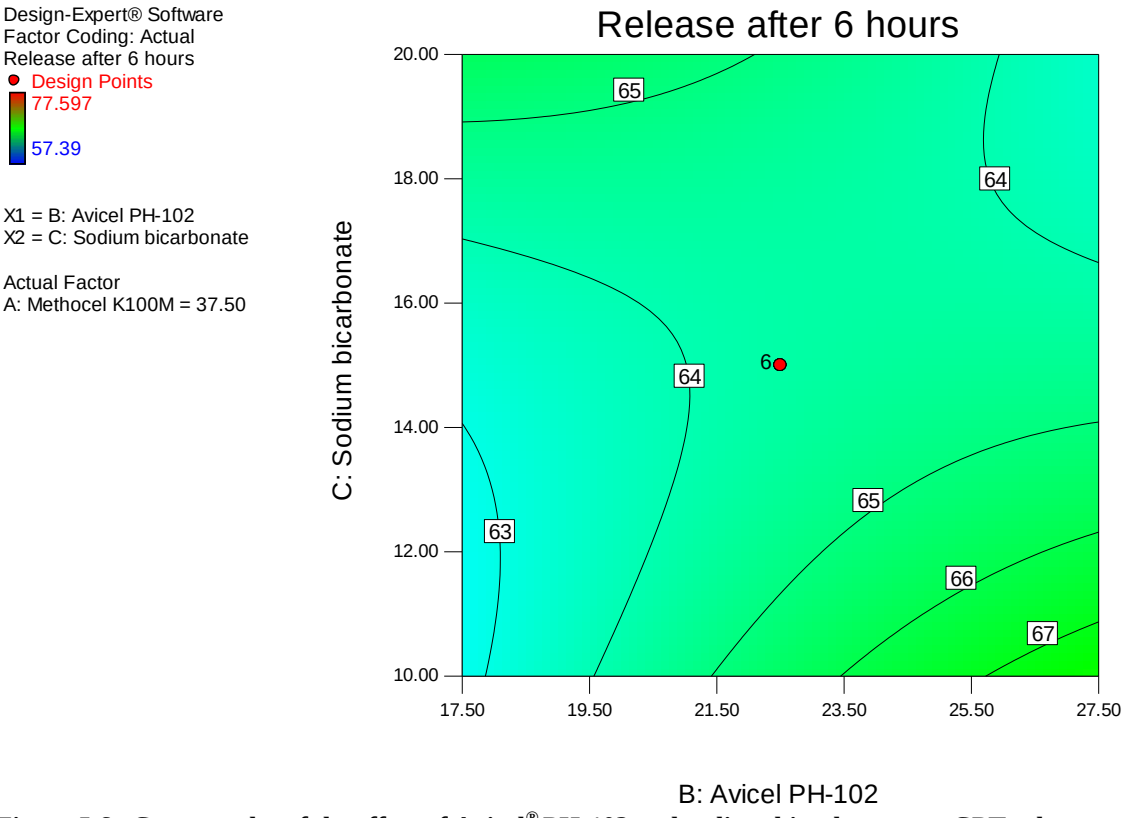

Figure 5.6a Contour plot of the effect of Avicel® PH-102 and sodium bicarbonate on CPT release at 6 hours

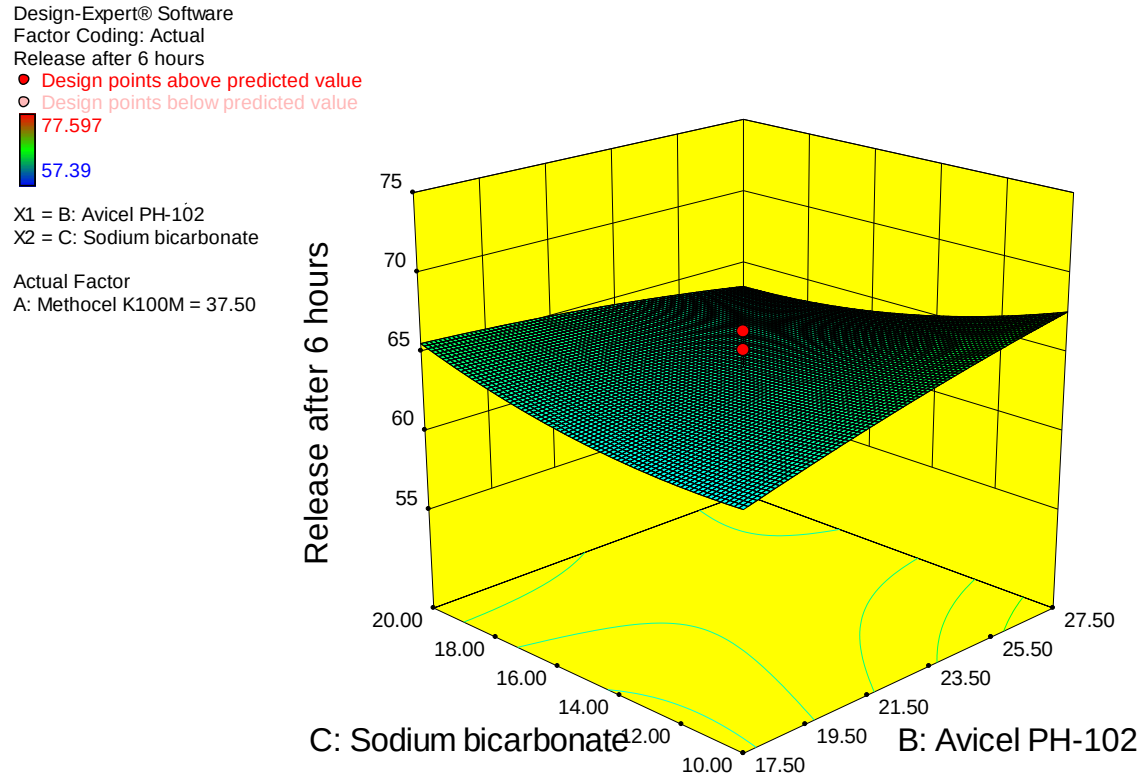

Figure 5.6b Three-dimensional contour plot of the effect of Avicel® PH-102 and sodium bicarbonate on CPT release at 6 hours

5.4.5 Evaluation of sustained release CPT tablets

The tablets manufactured were slightly off-white with flat, smooth surfaces and did not show evidence of capping, lamination, breaking or chipping. The tablet crushing strength ranged between 103.27 ± 3.5 and 124.39 N ± 3.45, and their tensile strength ranged between 1.31 ± 1.85 and 1.55 ± 4.25 N/mm^2, suggesting that the tablets would be able to withstand exposure to abrasive forces during handling, packaging and transportation. The friability of all the compressed tablet formulations was < 1% and indicated good mechanical resistance to abrasion. A summary of the physicochemical properties of the sustained release CPT tablets is listed in Table 5.6.

Table 5.6 Physicochemical assessment of CPT sustained release tablets

Batch	Thickness (mm)	Crushing strength (N)	Tensile strength (N/mm^2)	Weight (mg)	Friability (%)	CPT (%)	FLT (min)	TFT (hours)
C11	5.68 ± 1.43	107.47 ± 4.75	1.39 ± 2.04	341.00 ± 1.27	0.142 ± 2.36	98.20 ± 0.36	11.45 ± 3.33	> 12
C12	5.68 ± 1.17	112.78 ± 2.53	1.42 ± 3.68	342.71 ± 1.63	0.189 ± 1.26	101.25 ± 0.92	11.15 ± 2.46	> 12
C13	5.69 ± 1.05	109.73 ± 3.00	1.41 ± 2.38	342.99 ± 1.46	0.196 ± 1.71	99.46 ± 0.74	10.59 ± 3.50	> 12
C14	5.73 ± 0.86	104.19 ± 2.47	1.32 ± 2.59	340.10 ± 0.94	0.164 ± 2.63	97.52 ± 1.06	23.44 ± 4.54	> 12
C15	5.68 ± 1.63	114.46 ± 5.03	1.44 ± 4.05	339.26 ± 0.88	0.172 ± 1.47	96.26 ± 0.29	10.31 ± 3.02	> 12
C16	5.76 ± 0.44	106.85 ± 4.27	1.35 ± 1.85	340.29 ± 1.98	0.153 ± 3.70	97.36 ± 0.88	10.59 ± 2.96	> 12
C17	5.71 ± 1.34	114.72 ± 4.15	1.44 ± 3.76	343.51 ± 1.96	0.167 ± 1.48	100.26 ± 0.73	11.27 ± 5.03	> 12
C18	5.66 ± 1.14	110.45 ± 5.25	1.42 ± 3.55	345.10 ± 2.22	0.192 ± 2.96	99.14 ± 1.10	10.73 ± 2.83	> 12
C19	5.69 ± 1.49	105.76 ± 3.62	1.32 ± 1.24	341.70 ± 3.28	0.154 ± 1.12	96.76 ± 0.92	9.58 ± 1.76	> 12
C20	5.70 ± 1.17	104.50 ± 5.97	1.31 ± 3.72	338.92 ± 2.51	0.169 ± 3.56	97.95 ± 0.54	10.10 ± 2.98	> 12
C21	5.66 ± 1.18	111.80 ± 5.05	1.41 ± 1.98	345.44 ±1.66	0.117 ± 1.25	96.25 ± 0.79	10.53 ±2.60	> 12
C22	5.67 ± 1.27	103.86 ± 4.31	1.33 ± 2.47	340.92 ± 1.74	0.163 ± 2.46	99.29 ± 0.24	9.26 ± 1.47	> 12
C23	5.68 ± 1.27	115.28 ± 3.38	1.46 ± 3.11	345.27 ± 3.06	0.196 ± 3.15	97.55 ± 1.06	12.04 ± 2.83	> 12
C24	5.67 ± 0.27	104.28 ± 4.89	1.33 ± 4.83	338.01 ± 1.88	0.173 ± 1.66	99.02 ± 0.95	10.15 ± 2.69	> 12
C25	5.72 ± 1.69	118.87 ± 5.60	1.49 ± 2.72	345.47 ± 2.80	0.159 ± 3.48	98.25 ± 0.89	9.72 ± 3.28	> 12
C26	5.69 ± 1.05	105.66 ± 3.16	1.34 ± 3.20	341.11 ± 0.52	0.112 ± 3.86	96.41 ± 0.97	11.39 ± 4.70	> 12
C27	5.73 ± 0.73	112.37 ± 3.24	1.41 ± 2.43	342.01 ± 1.98	0.175 ± 1.46	99.68 ± 0.51	11.50 ± 4.25	> 12
C28	5.66 ± 1.07	103.27 ± 3.58	1.31 ± 4.16	346.68 ± 1.98	0.194 ± 1.25	98.13 ± 0.81	12.01 ± 3.87	> 12
C29	5.68 ± 0.98	108.98 ± 2.48	1.37 ± 3.72	342.08 ± 1.83	0.187 ± 3.14	99.09 ± 0.49	10.16 ± 3.33	> 12
C30	5.72 ± 0.86	124.39 ± 3.45	1.55 ± 4.25	336.19 ± 1.39	0.145 ± 2.73	97.49 ± 0.77	9.45 ± 4.13	> 12

The results from *in vitro* buoyancy tests revealed that all the formulations maintained *in vitro* buoyancy for up to 12 hours. The achievement and maintenance of *in vitro* buoyancy is attributed to the presence of the effervescent agent, sodium bicarbonate, which was dispersed in the tablet matrix. When the CPT sustained release tablets came into contact with HCl, an effervescent reaction occurred and carbon dioxide was released into the HPMC gel layer surrounding the tablets.

Visual inspection of the tablets during testing showed carbon dioxide bubbles on the surfaces of the tablets. The ability of the tablets to float for up to 12 hours suggests that Methocel® K100M Premium can form a durable gel layer around the tablets that can effectively entrap gas and promote *in vitro* buoyancy for at least 12 hours. Photographs (Figure 5.7) were taken with a 14-megapixel Kodak EasyShare digital camera (Model C1530, Eastman Kodak Company, New York, USA) at different time intervals during *in vitro* buoyancy testing of the tablets. Gas bubbles can be seen on the surface of the tablet shown in the photographs. The photographs reveal that the thickness of the tablets increased over time, indicating that the polymer matrix was hydrated and had swollen. Swelling behaviour studies were conducted at a later stage to confirm this phenomenon.

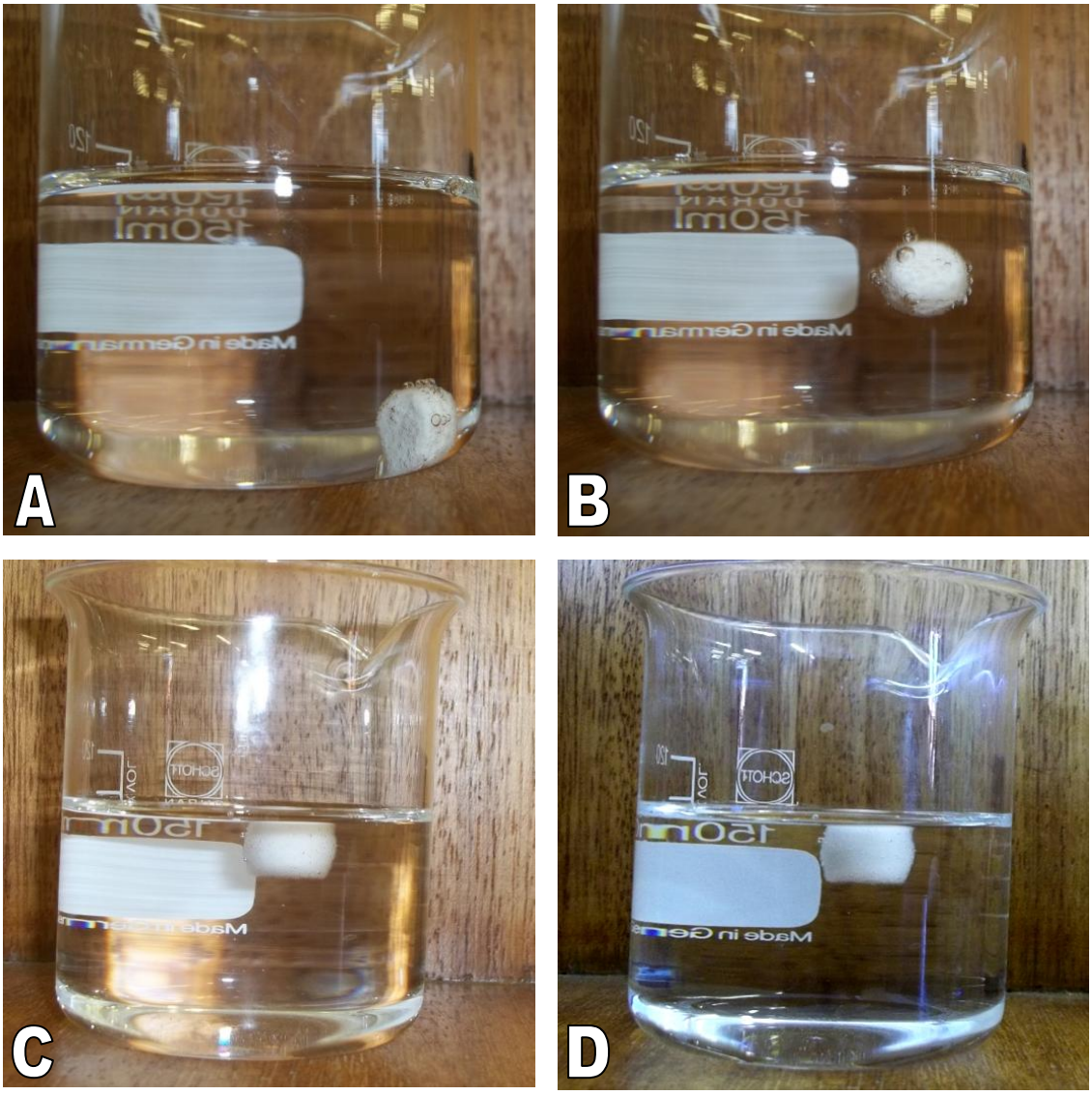

Figure 5.7 Photographs of a typical sustained release CPT floating matrix tablet at 1 min (A), 10 min (B), 4 hours (C) and 12 hours (D)

5.4.6 Mathematical modelling

The release kinetics of CPT were investigated by fitting release data to several mathematical models. The typical release pattern observed for all formulations showed an initial burst effect during the first 2 hours of dissolution testing, which may be attributed to rapid release of CPT from the tablet surface prior to the formation of a gel layer strong enough to modulate drug release [257,258]. In addition the physicochemical properties of CPT such as high water solubility provide the driving force for release and can lead to an initial burst [257,258]. The initial high release was generally followed by a phase characterised by a slower release of CPT up to the end of the dissolution test. The decrease in CPT release with time may be due to an increase in the thickness and stability of the gel layer that occurred as increased volumes of the dissolution medium entered the hydrophilic matrix resulting in a longer diffusional path length for drug release to occur, with a corresponding decrease in the release of CPT from the tablets [10,173,256].

Fickian diffusion is frequently used to describe the mechanism of drug release from the majority of polymeric systems [250,259]. However additional processes such as swelling, volume expansion and relaxation of polymer chains are characteristic for water swellable polymeric systems manufactured with HPMC. These processes must be considered when establishing the mechanism of release as they may also significantly influence the release process [259]. The Korsmeyer-Peppas model is useful for identifying the mechanism of drug transport from polymeric systems that may release an API by a combination of mechanisms [247,249-251]. The mechanism of API transport from the gastroretentive sustained CPT tablets was established by calculating the release exponent (*n*) obtained after fitting to the Korsmeyer-Peppas equation, the *in vitro* release data corresponding to up to 60% CPT released.

The results revealed that CPT release from the majority of the formulations occurred by an anomalous transport process, suggesting that CPT was released via a combination of diffusion (through the hydrated polymer matrix) and polymer relaxation [250]. In contrast the formulations exhibiting Fickian diffusion released CPT only via diffusion through the swollen polymer matrix and water-filled pores and channels that developed in the tablets [250]. The R^2 values obtained for the Korsmeyer-Peppas model ranged between 0.9515 and 0.9999, indicating that relatively good to excellent fit of the *in vitro* release data had been

achieved. The values of the constant incorporating the structural and geometrical characteristics of the tablets (*k*) that were obtained in the study were relatively high. Previous studies by Sinha *et al.* [250] revealed that high values of *k* reflect the occurrence of an initial burst release.

To further study CPT release kinetics, the experimental data were fitted to additional mathematical models including zero-order, first-order, Higuchi and the Hixson-Crowell model. The highest R^2 values were obtained when the data were fitted to the Korsmeyer-Peppas model. A tabular summary following mathematical modelling with associated parameters is listed in Table 5.7.

Table 5.7 Summary of mathematical model and release kinetic parameters

Batch	Zero-order		First-order		Higuchi		Hixson-Crowell		Korsmeyer-Peppas			
	R^2	k_0	R^2	k_1	R^2	k_H	R^2	k_{HC}	R^2	k	n	Drug transport mechanism
C11	0.9153	10.682	0.7457	0.0852	0.9497	19.383	0.7859	0.1087	0.9515	38.806	0.4317	Fickian
C12	0.9834	11.335	0.8592	0.1273	0.9946	25.364	0.8901	0.1492	0.9998	26.975	0.5039	Anomalous
C13	0.9839	11.669	0.8647	0.1230	0.9907	25.436	0.8962	0.1432	0.9999	26.016	0.5002	Anomalous
C14	0.9618	10.756	0.8506	0.1253	0.9576	25.412	0.8808	0.1477	0.9773	25.328	0.5476	Anomalous
C15	0.9816	11.146	0.8631	0.1267	0.9931	25.139	0.8889	0.1439	0.9999	26.756	0.5092	Anomalous
C16	0.9706	9.4856	0.8666	0.1077	0.9771	20.913	0.9002	0.1267	0.9928	26.828	0.4316	Fickian
C17	0.9595	10.158	0.7915	0.1134	0.9714	21.849	0.8331	0.1334	0.9914	26.467	0.5005	Anomalous
C18	0.9857	10.936	0.8783	0.1253	0.9931	25.613	0.9151	0.1488	0.9943	25.351	0.4857	Anomalous
C19	0.9716	10.732	0.8430	0.1169	0.9891	23.985	0.8827	0.1399	0.9998	27.120	0.4857	Anomalous
C20	0.9877	10.010	0.8611	0.1201	0.9960	22.723	0.9034	0.1397	0.9995	24.446	0.4857	Anomalous
C21	0.9801	11.476	0.8548	0.1279	0.9912	25.497	0.8976	0.1486	0.9998	26.998	0.5099	Anomalous
C22	0.9828	11.285	0.8657	0.1266	0.9896	26.346	0.9040	0.1512	0.9971	25.722	0.4984	Anomalous
C23	0.9249	10.793	0.7647	0.1004	0.9222	25.799	0.7618	0.1287	0.9798	35.975	0.4635	Anomalous
C24	0.9844	10.720	0.8747	0.1222	0.9919	24.818	0.9119	0.1451	0.9992	25.704	0.4716	Anomalous
C25	0.9862	10.030	0.8732	0.1264	0.9964	23.559	0.9109	0.1454	0.9981	22.951	0.5040	Anomalous
C26	0.9580	11.234	0.7692	0.1203	0.9639	24.081	0.8174	0.1456	0.9807	26.847	0.5714	Anomalous
C27	0.9845	11.133	0.8563	0.1232	0.9958	25.556	0.8971	0.1474	0.9999	26.266	0.5003	Anomalous
C28	0.9843	10.588	0.8443	0.1234	0.9956	24.111	0.8877	0.1449	0.9983	24.842	0.5110	Anomalous
C29	0.9826	11.165	0.8518	0.1229	0.9953	25.532	0.8925	0.1472	0.9999	26.412	0.5049	Anomalous
C30	0.9413	10.945	0.7538	0.0998	0.9685	21.387	0.7994	0.1236	0.9843	33.243	0.5110	Anomalous

5.4.7 Formulation optimisation

A numerical optimisation approach using Design Expert® (Version 7.0.1, Stat-Ease Inc., Minneapolis, MN, USA) statistical software was used to identify a formulation composition that would produce the desired responses. The statistical software was used to set goals that would generate minimal CPT release at 0.5 and 2 hours, a short FLT and maximum release of CPT at 12 hours. The combination of input parameters that produced the highest value of desirability was selected as the potential optimum tablet formulation composition (Table 5.8).

Table 5.8 Formulation composition for the optimised formulation

Ingredient	Amount (% w/w)
CPT	14.7
Methocel® K100M	41.81
Avicel® PH-102	26.73
Sodium bicarbonate	16.66
Talc	1.3
Magnesium stearate	1.0
Colloidal silicon dioxide	1.0

A 600 g batch of tablets corresponding to the optimal formula was manufactured and the experimental responses for these tablets were compared quantitatively to the values predicted by the statistical software. The results listed in Table 5.9 indicate that the experimental values were similar to the predicted values. In addition the values of the prediction error were < 5% for the majority of responses, suggesting that the proposed model has the potential to accurately predict experimental responses. The values for % prediction error for the responses Y_1 and Y_5 were slightly > 5%, suggesting that the CCD is a better predictor of responses Y_2 to Y_4. However this may be due to the fact that n=3 was used instead of n=6 and shows that the statistical experimental model developed in these studies has potential for further study and improvement.

Table 5.9 Predicted and average experimental responses (n=3) for the optimised formulation

Response	Predicted value (%)	Experimental value (%)	Prediction error (%)
Y_1	16.49	17.39	5.46
Y_2	31.80	32.27	1.48
Y_3	57.86	59.41	2.68
Y_4	84.12	86.21	2.48
Y_5	9.94	10.59	6.54

The tablets manufactured using the optimised formula were evaluated in terms of their physicochemical quality characteristics. They were slightly off-white with flat and smooth surfaces and without evidence of capping, lamination, breaking or chipping. The friability of the tablets was < 1% and the tensile strength was 1.34 ± 2.29 N/mm^2, suggesting that the tablets had good mechanical properties. The % RSD for weight variation and content uniformity were < 5%, indicating acceptable weight variation and uniformity respectively. The average CPT content in the tablets was approximately 98.92 ± 0.43% and the tablets maintained *in vitro* buoyancy for up to 12 hours.

The dissolution profile for the optimised formula is shown in Figure 5.8 and reveals sustained release of CPT over a 12 hour period.

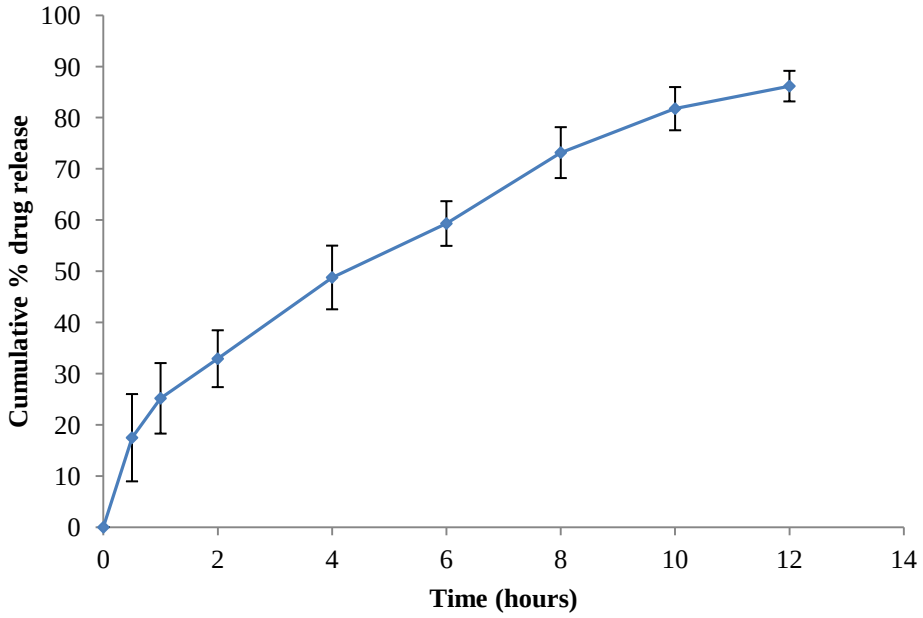

Figure 5.8 CPT release from the optimised formulation

The *in vitro* release data were fitted to mathematical models in an attempt to establish the mechanism of CPT release from these tablets. The R^2 values listed in Table 5.8 suggest that the data are best described using the Korsmeyer-Peppas model, as it yielded the highest R^2 value (0.9971). The release exponent for the Korsmeyer-Peppas was 0.4787 suggesting, that CPT release from the cylindrical tablet matrices occurs via an anomalous transport mechanism.

Table 5.10 Summary of mathematical model parameters for the optimised formulation

Model	*k*	R^2
Zero-order	10.997	0.9892
First-order	0.1289	0.8843
Higuchi	26.035	0.9943
Hixson-Crowell	0.1523	0.9926
Korsmeyer-Peppas	24.553	0.9971

5.4.8 Effect of agitation speed on *in vitro* CPT release

The hydrodynamic conditions used for dissolution testing can influence drug release from hydrophilic matrices [260]. For example variation of the agitation speed at which the dissolution apparatus is operated may alter the hydrodynamic conditions and mechanical stress around the dosage form that may influence the rate of polymer erosion [261]. It has been suggested that variation of dissolution rate due to changes of paddle speed may predict the possibility of variable *in vivo* behaviour and 'food effects' [173,262]. The dissolution profiles obtained from a study of the influence of different agitation speeds on CPT release from the tablets are shown in Figure 5.9.

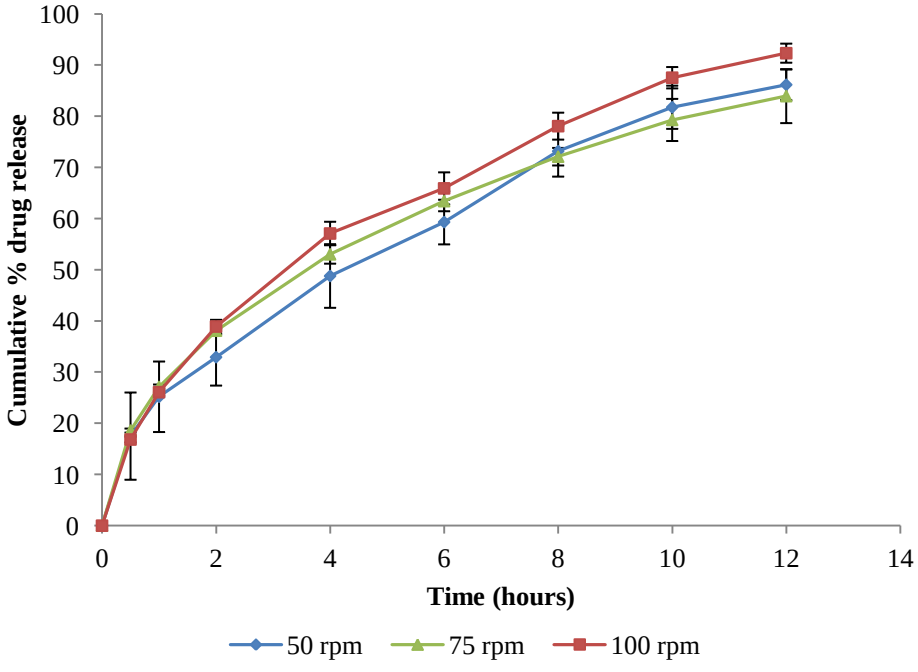

Figure 5.9 Effect of stirring rate on CPT release

The model-independent mathematical approaches proposed by Moore and Flanner in 1996 were used to quantitatively compare the dissolution profiles generated. The difference factor (f_1) is a measure of the percent error between two dissolution profiles at each dissolution time point and can be calculated using Equation 5.13 [248]. An f_1 value ≤ 15 indicates similarity between two dissolution profiles being compared [248].

$$f_1 = \frac{\sum_{j=1}^{n}|R_j - T_j|}{\sum_{j=1}^{n} R_j} \times 100 \quad \textbf{(Equation 5.13)}$$

Where

f_1 = Difference factor
n = Sampling number
R_j = Percent dissolved in the reference product at each time point
T_j = Percent dissolved in the test product at each time point

The similarity factor (f_2) measures the similarity in the percent of dissolution between two dissolution profiles [248]. The f_2 value is calculated as the logarithmic reciprocal square root transformation of the sum of squared error (Equation 5.14) and an f_2 value ≥ 50 indicates that two dissolution profiles being compared are similar [248].

$$f_2 = 50 \times log\left\{\left[1 + \left(\frac{1}{n}\right)\sum_{t=1}^{n} w_j\,|R_t - T_t|^2\right]^{-0.5} \times 100\right\} \quad \textbf{(Equation 5.14)}$$

Where

f_2 = Similarity factor
w_j = An optional weight factor
n = Sampling number
R_j = Percent dissolved in the reference product at each time point
T_j = Percent dissolved in the test product at each time point

The f_1 and f_2 values listed in Table 5.11 revealed that the dissolution profiles obtained when using different agitation speeds were similar, as indicated by f_1 values which are < 15 and f_2 values > 50. Theoretically an increase in agitation speed should decrease the thickness of the stagnant layer and result in an increase in the rate of dissolution [21,190]. However the slight change in dissolution rates observed when the agitation speed was increased may be a result of the high water solubility of CPT, which has been reported to outweigh the influence of agitation during dissolution testing [263]. Twelve units are usually required for the

calculation f_1 and f_2 values, it was therefore a limitation to use n=6 during these studies, however reports from previous work have revealed similar findings as those obtained in these studies [263].

Table 5.11 Difference and similarity factors for dissolution profiles obtained using different agitation speeds.

Profiles compared	f_1	f_2
50 rpm versus 75 rpm	4.7	74.1
50 rpm versus 100 rpm	8.3	65.5
75 rpm versus 100 rpm	6.4	64.5

5.4.9 Swelling studies

The hydrophilic nature of HPMC-based matrices facilitates the diffusion of water into the glassy (crystalline phase) material, resulting in the plasticization of the polymer [244]. As water infiltrates and plasticizes the polymer matrix the glass transition temperature (T_g) of HPMC is reduced to ambient temperature resulting in the conversion of the glassy phase to a rubbery state [244]. Over time the increasing volume of liquid entering the matrix results in an increase in the dimensions of the matrix manifested by swelling [244].

The swelling behaviour of a formulation may influence the mechanism of release, release kinetics and the buoyancy of floating tablets [244,245,250,264]. The presence of food in the stomach may alter the environment and osmolarity of the stomach contents and result in changes in the swelling characteristics of hydrophilic matrices [265-267]. The pH of the stomach under fasted conditions typically ranges between 1 and 3.5, however the presence of food may result in a temporary increase in pH up to pH 7 [10,268, 269, 270]. The osmolarity of the stomach contents also varies considerably during digestion and may increase to 1000 mOsm/L in the fed state [10].

The swelling behaviour of the tablets in different dissolution media was investigated in an attempt to gain an understanding of the effects of changes in pH and osmolarity on the swelling behaviour of the tablets. The results from the study of the effect of pH on the SI shown in Figure 5.10 revealed that continuous tablet swelling occurred over the 12 hour period regardless of the pH of the dissolution medium. There were only slight differences in

the swelling behaviour of the tablets when the pH of the dissolution medium was varied, and this is most probably the result of the non-ionic nature of HPMC [262]. These observations are in agreement with previous studies reporting that the pH of dissolution media did not have a significant effect on the swelling of HPMC-based matrix tablets [266,2719,272].

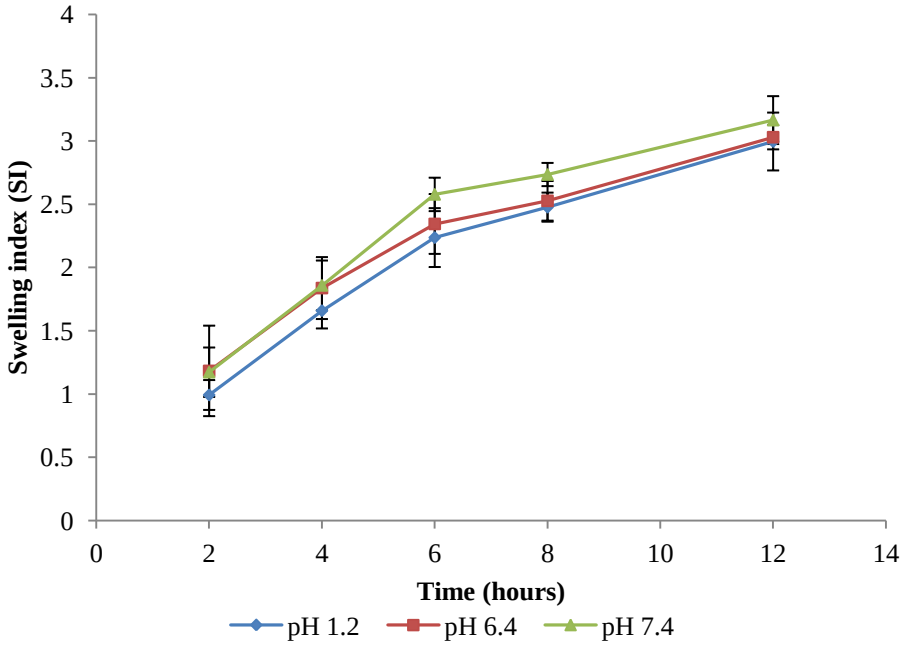

Figure 5.10 Effect of pH on the SI

The results from a study in which the effects of osmolarity on SI were determined are shown in Figure 5.11. They revealed that the swelling behaviour of tablets immersed in hypo-osmolar (200 mOsm/L) and iso-osmolar (308 mOsm/L) solutions was almost identical over the time interval, 2-6 hours. Thereafter a slight increase in the SI of tablets immersed in the iso-osmolar solution was observed. However the maximum SI values for the tablets immersed in the hypo-osmolar and iso-osmolar solutions were similar. Throughout the duration of the study, the values for SI recorded for the tablets immersed in hyper-osmolar solution were slightly higher than those reported for other dissolution media. In general, the swelling behaviour of the tablets was similar in the different solutions and suggests that changes in the composition of the stomach contents may not significantly affect the swelling behaviour of the tablets. In addition the solubility and/or stability of CPT in different dissolution media did not affect the water uptake and swelling of the tablet matrices. These observations are similar to those in previous studies in which variations of the osmolarity of dissolution media did not induce significant changes in the swelling behaviour of hydrophilic matrices [266,267,273].

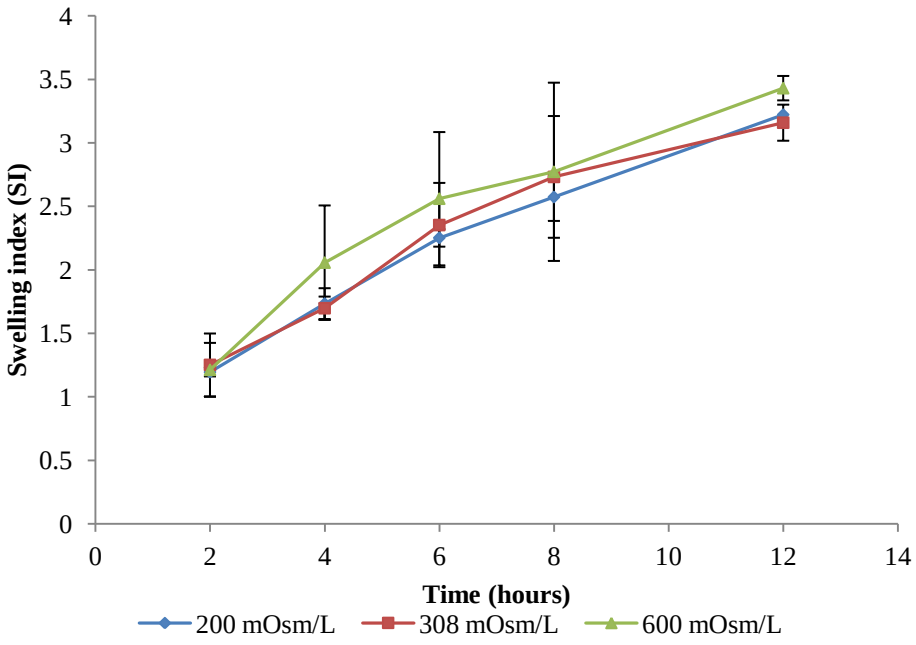

Figure 5.11 Effect of osmolarity on the SI

5.4.10 Matrix erosion studies

Hydrophilic matrices may also undergo erosion through slow disentanglement and dissolution of polymer chains at the interface between the gel layer and surrounding dissolution medium [245]. However for water-soluble drugs such as CPT, drug release through polymer erosion is insignificant and diffusion is the predominant mechanism of release [259]. The values for % E_p generated in matrix erosion studies were plotted to provide a visual presentation of the amount of polymer that had dissolved and matrix that had eroded over the 12 hours of dissolution testing. All tablets exhibited some degree of erosion regardless of which medium was used. For the study of the effect of pH on matrix erosion the tablets immersed in 0.1 M HCl (pH 1.2) exhibited the least erosion, with approximately 11.6% eroding within the first 2 hours of dissolution testing and approximately 22.9 % after 12 hours. In contrast the highest total % erosion was observed for the tablets immersed in a phosphate buffer (pH 7.4), with approximately 30.8% matrix erosion after 12 hours of dissolution testing (Figure 5.12).

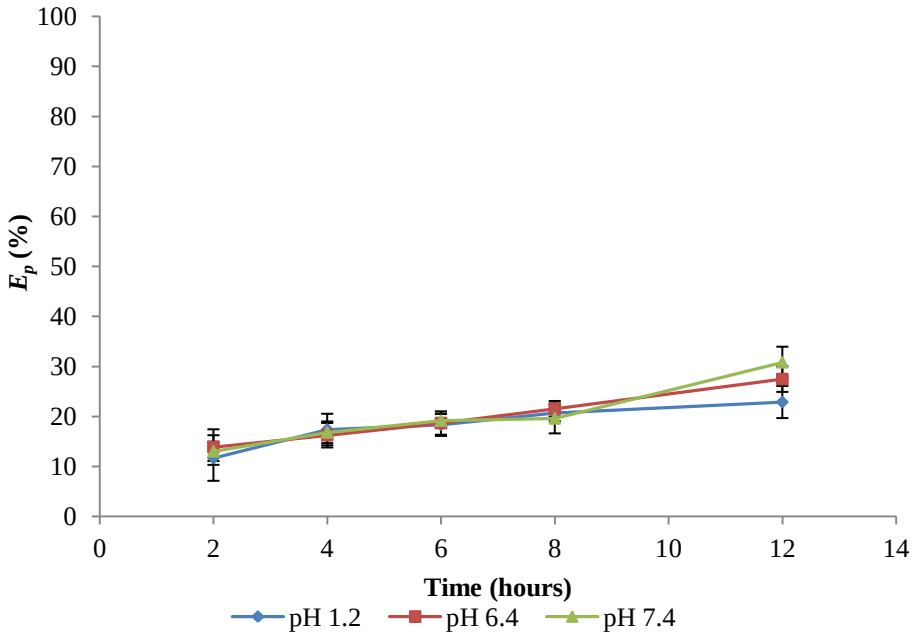

Figure 5.12 Effect of pH on the % erosion

The effect of osmolarity on matrix erosion revealed that tablets immersed in a hypo-osmolar (200 mOsm/L) solution exhibited the least % erosion, with only approximately 10.8% erosion occurring after the first 2 hours and approximately 20.7% after 12 hours. In contrast the highest total % erosion was observed for the tablets immersed in an iso-osmolar solution (308 mOsm/L), with approximately 24.5% matrix erosion after 12 hours of testing (Figure 5.13).

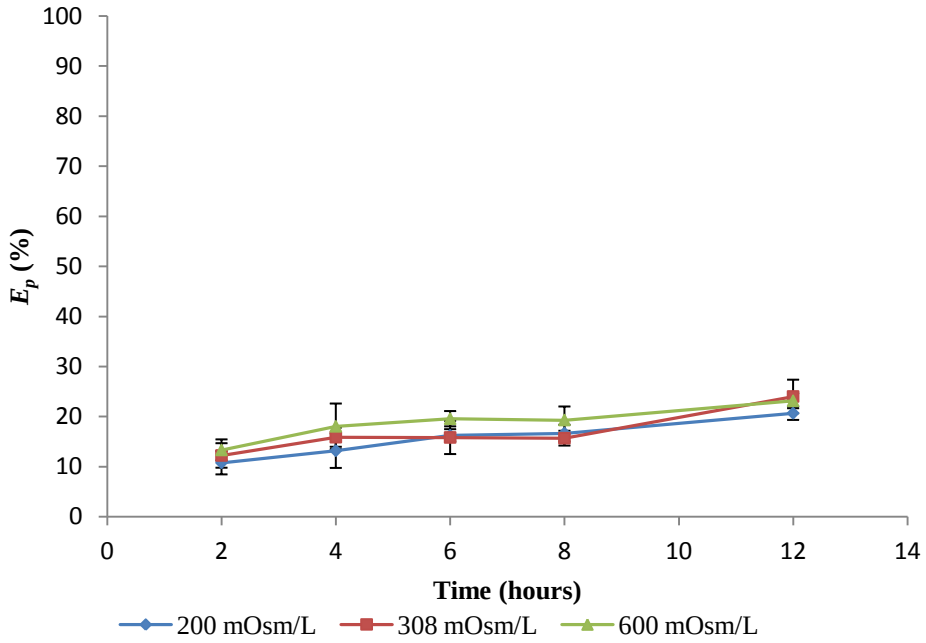

Figure 5.13 Effect of osmolarity on the % erosion

The rate of erosion was established by fitting the experimental data to the Hixson-Crowell cube root Equation 5.15 [245].

$$\left(\frac{W_d}{W_i}\right)^{\frac{1}{3}} = 1 - k_2 t \qquad \textbf{(Equation 5.15)}$$

Where

W_d = Dry weight of the tablet at time t
W_i = Initial weight of the tablet
k_2 = Polymer erosion rate constant
t = Time

A tabular summary of the parameters for the estimates for erosion obtained after fitting the data to the Hixson-Crowell cube root model is presented in Table 5.12. The results reveal that the erosion rate constants were low, suggesting that although polymer erosion occurred the role of this phenomenon in CPT release is, as expected, not as significant as that of diffusion.

Table 5.12 Summary of the kinetic parameters for tablet erosion in different dissolution media

Dissolution medium	R^2	Erosion rate constant ($hour^{-1}$)
pH 1.2	0.8844	0.0039
pH 6.4	0.9949	0.0053
pH 7.4	0.9219	0.0066
200 mOsm/L	0.9721	0.0036
308 mOsm/L	0.7171	0.0039
600 mOsm/L	0.8733	0.0033

5.4.11 Stability testing

Stability testing is an important component of the product development process [10,21]. A stable formulation should maintain aesthetic appeal and elegance from the time of manufacture until administration. If the organoleptic properties of the product such as the taste, odour and colour change over time it may result in the patient losing confidence in the effectiveness and safety of the product [21]. In addition degradation of the API on storage may lead to a reduced dosage and a lack of clinical effectiveness [21].

The results from stability tests revealed that the shape and colour of the tablets did not change throughout the duration of the study. In addition no significant changes in the

physicochemical properties of the tablets were observed after 60 days of storage. The results from short term stability testing are summarized in Tables 5.13 and 5.14.

Table 5.13 Results from stability testing for the optimised formulation stored at 25°C/60% RH

Physicochemical property	Day 1	Day 7	Day 15	Day 30	Day 60
Appearance	Slightly off-white; flat; smooth surface; no capping, lamination, breaking or chipping				
FLT (min)	11.59 ± 3.86	11.47 ± 3.16	10.44 ± 3.35	10.57 ± 3.90	11.33 ± 2.75
TFT (hours)	> 12	> 12	> 12	> 12	> 12
CPT content (%)	98.9± 0.43	98.3 ± 0.35	97.9 ± 0.71	98.1 ± 0.39	98.7 ± 0.22
Weight uniformity (mg)	338.59 ± 2.80	337.50 ± 1.65	339.06 ± 2.27	339.17 ± 1.12	340.29 ± 2.85
Content uniformity (mg)	49.16 ± 4.56	48.92 ± 3.91	49.80 ± 2.14	49.58 ± 2.69	49.75 ± 2.73
Crushing strength (N/mm^2)	105.12 ± 2.74	99.96 ± 4.93	105.63 ± 3.62	101.97 ± 2.80	102.31 ± 4.99
Friability (%)	0.169	0.153	0.177	0.194	0.172

Table 5.14 Results from stability testing for the optimised formulation stored at 40°C/75% RH

Physicochemical property	Day 1	Day 7	Day 15	Day 30	Day 60
Appearance	Slightly off-white; flat; smooth surface; no capping, lamination, breaking or chipping				
FLT (min)	11.59 ± 3.86	10.29 ± 4.92	10.11 ± 3.12	10.57 ± 2.22	11.05 ± 1.51
TFT (hours)	> 12	> 12	> 12	> 12	> 12
CPT content (%)	98.9 ± 0.43	99.1 ± 0.54	98.6 ± 0.32	98.8 ± 0.44	98.6 ± 0.61
Weight uniformity (mg)	338.59 ± 2.80	339.33 ± 3.64	340.69 ± 1.93	338.77 ± 2.49	339.15 ± 3.07
Content uniformity (mg)	49.16 ± 4.56	49.91 ± 2.49	49.24 ± 2.15	49.82 ± 3.31	49.06 ± 1.47
Crushing strength (N/mm^2)	105.12 ± 2.74	102.23 ± 3.44	101.15 ± 6.57	103.67 ± 2.82	101.68 ± 3.85
Friability (%)	0.169	0.179	0.166	0.171	0.169

The statistical stability evaluation procedure described by Timm *et al.* was used to quantitatively determine whether the observed differences in changes of the physicochemical properties of the tablets were statistically relevant and/or significant. The method described by Timm *et al.* is based on the construction of a 90% confidence interval for the true difference of responses obtained from freshly prepared and stored samples [274]. The upper and lower limits of the confidence interval are calculated using the % response difference between freshly prepared and stored samples, and the true % change of the response lies within that confidence interval [274]. If both the values of the upper limit (UL) and lower limit (LL) of the confidence interval for the change of a response after storage are either < -10% or > +10%, then the change is considered to be statistically relevant [275].

The procedure described by Timm *et al.* was used to construct confidence intervals for CPT content, FLT, weight uniformity, content uniformity and crushing strength. The % difference between the initial response factors and the responses obtained after storing the tablets at accelerated test conditions was used to calculate the confidence interval for each physicochemical property. The tablets were considered to be stable if both the UL and LL of the confidence intervals were between -10% and +10%. Within this range, there was no statistically relevant and/or significant difference between the initial physicochemical properties of the tablets and physicochemical properties after storage.

The results obtained from the statistical test of the stability of the CPT tablets according to procedure described by Timm *et al.* are shown in Tables 5.15 and 5.16 for the tablets stored at 25°/60% RH and 40°/75% RH respectively. The results revealed that there were no statistically relevant and significant changes of the physicochemical properties of the CPT tablets after 60 days of storage at 25°/60% RH and 40°/75% RH. Consequently, the tablets were regarded as stable for the duration of the stability test.

Table 5.15 Results from the Timm *et al.* test for the effect of stability test conditions on the physicochemical properties of CPT tablets after storage at 25°C/60% RH for 60 days

Storage conditions	25°C/60% RH									
	CPT content (n=3)		FLT (n=6)		Weight uniformity (n=20)		Content uniformity (n=10)		Crushing strength (n=20)	
	LL	UL	LL	UL	LL	UL	LL	UL	LL	UL
Day 7	-1.46	0.59	-0.12	0.36	-0.96	3.14	-0.75	1.23	3.35	6.97
Day 15	0.18	1.47	0.92	1.38	-3.3	2.36	-1.19	-0.09	-0.90	1.92
Day 30	-0.15	2.19	0.74	1.30	-1.98	0.82	-1.11	0.27	2.12	4.22
Day 60	-0.05	1.19	0.05	0.47	-1.87	5.27	-1.30	0.12	0.93	4.69

* Where LL = Lower limit and UP = Upper limit. Acceptable interval = -10% to +10%.

Table 5.16 Results from the Timm *et al.* test for the effect of stability test conditions on the physicochemical properties of CPT tablets after storage at 40°C/75% RH for 60 days

Storage conditions	40°C/75% RH									
	CPT content (n=3)		FLT (n=6)		Weight uniformity (n=20)		Content uniformity (n=10)		Crushing strength (n=20)	
	LL	UL	LL	UL	LL	UL	LL	UL	LL	UL
Day 7	-0.69	1.33	0.96	1.64	-3.8	5.28	-1.4	-0.10	1.60	4.18
Day 15	-0.61	0.85	1.27	1.69	-0.32	4.52	-0.47	0.63	1.53	6.41
Day 30	0.21	0.85	0.86	1.18	-2.92	3.28	-1.52	0.20	0.37	2.53
Day 60	-0.52	1.22	0.43	0.65	-4.39	3.27	-0.28	0.48	2.00	4.88

* Where LL = Lower limit and UP = Upper limit. Acceptable interval = -10% to +10%

5.5 CONCLUSIONS

Gastroretentive sustained release CPT tablets were manufactured using a direct compression process and a RSM approach was used to study the main, interactive and quadratic effects of formulation variables on CPT release and the floating properties of the tablets. The RSM approach was successful and reduced the time and resources required for formulation development and optimisation. A three-factor CCD was used to determine the effects of the composition of Methocel® K100M, Avicel® PH-102 and sodium bicarbonate on several responses. ANOVA was used to quantitatively analyse the significance and relevance of the independent variables. The results revealed that the Methocel® K100M content in the formulations had a statistically significant effect on the % CPT released from the tablets. However, the concentration levels of Avicel® PH-102 and sodium bicarbonate did not have a statistically significant effect on the cumulative % CPT released when used in the ranges studied. Two-dimensional contour and three-dimensional response surface plots were used to gain further insight into the impact of independent variables on the responses.

A numerical optimisation approach was used to predict a formulation composition that would produce low initial CPT release and a short FLT with maximum release of CPT observed at 12 hours. In an effort to validate the results from the CCD the experimental responses of the proposed optimal formulation were compared with the predicted responses. The results revealed that the majority of the predicted and experimental values were similar, as indicated by values of % prediction error < 5%.

The release kinetics of CPT from the formulations were established by fitting the *in vitro* release data to mathematical models. The model that best described that data was established by selecting the model that produced the highest R^2 values. The highest R^2 values were obtained when the *in vitro* release data were fitted to the Korsmeyer-Peppas model. The values of the release exponent (*n*) that were obtained when the data were fitted to the Korsmeyer-Peppas model revealed that the majority of the tablet formulations exhibited anomalous release kinetics which resulted in sustained CPT release throughout 12 hours of dissolution testing.

Tablets from each batch that was manufactured were subjected to several quality control tests and the results revealed that the tablets met compendial specifications with regard to weight uniformity, content uniformity, CPT content and friability. In addition all the formulations remained buoyant for up to 12 hours. The optimised formulation was subjected to additional testing in an attempt to investigate the effects of pH and osmolarity on the swelling characteristics of the tablets. The results revealed that the swelling characteristics of the proposed formulation were not significantly altered by a change in pH and osmolarity. In addition the solubility and/or stability of CPT in different dissolution media did not affect the water uptake and swelling of the tablet matrices.

The effect of increasing agitation rate of USP Apparatus 2 from 50 to 100 rpm was investigated. The results revealed that the agitation speed of the paddle had a relatively low impact on the *in vitro* release behaviour of the tablets, possibly due to the high water solubility of CPT. The short-term stability of the optimised formulation was established by performing stability studies at 25°/60% RH and 40°/75% RH. No significant changes in the appearance and physicochemical properties of the tablets were observed over the 60 days.

In conclusion a statistical experimental design approach was successfully applied to study the effect of formulation variables on several responses and to identify a gastroretentive formulation composition that has the potential for further development and improvement. Further studies to improve this formulation would include approaches to reduce the initial burst effect and performing dissolution studies using Simulated Gastric Fluid (SGF) to predict the *in vivo* behaviour of the formulation. These studies serve as a starting point for the development of gastroretentive sustained release formulations for API that are highly water soluble and/or may require gastric retention to improve *in vivo* stability and/or solubility **.**

CHAPTER 6

CONCLUSIONS

CVD is the leading cause of death worldwide, and global projections predict that the number of deaths due to CVD will continue to increase over the next 17 years. The development of new compounds to combat CVD is time consuming and expensive, and therefore the design and development of formulations that can optimise the delivery of existing compounds such as CPT may be an approach to improving the management of patients with CVD.

CPT is an ACE inhibitor with a well-established pharmacokinetic, efficacy and safety profile. CPT is indicated for the treatment of hypertension, cardiac failure and diabetic nephropathy. It has a relatively short half-life of 2-3 hours, and typical dosage regimens require administration every 8-12 hours. CPT is therefore a potential candidate for sustained oral drug delivery, however the poor stability profile and high water solubility of the molecule present significant formulation challenges. CPT exhibits optimal stability at pH < 4 and is therefore unstable in the alkaline environment of intestinal fluids. The development of a gastro-retentive sustained release formulation of CPT may be an approach to increasing the residence time of CPT in the stomach where it is most stable. A gastro-retentive sustained release formulation may improve the *in vivo* stability of CPT and may also reduce the occurrence of drug-related adverse effects such as the dry hacking cough associated with the use of CPT. Consequently the overall aim of this study was to develop, manufacture and assess gastro-retentive sustained release CPT tablets.

A CZE method for the quantitation of CPT in pharmaceutical dosage forms was developed and optimised using a RSM approach and a CCD. On the basis of a study of the influence of electrolyte and system variables on the electrophoretic separation, the buffer pH and molarity, applied voltage and capillary length were found to be key variables that required optimisation. The key responses that were monitored were peak resolution and CPT migration. The latter was considered the most important parameter as it has a significant impact on the total analytical run time. The least squares linear regression method was used to establish the mathematical model that best described the experimental data, and ANOVA was used to determine the significance and relevance of the input factors on responses. The results revealed that buffer molarity and pH had no significant effect on the migration time of

CPT, whereas applied voltage and capillary length had a significant effect on the migration time of CPT in the ranges investigated. A numerical optimisation approach was used to establish the optimal separation conditions for the CZE method. These were achieved using a fused silica capillary with an effective length = 57.5 cm and total length = 67.5 cm, 20 mM phosphate buffer adjusted to pH 7.0 and a separation voltage of 23.9 kV. The use of a RSM approach significantly reduced the development and optimisation time of the CZE method.

Due to the poor stability profile of the CPT molecule and its susceptibility to oxidative degradation at pH > 4, the stability of test solutions in the running buffer was established prior to proceeding with method validation studies. This included an analysis of the stability of calibration solutions stored under a range of conditions. The results revealed that the presence of 0.2 % m/v sodium metabisulphite in sample solutions was necessary and sufficient to delay oxidative degradation over 24 hours. The CZE method was validated and the detector response was found to be linear over the concentration range of 10-70 µg/mL. The LOQ and LOD of the method were 3 µg/mL and 10 µg/mL respectively. The CZE method demonstrated acceptable accuracy and precision, as indicated by the values of % RSD that were < 5%, and were within the limits set in our laboratory. The CZE method developed, validated and reported in this study was successfully applied to the analysis of CPT in dosage forms and may be suitable for routine analysis of CPT dosage forms for quality control purposes.

Preformulation studies were conducted as part of the preparative work required to manufacture a high quality and stable gastroretentive sustained release CPT tablets. SEM was used to determine the shape and size of excipients used in the study, and the results revealed differences in the shape and size of the particles. Consequently two sieving steps were included in the manufacturing process in an attempt to achieve uniform size distribution and improve the flow properties of the powder blends. The flow properties of the powder blends used to manufacture the tablets were established by determining CI, HR and AOR. The results revealed that the flowability of the majority of the powder blends was suitable for manufacturing tablets using a direct compression manufacturing process.

Thermal decomposition of CPT was investigated using TGA, and the results revealed that CPT is stable up to 150°C, after which > 95% mass loss is observed between 150 and 500°C. The results suggest that degradation of CPT is unlikely under normal tableting conditions,

which rarely exceed 100°C. API-excipient compatibility studies using DSC and FT-IR were undertaken in an attempt to identify excipients that may be incompatible with CPT. DSC results suggested a possible interaction between CPT and magnesium stearate could occur, however chemical incompatibility between the two compounds was not confirmed in FT-IR studies. Long-term stability studies would be required to ensure that such an incompatibility does not exist. FT-IR studies did not reveal any potential incompatibility between CPT and potential excipients, and any slight shifts observed in the characteristic bands for CPT were possibly a result of hydrogen bonding in the powder mixtures. Since there was no definite evidence to support interactions between CPT and the excipients to be used to manufacture CPT sustained release gastro-retentive tablets, CPT formulations were developed using these excipients.

A direct compression procedure was used to manufacture CPT sustained release gastro-retentive tablets due to its simplicity, and to avoid unnecessary exposure of CPT to heat and moisture that would be necessary for a wet granulation process. All formulations were manufactured with an HPMC-based matrix and included sodium bicarbonate. The effect of different grades of HPMC on CPT release from the tablets was investigated. The results revealed that formulations manufactured with high viscosity grades of HPMC exhibited lower release of CPT after 12 hours of dissolution testing than formulations containing lower viscosity grades of the polymer. The effect of varying HPMC content in formulations was also investigated, and the results generated revealed that reducing the HPMC content resulted in an increase in the cumulative % CPT released after 12 hours of dissolution testing. In addition, the effect of combining HPMC with ethylcellulose or Carbopol® 974P NF on the initial burst release of CPT from the tablets was investigated. The results revealed that there was no significant benefit from using such combinations in the ranges under investigation, and the initial release of CPT observed using such combinations was similar to that obtained when HPMC was used alone. Consequently, HPMC was used as the only rate-controlling polymer in subsequent formulation studies. However further research would be required to fully establish the effects of using different amounts of these polymers on the release of CPT in more exhaustive development studies.

A RSM approach with the use of CCD was undertaken to investigate the effects of formulation variables on CPT release and the floating properties of the tablets. The HPMC, MCC and sodium bicarbonate content in the formulations were key variables that required

further study and optimisation. The key responses that were monitored were cumulative % CPT released after 0.5, 2, 6 and 12 hours of dissolution testing and FLT. ANOVA models were used to quantitatively analyse the significance and relevance of the independent variables. The results revealed that the linear contributions of MCC and sodium bicarbonate content in the formulations did not have a statistically significant effect on CPT release in the ranges studied. One exception indicted that there was a synergistic linear contribution of MCC at 0.5 hours which was found to be statistically significant. The HPMC content in the formulations had a statistically significant and antagonistic effect on the % CPT released from the tablets. Therefore an increase in the HPMC content in the formulations resulted in a decrease in the % CPT released during dissolution testing. The decrease in CPT release observed when the HPMC content was increased was a result of an increase in the thickness and viscosity of the HPMC gel layer that formed and surrounded the tablets, and which consequently increased the diffusional path length, thereby slowing down and decreasing the release of CPT. The sodium bicarbonate content had a significant and antagonistic effect on the FLT, and this was due to an increase in the amount of carbon dioxide generated by the effervescent reaction between the dissolution medium and sodium bicarbonate that promoted rapid *in vitro* buoyancy.

Tablets from each batch that was manufactured were subjected to quality control testing and the results revealed that the tablets met compendial specifications with regard to weight uniformity, content uniformity, CPT content and friability. In addition, all formulations remained buoyant for up to 12 hours. The typical release pattern observed for all formulations exhibited an initial burst effect during the first 2 hours of dissolution testing, attributed to the high water solubility of CPT that provided the driving force for drug release. The initial high release was followed by a phase characterised by a slower release rate of CPT from the tablets that continued until the end of dissolution testing. The release kinetics of CPT from the formulations were established by fitting *in vitro* release data to several mathematical models. The *in vitro* release data were best described using the Korsmeyer-Peppas model, and values of release exponent (*n*) suggested that the majority of the tablets exhibited an anomalous drug transport mechanism.

A numerical optimisation approach was used to predict a formulation composition that would produce a minimal initial CPT release, short FLT and maximum CPT release after 12 hours of dissolution testing. The effect of increasing the agitation speed of USP Apparatus 2 from

50 to 100 rpm on the release of CPT from the optimised formulation was investigated. The results revealed that varying the speed of the paddle apparatus had a relatively small impact on the *in vitro* release behaviour of CPT from the tablets. A small change in dissolution rate was observed when agitation was increased, which may be a result of the high water solubility of CPT. This has been reported to outweigh the influence of the paddle speed during dissolution testing. The optimised formulation was subjected to additional testing in an attempt to investigate the effects of pH and osmolarity on the swelling and erosion characteristics of the dosage form. The results generated from swelling studies revealed that the swelling characteristics of the proposed formulation were not significantly altered by a change in pH and osmolarity, and this is due to the non-ionic nature of HPMC. The results revealed the erosion rate constants were low, and suggest that although polymer erosion occurred, its role in CPT release may not be as significant as that of diffusion. The short-term stability of the optimised formulation was established by undertaking stability studies at 25°/60% RH and 40°/75% RH. The results revealed that there was no significant change in appearance and physicochemical properties of the tablets over 60 days. However, long-term stability studies would be required to determine the shelf-life and physicochemical stability of the tablets.

In conclusion, sustained release gastro-retentive CPT tablets with the potential for further development have been developed in these studies. The optimised formulation released 86% CPT after 12 hours of dissolution testing in 0.1 M HCl, and remained buoyant for the duration of the dissolution test. Further studies to improve this formulation would include investigating the application of a polymeric coat to reduce the initial burst effect, and performing dissolution studies using Simulated Gastric Fluid (SGF) to predict the *in vivo* behaviour of the formulation. These research studies have provided a starting point for the development of sustained release gastroretentive formulations for API that exhibit high water solubility and/or may require gastric retention in order to improve *in vivo* stability and/or solubility.

Reference List

(1) Cardivascular Diseases (CVDs) Fact Sheet. World Health Organization 2013 March [cited 2013 Aug 16];Available from: URL: http://www.who.int/mediacentre/factsheets/fs317/en/index.html

(2) Gibbon JC (Editor). South African Medicines Formulary. 8 ed. Cape Town: Health and Medical Publishing Group; 2012,pp 157-158.

(3) Lacy C, Armstrong LL, Goldman MP, Lance LL. Drug Information Handbook. 15 ed. Ohio: Lexi-comp Hudson; 1999, pp 184-186.

(4) Reynolds JEF.(Editor). Martindale: The Extra Pharmacopoeia. 30 ed. London: The Pharmaceutical Press; 2012, pp 342-349

(5) Florey KE. Analytical Profiles of Drug Substances. 11 ed. London: Academic Press, Inc; 2012, pp79-128

(6) Mendis S, Puska P, Norrving B. Global atlas on cardiovascular disease prevention and control. World Health Organization; 2011, pp 1-114. [cited 2013 Aug 16]; Available from: URL: http://whqlibdoc.who.int/publications/2011/9789241564373_eng.pdf?ua=1

(7) Mendis S, Banerjee A. Cardiovascular disease: equity and social determinants 3. Equity, social determinants and public health programmes 2010; pp 31-40. [cited 2013 Aug 16]; Available from: URL: http://whqlibdoc.who.int/publications/2010/9789241563970_eng.pdf

(8) Kubo SH, Cody RJ. Clinical pharmacokinetics of the angiotensin converting enzyme inhibitors. Clinical pharmacokinetics 1985; 10(5): 377-91.

(9) Sabroe RA, Black AK. Angiotensin-converting enzyme (ACE) inhibitors and angio-oedema. British Journal of Dermatology 1997 Feb 1; 136(2): 153-8.

(10) Wen H, Park K (Editors). Oral Controlled Release Formulation Design and Drug Delivery. 2011,1-332.

(11) Siepmann J, Siegel RA, Rathbone MJ (Editors). Fundamentals and applications of controlled release drug delivery. New York: Springer; 2012, pp 19.

(12) Captopril. British Pharmacopoeia Online 2013. [cited 2013 Aug 16]; Available from: URL: http://0-www.pharmacopoeia.co.uk.wam.seals.ac.za/bp2013

(13) United States Pharmacopoeia-National Formulary 2013. [cited 2013 Aug 16]; Available from: URL http://0-www.uspnf.com.wam.seals.ac.za/uspnf

(14) Felton LE (Editor). Remington: Essentials of Pharmaceutics. London: Pharmaceutical Press; 2013, pp 188-189.

(15) Rabenstein DL, Isab AA. Conformational and acid-base equilibriums of captopril in aqueous solution. Anal Chem 1982 Mar 1; 54(3): 526-9.

(16) Wang SL, Lin SY, Chen TF, Chuang CH. Solid-state *trans-cis* isomerization of captopril determined by thermal Fourier transform infrared (FT-IR) microspectroscopy. J Pharm Sci 2001 Aug 1; 90(8): 1034-9.

(17) Mariappan SVS, Rabenstein DL. Kinetics and thermodynamics of *cis-trans* isomerization of captopril and related compounds. J Org Chem 1992 Nov 1; 57(24): 6675-8.

(18) Wang SL, Lin SY, Chen TF, Chuang CH. Solid-state *trans-cis* isomerization of captopril determined by thermal Fourier transform infrared (FT-IR) microspectroscopy. J Pharm Sci 2001 Aug 1; 90(8): 1034-9.

(19) Lund W, Royal Pharmaceutical Society of Great Britain. The Pharmaceutical Codex: Principles and Practice of Pharmaceutics. 12th (Ed). London: The Pharmaceutical press; 1994, pp 772-774.

(20) Nur AO, Zhang JS. Recent progress in sustained/controlled oral delivery of captopril: an overview. International Journal of Pharmaceutics 2000 Jan 25; 194(2): 139-46.

(21) Troy, D.B. (Ed.), Remington The Science and Practice of Pharmacy, 21st Ed. Philadelphia: Lippincott Williams & Wilkins; 2013, pp 450, 477-478, 1354-1355, 2190.

(22) O'Neil MJ (Editor). The Merck Index: An Encyclopedia of Chemicals, Drugs, and Biologicals.New Jersey: Whitehouse station; 2001, pp 1783.

(23) Ivanovic D, Medenica M, Malenovic A, Jancic B. Validation of the RP□HPLC method for analysis of hydrochlorothiazide and captopril in tablets. Accred Qual Assur 2004; 9(1-2): 76-81.

(24) Lindenberg M, Kopp S, Dressman JB. Classification of orally administered drugs on the World Health Organization Model list of Essential Medicines according to the biopharmaceutics classification system. European Journal of Pharmaceutics and Biopharmaceutics 2004 Sep; 58(2): 265-78.

(25) Wu CY, Benet LZ. Predicting drug disposition via application of BCS: transport/absorption/elimination interplay and development of a biopharmaceutics drug disposition classification system. Pharmaceutical Research 2005; 22(1): 11-23.

(26) Foye WO, Lemke TL, Williams DA. Foye's Principles of Medicinal Chemistry. 7th Ed. Baltimore: Lippincott Williams & Wilkins; 2008, pp 748-761.

(27) Kasim NA, Whitehouse M, Ramachandran C, Bermejo M, Lennernäs H, Hussain AS, et al. Molecular Properties of WHO Essential Drugs and Provisional Biopharmaceutical Classification. Mol Pharmaceutics 2003 Dec 17; 1(1): 85-96.

(28) World Health Organization. International Pharmacopoeia 2006. World Health Organization; 2006. [cited 2013 Aug 19]; Available from: URL http://apps.who.int/phint/en/p/docf/

(29) Settle FA. Handbook of Instrumental Techniques for Analytical Chemistry. New Jersey: Prentice hall; 1997; 249: 247-83.

(30) Coates J. Interpretation of Infrared Spectra in A Practical Approach. Encyclopedia of Analytical Chemistry. Chichester: John Wiley and Sons Ltd; 2000; 1-23.

(31) Stuart BH. Infrared spectroscopy: Fundamentals and Applications. Chichester: John Wiley and Sons Ltd; 2004; pp 1-14.

(32) Stulzer HK, Rodrigues PO, Cardoso TM, Matos JSR, Silva MAS. Compatibility studies between captopril and pharmaceutical excipients used in tablets formulations. Journal of Thermal Analysis & Calorimetry 2008 Jan; 91(1): 323-8.

(33) Ondetti MA. Structural relationships of angiotensin converting-enzyme inhibitors to pharmacologic activity. Circulation 1988; 77(6 Pt 2): I74.

(34) Kristensen S, Lao YE, Brustugun J, Braenden JU. Influence of formulation properties on chemical stability of captopril in aqueous preparations. Die Pharmazie-An International Journal of Pharmaceutical Sciences 2008; 63(12): 872-7.

(35) Hillaert S, Van den Bossche W. Determination of captopril and its degradation products by capillary electrophoresis. Journal of Pharmaceutical and Biomedical Analysis 1999 Oct; 21(1): 65-73.

(36) Brustugun J, Lao YE, Fagernaes C, Braenden J, Kristensen S. Long-term stability of extemporaneously prepared captopril oral liquids in glass bottles. American Journal of Health-System Pharmacy 2009; 66(19): 1722-5.

(37) Frohlich ED, Richard N (Editors). The local cardiac renin angiotensin-aldosterone system. 20 Ed.New York: Springer; 2006, pp 7-8.

(38) DeMello WC, Frohlich ED (Editors). Renin Angiotensin System and Cardiovascular Disease. New York: Springer; 2009, pp 35-36 .

(39) Chapter 26. Renin and Angiotensin. In: Brunton LL, Chabner BA, Knollmann BC, eds. Goodman & Gilman's The Pharmacological Basis of Therapeutics. 12nd ed. New York: McGraw-Hill; 2013; pp 434-484.

(40) Katzung BGED. Basic and Clinical Pharmacology. 11th Ed. New York: McGraw-Hill Medical; 2009; pp 219-297.

(41) Greenstein B, Wood D. The Endocrine System at a Glance. 42 Ed. London: Wiley-Blackwell; 2011, pp 78-81.

(42) Lullmann H, Morh K, Hein L, Beiger D. Color Atlas of Pharmacology. 3rd Ed. Teningen: Thieme; 2005, pp 128-129.

(43) Frohlich ED. ACE Inhibition in Hypertension: From principle to practice. New York: Biomedical Information Corporation; 1982, pp 1-17.

(44) Donnelly P. Nurse's Handbook of Combination Drugs. Sudbury: Jones & Bartlett Publishers; 2010, pp 101-102.

(45) Bonow RO, Mann DL, Zipes DP, Libby P. Braunwald's Heart Disease: A Textbook of Cardiovascular Medicine, 2-Volume Set. Philadelphia: Saunders; 2011, 239-253.

(46) Craig CR, Stitzel RE. Modern Pharmacology with Clinical Applications, 6e.Baltimore: Lippincott Williams & Wilkins; 2004, pp 210-212.

(47) Captopril. Micromedex 2013 [cited 2013 May 8]; Available from: URL: http://0-www.thomsonhc.com.wam.seals.ac.za/micromedex2/librarian/ND_T/evidencexpert/ND_PR/evidencexpert/CS/8B95D2/ND_AppProduct/evidencexpert/DUPLICATIONSHIELDSYNC/145E0E/ND_PG/evidencexpert/ND_B/evidencexpert/ND_P/evidencexpert/PFActionId/evidencexpert.IntermediateToFullDocumentLink/docId/0591/contentSetId/31/title/CAPTOPRIL/servicesTitle/CAPTOPRIL

(48) Munoz R, Vetterly C, Roth SJ, da Cruz E. Handbook of Pediatric Cardiovascular Drugs. London: Springer; 2007, pp 77-79.

(49) Golan DE, Tashjian AH, Armstrong EJ, Armstrong AW. Principles of pharmacology: The Pathophysiologic Basis of Drug Therapy. Philadelphia Lipincott Williams and Wilkins; 2011; pp 343-458.

(50) Ceyhan B, Karaaslan Y, Caymaz O, Oto A, Oram E, Oram A, et al. Comparison of sublingual captopril and sublingual nifedipine in hypertensive emergencies. Japanese Journal of Pharmacology 1990; 52(2): 189.

(51) Biollaz J, Waeber B, Brunner HR. Hypertensive crisis treated with orally administered captopril. Eur J Clin Pharmacol 1983; 25(2): 145-9.

(52) Dollery C (Editor). Therapeutic drugs. Edinurgh: Churchill Livingstone; 1991, C44-C48.

(53) United States Pharmacopeia, United States Pharmacopeial Convention. USP DI.: Drug Information for the Health Care Professional. Rockville: United States Pharmacopeial Convention Inc; 1990; pp 166-173.

(54) Kauffman RE, Banner Jr W, Berlin Jr CM, Blumer JL, Gormer RL, Lambert GH, et al. The transfer of drugs and other chemicals into human milk. Pediatrics 1994; 93(1): 137-50.

(55) Devlin RG, Fleiss PM. Captopril in human blood and breast milk. The Journal of Clinical Pharmacology 1981; 21(2): 110-3.

(56) Turner L. Daily Drug Use: A Guide for the Health Professional. 9th ed. Cape Western Branch of the Pharmaceutical Society of South Africa; 2010, pp 132-136.

(57) Israili ZH, Hall WD. Cough and angioneurotic edema associated with angiotensin-converting enzyme inhibitor therapy. Annals of Internal Medicine 1992 Aug 8; 117(3): 234.

(58) Coulter DM, Edwards IR. Cough associated with captopril and enalapril. British medical journal (Clinical research ed) 1987; 294(6586): 1521.

(59) Stoller JK, Elghazawi A, Mehta AC, Vidt DG. Captopril-induced cough. CHEST Journal 1988; 93(3): 659-61.

(60) Woo KS, Nicholls MG. High prevalence of persistent cough with angiotensin converting enzyme inhibitors in Chinese. British Journal of Clinical Pharmacology 1995; 40(2): 141.

(61) McNeil JJ, Anderson A, Christophidis N, Jarrott B, Louis WJ. Taste loss associated with captopril treatment. British Medical Journal 1979; 2(6204): 1555.

(62) Havelka J, Boerlin HJ, Studer A, Greminger P, Tenschert W, Luescher T, et al. Long-term experience with captopril in severe hypertension. British Journal of Clinical Pharmacology 1982; 14(S2): 71S-6S.

(63) Ackerman BH, Kasbekar N. Disturbances of taste and smell induced by drugs. Pharmacotherapy: The Journal of Human Pharmacology and Drug Therapy 1997 May 6; 17(3): 482-96.

(64) Doty RL, Shah M, Bromley SM. Drug-induced taste disorders. Drug Safety 2008 Feb; 31(3): 199-215.

(65) Bromley SM. Smell and taste disorders: A primary care approach. Am Fam Physician 2000; 61(2): 427-36.

(66) Edwards IR, Coulter DM, Beasley DM, MacIntosh D. Captopril: 4 years of post marketing surveillance of all patients in New Zealand. British Journal of Clinical Pharmacology 1987; 23(5): 529-36.

(67) Coulter DM. Eye pain with nifedipine and disturbance of taste with captopril: A mutually controlled study showing a method of postmarketing surveillance. British Medical Journal (Clinical Research Ed) 1988;296(6629):1086.

(68) Gavras H, Gavras I. Angiotensin converting enzyme inhibitors. Properties and side effects. Hypertension 1988; 11(3 Pt 2): II37.

(69) Wilkin JK, Walter K. Pityriasis rosea-like rash from captopril. Archives of Dermatology 1982 Mar 1; 118(3): 186-7.

(70) Frohlich ED, Cooper RA, Lewis EJ. Review of the overall experience of captopril in hypertension. Archives of Internal Medicine 1984; 144(7): 1441.

(71) Heel RC, Brogden RN, Speight TM, Avery GS. Captopril: A preliminary review of its pharmacological properties and therapeutic efficacy. Drugs 1980; 20(6): 409-52.

(72) Groel JT, Tadros SS, Dreslinski GR, Jenkins AC. Long-term antihypertensive therapy with captopril. Hypertension 1983; 5(5 Pt 2): III145.

(73) Grosbois B, Milton D, Beneton C, Jacomy D. Thrombocytopenia induced by angiotensin converting enzyme inhibitors. BMJ: British Medical Journal 1989; 298(6667): 189.

(74) Chalmers D, Whitehead A, Lawson DH. Postmarketing surveillance of captopril for hypertension. British Journal of Clinical Pharmacology 1992; 34(3): 215-23.

(75) Walley T, Winstanley P, Roberts D, Grimmer M, Orme M, Breckenridge A. Adverse effects of captopril in hospital outpatients with hypertension. Postgraduate Medical Journal 1990 Feb 1; 66(772): 106-9.

(76) Vleeming W, van Amsterdam JGC, Stricker BHC, de Wildt DJ. ACE inhibitor-induced angioedema: Incidence, Prevention and Management. Drug Safety 1998 Mar; 18(3): 171-88.

(77) Duchin KL, McKinstry DN, Cohen AI, Migdalof BH. Pharmacokinetics of captopril in healthy subjects and in patients with cardiovascular diseases. Clin-Pharmacokinet 1988; 14(4): 241-59.

(78) Endoh M, Suzuki M, Katayama K, Kakemi M, Koizumi T. Kinetic studies of the pharmacologic response to captopril in rats. II. Hypotensive effect and plasma angiotensin converting enzyme activity. Journal of Pharmacobio-dynamics 1989; 12(1): 10.

(79) Ohman KP, Kagedal B, Larsson R, Karlberg BE. Pharmacokinetics of Captopril and its effects on blood pressure during acute and chronic administration and in relation to food intake. Journal of Cardiovascular Pharmacology 1985; 7(1).

(80) Salvetti A, Pedrinelli R, Magagna A, Abdel-Haq B, Graziadei L, Taddei S, et al. Influence of food on acute and chronic effects of captopril in essential hypertensive patients. Journal of Cardiovascular Pharmacology 1985; 7(1): S25-S29.

(81) Muller HM, Overlack A, Heck I, Kolloch R, Stumpe KO. The influence of food intake on pharmacodynamics and plasma concentration of captopril. Journal of Hypertension Supplement: Official Journal of the International Society of Hypertension 1985; 3(2): S135.

(82) Duchin KL, Singhvi SM, Willard DA, Migdalof BH, McKinstry DN. Captopril kinetics. Clin Pharm Ther 1982 Apr; 31(4): 452-8.

(83) Rendic S. Summary of information on human CYP enzymes: Human P450 metabolism data. Drug Metabolism Reviews 2002 Feb; 34(1/2): 83.

(84) Vesterberg O. History of electrophoretic methods. Journal of Chromatography A 1989; 480: 3-19.

(85) Jorgenson JW, Lukacs KD. High-resolution separations based on electrophoresis and electro-osmosis. Journal of Chromatography A 1981; 218: 209-16.

(86) Altria KD. Capillary Electrophoresis Guidebook: Principles, Operation, and Applications. 52 ed. New Jersey: Springer; 1996, pp 3-345.

(87) Li SFY. Capillary electrophoresis: principles, practice and applications. Access Online via Elsevier; 1992.

(88) Neubert RH, Ruttinger HH. Affinity capillary electrophoresis in pharmaceutics and biopharmaceutics. New York: CRC Press; 2003; pp 1-280.

(89) Xu Y. Tutorial: Capillary electrophoresis. The Chemical Educator. 1996; 1(2): 1-14.

(90) Lauer HH, McManigill D. Capillary zone electrophoresis of proteins in untreated fused silica tubing. Anal Chem 1986; 58(1): 166-70.

(91) Foret F, Fanali S, Nardi A, Bocek P. Capillary zone electrophoresis of rare earth metals with indirect UV absorbance detection. Electrophoresis 1990; 11(9): 780-3.

(92) McCormick RM. Capillary zone electrophoretic separation of peptides and proteins using low pH buffers in modified silica capillaries. Anal Chem 1988; 60(21): 2322-8.

(93) Faria AF, de Souza MV, de Almeida MV, de Oliveira MA. Simultaneous separation of five fluoroquinolone antibiotics by capillary zone electrophoresis. Analytica Chimica Acta 2006; 579(2): 185-92.

(94) Frazier RA, Nursten HE, Ames JM. Capillary Electrophoresis for Food Analysis: Method development. Cambridge: Royal Society of Chemistry; 2000, pp 16-18.

(95) Towns JK, Regnier FE. Polyethyleneimine-bonded phases in the separation of proteins by capillary electrophoresis. Journal of Chromatography A 1990; 516(1): 69-78.

(96) Cohen AS, Najarian DR, Karger BL. Separation and analysis of DNA sequence reaction products by capillary gel electrophoresis. Journal of Chromatography A 1990; 516(1): 49-60.

(97) Jensen PK, Paia-Tolic L, Peden KK, Martinovic S, Lipton MS, Anderson GA, et al. Mass spectrometic detection for capillary isoelectric focusing separations of complex protein mixtures. Electrophoresis 2000;21(7):1372-80.

(98) Shen Y, Smith RD. High-resolution capillary isoelectric focusing of proteins using highly hydrophilic-substituted cellulose-coated capillaries. Journal of Microcolumn Separations 2000; 12(3): 135-41.

(99) Shen Y, Berger SJ, Anderson GA, Smith RD. High-efficiency capillary isoelectric focusing of peptides. Anal Chem 2000; 72(9): 2154-9.

(100) Righetti PG. Isoelectric Focusing: Theory, Methodology and Application: Theory, Methodology and Application. Amsterdam: Elsevier Science; 2000; pp 1-39.

(101) Colon LA, Burgos G, Maloney TD, Cintron JM, Rodriguez RL. Recent progress in capillary electrochromatography. Electrophoresis 2000;21(18):3965-93.

(102) Svec F, Deyl Z. Capillary Electrochromatography. Amsterdam: Elsevier Science; 2001 pp 1-413.

(103) Bartle KD, Myers P, Myers P, Royal Society of Chemistry (Great Britain). Capillary Electrochromatography. Cambridge: Royal Society of Chemistry; 2001; pp 1-144.

(104) Camilleri P. Capillary Electrophoresis: Theory and Practice, 2nd Ed. Florida: Taylor & Francis; 1997; pp 23-397.

(105) Buszewski B, Dziubakiewicz E, Szumski M (Editors). Electromigration Techniques: Theory and Practice. Springer; 2013; pp 1-37.

(106) Capillary Electrophoresis. European Pharmacopoeia 5.0; pp 74-79. [cited 2013 May 20]; Available from: URL: http://lib.njutcm.edu.cn/yaodian/ep/EP5.0/02_methods_of_analysis/2.2._physical_and_physicochemical_methods/2.2.47.%20Capillary%20electrophoresis.pdf

(107) Ahuja S, Jimidar M. Capillary electrophoresis methods for pharmaceutical analysis. 9 Ed. London: Elsiever Inc;2008; pp 1-434.

(108) Ewing AG, Wallingford RA, Olefirowicz TM. Capillary electrophoresis. Anal Chem 1989; 61(4): 292A-303A.

(109) Hempel G. Strategies to improve the sensitivity in capillary electrophoresis for the analysis of drugs in biological fluids. Electrophoresis 2000; 21(4): 691-8.

(110) Chervet JP, Van Soest REJ, Ursem M. Z-shaped flow cell for UV detection in capillary electrophoresis. Journal of Chromatography A 1991; 543: 439-49.

(111) Albin M, Grossman PD, Moring SE. Sensitivity enhancement for capillary electrophoresis. Anal Chem 1993; 65(10): 489A-97A.

(112) Landers JP. Handbook of Capillary Electrophoresis, 2cnd Ed. Florida: CRC Press; 1996; pp 1-139.

(113) Marina ML, Rios A, Valcarcel M. Analysis and Detection by Capillary Electrophoresis. Amsterdam: Elsevier Science; 2005, pp 225-227.

(114) David GL. Analytical Chemistry. Hyderabad: University Press; 2001, pp 128-131.

(115) Macka M, Andersson P, Haddad PR. Changes in electrolyte pH due to electrolysis during capillary zone electrophoresis. Anal Chem 1998; 70(4): 743-9.

(116) Lewis GA, Mathieu D, Phan-Tan-Luu R. Pharmaceutical experimental design. New York: Marcel Dekker; 1999; pp 1-282.

(117) Bezerra MA, Santelli RE, Oliveira EP, Villar LS, Escaleira LAl. Response surface methodology (RSM) as a tool for optimization in analytical chemistry. Talanta 2008; 76(5): 965-77.

(118) Cox DR, Reid N. The Theory of The Design of Experiments. Florida: CRC Press; 2002; pp 1-182.

(119) Bas D, Boyaci IH. Modeling and optimization I: Usability of response surface methodology. Journal of Food Engineering 2007; 78(3): 836-45.

(120) Vander Heyden Y, Khots MS, Massart DL. Three-level screening designs for the optimisation or the ruggedness testing of analytical procedures. Analytica Chimica Acta 1993 Apr 15; 276(1): 189-95.

(121) Ferreira SLC, Bruns RE, da Silva EGP, dos Santos WNL, Quintella CM, David JM, et al. Statistical designs and response surface techniques for the optimization of chromatographic systems. Journal of Chromatography A 2007; 1158(1): 2-14.

(122) Varesio E, Gauvrit J, Longeray R, Longeray P, Veuthey J. Central composite design in the chiral analysis of amphetamines by capillary electrophoresis. Electrophoresis 1997; 18(6): 931-7.

(123) Morris VM, Hargreaves C, Overall K, Marriott PJ, Hughes JG. Optimization of the capillary electrophoresis separation of ranitidine and related compounds. Journal of Chromatography A 1997 Apr 4;766(1-2):245-54.

(124) Mamani MCV, Farfan JA, Reyes FGR, Rath S. Simultaneous determination of tetracyclines in pharmaceuticals by CZE using experimental design. Talanta 2006 Sep 15; 70(2): 236-43.

(125) Torrealday N, Gonzalez L, Alonso RM, Jimenez RM, Ortiz Lastra E. Experimental design approach for the optimisation of a HPLC-fluorimetric method for the quantitation of the angiotensin II receptor antagonist telmisartan in urine. Journal of Pharmaceutical and Biomedical Analysis 2003 Aug 8; 32(4-5): 847-57.

(126) Stalikas CD, Pilidis GA. Development of a method for the simultaneous determination of phosphoric and amino acid group containing pesticides by gas chromatography with mass-selective detection: Optimization of the derivatization procedure using an experimental design approach. Journal of Chromatography A 2000 Mar 3; 872(1-2): 215-25.

(127) Both DA, Jemal M. Stereoisomeric purity determination of captopril by capillary gas chromatography. Journal of Chromatography A 1991 Sep 27; 558(1): 257-63.

(128) Ito T, Matsuki Y, Kurihara H, Nambara T. Sensitive method for determination of captopril in biological fluids by gas chromatography-mass spectrometry. Journal of Chromatography B: Biomedical Sciences and Applications 1987; 417(0): 79-87.

(129) Chik Z, Mustafa M, Mohamed Z, Lee C. Analysis of Captopril in human plasma using gas chromatography-mass spectrometry (GCMS) with Solid-Phase Extraction (SPE). Current Analytical Chemistry 2010; 6(4): 329-33.

(130) Franklin ME, Addison RS, Baker PV, Hooper WD. Improved analytical procedure for the measurement of captopril in human plasma by gas chromatography-mass spectrometry and its application to pharmacokinetic studies. Journal of

Chromatography B: Biomedical Sciences and Applications 1998 Jan 23; 705(1): 47-54.

(131) Kusierek K, Bald E. A simple liquid chromatography method for the determination of captopril in urine. Chromatographia 2007 Jul 1; 66(1): 71-4.

(132) Jankowski A, Skorek A, Krzysko K, Zarzycki PK, Ochocka RJ, Lamparczyk H. Captopril: Determination in blood and pharmacokinetics after single oral dose. Journal of Pharmaceutical and Biomedical Analysis 1995 Apr; 13: 655-60.

(133) Amini M, Zarghi A, Vatanpour H. Sensitive high-performance liquid chromatographic method for determination of captopril in plasma. Pharmaceutica Acta Helvetiae 1999; 73(6): 303-6.

(134) Bahmaei M, Khosravi A, Zamiri C, Massoumi A, Mahmoudian M. Determination of captopril in human serum by high performance liquid chromatography using solid-phase extraction. Journal of Pharmaceutical and Biomedical Analysis 1997 May; 15(8): 1181-6.

(135) Tache F, Farca A, Medvedovici A, David V. Validation of a LC-fluorescence method for determination of free captopril in human plasma, using a pre-column derivatization reaction with monobromobimane. Journal of Pharmaceutical and Biomedical Analysis 2002 May 15; 28: 549-57.

(136) Khamanga SM, Walker RB. The use of experimental design in the development of an HPLC-ECD method for the analysis of captopril. Talanta 2011 Jan 15; 83(3): 1037-49.

(137) Altria KD, Chen AB, Clohs L. Capillary electrophoresis as a routine analytical tool in pharmaceutical analysis. LC GC North America 2001; 19(9): 972-85.

(138) Neubert RH, Schwarz MA, Mrestani Y, Platzer M, Raith K. Affinity capillary electrophoresis in pharmaceutics. Pharmaceutical research 1999; 16(11): 1663-73.

(139) Hernandez M, Borrull F, Calull M. Capillary zone electrophoresis determination of oxytetracycline in pig tissue samples at maximum residue limits. Chromatographia 2001; 54(5-6): 355-9.

(140) Mohammadi A, Kanfer I, Walker RB. A capillary zone electrophoresis (CZE) method for the determination of cyclizine hydrochloride in tablets and suppositories. Journal of Pharmaceutical and Biomedical Analysis 2004 Apr 1; 35(1): 233-9.

(141) Matsuki Y, Fukuhara K, Ito T, Ono H, Ohara N, Yui T, et al. Determinatin of captopril in biological fluids by gas-liquid chromatography. Journal of Chromatography A 1980 Jan 25; 188(1): 177-83.

(142) Matsuki Y, Ito T, Fukuhara K, Nakamura T, Kimura M, Ono H, et al. Determination of captopril and its disulphide in biological fluids. Journal of Chromatography A 1982; 239: 585-94.

(143) Li K, Tan L, Zhou Jh. HPLC Determination of Captopril in human plasma and its pharmacokinetic study. Biomed Chromatogr 1996 Sep 1; 10(5): 237-9.

(144) Pérez-Ruiz T, Martínez-Lozano C, Galera R. Development and validation of a capillary electrophoresis method with laser-induced fluorescence detection for the determination of captopril in human urine and pharmaceutical preparations. Electrophoresis 2006; 27(12): 2310-6.

(145) Bretnall AE, Clarke GS. Selectivity of capillary electrophoresis for the analysis of cardiovascular drugs. Journal of Chromatography A 1996 Sep 20; 745(1-2): 145-54.

(146) Robinson JW, Frame EMS, Frame GM. Undergraduate Instrumental Analysis, 6th Edition. New York: Marcel & Dekker; 2004; pp 87-89.

(147) Altria K, Rudd D. An overview of method validation and system suitability aspects in capillary electrophoresis. Chromatographia 1995 Sep 1; 41(5): 325-31.

(148) Dolan JW. Peak Tailing and Resolution. Walnut Creek, California, USA: LC Resources Inc; 2002 June, pp 1-4. [cited 2013 May 28]; Available from: URL: http://www.chromatographyonline.com/lcgc/data/articlestandard/lcgceurope/202002/19199/article.pdf

(149) Ermer J, Miller JHMB. Method Validation in Pharmaceutical Analysis: A Guide to Best Practice. Darmastardt: John Wiley & Sons; 2006 pp 1-396.

(150) Guideline T. Q2A Text on Validation of Analytical Procedures. Fed Regist 2005; 60.

(151) Ahuja S, Scypinski S. Handbook of Modern Pharmaceutical Analysis. London: Elsevier Science; 2001, pp 18-283.

(152) Chan CC, Lee YC, Lam H, Zhang XM. Analytical Method Validation and Instrument Performance Verification. New Jersey.:John Wiley & Sons; 2004; 1-277.

(153) Green JM. Peer Reviewed: A Practical Guide to Analytical Method Validation. Anal Chem 1996;68(9): 305A-9A.

(154) Guideline T. Q2B validation of analytical procedures: methodology. Fed Regist 1997;62.

(155) Altria KD, Chanter YL. Validation of a capillary electrophoresis method for the determination of a quinolone antibiotic and its related impurities. Journal of Chromatography A 1993; 652(2): 459-63.

(156) Emaldi P, Fapanni S, Baldini A. Validation of a capillary electrophoresis method for the determination of cephradine and its related impurities. Journal of Chromatography A 1995 Sep 22; 711(2): 339-46.

(157) Yesilada A, Gokhan N, Tozkoparan B, Ertan M, Aboul-Enein HY. Method validation in pharmaceutical analysis: From a general approach to capillary electrophoresis. Journal of Liquid Chromatography & Related Technologies 1998;21(17):2619-32.

(158) Shabir GA, John Lough W, Arain SA, Bradshaw TK. Evaluation and application of best practice in analytical method validation. Journal of Liquid Chromatography & Related Technologies 2007; 30(3): 311-33.

(159) Riley CM, Rosanske TW (Editors). Development and Validation of Analytical Methods. Elsevier Science; 1996; pp 1-15.

(160) Guideline T. Q2A Text on Validation of Analytical Procedures. Fed Regist 1995; 60.

(161) Babu VS, Kumar SS, Murali RV, Rao MM. Investigation and validation of optimal cutting parameters for least surface roughness in EN24 with response surface method. International Journal of Engineering, Science and Technology 2011; 3(6): 146-60.

(162) Kim MJ, Kim HJ, Kihm KD. Micro-scale PIV for electroosmotic flow measurement. Proceedings of PSFVIP-3, Maui, Hawaii, USA 2001; 18-21.

(163) Prieto J, Akesolo U, Jimenez R, Alonso R. Capillary zone electrophoresis applied to the determination of the angiotensin-converting enzyme inhibitor cilazapril and its active metabolite in pharmaceuticals and urine. Journal of Chromatography A 2001 May 4; 916: 279-88.

(164) Lieberman H, Lachman L, Schwartz JB. Pharmaceutical Dosage Forms: Tablets, Volume 1, 2nd Ed. New York: Taylor & Francis; 1989; pp 1-584.

(165) Lawrence XY. Pharmaceutical quality by design: Product and process development, understanding, and control. Pharmaceutical research 2008; 25(4): 781-91.

(166) Ahuja S, Scypinski S. Handbook of Modern Pharmaceutical Analysis. London: Elsevier Science; 2001, pp 18-283.

(167) Di Feo TJ. Drug product development: Atechnical review of chemistry, manufacturing, and controls information for the support of pharmaceutical compound licensing activities. Drug Development and Industrial Pharmacy 2003; 29(9): 939-58.

(168) Steinberg M, Borzelleca JF, Enters EK, Kinoshita FK, Loper A, Mitchell DB, et al. A new approach to the safety assessment of pharmaceutical excipients: the Safety Committee of the International Pharmaceutical Excipients Council. Regulatory Toxicology and Pharmacology 1996; 24(2): 149-54.

(169) Pifferi G, Restani P. The safety of pharmaceutical excipients. Il Farmaco 2003 Aug; 58(8): 541-50.

(170) Sam T. Regulatory implications of excipient changes in medicinal products. Drug information journal 2000; 34(3): 875-94.

(171) Rowe RC, Sheskey PJ, Quinn ME, Press P. Handbook of pharmaceutical excipients. 6 ed. London: Pharmaceutical Press; 2009; pp 129-732.

(172) Li CL, Martini LG, Ford JL, Roberts M. The use of hypromellose in oral drug delivery. Journal of Pharmacy and Pharmacology 2005 May 1;57(5): 533-46.

(173) Tiwari SB, Rajabi-Siahboomi AR. Modulation of drug release from hydrophilic matrices. Pharmaceutical Technology Europe. 2008. [cited 2013 November 28]; Available from: URL: http://www.pharmtech.com/pharmtech/article/articleDetail.jsp?id=547891

(174) Jivraj M, Martini LG, Thomson CM. An overview of the different excipients useful for the direct compression of tablets. Pharmaceutical Science & Technology Today 2000 Feb 1; 3(2): 58-63.

(175) Saigal N, Baboota S, Ahuja A, Ali J. Microcrystalline cellulose as a versatile excipient in drug research. Journal of Young Pharmacists 2009; 1(1): 6.

(176) Crowley MM, Schroeder B, Fredersdorf A, Obara S, Talarico M, Kucera S, et al. Physicochemical properties and mechanism of drug release from ethyl cellulose matrix tablets prepared by direct compression and hot-melt extrusion. International Journal of Pharmaceutics 2004; 269(2): 509-22.

(177) Katikaneni PR, Upadrashta SM, Neau SH, Mitra AK. Ethylcellulose matrix controlled release tablets of a water-soluble drug. International Journal of Pharmaceutics 1995 Aug 29; 123(1): 119-25.

(178) Sánchez-Lafuente C, Teresa Faucci M, Fernández-Arévalo M, Álvarez-Fuentes J, Rabasco AM, Mura P. Development of sustained release matrix tablets of didanosine containing methacrylic and ethylcellulose polymers. International Journal of Pharmaceutics 2002 Mar 2; 234(1-2): 213-21.

(179) Jaimini M, Rana AC, Tanwar YS. Formulation and evaluation of famotidine floating tablets. Current Drug Delivery 2007; 4(1): 51-5.

(180) Ichikawa M, Watanabe S, Miyake Y. A new multiple-unit oral floating dosage system. I: Preparation and in vitro evaluation of floating and sustained□release characteristics. J Pharm Sci 1991; 80(11): 1062-6.

(181) Basak SC, Nageswara Rao K, Manavalan R, Rama Rao P. Development and in vitro evaluation of an oral floating matrix tablet formulation of ciprofloxacin. Indian Journal of Pharmaceutical Sciences 2004; 66(3): 313-6.

(182) Rahman Z, Ali M, Khar RK. Design and evaluation of bilayer floating tablet of captopril. ACTA Pharmaceutica-Zagreb- 2006; 56(1): 49.

(183) Strickland WA, Nelson E, Busse LW, Higuchi T. The physics of tablet compression IX. Fundamental aspects of tablet lubrication. Journal of the American Pharmaceutical Association 1956 Jan 1; 45(1): 51-5.

(184) Zuurman K, Voort Maarschalk K, Bolhuis GK. Effect of magnesium stearate on bonding and porosity expansion of tablets produced from materials with different consolidation properties. International Journal of Pharmaceutics 1999 Mar 1; 179(1): 107-15.

(185) Zazenski R, Ashton WH, Briggs D, Chudkowski M, Kelse JW, Maceachern L, et al. Talc: Occurrence, Characterization, and Consumer Applications. Regulatory Toxicology and Pharmacology 1995 Apr; 21(2): 218-29.

(186) Tousey MD. The Granulation Process 101. Pharm Tech 2002; 8-13.

(187) Aulton ME (Editor), Wells TI. Pharmaceutics: The Science of Dosage form Design. 2nd Ed. London: Churchill Livingston. 2002; pp 139-197.

(188) Aulton ME, Taylor KMG. Aulton's Pharmaceutics: The Design and Manufacture of Medicines. London: Elsevier Health Sciences UK; 2013 pp 138-527.

(189) Verma RK, Garg S. Selection of excipients for extended release formulations of glipizide through drug-excipient compatibility testing. Journal of Pharmaceutical and Biomedical Analysis 2005 Jul 15;38(4):633-44.

(190) Qiu Y, Chen Y, Zhang GGZ, Liu L, Porter W. Developing Solid Oral Dosage Forms: Pharmaceutical Theory & Practice. New York: Elsevier Science; 2009 pp 125-143.

(191) Narang AS, Desai D, Badawy S. Impact of excipient interactions on solid dosage form stability. Pharmaceutical Research 2012; 29(10): 2660-83.

(192) Crowley P, Martini LG. Drug-excipient interactions. Pharm Technol 2001;4:7-12.

(193) Bruni G, Berbenni V, Milanese C, Girella A, Marini A. Drug-excipient compatibility studies in binary and ternary mixtures by physico-chemical techniques. Journal of Thermal Analysis & Calorimetry 2010 Oct; 102(1): 193-201.

(194) Van Dooren AA. Design for Drug-Excipient Interaction Studies. Drug Development and Industrial Pharmacy 1983 Jan 1; 9(1-2): -55.

(195) Adeyeye MC, Brittain HG. Preformulation in Solid Dosage Form Development. London: Taylor & Francis; 2008; pp 1-616.

(196) Shekunov BY, Chattopadhyay P, Tong HH, Chow AH. Particle size analysis in pharmaceutics: principles, methods and applications. Pharmaceutical research 2007; 24(2): 203-27.

(197) Liu LX, Marziano I, Bentham AC, Litster JD, E.T.White, Howes T. Effect of particle properties on the flowability of ibuprofen powders. International Journal of Pharmaceutics 2008 Oct 1; 362(1-2): 109-17.

(198) Meka L, Kesavan B, Chinnala KM, Vobalaboina V, Yamsani MR. Preparation of a matrix type multiple-unit gastro retentive floating drug delivery system for captopril based on gas formation technique: in vitro evaluation. AAPS PharmSciTech 2008; 9(2): 612-9.

(199) Macëdo RO, Gomes do Nascimento T, Soares Aragão CF, Barreto Gomes AP. Application of thermal analysis in The characterization of anti-hypertensive drugs. Journal of Thermal Analysis and Calorimetry 2000; 59(3): 657-61.

(200) Pani N, Nath L, Acharya S, Bhuniya B. Application of DSC, IST, and FTIR study in the compatibility testing of nateglinide with different pharmaceutical excipients. Journal of Thermal Analysis & Calorimetry 2012 Apr; 108(1): 219-26.

(201) Peres-Filho M, Gaeti M, Oliveira S, Marreto R, Lima E. Thermoanalytical investigation of olanzapine compatibility with excipients used in solid oral dosage forms. Journal of Thermal Analysis & Calorimetry 2011 Apr; 104(1): 255-60.

(202) Verma RK, Krishna DM, Garg S. Formulation aspects in the development of osmotically controlled oral drug delivery systems. Journal of Controlled Release 2002 Feb 19; 79(1-3): 7-27.

(203) Hjalmarson Â, Goldstein S, Fagerberg B, Wedel H, Waagstein F, Kjekshus J, et al. Effects of controlled-release metoprolol on total mortality, hospitalizations, and well-being in patients with heart failure. JAMA: the journal of the American Medical Association 2000; 283(10): 1295-302.

(204) Gimbel JS, Richards P, Portenoy RK. Controlled-release oxycodone for pain in diabetic neuropathy A randomized controlled trial. Neurology 2003; 60(6): 927-34.

(205) Singh B, Chakkal SK, Ahuja N. Formulation and optimization of controlled release mucoadhesive tablets of atenolol using response surface methodology. AAPS PharmSciTech 2006; 7(1): E19-E28.

(206) CR IM. Effect of metoprolol CR/XL in chronic heart failure: Metoprolol CR/XL randomised intervention trial in congestive heart failure (MERIT-HF). Lancet 1999; 353: 2001-7.

(207) Gelenberg AJ, Lydiard RB, Rudolph RL, Aguiar L, Haskins JT, Salinas E. Efficacy of venlafaxine extended-release capsules in nondepressed outpatients with generalized anxiety disorder. JAMA: the journal of the American Medical Association 2000; 283(23): 3082-8.

(208) Kane J, Canas F, Kramer M, Ford L, Gassmann-Mayer C, Lim P, et al. Treatment of schizophrenia with paliperidone extended-release tablets: a 6-week placebo-controlled trial. Schizophrenia research 2007;90(1):147-61.

(209) Uhrich KE, Cannizzaro SM, Langer RS, Shakesheff KM. Polymeric systems for controlled drug release. Chemical Reviews 1999; 99(11): 3181-98.

(210) Salsa T, Veiga F, Pina ME. Oral controlled-release dosage forms. I. Cellulose ether polymers in hydrophilic matrices. Drug development and industrial pharmacy 1997; 23(9): 929-38.

(211) Perrie Y, Rades T. Pharmaceutics: Drug Delivery and Targeting. London: Pharmaceutical Press; 2012; pp 87-139.

(212) Wise DL. Handbook of Pharmaceutical Controlled Release Technology. New York: Taylor & Francis; 2000; pp 1-26, 435-44.

(213) Uhrich KE, Cannizzaro SM, Langer RS, Shakesheff KM. Polymeric systems for controlled drug release. Chemical Reviews 1999; 99(11): 3181-98.

(214) Ghosh TK, Jasti BR. Theory and Practice of Contemporary Pharmaceutics. Florida: Taylor & Francis; 2010 pp 346-54.

(215) Wilson CG, Crowley PJ. Controlled Release in Oral Drug Delivery. New York: Springer; 2011 pp 109-130.

(216) Keraliya Rajesh A, Chirag P, Pranav P, Vipul K, Soni Tejal G, Patel Rajnikant C, et al. Osmotic Drug Delivery System as a Part of Modified Release Dosage Form. ISRN pharmaceutics 2012; 2012.

(217) Verma RK, Mishra B, Garg S. Osmotically Controlled Oral Drug Delivery 1*. Drug Development and Industrial Pharmacy 2000;26(7):695-708.

(218) Sriwongjanya M, Bodmeier R. Effect of ion exchange resins on the drug release from matrix tablets. European Journal of Pharmaceutics and Biopharmaceutics 1998 Nov 1;46(3):321-7.

(219) Iannuccelli V, Coppi G, Bernabei MT, Cameroni R. Air compartment multiple-unit system for prolonged gastric residence. Part I. Formulation study. International Journal of Pharmaceutics 1998 Nov 15; 174(1-2): 47-54.

(220) Arora S, Ali J, Ahuja A, Khar RK, Baboota S. Floating drug delivery systems: a review. AAPS PharmSciTech 2005; 6(3): E372-E390.

(221) Garg R, Gupta GD. Progress in controlled gastroretentive delivery systems. Tropical Journal of Pharmaceutical Research 2008; 7(3): 1055-66.

(222) Talukder R, Fassihi R. Gastroretentive delivery systems: a mini review. Drug Development and Industrial Pharmacy 2004; 30(10): 1019-28.

(223) Davis SS. Formulation strategies for absorption windows. Drug Discovery Today 2005; 10(4): 249-57.

(224) Tye CK, Sun CC, Amidon GE. Evaluation of the effects of tableting speed on the relationships between compaction pressure, tablet tensile strength, and tablet solid fraction. J Pharm Sci 2005; 94(3): 465-72.

(225) Jiménez-Castellanos MR, Zia H, Rhodes CT. Design and testing in vitro of a bioadhesive and floating drug delivery system for oral application. International Journal of Pharmaceutics 1994; 105(1): 65-70.

(226) Pitt KG, Heasley MG. Determination of the tensile strength of elongated tablets. Powder Technology 2013 Apr; 238(0): 169-75.

(227) Baumgartner S, Kristl J, Vrecer F, Vodopivec P, Zorko B. Optimisation of floating matrix tablets and evaluation of their gastric residence time. International Journal of Pharmaceutics 2000 Feb 15; 195(1-2): 125-35.

(228) Yang L, Johnson B, Fassihi R. Determination of continuous changes in the gel layer thickness of poly (ethylene oxide) and HPMC tablets undergoing hydration: A texture analysis study. Pharmaceutical research 1998; 15(12): 1902-6.

(229) Levina M, Gothoskar A, Rajabi-Siaboomi. Application of a modelling system in the formulation of extended release hydrophilic matrices. 2006. [cited 2013 November 30]; Available from: URL: [cited 2013 November 28]; Available from: URL: http://www.colorcon.com/literature/marketing/mr/Extended%20Release/METHOCEL/English/hyperstart_form_er_matrices.pdf

(230) Dortunç B, Gunal N. Release of acetazolamide from swellable hydroxypropylmethylcellulose matrix tablets. Drug Development and Industrial Pharmacy 1997; 23(12): 1245-9.

(231) Campos-Aldrete MaE, Villafuerte-Robles L. Influence of the viscosity grade and the particle size of HPMC on metronidazole release from matrix tablets. European Journal of Pharmaceutics and Biopharmaceutics 1997;43(2):173-8.

(232) Tiwari SB, Rajabi-Siahboomi AR. Applications of complementary polymers in HPMC hydrophilic extended release matrices. Drug Deliv Tech 2009; 9(7): 20-7.

(233) Li S, Lin S, Daggy BP, Mirchandani HL, Chien YW. Effect of HPMC and Carbopol on the release and floating properties of Gastric Floating Drug Delivery System using factorial design. International Journal of Pharmaceutics 2003 Mar 6;253(1-2): 13-22.

(234) Ethers MC. Technical Handbook. Dow Chemical Company, Midland, Michingan, USA 1997. [cited 2013 November 29]; Available from: URL: http://www.dow.com/dowwolff/en/pdf/192-01062.pdf

(235) Hu L, Li L, Yang X, Liu W, Yang J, Jia Y, et al. Floating matrix dosage form for dextromethorphan hydrobromide based on gas forming technique: In vitro and in vivo evaluation in healthy volunteers. European Journal of Pharmaceutical Sciences 2011 Jan 18;42(1-2):99-105.

(236) Patel RP, Kamani R. Formulation Optimization and Evaluation of Mometasone Furoate Cream. Journal of Pharmacy Research 2009; 2(10).

(237) Kim MS, Kim JS, You YH, Park HJ, Lee S, Park JS, et al. Development and optimization of a novel oral controlled delivery system for tamsulosin hydrochloride using response surface methodology. International Journal of Pharmaceutics 2007; 341(1): 97-104.

(238) Singh B, Chakkal SK, Ahuja N. Formulation and optimization of controlled release mucoadhesive tablets of atenolol using response surface methodology. AAPS PharmSciTech 2006; 7(1): E19-E28.

(239) Nazzal S, Nutan M, Palamakula A, Shah R, Zaghloul AA, Khan MA. Optimization of a self-nanoemulsified tablet dosage form of Ubiquinone using response surface methodology: effect of formulation ingredients. International Journal of Pharmaceutics 2002; 240(1): 103-14.

(240) Mandal U, Gowda V, Ghosh A, Selvan S, Solomon S, Pal TK. Formulation and optimization of sustained release matrix tablet of metformin HCl 500 mg using response surface methodology. Yakugaku Zasshi 2007; 127(8): 1281-90.

(241) Hanrahan G, Lu K. Application of Factorial and Response Surface Methodology in Modern Experimental Design and Optimization. Critical Reviews in Analytical Chemistry 2006 Sep; 36(3/4): 141-51.

(242) Shah SNH, Asghar S, Choudhry MA, Akash MSH, Rehman Nu, Baksh S. Formulation and evaluation of natural gum-based sustained release matrix tablets of flurbiprofen using response surface methodology. Drug Development & Industrial Pharmacy 2009 Dec; 35(12): 1470-8.

(243) Kincl M, Turk S, Vre-ìer F. Application of experimental design methodology in development and optimization of drug release method. International Journal of Pharmaceutics 2005 Mar 3; 291(1-2): 39-49.

(244) Tadros MI. Controlled-release effervescent floating matrix tablets of ciprofloxacin hydrochloride: Development, optimization and *in vitro-in vivo* evaluation in healthy human volunteers. European Journal of Pharmaceutics and Biopharmaceutics 2010; 74(2): 332-9.

(245) Tahara K, Yamamoto K, Nishihata T. Overall mechanism behind matrix sustained release (SR) tablets prepared with hydroxypropyl methylcellulose 2910. Journal of Controlled Release 1995 Jul; 35(1): 59-66.

(246) Dash S, Murthy PN, Nath L, Chowdhury P. Kinetic modeling on drug release from controlled drug delivery systems. Acta Pol Pharm 2010; 67(3): 217-23.

(247) Palmeri A. Dissolution Theory, Methodology and Testing. Hockessin, DE: Dissolution Technologies, Incorporated; 2007 pp 1-307.

(248) Costa P, Sousa Lobo JM. Modeling and comparison of dissolution profiles. European Journal of Pharmaceutical Sciences 2001; 13(2): 123-33.

(249) Siepmann J, Peppas NA. Modeling of drug release from delivery systems based on hydroxypropyl methylcellulose (HPMC). Advanced Drug Delivery Reviews 2001; 48(2-3): 139-157.

(250) Sinha Roy D, Rohera BD. Comparative evaluation of rate of hydration and matrix erosion of HEC and HPC and study of drug release from their matrices. European Journal of Pharmaceutical Sciences 2002 Aug; 16(3): 193-9.

(251) Ritger PL, Peppas NA. A simple equation for description of solute release II. Fickian and anomalous release from swellable devices. Journal of Controlled Release 1987; 5(1): 37-42.

(252) Anderson MJ, Whitcomb PJ. Response Surface Methods Simplified. New York: Productivity Press; 2005 pp 82.

(253) Ishikawa T, Watanabe Y, Takayama K, Endo H, Matsumoto M. Effect of hydroxypropylmethylcellulose (HPMC) on the release profiles and bioavailability of a poorly water-soluble drug from tablets prepared using macrogol and HPMC. International Journal of Pharmaceutics 2000;202(1):173-8.

(254) Mohamed FA, Roberts M, Seton L, Ford JL, Levina M, Rajabi-Siahboomi AR. The influence of HPMC concentration on release of theophylline or hydrocortisone from extended release mini-tablets. Drug development and industrial pharmacy 2012; (00): 1-8.

(255) Chavanpatil M, Jain P, Chaudhari S, Shear R, Vavia P. Development of sustained release gastroretentive drug delivery system for ofloxacin: In vitro and in vivo evaluation. International Journal of Pharmaceutics 2005; 304(1): 178-84.

(256) Nerurkar J, Jun HW, Price JC, Park MO. Controlled-release matrix tablets of ibuprofen using cellulose ethers and carrageenans: effect of formulation factors on dissolution rates. European Journal of Pharmaceutics and Biopharmaceutics 2005 Sep; 61(1-2): 56-68.

(257) Huang X, Brazel CS. On the importance and mechanisms of burst release in matrix-controlled drug delivery systems. Journal of Controlled Release 2001 Jun 15;73(2-3):121-36.

(258) Tiwari SB, Murthy TK, Pai MR, Mehta PR, Chowdary PB. Controlled release formulation of tramadol hydrochloride using hydrophilic and hydrophobic matrix system. AAPS PharmSciTech 2003; 4(3): 18-23.

(259) Baumgartner S, Kristl J, Vrecer F, Vodopivec P, Zorko B. Optimisation of floating matrix tablets and evaluation of their gastric residence time. International Journal of Pharmaceutics 2000;195(1): 125-35.

(260) Kim H, Fassihi R. Application of binary polymer system in drug release rate modulation. 2. Influence of formulation variables and hydrodynamic conditions on release kinetics. J Pharm Sci 1997; 86(3): 323-8.

(261) Krishna R, Yu L (Editors). Biopharmaceutics Applications in Drug Development. New York: Springer; 2007; pp 55.

(262) Kavanagh N, Corrigan OI. Swelling and erosion properties of hydroxypropylmethylcellulose (Hypromellose) matrices: Influence of agitation rate and dissolution medium composition. International Journal of Pharmaceutics 2004 Jul 26; 279(1-2): 141-52.

(263) Nur AO, Zhang JS. Captopril floating and/or bioadhesive tablets: Design and release kinetics. Drug development and Industrial Pharmacy 2000; 26(9): 965-9.

(264) Jimenez-Martinez Iz, Quirino-Barreda T, Villafuerte-Robles L. Sustained delivery of captopril from floating matrix tablets. International Journal of Pharmaceutics 2008;362(1):37-43.

(265) Florence AT, Attwood D, Physicochemical Principles of Pharmacy. London: Pharmaceutical Press; 2011; pp 361-362.

(266) Garse H, Vij M, Yamgar M, Kadam V, Hirlekar R. Formulation and evaluation of a gastroretentive dosage form of labetalol hydrochloride. Archives of Pharmacal Research 2010; 33(3): 405-10.

(267) Patel P, Dand N, Somwanshi A, Kadam VJ, Hirlekar RS. Design and evaluation of a sustained release gastroretentive dosage form of captopril: a technical note. AAPS PharmSciTech 2008; 9(3): 836-9.

(268) Marques MR, Loebenberg R, Almukainzi M. Simulated biological fluids with possible application in dissolution testing. Dissolution Technol 2011; 18(3): 15-28.

(269) McConell EL, Basit AW, Murdan S. Measurements of rat annd mouse gastrointestinal pH, fluid and lymphoid tissue, and implications for in-vivo experiments. Journal of Pharmacy and Pharmacology 2008; 60(1):63-70

(270) Ibekwe VC, Fadda HM, McConnell EL, Khela MK, Evans DF, Basit AW. Interplay between intestinal pH, transit time and feed status on the in vivo performace of pH responsive ileo-colonic release sysyems. Pharmaceutical Research 2008; 25(8): 1828-35

(271) Conti S, Maggi L, Segale L, Ochoa Machiste E, Conte U, Grenier P, et al. Matrices containing NaCMC and HPMC: 2. Swelling and release mechanism study. International Journal of Pharmaceutics 2007 Mar 21; 333(1-2): 143-51.

(272) Patel P, Dand N, Somwanshi A, Kadam VJ, Hirlekar RS. Design and evaluation of a sustained release gastroretentive dosage form of captopril: Atechnical note. AAPS PharmSciTech 2008; 9(3): 836-9.

(273) Jain SK, Kadam VJ, Hirlekar RS. study of effects of post-compression curing on Kollidon® SR based floating tablets. Int J Pharm Pharm Sci 2011; 3(2): 90.

(274) Timm U, Wall M, Dell D. A new approach for dealing with the stability of drugs in biological fluids. J Pharm Sci 1985; 74(9): 972-7.

(275) Setti I, Celeste R, Mariani G, Dal Fiume D, Morisetti A, Lorusso V. High-performance liquid chromatographic determination of the magnetic resonance imaging contrast agent Gadocoletate ion in human plasma, urine and faeces. Journal of Chromatography B 2006 May 1;835(1-2): 1-15.

APPENDIX I

BATCH MANUFACTURING RECORD – C1

LABORATORY SCALE MANUFACTURE

A sample batch production record for batch C1, a laboratory scale tablet formulation is included. The batch production records for the other batches are available on request.

BATCH PRODUCTION RECORD

Faculty of Pharmacy, Rhodes University, Grahamstown 6140, South Africa

Product name: CPT tablets	**Batch number:** C1
Batch size:300 g	Page 1 of 4

Manufacturing approvals

Batch record issued by:	Date:
Master record issued by:	Date:

BATCH PRODUCTION RECORD

Faculty of Pharmacy, Rhodes University, Grahamstown 6140, South Africa

Product name: CPT tablets	**Batch number:** C1
Batch size: 300 g	Page 2 of 4

Equipment verification

Description	**Type**	**Verified by**	**Confirmed by**
Weighing balance	Model PM, Mettler®		
Sieve A	# 20 mesh size		
Sieve B	#44 mesh size		
Cube Blender			
Tableting instrumentation	Manesty® B3B Rotary Press		

BATCH PRODUCTION RECORD

Faculty of Pharmacy, Rhodes University, Grahamstown 6140, South Africa

Product name: CPT tablets	**Batch number:** C1
Batch size: 300 g	Page 3 of 4

Material	**Rhodes number**	**Quantity (w/w)**	**Amount dispensed**	**Dispensed by**	**Checked by**
CPT	RM000348	14.7	44.1		
$NaHCO_3$	RM000924	15.0	45.0		
Avicel® PH102	RM000038	67.0	201.0		
Colloidal silicon dioxide	RM000305	1.0	3.0		
Talc	RM000050	1.3	3.9		
Magnesium stearate	RM000304	1.0	3.0		

BATCH PRODUCTION RECORD

Faculty of Pharmacy, Rhodes University, Grahamstown 6140, South Africa

Product name: CPT tablets	**Batch number:** C1
Batch size: 300 g	Page 4 of 4

Method of manufacture

Method of manufacture			
Steps	**Procedure**	**Done by**	**Checked by**
1	Screen all weighed materials excluding talc, magnesium stearate and colloidal silicon dioxide through # 20 screen mesh. Use # 44 screen mesh for talc, magnesium stearate and colloidal silicon dioxide.		
2	Blend the excipients screened using the # 20 screen mesh in a cube blender rotating at 100 rpm for 20 minutes.		
3	Add talc, magnesium stearate and colloidal silicon dioxide and blend for further 3 minutes.		
4	Assess powder flowability by determining the angle of repose, Carr's index and Hausner ratio.		
5	Compress the powder blend on Manesty® B3B Rotary Press manually to set tablet weight and crushing strength.		
6	Set the instrument to automatic mode and check for weight and crushing strength every minute.		
7	Calculate % yield when manufacturing is complete.		
8	Store the tablets in self-sealing plastic bags for analysis.		

APPENDIX II

BATCH SUMMARIES

BATCH SUMMARY BATCH SUMMARY – C1

Faculty of Pharmacy, Rhodes University, Grahamstown, 6140, South Africa

Formulator: Samantha Mukozhiwa	**Batch number:** C1
Product: CPT 50 mg tablets	**Batch size: 300 g**
Powder blending date: 2013/09/20	**Humidity:** 60%
Tableting date: 2013/09/20	**Tooling:** 9.00 mm flat punches
Temperature: 15° C	**Actual weight:** 338.85 ± 1.30 mg
Tablet press: Manesty® B3B Rotary Press	**Actual crushing strength:** 112.9 ± 6.86 N
Target weight: 340 mg	**Yield:** 74.6 %
Target crushing strength: 100-140 N	**CPT content:** 100.1 ± 1.12 %
Friability: 0.143 ± 3.02 %	**FLT:** N/A
TFT: N/A	

FORMULA

Material	% w/w	Amount added (g)	Rhodes number
CPT	14.7	44.1	RM000348
$NaHCO_3$	15.0	45.0	RM000924
Avicel® PH102	67.0	201.0	RM000038
Colloidal silicon dioxide	1.0	3.0	RM000305
Talc	1.3	3.9	RM000050
Magnesium stearate	1.0	3.0	RM000304

***In vitro* release profile**

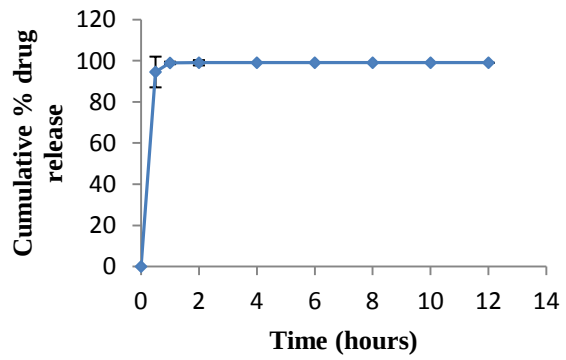

Comments and observations

- Slightly off-white
- Flat, smooth surfaces
- No sticking
- No lamination
- No capping
- No chipping
- No breaking

BATCH SUMMARY BATCH SUMMARY – C2

Faculty of Pharmacy, Rhodes University, Grahamstown, 6140, South Africa

Formulator: Samantha Mukozhiwa	**Batch number:** C2
Product: CPT 50 mg tablets	**Batch size: 300 g**
Powder blending date: 2013/09/20	**Humidity:** 60%
Tableting date: 2013/09/20	**Tooling:** 9.00 mm flat punches
Temperature: 15° C	**Actual weight:** 345.90 ± 1.64 mg
Tablet press: Manesty® B3B Rotary Press	**Actual crushing strength:** 114.5 ± 6.56 N
Target weight: 340 mg	**Yield:** 71.4 %
Target crushing strength: 100-140 N	**CPT content:** 99.3 ± 1.45 %
Friability: 0.186 ± 1.14 %	**FLT:** 16.2 ± 3.63 min
TFT: > 12 hours	

FORMULA

Material	% w/w	Amount added (g)	Rhodes number
CPT	14.7	44.1	RM000348
Methocel® K100M	60.0	180.0	RM000602
$NaHCO_3$	15.0	45.0	RM000924
Avicel® PH102	7.0	21.0	RM000038
Colloidal silicon dioxide	1.0	3.0	RM000305
Talc	1.3	3.9	RM000050
Magnesium stearate	1.0	3.0	RM000304

***In vitro* release profile**

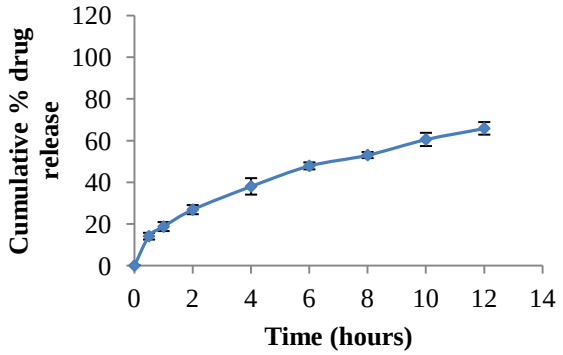

Comments and observations

- Slightly off-white
- Flat, smooth surfaces
- No sticking
- No lamination
- No capping
- No chipping
- No breaking

BATCH SUMMARY BATCH SUMMARY – C3

Faculty of Pharmacy, Rhodes University, Grahamstown, 6140, South Africa

Formulator: Samantha Mukozhiwa	**Batch number:** C3
Product: CPT 50 mg tablets	**Batch size: 300 g**
Powder blending date: 2013/09/20	**Humidity:** 60%
Tableting date: 2013/09/20	**Tooling:** 9.00 mm flat punches
Temperature: 15° C	**Actual weight:** 342.50 ± 2.27 mg
Tablet press: Manesty® B3B Rotary Press	**Actual crushing strength:** 91.54 ± 2.79 N
Target weight: 340 mg	**Yield:** 77.1 %
Target crushing strength: 100-140 N	**CPT content:** 98.7 ± 2.36 %
Friability: 0.161 ± 2.39 %	**FLT:** 15.3 ± 4.08 min
TFT: > 12 hours	

FORMULA

Material	% w/w	Amount added (g)	Rhodes number
CPT	14.7	44.1	RM000348
Methocel® K15M	60.0	180.0	RM000250
$NaHCO_3$	15.0	45.0	RM000924
Avicel® PH102	7.0	21.0	RM000038
Colloidal silicon dioxide	1.0	3.0	RM000305
Talc	1.3	3.9	RM000050
Magnesium stearate	1.0	3.0	RM000304

***In vitro* release profile**

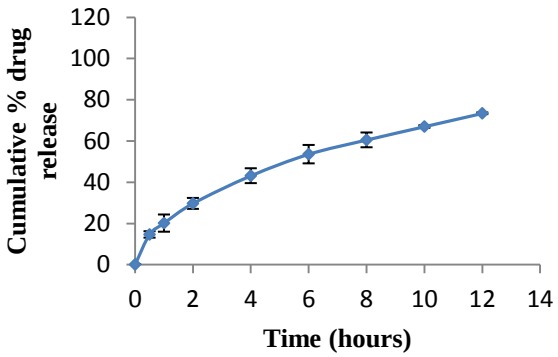

Comments and observations

- Slightly off-white
- Flat, smooth surfaces
- No sticking
- No lamination
- No capping
- No chipping
- No breaking

BATCH SUMMARY BATCH SUMMARY – C4

Faculty of Pharmacy, Rhodes University, Grahamstown, 6140, South Africa

Formulator: Samantha Mukozhiwa	**Batch number:** C4
Product: CPT 50 mg tablets	**Batch size: 300 g**
Powder blending date: 2013/09/21	**Humidity:** 51%
Tableting date: 2013/09/21	**Tooling:** 9.00 mm flat punches
Temperature: 14° C	**Actual weight:** ± 332.16 mg
Tablet press: Manesty® B3B Rotary Press	**Actual crushing strength:** 108.3 ± 4.90 N
Target weight: 340 mg	**Yield:** 79.2 %
Target crushing strength: 100-140 N	**CPT content:** 97.5 ± 2.97 %
Friability: 0.164 ± 1.57 %	**FLT:** 15.2 ± 3.27 min
TFT: > 12 hours	

FORMULA

Material	% w/w	Amount added (g)	Rhodes number
CPT	14.7	44.1	RM000348
Methocel® K100-LV	60.0	180.0	RM000115
$NaHCO_3$	15.0	45.0	RM000924
Avicel® PH102	7.0	21.0	RM000038
Colloidal silicon dioxide	1.0	3.0	RM000305
Talc	1.3	3.9	RM000050
Magnesium stearate	1.0	3.0	RM000304

***In vitro* release profile**

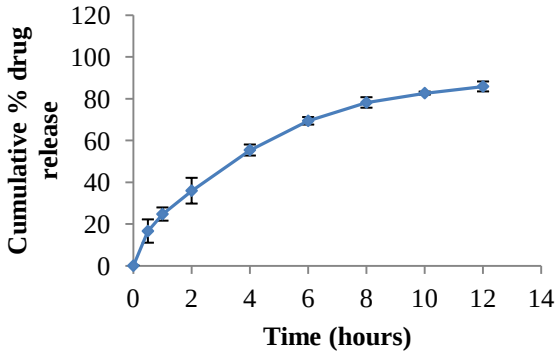

Comments and observations

- Slightly off-white
- Flat, smooth surfaces
- No sticking
- No lamination
- No capping
- No chipping
- No breaking

BATCH SUMMARY BATCH SUMMARY – C5

Faculty of Pharmacy, Rhodes University, Grahamstown, 6140, South Africa

Formulator: Samantha Mukozhiwa	**Batch number:** C5
Product: CPT 50 mg tablets	**Batch size: 300 g**
Powder blending date: 2013/09/21	**Humidity:** 51%
Tableting date: 2013/09/21	**Tooling:** 9.00 mm flat punches
Temperature: 14° C	**Actual weight:** 33.92 ± 1.02 mg
Tablet press: Manesty® B3B Rotary Press	**Actual crushing strength:** 99.8 ± 3.29 N
Target weight: 340 mg	**Yield:** 75.5 %
Target crushing strength: 100-140 N	**CPT content:** 99.6 ± 3.04 %
Friability: 0.177 ± 2.76 %	
	FLT: 8.0 ± 4.53 min
TFT: > 12 hours	

FORMULA

Material	% w/w	Amount added (g)	Rhodes number
CPT	14.7	44.1	RM000348
Methocel® K100M	30.0	90.0	RM000602
Methocel® K100-LV	30.0	90.0	RM000115
$NaHCO_3$	15.0	45.0	RM000924
Avicel® PH102	7.0	21.0	RM000038
Colloidal silicon dioxide	1.0	3.0	RM000305
Talc	1.3	3.9	RM000050
Magnesium stearate	1.0	3.0	RM000304

***In vitro* release profile**

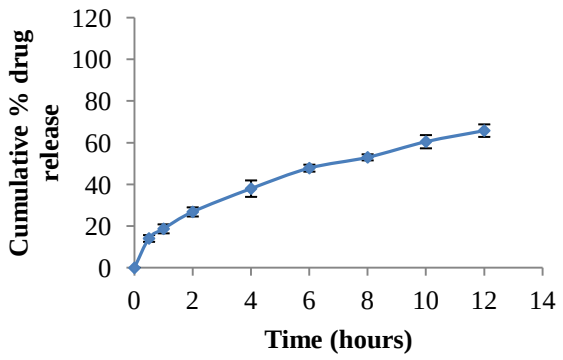

Comments and observations

- Slightly off-white
- Flat, smooth surfaces
- No sticking
- No lamination
- No capping
- No chipping
- No breaking

BATCH SUMMARY BATCH SUMMARY – C6

Faculty of Pharmacy, Rhodes University, Grahamstown, 6140, South Africa

Formulator: Samantha Mukozhiwa

Batch number: C6

Product: CPT 50 mg tablets

Batch size: 300 g

Powder blending date: 2013/09/21

Humidity: 51%

Tableting date: 2013/09/21

Tooling: 9.00 mm flat punches

Temperature: 14° C

Actual weight: 336.95 ± 1.94 mg

Tablet press: Manesty® B3B Rotary Press

Actual crushing strength: 106.7 ± 4.72 N

Target weight: 340 mg

Yield: 79.1 %

Target crushing strength: 100-140 N

CPT content: 101.6 ± %

Friability: 0.159 ± 1.46 %

FLT: 11.3 ± 4.68 min

TFT: > 12 hours

FORMULA

Material	% w/w	Amount added (g)	Rhodes number
CPT	14.7	44.1	RM000348
Methocel® K100M	50.0	150.0	RM000602
$NaHCO_3$	15.0	45.0	RM000924
Avicel® PH102	17.0	51.0	RM000038
Colloidal silicon dioxide	1.0	3.0	RM000305
Talc	1.3	3.9	RM000050
Magnesium stearate	1.0	3.0	RM000304

***In vitro* release profile**

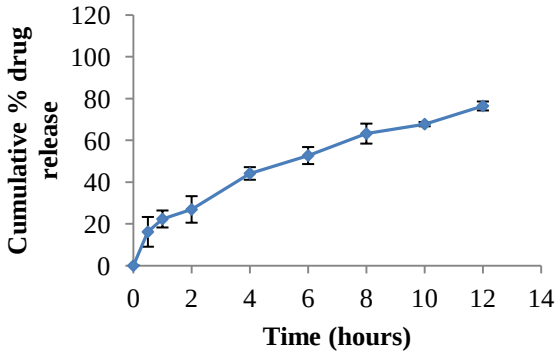

Comments and observations

- Slightly off-white
- Flat, smooth surfaces
- No sticking
- No lamination
- No capping
- No chipping
- No breaking

BATCH SUMMARY BATCH SUMMARY – C7

Faculty of Pharmacy, Rhodes University, Grahamstown, 6140, South Africa

Formulator: Samantha Mukozhiwa	**Batch number:** C7
Product: CPT 50 mg tablets	**Batch size: 300 g**
Powder blending date: 2013/09/22	**Humidity:** 52%
Tableting date: 2013/09/22	**Tooling:** 9.00 mm flat punches
Temperature: 23° C	**Actual weight:** 340 ± 1.24 mg
Tablet press: Manesty® B3B Rotary Press	**Actual crushing strength:** 91.3 ± 1.93 N
Target weight: 340 mg	**Yield:** 75.9 %
Target crushing strength: 100-140 N	**CPT content:** 98.1 ± 2.77 %
Friability: 0.148 ± 2.25 %	
	FLT: 11.9 ± 3.96 min
TFT: > 12 hours	

FORMULA

Material	% w/w	Amount added (g)	Rhodes number
CPT	14.7	44.1	RM000348
Methocel® K100M	40.0	120.0	RM000602
$NaHCO_3$	15.0	45.0	RM000924
Avicel® PH102	27.0	81.0	RM000038
Colloidal silicon dioxide	1.0	3.0	RM000305
Talc	1.3	3.9	RM000050
Magnesium stearate	1.0	3.0	RM000304

***In vitro* release profile**

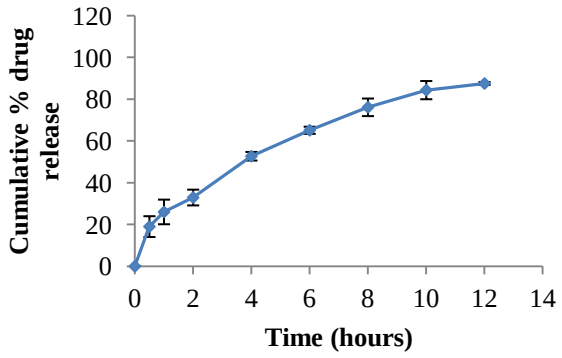

Comments and observations

- Slightly off-white
- Flat, smooth surfaces
- No sticking
- No lamination
- No capping
- No chipping
- No breaking

BATCH SUMMARY BATCH SUMMARY – C8

Faculty of Pharmacy, Rhodes University, Grahamstown, 6140, South Africa

Formulator: Samantha Mukozhiwa	**Batch number:** C8
Product: CPT 50 mg tablets	**Batch size: 300 g**
Powder blending date: 2013/09/22	**Humidity:** 52%
Tableting date: 2013/09/22	**Tooling:** 9.00 mm flat punches
Temperature: 23° C	**Actual weight:** 337.55 ± 2.28 mg
Tablet press: Manesty® B3B Rotary Press	**Actual crushing strength:** 117.8 ± 2.51 N
Target weight: 340 mg	**Yield:** 76.3 %
Target crushing strength: 100-140 N	**CPT content:** 96.8 ± 3.95 %
Friability: 0.187 ± 1.69 %	**FLT:** 4.1 ± 4.78 min
TFT: > 12 hours	

FORMULA

Material	% w/w	Amount added (g)	Rhodes number
CPT	14.7	44.1	RM000348
Methocel® K100M	40.0	120.0	RM000602
Ethylcellulose	20.0	60.0	RM000100
$NaHCO_3$	15.0	45.0	RM000924
Avicel® PH102	7.0	21.0	RM000038
Colloidal silicon dioxide	1.0	3.0	RM000305
Talc	1.3	3.9	RM000050
Magnesium stearate	1.0	3.0	RM000304

***In vitro* release profile**

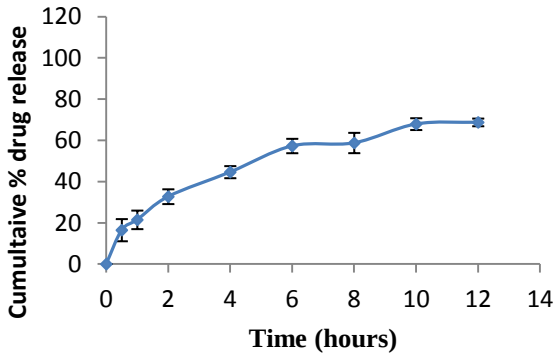

Comments and observations

- Slightly off-white
- Flat, smooth surfaces
- No sticking
- No lamination
- No capping
- No chipping
- No breaking

BATCH SUMMARY BATCH SUMMARY – C9

Faculty of Pharmacy, Rhodes University, Grahamstown, 6140, South Africa

Formulator: Samantha Mukozhiwa	**Batch number:** C9
Product: CPT 50 mg tablets	**Batch size: 300 g**
Powder blending date: 2013/09/22	**Humidity:** 52%
Tableting date: 2013/09/22	**Tooling:** 9.00 mm flat punches
Temperature: 23° C	**Actual weight:** 339.89 ± 2.11 mg
Tablet press: Manesty® B3B Rotary Press	**Actual crushing strength:** 98.6 ± 4.27 N
Target weight: 340 mg	**Yield:** 77.8 %
Target crushing strength: 100-140 N	**CPT content:** 98.2 ± 1.24 %
Friability: 0.173 ± 3.04 %	
	FLT: 1.1 ± 2.05 min
TFT: > 12 hours	

FORMULA

Material	% w/w	Amount added (g)	Rhodes number
CPT	14.7	44.1	RM000348
Methocel® K100M	50.0	150.0	RM000602
Ethylcellulose	10.0	30.0	RM000100
$NaHCO_3$	15.0	45.0	RM000924
Avicel® PH102	7.0	21.0	RM000038
Colloidal silicon dioxide	1.0	3.0	RM000305
Talc	1.3	3.9	RM000050
Magnesium stearate	1.0	3.0	RM000304

***In vitro* release profile**

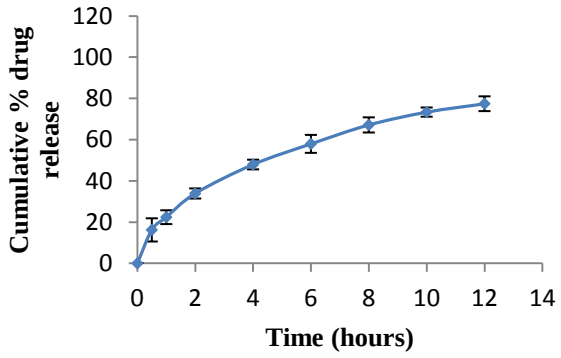

Comments and observations

- Slightly off-white
- Flat, smooth surfaces
- No sticking
- No lamination
- No capping
- No chipping
- No breaking

BATCH SUMMARY BATCH SUMMARY – C10

Faculty of Pharmacy, Rhodes University, Grahamstown, 6140, South Africa

Formulator: Samantha Mukozhiwa	**Batch number:** C10
Product: CPT 50 mg tablets	**Batch size: 300 g**
Powder blending date: 2013/09/23	**Humidity:** 34%
Tableting date: 2013/09/23	**Tooling:** 9.00 mm flat punches
Temperature: 31° C	**Actual weight:** 338.42 ± 3.43 mg
Tablet press: Manesty® B3B Rotary Press	**Actual crushing strength:** 139.9 ± 1.13 N
Target weight: 340 mg	**Yield:** 78.8 %
Target crushing strength: 100-140 N	**CPT content:** 97.8 ± 2.55 %
Friability: 0.168 ± 2.38 %	**FLT:** 24.4 ± 2.71 min
TFT: > 12 hours	

FORMULA

Material	% w/w	Amount added (g)	Rhodes number
CPT	14.7	44.1	RM000348
Methocel® K100M	50.0	150.0	RM000602
Carbopol® 974P NF	10.0	30.0	RM000245
$NaHCO_3$	15.0	45.0	RM000924
Avicel® PH102	7.0	21.0	RM000038
Colloidal silicon dioxide	1.0	3.0	RM000305
Talc	1.3	3.9	RM000050
Magnesium stearate	1.0	3.0	RM000304

***In vitro* release profile**

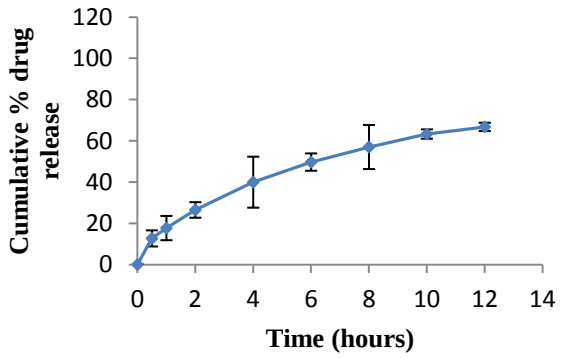

Comments and observations

- Slightly off-white
- Flat, smooth surfaces
- No sticking
- No lamination
- No capping
- No chipping
- No breaking

BATCH SUMMARY BATCH SUMMARY – C11

Faculty of Pharmacy, Rhodes University, Grahamstown, 6140, South Africa

Formulator: Samantha Mukozhiwa	**Batch number:** C11
Product: CPT 50 mg tablets	**Batch size: 300 g**
Powder blending date: 2013/10/18	**Humidity:** 78%
Tableting date: 2013/10/18	**Tooling:** 9.00 mm flat punches
Temperature: 21° C	**Actual weight:** 341.00 ± 1.27 mg
Tablet press: Manesty® B3B Rotary Press	**Actual crushing strength:** 107.47 ± 4.75 N
Target weight: 340 mg	**Yield:** 77.4 %
Target crushing strength: 100-140 N	**CPT content:** 98.2 ± 0.36%
Friability: 0.142 ± 2.36 %	**FLT:** 11.45 ± 3.33 min
TFT: > 12	

FORMULA

Material	% w/w	Amount added (g)	Rhodes number
CPT	14.7	52.1	RM000348
Methocel® K100M	29.09	103.2	RM000602
$NaHCO_3$	15.0	53.2	RM000924
Avicel® PH102	22.5	79.8	RM000038
Colloidal silicon dioxide	1.0	3.5	RM000305
Talc	1.3	4.6	RM000050
Magnesium stearate	1.0	3.5	RM000304

***In vitro* release profile**

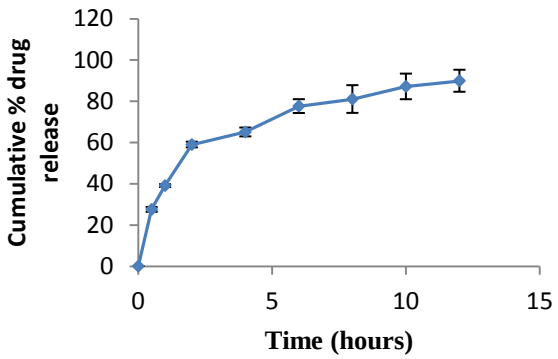

Comments and observations

- Slightly off-white
- Flat, smooth surfaces
- No sticking
- No lamination
- No capping
- No chipping
- No breaking

BATCH SUMMARY BATCH SUMMARY – C12

Faculty of Pharmacy, Rhodes University, Grahamstown, 6140, South Africa

Formulator: Samantha Mukozhiwa	**Batch number:** C12
Product: CPT 50 mg tablets	**Batch size: 300 g**
Powder blending date: 2013/10/18	**Humidity:** 78%
Tableting date: 2013/10/18	**Tooling:** 9.00 mm flat punches
Temperature: 21° C	**Actual weight:** 342.71 ± 1.63 mg
Tablet press: Manesty® B3B Rotary Press	**Actual crushing strength:** 112.78 ± 2.53 N
Target weight: 340 mg	**Yield:** 81.2 %
Target crushing strength: 100-140 N	**CPT content:** 101.25 ± 0.92%
Friability: 0.189 ± 1.26%	**FLT:** 11.15 ± 2.46 min
TFT: > 12 hours	

FORMULA

Material	% w/w	Amount added (g)	Rhodes number
CPT	14.7	47.4	RM000348
Methocel® K100M	37.5	120.9	RM000602
$NaHCO_3$	15.0	48.4	RM000924
Avicel® PH102	22.5	72.6	RM000038
Colloidal silicon dioxide	1.0	3.2	RM000305
Talc	1.3	4.2	RM000050
Magnesium stearate	1.0	3.2	RM000304

***In vitro* release profile**

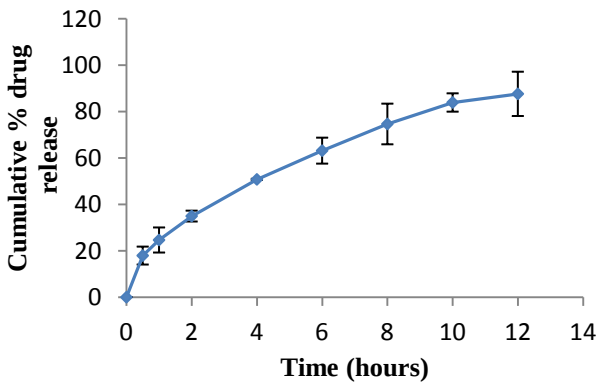

Comments and observations

- Slightly off-white
- Flat, smooth surfaces
- No sticking
- No lamination
- No capping
- No chipping
- No breaking

BATCH SUMMARY BATCH SUMMARY – C13

Faculty of Pharmacy, Rhodes University, Grahamstown, 6140, South Africa

Formulator: Samantha Mukozhiwa	**Batch number:** C13
Product: CPT 50 mg tablets	**Batch size: 300 g**
Powder blending date: 2013/10/18	**Humidity:** 78%
Tableting date: 2013/10/18	**Tooling:** 9.00 mm flat punches
Temperature: 21° C	**Actual weight:** 342.99 ± 1.46 mg
Tablet press: Manesty® B3B Rotary Press	**Actual crushing strength:** 109.73 ± 3.00 N
Target weight: 340 mg	**Yield:** 79.7 %
Target crushing strength: 100-140 N	**CPT content:** 99.46 ± 0.74%
Friability: 0.196 ± 1.46%	**FLT:** 10.59 ± 3.50 min
TFT: > 12 hours	

FORMULA

Material	% w/w	Amount added (g)	Rhodes number
CPT	14.7	47.4	RM000348
Methocel® K100M	37.5	120.9	RM000602
$NaHCO_3$	15.0	48.4	RM000924
Avicel® PH102	22.5	72.6	RM000038
Colloidal silicon dioxide	1.0	3.2	RM000305
Talc	1.3	4.2	RM000050
Magnesium stearate	1.0	3.2	RM000304

***In vitro* release profile**

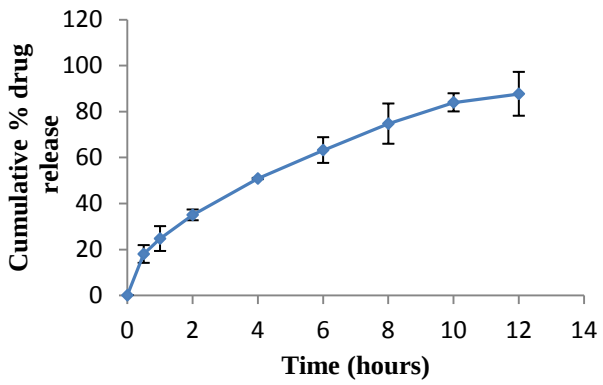

Comments and observations

- Slightly off-white
- Flat, smooth surfaces
- No sticking
- No lamination
- No capping
- No chipping
- No breaking

BATCH SUMMARY BATCH SUMMARY – C14

Faculty of Pharmacy, Rhodes University, Grahamstown, 6140, South Africa

Formulator: Samantha Mukozhiwa	**Batch number:** C14
Product: CPT 50 mg tablets	**Batch size: 300 g**
Powder blending date: 2013/10/19	**Humidity:** 64%
Tableting date: 2013/10/19	**Tooling:** 9.00 mm flat punches
Temperature: 24° C	**Actual weight:** 340.10 ± 0.94 mg
Tablet press: Manesty® B3B Rotary Press	**Actual crushing strength:** 104.19 ± 2.47 N
Target weight: 340 mg	**Yield:** 71.6 %
Target crushing strength: 100-140 N	**CPT content:** 97.52 ± 1.06%
Friability: 0.164 ± 2.63%	**FLT:** 23.44 ± 4.54 min
TFT: > 12 hours	

FORMULA

Material	% w/w	Amount added (g)	Rhodes number
CPT	14.7	52.1	RM000348
Methocel® K100M	37.5	132.9	RM000602
$NaHCO_3$	6.59	23.4	RM000924
Avicel® PH102	22.5	79.8	RM000038
Colloidal silicon dioxide	1.0	3.5	RM000305
Talc	1.3	4.6	RM000050
Magnesium stearate	1.0	3.5	RM000304

***In vitro* release profile**

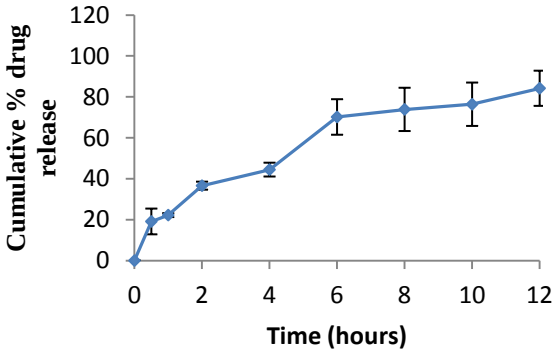

Comments and observations

- Slightly off-white
- Flat, smooth surfaces
- No sticking
- No lamination
- No capping
- No chipping
- No breaking

BATCH SUMMARY BATCH SUMMARY – C15

Faculty of Pharmacy, Rhodes University, Grahamstown, 6140, South Africa

Formulator: Samantha Mukozhiwa	**Batch number:** C15
Product: CPT 50 mg tablets	**Batch size: 300 g**
Powder blending date: 2013/10/19	**Humidity:** 64%
Tableting date: 2013/10/19	**Tooling:** 9.00 mm flat punches
Temperature: 24° C	**Actual weight:** 339.26 ± 0.88 mg
Tablet press: Manesty® B3B Rotary Press	**Actual crushing strength:** 114.46 ± 5.03 N
Target weight: 340 mg	**Yield:** 79.2 %
Target crushing strength: 100-140 N	**CPT content:** 96.26 ± 0.29%
Friability: 0.172 ± 1.47 %	**FLT:** 10.31 ± 3.02 min
TFT: > 12 hours	

FORMULA

Material	% w/w	Amount added (g)	Rhodes number
CPT	14.7	47.4	RM000348
Methocel® K100M	37.5	120.9	RM000602
$NaHCO_3$	15.0	48.4	RM000924
Avicel® PH102	22.5	72.6	RM000038
Colloidal silicon dioxide	1.0	3.2	RM000305
Talc	1.3	4.2	RM000050
Magnesium stearate	1.0	3.2	RM000304

***In vitro* release profile**

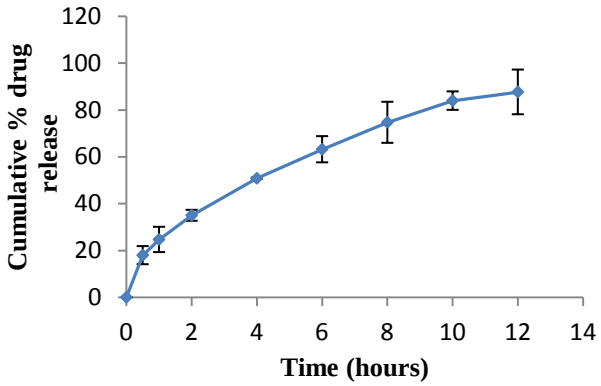

Comments and observations

- Slightly off-white
- Flat, smooth surfaces
- No sticking
- No lamination
- No capping
- No chipping
- No breaking

BATCH SUMMARY BATCH SUMMARY – C16

Faculty of Pharmacy, Rhodes University, Grahamstown, 6140, South Africa

Formulator: Samantha Mukozhiwa	**Batch number:** C16
Product: CPT 50 mg tablets	**Batch size: 300 g**
Powder blending date: 2013/10/19	**Humidity:** 64%
Tableting date: 2013/10/19	**Tooling:** 9.00 mm flat punches
Temperature: 24° C	**Actual weight:** 340.29 ± 1.98 mg
Tablet press: Manesty® B3B Rotary Press	**Actual crushing strength:** 106.85 ± 4.27 N
Target weight: 340 mg	**Yield:** 77.4 %
Target crushing strength: 100-140 N	**CPT content:** 106.85 ± 4.27%
Friability: 0.153 ± 3.70%	**FLT:** 10.59 ± 2.96 min
TFT: > 12 hours	

FORMULA

Material	% w/w	Amount added (g)	Rhodes number
CPT	14.7	47.4	RM000348
Methocel® K100M	37.5	120.9	RM000602
$NaHCO_3$	10.0	32.3	RM000924
Avicel® PH102	27.5	88.7	RM000038
Colloidal silicon dioxide	1.0	3.2	RM000305
Talc	1.3	4.2	RM000050
Magnesium stearate	1.0	3.2	RM000304

***In vitro* release profile**

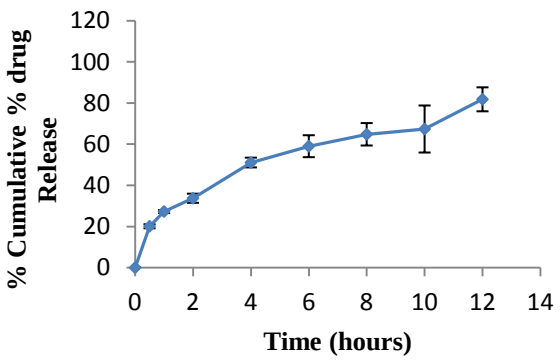

Comments and observations

- Slightly off-white
- Flat, smooth surfaces
- No sticking
- No lamination
- No capping
- No chipping
- No breaking

BATCH SUMMARY BATCH SUMMARY – C17

Faculty of Pharmacy, Rhodes University, Grahamstown, 6140, South Africa

Formulator: Samantha Mukozhiwa	**Batch number:** C17
Product: CPT 50 mg tablets	**Batch size: 300 g**
Powder blending date: 2013/10/20	**Humidity:** 76%
Tableting date: 2013/10/20	**Tooling:** 9.00 mm flat punches
Temperature: 21° C	**Actual weight:** 343.51 ± 1.96 mg
Tablet press: Manesty® B3B Rotary Press	**Actual crushing strength:** 114.72 ± 4.15 N
Target weight: 340 mg	**Yield:** 77.5 %
Target crushing strength: 100-140 N	**CPT content:** 100.26 ± 0.73%
Friability: 0.167 ± 1.48%	**FLT:** 11.27 ± 5.03 min
TFT: > 12 hours	

FORMULA

Material	% w/w	Amount added (g)	Rhodes number
CPT	14.7	50.1	RM000348
Methocel® K100M	42.5	144.9	RM000602
$NaHCO_3$	10.0	34.1	RM000924
Avicel® PH102	17.5	59.7	RM000038
Colloidal silicon dioxide	1.0	3.4	RM000305
Talc	1.3	4.4	RM000050
Magnesium stearate	1.0	3.4	RM000304

***In vitro* release profile**

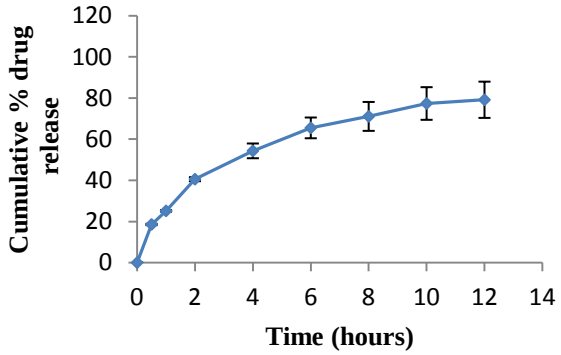

Comments and observations

- Slightly off-white
- Flat, smooth surfaces
- No sticking
- No lamination
- No capping
- No chipping
- No breaking

BATCH SUMMARY BATCH SUMMARY – C18

Faculty of Pharmacy, Rhodes University, Grahamstown, 6140, South Africa

Formulator: Samantha Mukozhiwa	**Batch number:** C18
Product: CPT 50 mg tablets	**Batch size: 300 g**
Powder blending date: 2013/10/20	**Humidity:** 76%
Tableting date: 2013/10/20	**Tooling:** 9.00 mm flat punches
Temperature: 21° C	**Actual weight:** 345.10 ± 2.22 mg
Tablet press: Manesty® B3B Rotary Press	**Actual crushing strength:** 110.45 ± 5.25 N
Target weight: 340 mg	**Yield:** 71.4 %
Target crushing strength: 100-140 N	**CPT content:** 99.14 ± 1.10%
Friability: 0.912 ± 2.96%	**FLT:** 10.73 ± 2.83 min
TFT: > 12 hours	

FORMULA

Material	% w/w	Amount added (g)	Rhodes number
CPT	14.7	45.7	RM000348
Methocel® K100M	32.5	101.1	RM000602
$NaHCO_3$	23.41	72.8	RM000924
Avicel® PH102	22.5	70.0	RM000038
Colloidal silicon dioxide	1.0	3.1	RM000305
Talc	1.3	4.0	RM000050
Magnesium stearate	1.0	3.1	RM000304

***In vitro* release profile**

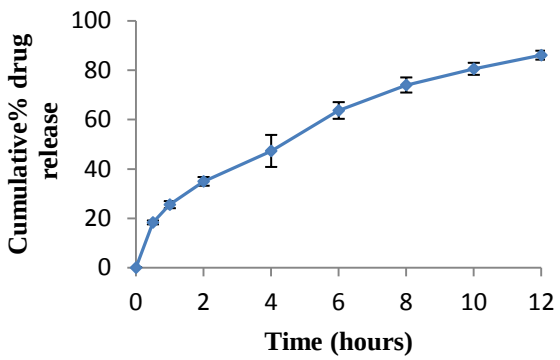

Comments and observations

- Slightly off-white
- Flat, smooth surfaces
- No sticking
- No lamination
- No capping
- No chipping
- No breaking

BATCH SUMMARY BATCH SUMMARY – C19

Faculty of Pharmacy, Rhodes University, Grahamstown, 6140, South Africa

Formulator: Samantha Mukozhiwa	**Batch number:** C19
Product: CPT 50 mg tablets	**Batch size: 300 g**
Powder blending date: 2013/10/20	**Humidity:** 76%
Tableting date: 2013/10/20	**Tooling:** 9.00 mm flat punches
Temperature: 21° C	**Actual weight:** 341.70± 3.28 mg
Tablet press: Manesty® B3B Rotary Press	**Actual crushing strength:** 105.76 ± 3.62 N
Target weight: 340 mg	**Yield:** 76.8 %
Target crushing strength: 100-140 N	**CPT content:** 96.76 ± 0.92%
Friability: 0.154 ± 1.12%	**FLT:** 9.58 ± 1.76 min
TFT: > 12 hours	

FORMULA

Material	% w/w	Amount added (g)	Rhodes number
CPT	14.7	47.4	RM000348
Methocel® K100M	37.5	120.9	RM000602
$NaHCO_3$	20.0	64.5	RM000924
Avicel® PH102	17.5	56.5	RM000038
Colloidal silicon dioxide	1.0	3.2	RM000305
Talc	1.3	4.2	RM000050
Magnesium stearate	1.0	3.2	RM000304

***In vitro* release profile**

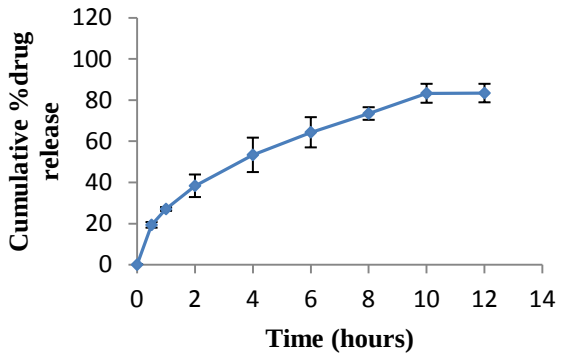

Comments and observations

- Slightly off-white
- Flat, smooth surfaces
- No sticking
- No lamination
- No capping
- No chipping
- No breaking

BATCH SUMMARY BATCH SUMMARY – C20

Faculty of Pharmacy, Rhodes University, Grahamstown, 6140, South Africa

Formulator: Samantha Mukozhiwa	**Batch number:** C20
Product: CPT 50 mg tablets	**Batch size: 300 g**
Powder blending date: 2013/10/21	**Humidity:** 92%
Tableting date: 2013/10/21	**Tooling:** 9.00 mm flat punches
Temperature: 16° C	**Actual weight:** 338.92 ± 2.51 mg
Tablet press: Manesty® B3B Rotary Press	**Actual crushing strength:** 104.50 ± 5.97 N
Target weight: 340 mg	**Yield:** 76.1%
Target crushing strength: 100-140 N	**CPT content:** 97.95 ± 0.54%
Friability: 0.169 ± 3.56%	**FLT:** 10.10 ± 2.98 min
TFT: > 12 hours	

FORMULA

Material	% w/w	Amount added (g)	Rhodes number
CPT	14.7	40.8	RM000348
Methocel® K100M	42.5	118.1	RM000602
$NaHCO_3$	20.0	55.6	RM000924
Avicel® PH102	27.5	76.4	RM000038
Colloidal silicon dioxide	1.0	2.8	RM000305
Talc	1.3	3.6	RM000050
Magnesium stearate	1.0	2.8	RM000304

***In vitro* release profile**

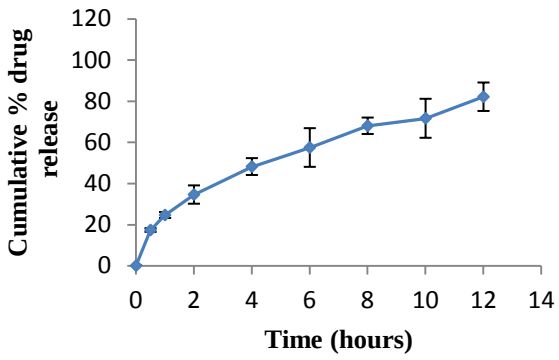

Comments and observations

- Slightly off-white
- Flat, smooth surfaces
- No sticking
- No lamination
- No capping
- No chipping
- No breaking

BATCH SUMMARY BATCH SUMMARY – C21

Faculty of Pharmacy, Rhodes University, Grahamstown, 6140, South Africa

Formulator: Samantha Mukozhiwa	**Batch number:** C21
Product: CPT 50 mg tablets	**Batch size: 300 g**
Powder blending date: 2013/10/21	**Humidity:** 92%
Tableting date: 2013/10/21	**Tooling:** 9.00 mm flat punches
Temperature: 16° C	**Actual weight:** 345.44 ± 1.66 mg
Tablet press: Manesty® B3B Rotary Press	**Actual crushing strength:** 111.80 ± 5.05 N
Target weight: 340 mg	**Yield:** 78.9 %
Target crushing strength: 100-140 N	**CPT content:** 96.25 ± 0.79%
Friability: 0.117 ± 1.25%	**FLT:** 10.53 ± 2.60 min
TFT: > 12 hours	

FORMULA

Material	% w/w	Amount added (g)	Rhodes number
CPT	14.7	45	RM000348
Methocel® K100M	42.5	130.1	RM000602
$NaHCO_3$	15.0	45.9	RM000924
Avicel® PH102	22.5	68.9	RM000038
Colloidal silicon dioxide	1.0	3.1	RM000305
Talc	1.3	3.9	RM000050
Magnesium stearate	1.0	3.1	RM000304

***In vitro* release profile**

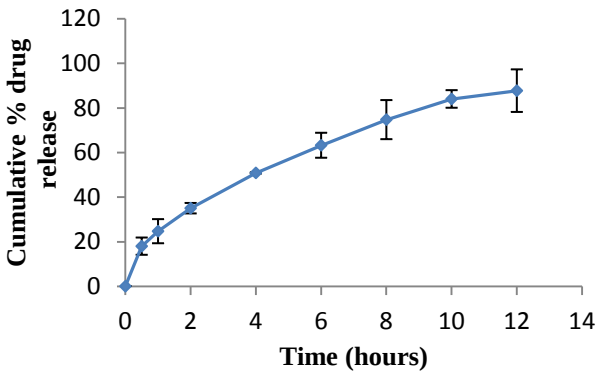

Comments and observations

- Slightly off-white
- Flat, smooth surfaces
- No sticking
- No lamination
- No capping
- No chipping
- No breaking

BATCH SUMMARY BATCH SUMMARY – C22

Faculty of Pharmacy, Rhodes University, Grahamstown, 6140, South Africa

Formulator: Samantha Mukozhiwa	**Batch number:** C22
Product: CPT 50 mg tablets	**Batch size: 300 g**
Powder blending date: 2013/10/21	**Humidity:** 92%
Tableting date: 2013/10/21	**Tooling:** 9.00 mm flat punches
Temperature: 16° C	**Actual weight:** 340.92 ± 1.74 mg
Tablet press: Manesty® B3B Rotary Press	**Actual crushing strength:** 103.86 ± 4.31 N
Target weight: 340 mg	**Yield:** 80.7 %
Target crushing strength: 100-140 N	**CPT content:** 99.29 ± 0.24%
Friability: 0.163 ± 2.46%	**FLT:** 9.26 ± 1.47 min
TFT: > 12 hours	

FORMULA

Material	% w/w	Amount added (g)	Rhodes number
CPT	14.7	43.5	RM000348
Methocel® K100M	37.5	110.9	RM000602
$NaHCO_3$	15.0	44.4	RM000924
Avicel® PH102	30.91	91.4	RM000038
Colloidal silicon dioxide	1.0	2.9	RM000305
Talc	1.3	3.8	RM000050
Magnesium stearate	1.0	2.9	RM000304

***In vitro* release profile**

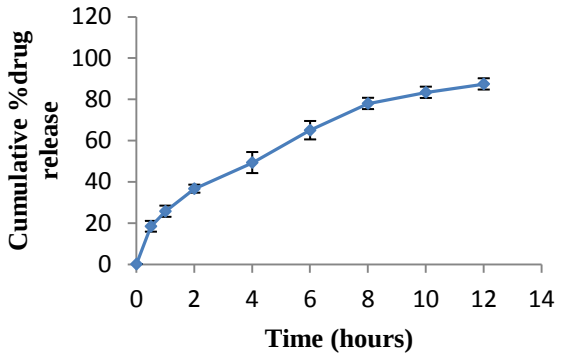

Comments and observations

- Slightly off-white
- Flat, smooth surfaces
- No sticking
- No lamination
- No capping
- No chipping
- No breaking

BATCH SUMMARY BATCH SUMMARY – C23

Faculty of Pharmacy, Rhodes University, Grahamstown, 6140, South Africa

Formulator: Samantha Mukozhiwa	**Batch number:** C23
Product: CPT 50 mg tablets	**Batch size: 300 g**
Powder blending date: 2013/10/22	**Humidity:** 62%
Tableting date: 2013/10/22	**Tooling:** 9.00 mm flat punches
Temperature: 18° C	**Actual weight:** 345.27 ± 3.06 mg
Tablet press: Manesty® B3B Rotary Press	**Actual crushing strength:** 115.28 ± 3.38 N
Target weight: 340 mg	**Yield:** 74.3 %
Target crushing strength: 100-140 N	**CPT content:** 97.55 ± 1.06%
Friability: 0.196 ± 3.15%	**FLT:** 12.04 ± 2.83 min
TFT: > 12 hours	

FORMULA

Material	% w/w	Amount added (g)	Rhodes number
CPT	14.7	50.11	RM000348
Methocel® K100M	32.5	110.8	RM000602
$NaHCO_3$	10.0	34.1	RM000924
Avicel® PH102	27.5	93.8	RM000038
Colloidal silicon dioxide	1.0	3.4	RM000305
Talc	1.3	4.4	RM000050
Magnesium stearate	1.0	3.4	RM000304

***In vitro* release profile**

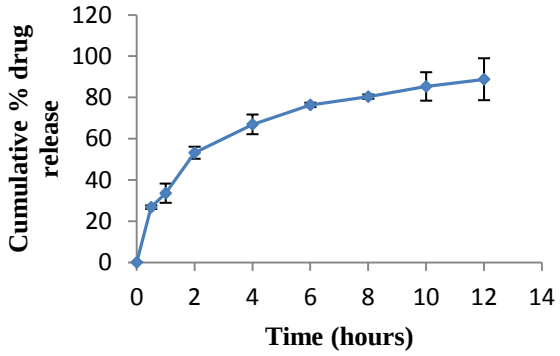

Comments and observations

- Slightly off-white
- Flat, smooth surfaces
- No sticking
- No lamination
- No capping
- No chipping
- No breaking

BATCH SUMMARY BATCH SUMMARY – C24

Faculty of Pharmacy, Rhodes University, Grahamstown, 6140, South Africa

Formulator: Samantha Mukozhiwa	**Batch number:** C24
Product: CPT 50 mg tablets	**Batch size: 300 g**
Powder blending date: 2013/10/22	**Humidity:** 62%
Tableting date: 2013/10/22	**Tooling:** 9.00 mm flat punches
Temperature: 18° C	**Actual weight:** 338.01 ± 1.88 mg
Tablet press: Manesty® B3B Rotary Press	**Actual crushing strength:** 104.28 ± 4.89 N
Target weight: 340 mg	**Yield:** 71.2 %
Target crushing strength: 100-140 N	**CPT content:** 99.02 ± 0.95%
Friability: 0.173 ± 1.66%	**FLT:** 10.15 ± 2.69 min
TFT: > 12 hours	

FORMULA

Material	% w/w	Amount added (g)	Rhodes number
CPT	14.7	50.1	RM000348
Methocel® K100M	42.5	144.9	RM000602
$NaHCO_3$	10.0	34.1	RM000924
Avicel® PH102	17.5	59.7	RM000038
Colloidal silicon dioxide	1.0	3.4	RM000305
Talc	1.3	4.4	RM000050
Magnesium stearate	1.0	3.4	RM000304

***In vitro* release profile**

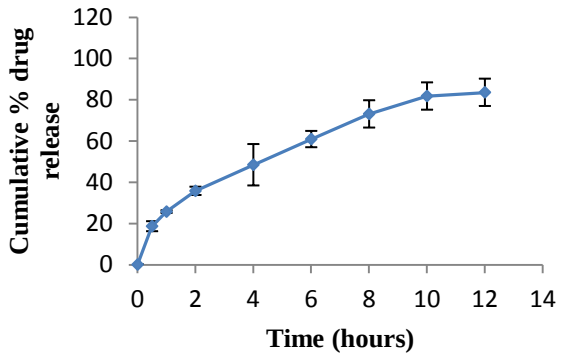

Comments and observations

- Slightly off-white
- Flat, smooth surfaces
- No sticking
- No lamination
- No capping
- No chipping
- No breaking

BATCH SUMMARY BATCH SUMMARY – C25

Faculty of Pharmacy, Rhodes University, Grahamstown, 6140, South Africa

Formulator: Samantha Mukozhiwa	**Batch number:** C25
Product: CPT 50 mg tablets	**Batch size: 300 g**
Powder blending date: 2013/10/22	**Humidity:** 62%
Tableting date: 2013/10/22	**Tooling:** 9.00 mm flat punches
Temperature: 18° C	**Actual weight:** 345.47 ± 2.80 mg
Tablet press: Manesty® B3B Rotary Press	**Actual crushing strength:** 118.87 ± 5.60 N
Target weight: 340 mg	**Yield:** 73.3 %
Target crushing strength: 100-140 N	**CPT content:** 98.25 ± 3.28%
Friability: 0.159 ± 3.48%	**FLT:** 9.72 ± 3.28 min
TFT: > 12 hours	

FORMULA

Material	% w/w	Amount added (g)	Rhodes number
CPT	14.7	43.5	RM000348
Methocel® K100M	45.91	135.8	RM000602
$NaHCO_3$	15.00	44.4	RM000924
Avicel® PH102	22.5	66.6	RM000038
Colloidal silicon dioxide	1.0	2.9	RM000305
Talc	1.3	3.8	RM000050
Magnesium stearate	1.0	2.9	RM000304

***In vitro* release profile**

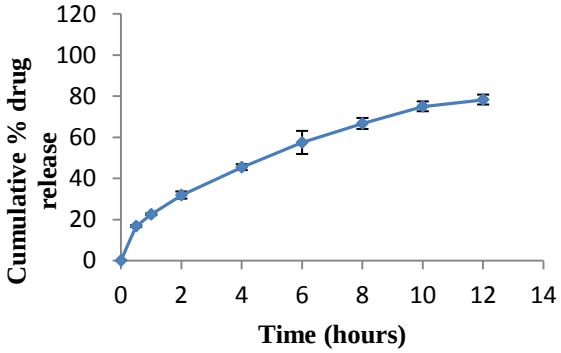

Comments and observations

- Slightly off-white
- Flat, smooth surfaces
- No sticking
- No lamination
- No capping
- No chipping
- No breaking

BATCH SUMMARY BATCH SUMMARY – C26

Faculty of Pharmacy, Rhodes University, Grahamstown, 6140, South Africa

Formulator: Samantha Mukozhiwa	**Batch number:** C26
Product: CPT 50 mg tablets	**Batch size: 300 g**
Powder blending date: 2013/10/23	**Humidity:** 67%
Tableting date: 2013/10/23	**Tooling:** 9.00 mm flat punches
Temperature: 22° C	**Actual weight:** 341.11 ± 0.52 mg
Tablet press: Manesty® B3B Rotary Press	**Actual crushing strength:** 105.66 ± 3.16 N
Target weight: 340 mg	**Yield:** 79.6 %
Target crushing strength: 100-140 N	**CPT content:** 96.41 ± 0.97%
Friability: 0.112 ± 3.86%	**FLT:** 11.59 ± 4.70 min
TFT: > 12 hours	

FORMULA

Material	% w/w	Amount added (g)	Rhodes number
CPT	14.7	50.1	RM000348
Methocel® K100M	32.5	110.8	RM000602
$NaHCO_3$	20.0	68.2	RM000924
Avicel® PH102	17.5	59.7	RM000038
Colloidal silicon dioxide	1.0	3.4	RM000305
Talc	1.3	4.4	RM000050
Magnesium stearate	1.0	3.4	RM000304

***In vitro* release profile**

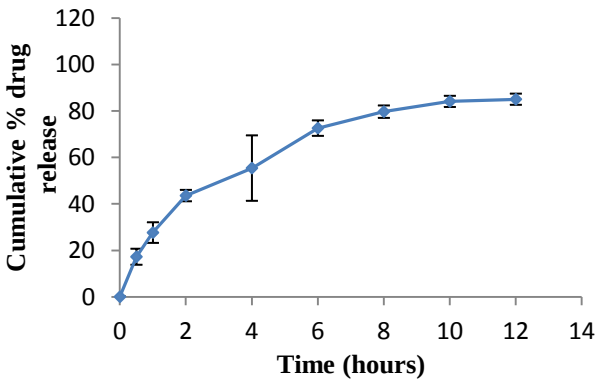

Comments and observations

- Slightly off-white
- Flat, smooth surfaces
- No sticking
- No lamination
- No capping
- No chipping
- No breaking

BATCH SUMMARY BATCH SUMMARY – C27

Faculty of Pharmacy, Rhodes University, Grahamstown, 6140, South Africa

Formulator: Samantha Mukozhiwa	**Batch number:** C27
Product: CPT 50 mg tablets	**Batch size: 300 g**
Powder blending date: 2013/10/23	**Humidity:** 67%
Tableting date: 2013/10/23	**Tooling:** 9.00 mm flat punches
Temperature: 22° C	**Actual weight:** 342.01 ± 1.98 mg
Tablet press: Manesty® B3B Rotary Press	**Actual crushing strength:** 112.37 ± 3.24 N
Target weight: 340 mg	**Yield:** 77.1 %
Target crushing strength: 100-140 N	**CPT content:** 99.68 ± 0.51%
Friability: 0.175 ± 1.46%	**FLT:** 11.50 ± 4.25 min
TFT: >12 hours	

FORMULA

Material	% w/w	Amount added (g)	Rhodes number
CPT	14.7	47.4	RM000348
Methocel® K100M	37.5	120.9	RM000602
$NaHCO_3$	15.0	48.4	RM000924
Avicel® PH102	22.5	72.6	RM000038
Colloidal silicon dioxide	1.0	3.2	RM000305
Talc	1.3	4.2	RM000050
Magnesium stearate	1.0	3.2	RM000304

***In vitro* release profile**

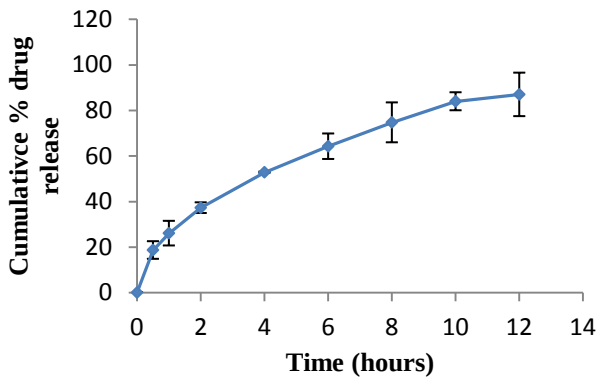

Comments and observations

- Slightly off-white
- Flat, smooth surfaces
- No sticking
- No lamination
- No capping
- No chipping
- No breaking

BATCH SUMMARY BATCH SUMMARY – C28

Faculty of Pharmacy, Rhodes University, Grahamstown, 6140, South Africa

Formulator: Samantha Mukozhiwa	**Batch number:** C28
Product: CPT 50 mg tablets	**Batch size: 300 g**
Powder blending date: 2013/10/23	**Humidity:** 67%
Tableting date: 2013/10/23	**Tooling:** 9.00 mm flat punches
Temperature: 22° C	**Actual weight:** 346.68 ± 1.98 mg
Tablet press: Manesty® B3B Rotary Press	**Actual crushing strength:** 103.27 ± 3.58 N
Target weight: 340 mg	**Yield:** 79.0 %
Target crushing strength: 100-140 N	**CPT content:** 98.13 ± 0.81%
Friability: 0.197 ± 1.25%	**FLT:** 12.01 ± 3.87 min
TFT: > 12 hours	

FORMULA

Material	% w/w	Amount added (g)	Rhodes number
CPT	14.7	52.1	RM000348
Methocel® K100M	37.5	132.9	RM000602
$NaHCO_3$	15.0	53.2	RM000924
Avicel® PH102	14.09	49.9	RM000038
Colloidal silicon dioxide	1.0	3.5	RM000305
Talc	1.3	4.6	RM000050
Magnesium stearate	1.0	3.5	RM000304

***In vitro* release profile**

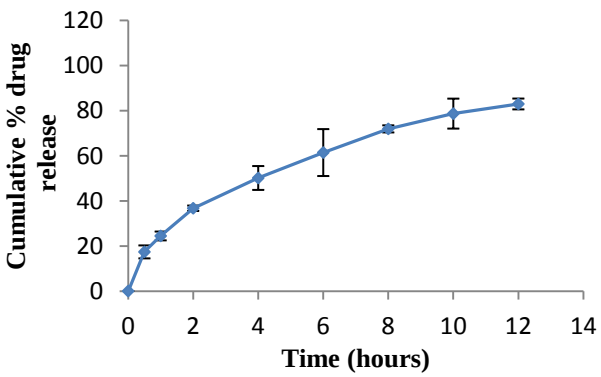

Comments and observations

- Slightly off-white
- Flat, smooth surfaces
- No sticking
- No lamination
- No capping
- No chipping
- No breaking

BATCH SUMMARY BATCH SUMMARY – C29

Faculty of Pharmacy, Rhodes University, Grahamstown, 6140, South Africa

Formulator: Samantha Mukozhiwa	**Batch number:** C29
Product: CPT 50 mg tablets	**Batch size: 300 g**
Powder blending date: 2013/10/24	**Humidity:** 54%
Tableting date: 2013/10/24	**Tooling:** 9.00 mm flat punches
Temperature: 29° C	**Actual weight:** 342.08 ± 1.83 mg
Tablet press: Manesty® B3B Rotary Press	**Actual crushing strength:** 108.98 ± 2.48 N
Target weight: 340 mg	**Yield:** 74.3 %
Target crushing strength: 100-140 N	**CPT content:** 99.09 ± 0.49%
Friability: 0.187 ± 3.14%	**FLT:** 10.16 ± 3.33 min
TFT: > 12 hours	

FORMULA

Material	% w/w	Amount added (g)	Rhodes number
CPT	14.7	47.4	RM000348
Methocel® K100M	37.5	120.9	RM000602
$NaHCO_3$	15.0	48.4	RM000924
Avicel® PH102	22.5	72.6	RM000038
Colloidal silicon dioxide	1.0	3.2	RM000305
Talc	1.3	4.2	RM000050
Magnesium stearate	1.0	3.2	RM000304

***In vitro* release profile**

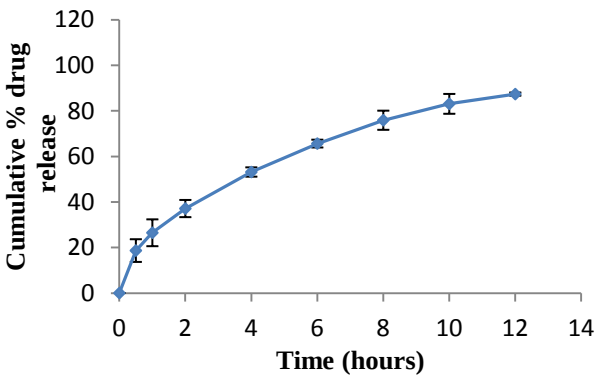

Comments and observations

- Slightly off-white
- Flat, smooth surfaces
- No sticking
- No lamination
- No capping
- No chipping
- No breaking

BATCH SUMMARY BATCH SUMMARY – C30

Faculty of Pharmacy, Rhodes University, Grahamstown, 6140, South Africa

Formulator: Samantha Mukozhiwa	**Batch number:** C30
Product: CPT 50 mg tablets	**Batch size: 300 g**
Powder blending date: 2013/10/24	**Humidity:** 54%
Tableting date: 2013/10/24	**Tooling:** 9.00 mm flat punches
Temperature: 29° C	**Actual weight:** 336.19 ± 1.39 mg
Tablet press: Manesty® B3B Rotary Press	**Actual crushing strength:** 124.39 ± 3.45 N
Target weight: 340 mg	**Yield:** 76.4 %
Target crushing strength: 100-140 N	**CPT content:** 97.49 ± 0.77%
Friability: 0.145 ± 2.73%	**FLT:** 9.45 ± 4.13 min
TFT: > 12 hours	

FORMULA

Material	% w/w	Amount added (g)	Rhodes number
CPT	14.7	45	RM000348
Methocel® K100M	32.5	99.5	RM000602
$NaHCO_3$	20.0	61.2	RM000924
Avicel® PH102	27.5	84.2	RM000038
Colloidal silicon dioxide	1.0	3.1	RM000305
Talc	1.3	3.9	RM000050
Magnesium stearate	1.0	3.1	RM000304

***In vitro* release profile**

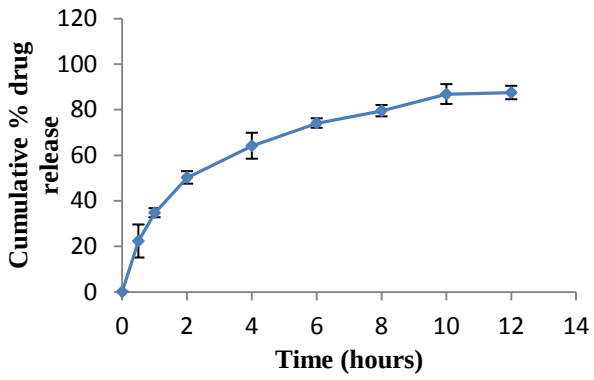

Comments and observations

- Slightly off-white
- Flat, smooth surfaces
- No sticking
- No lamination
- No capping
- No chipping
- No breaking

BATCH SUMMARY BATCH SUMMARY – C31

Faculty of Pharmacy, Rhodes University, Grahamstown, 6140, South Africa

Formulator: Samantha Mukozhiwa	**Batch number:** C31
Product: CPT 50 mg tablets	**Batch size: 300 g**
Powder blending date: 2013/11/05	**Humidity:** 51%
Tableting date: 2013/11/05	**Tooling:** 9.00 mm flat punches
Temperature: 36° C	**Actual weight:** 338.59 ± 2.80 mg
Tablet press: Manesty® B3B Rotary Press	**Actual crushing strength:** 105.12 ± 2.74 N
Target weight: 340 mg	**Yield:** 76.8 %
Target crushing strength: 100-140 N	**CPT content:** 98.8 ± 0.43%
Friability: 0.169 ± 1.96%	
TFT: > 12 hours	

FORMULA

Material	% w/w	Amount added (g)	Rhodes number
CPT	14.7	42.5	RM000348
Methocel® K100M	41.81	121.5	RM000602
$NaHCO_3$	26.73	77.7	RM000924
Avicel® PH102	16.66	48.4	RM000038
Colloidal silicon dioxide	1.0	2.9	RM000305
Talc	1.3	3.8	RM000050
Magnesium stearate	1.0	2.9	RM000304

***In vitro* release profile**

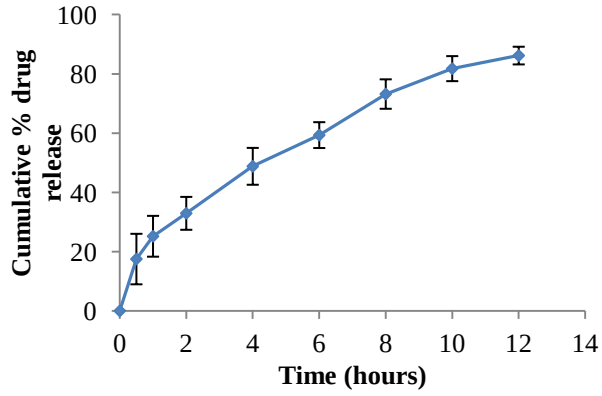

Comments and observations

- Slightly off-white
- Flat, smooth surfaces
- No sticking
- No lamination
- No capping
- No chipping
- No breaking

BATCH SUMMARY BATCH SUMMARY – C32

Faculty of Pharmacy, Rhodes University, Grahamstown, 6140, South Africa

Formulator: Samantha Mukozhiwa	**Batch number:** C32
Product: CPT 50 mg tablets	**Batch size: 300 g**
Powder blending date: 2013/11/06	**Humidity:** 71%
Tableting date: 2013/11/06	**Tooling:** 9.00 mm flat punches
Temperature: 36° C	**Actual weight:** 338.59 ± 2.80 mg
Tablet press: Manesty® B3B Rotary Press	**Actual crushing strength:** 105.12 ± 2.74 N
Target weight: 340 mg	**Yield:** 76.8 %
Target crushing strength: 100-140 N	**CPT content:** 98.8 ± 0.43%
Friability: 0.169 ± 1.96%	
TFT: > 12 hours	

FORMULA

Material	% w/w	Amount added (g)	Rhodes number
CPT	14.7	42.5	RM000348
Methocel® K100M	41.81	121.5	RM000602
$NaHCO_3$	26.73	77.7	RM000924
Avicel® PH102	16.66	48.4	RM000038
Colloidal silicon dioxide	1.0	2.9	RM000305
Talc	1.3	3.8	RM000050
Magnesium stearate	1.0	2.9	RM000304

***In vitro* release profile**

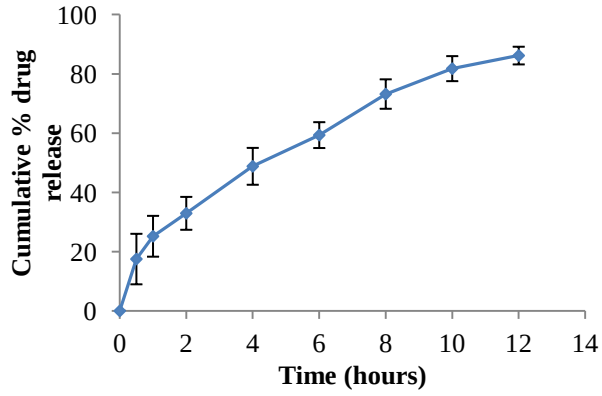

Comments and observations

- Slightly off-white
- Flat, smooth surfaces
- No sticking
- No lamination
- No capping
- No chipping
- No breaking

BATCH SUMMARY BATCH SUMMARY – C33

Faculty of Pharmacy, Rhodes University, Grahamstown, 6140, South Africa

Formulator: Samantha Mukozhiwa	**Batch number:** C33
Product: CPT 50 mg tablets	**Batch size: 300 g**
Powder blending date: 2013/11/07	**Humidity:** 62%
Tableting date: 2013/11/07	**Tooling:** 9.00 mm flat punches
Temperature: 24° C	**Actual weight:** 338.59 ± 2.80 mg
Tablet press: Manesty® B3B Rotary Press	**Actual crushing strength:** 105.12 ± 2.74 N
Target weight: 340 mg	**Yield:** 76.8 %
Target crushing strength: 100-140 N	**CPT content:** 98.8 ± 0.43%
Friability: 0.169 ± 1.96%	
TFT: > 12 hours	

FORMULA

Material	% w/w	Amount added (g)	Rhodes number
CPT	14.7	42.5	RM000348
Methocel® K100M	41.81	121.5	RM000602
$NaHCO_3$	26.73	77.7	RM000924
Avicel® PH102	16.66	48.4	RM000038
Colloidal silicon dioxide	1.0	2.9	RM000305
Talc	1.3	3.8	RM000050
Magnesium stearate	1.0	2.9	RM000304

***In vitro* release profile**

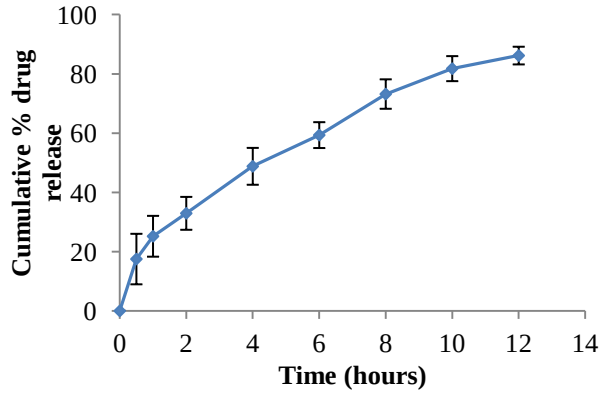

Comments and observations

- Slightly off-white
- Flat, smooth surfaces
- No sticking
- No lamination
- No capping
- No chipping
- No breaking

APPENDIX III

Diagnostic plots, two-dimensional and three-dimensional response surface plots monitored in the CCD optimisation process

1. Diagnostic plots for response Y_1: CPT release after 0.5 hours – Quadratic model

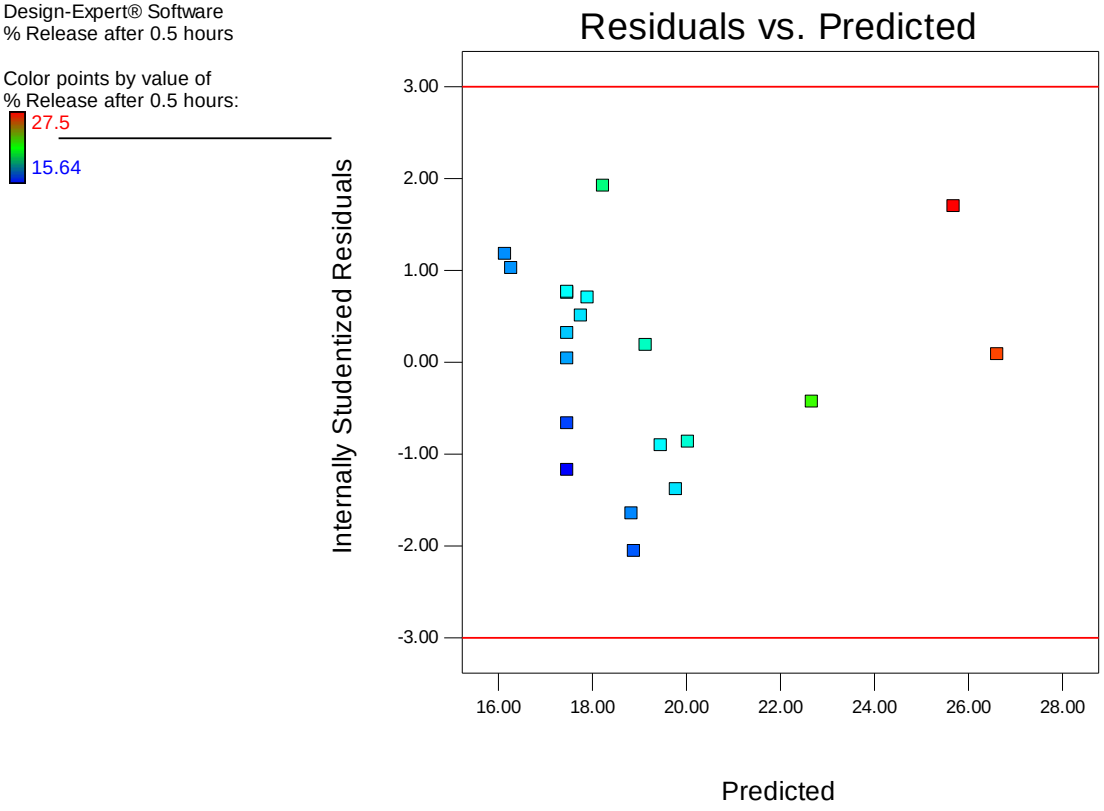

Figure Ap. 3.1 Normal plot of residuals for response Y_1

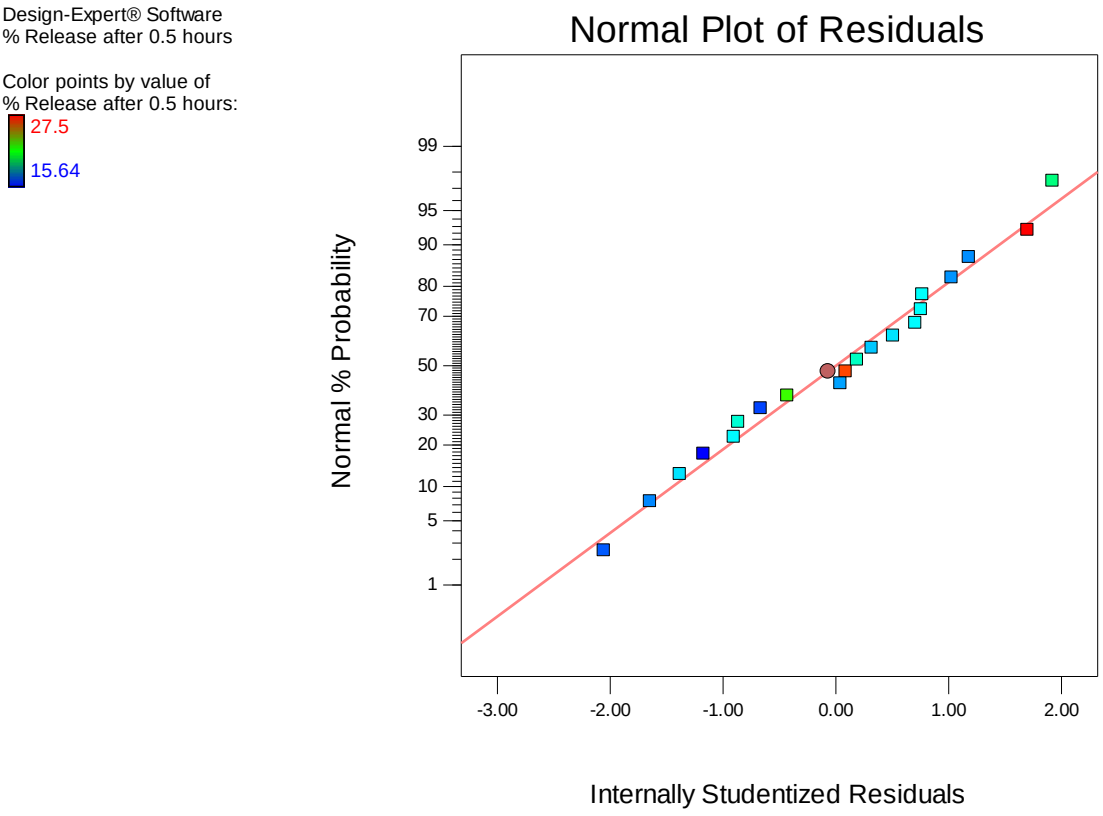

Figure Ap. 3.2 Plot of residuals vs. Predicted for response Y_1

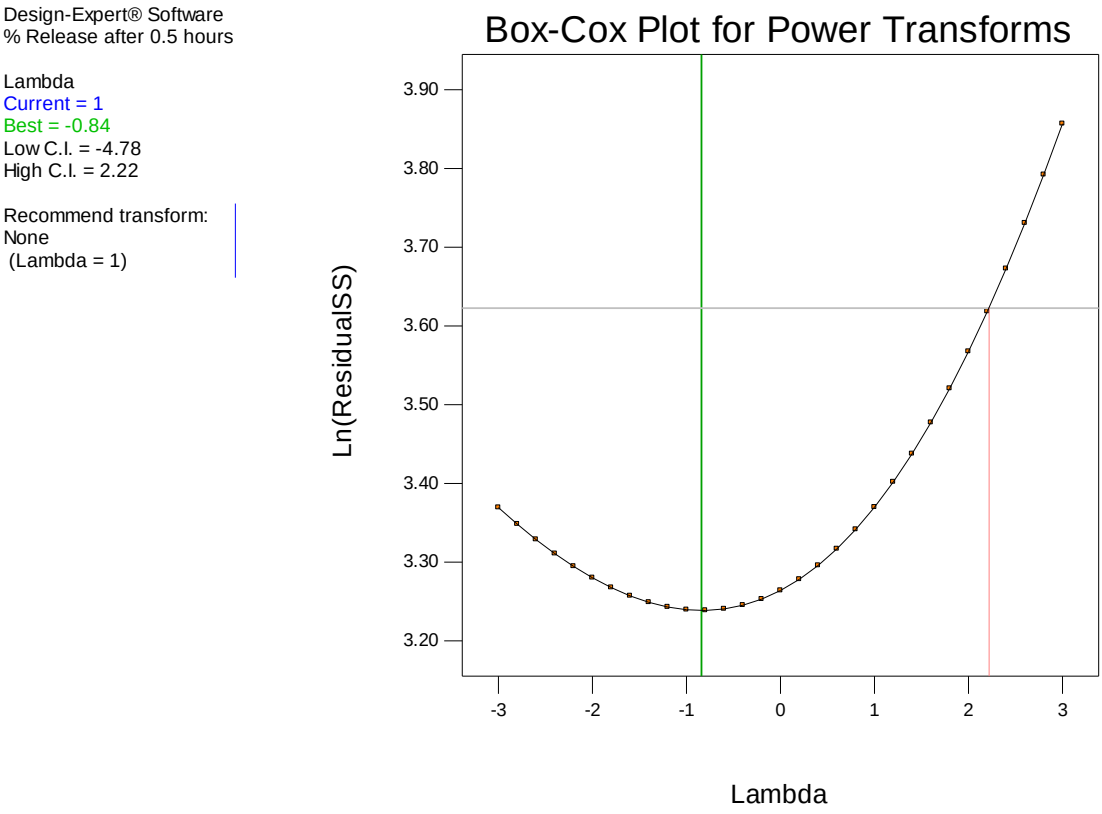

Figure Ap. 3.3 Box-Cox plot for power transformation for response Y_1

2. Response surface plots for response Y_1

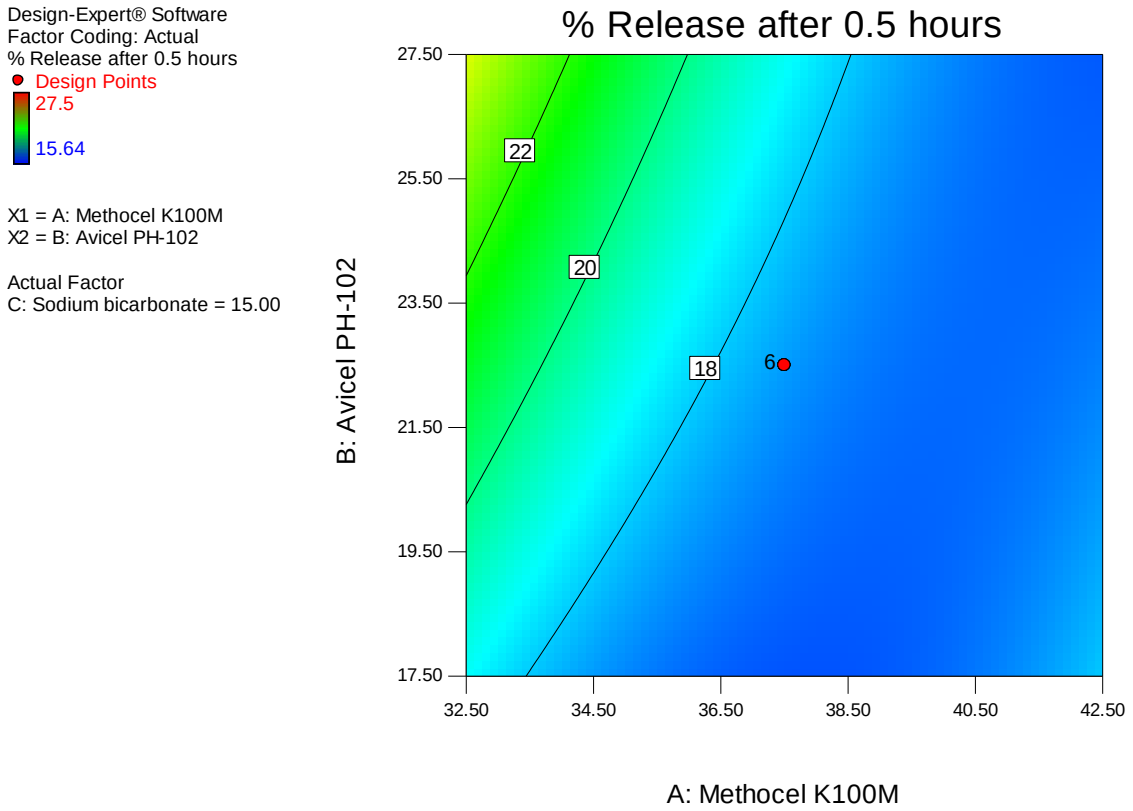

Figure Ap. 3.4 Two-dimensional contour plot of the effect of Avicel® PH-102 and Methocel® K100M on response Y_1

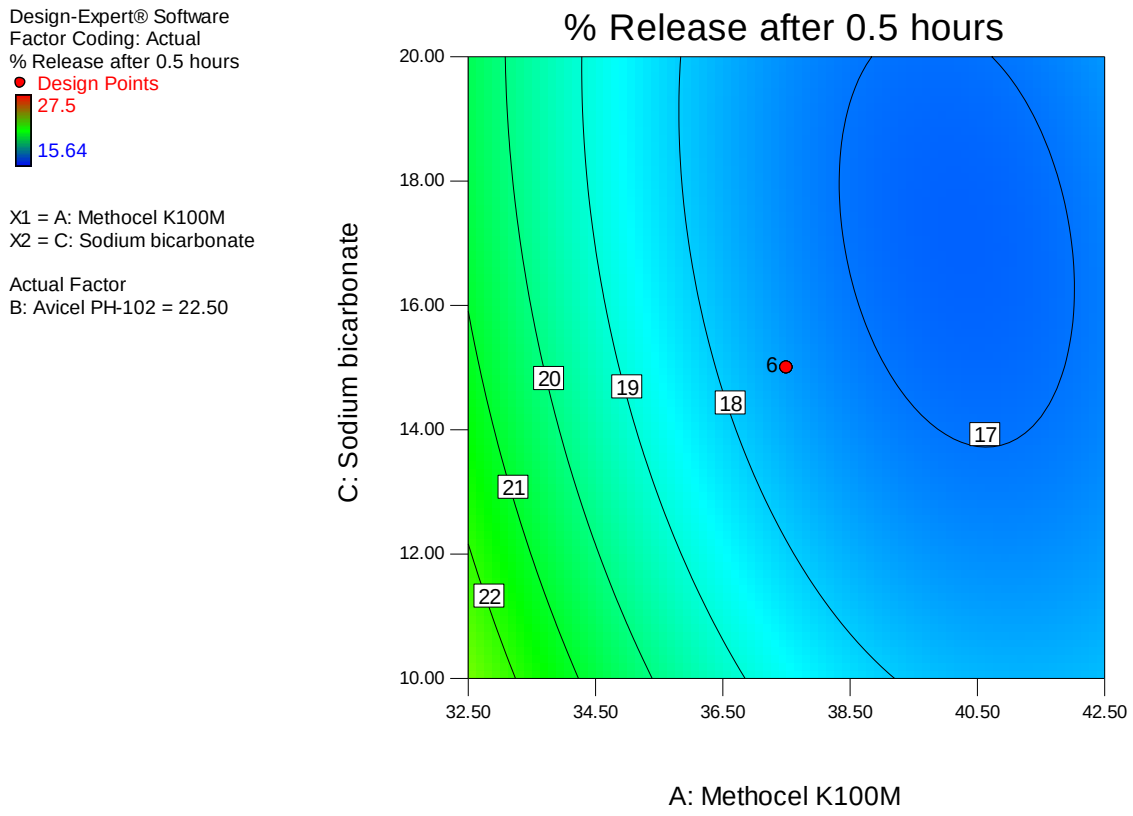

Figure Ap. 3.5 Two-dimensional contour plot of the effect of sodium bicarbonate and Methocel® K100M on response Y_1

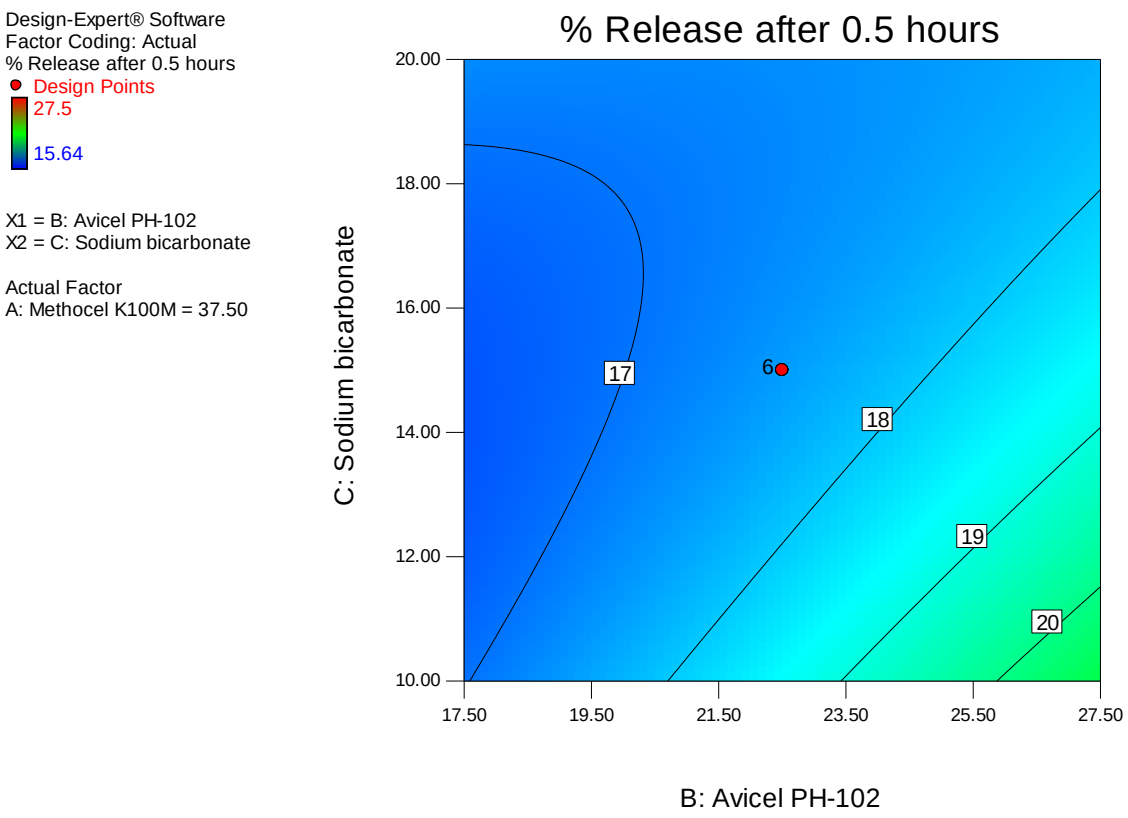

Figure Ap. 3.6 Two-dimensional contour plot of the effect of Avicel® PH-102 sodium bicarbonate on response Y_1

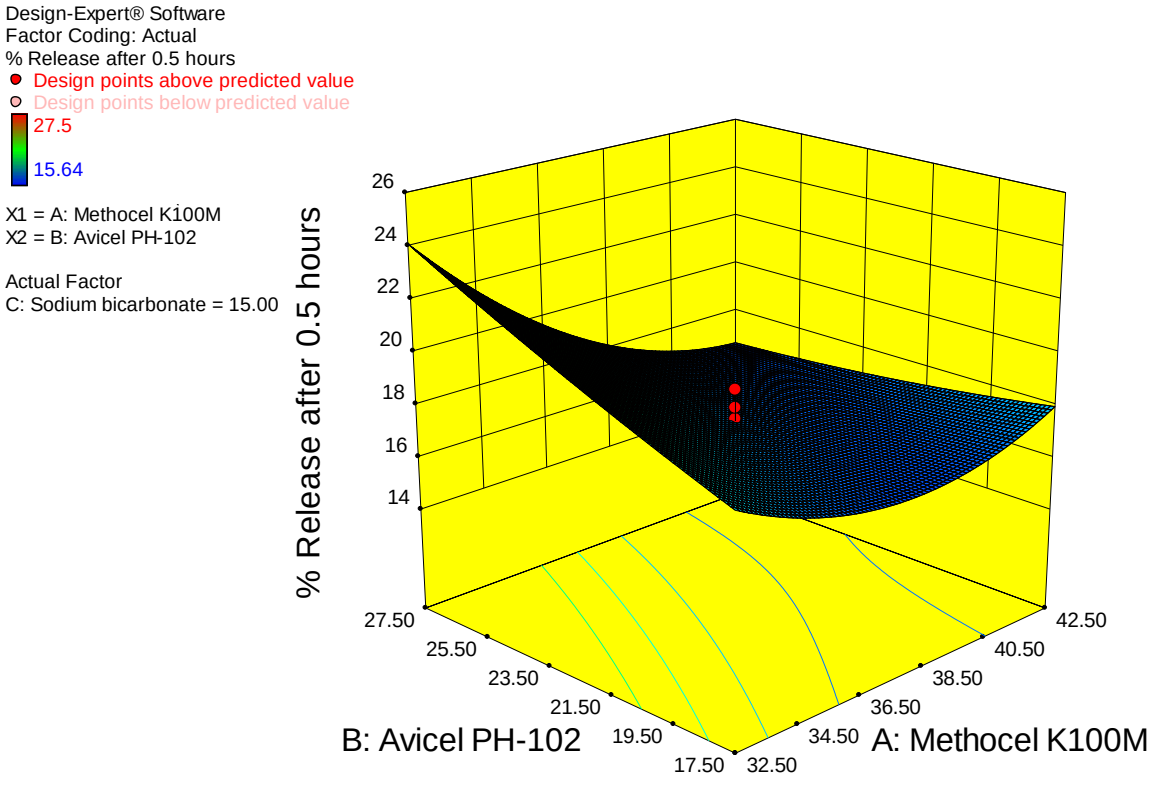

Figure Ap. 3.7 Three-dimensional contour plot of the effect of Avicel® PH-102 and Methocel® K100M on response Y_1

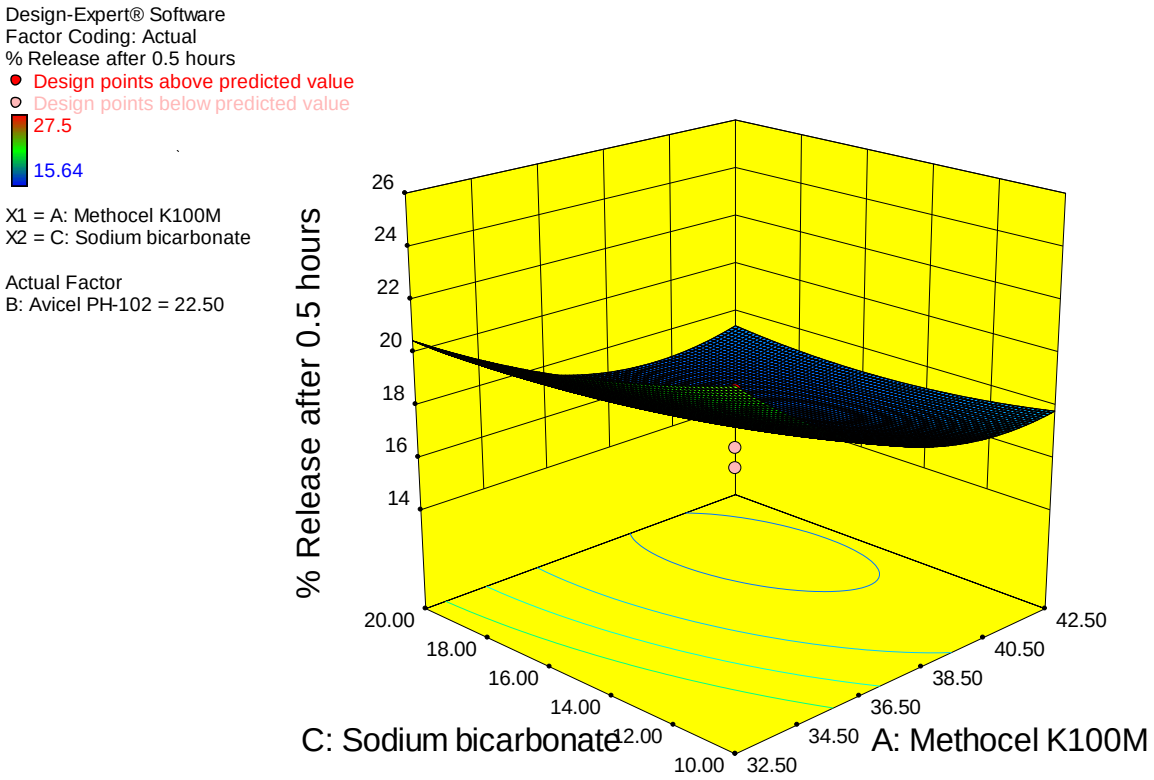

Figure Ap. 3.8 Three-dimensional contour plot of the effect of sodium bicarbonate and Methocel® K100M on response Y_1

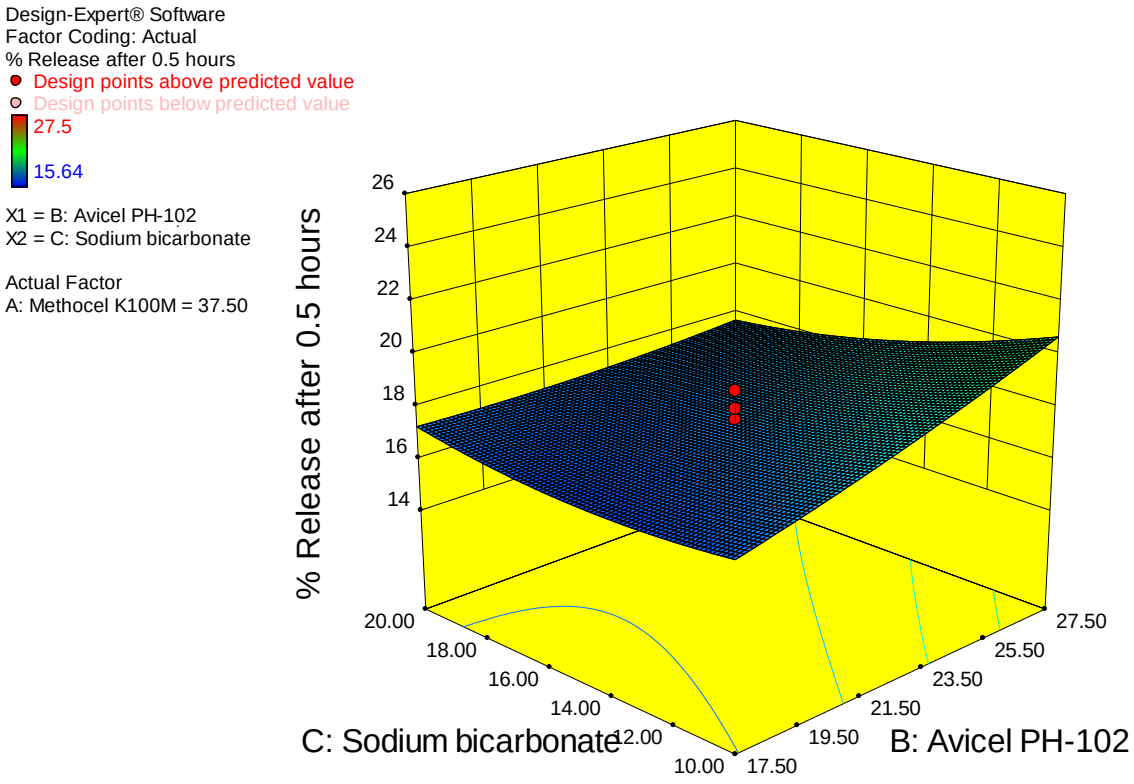

Figure Ap. 3.9 Three-dimensional contour plot of the effect of Avicel® PH-102 sodium bicarbonate on response Y_1

Diagnostic plots for response Y_2: CPT release after 2 hours – Quadratic model

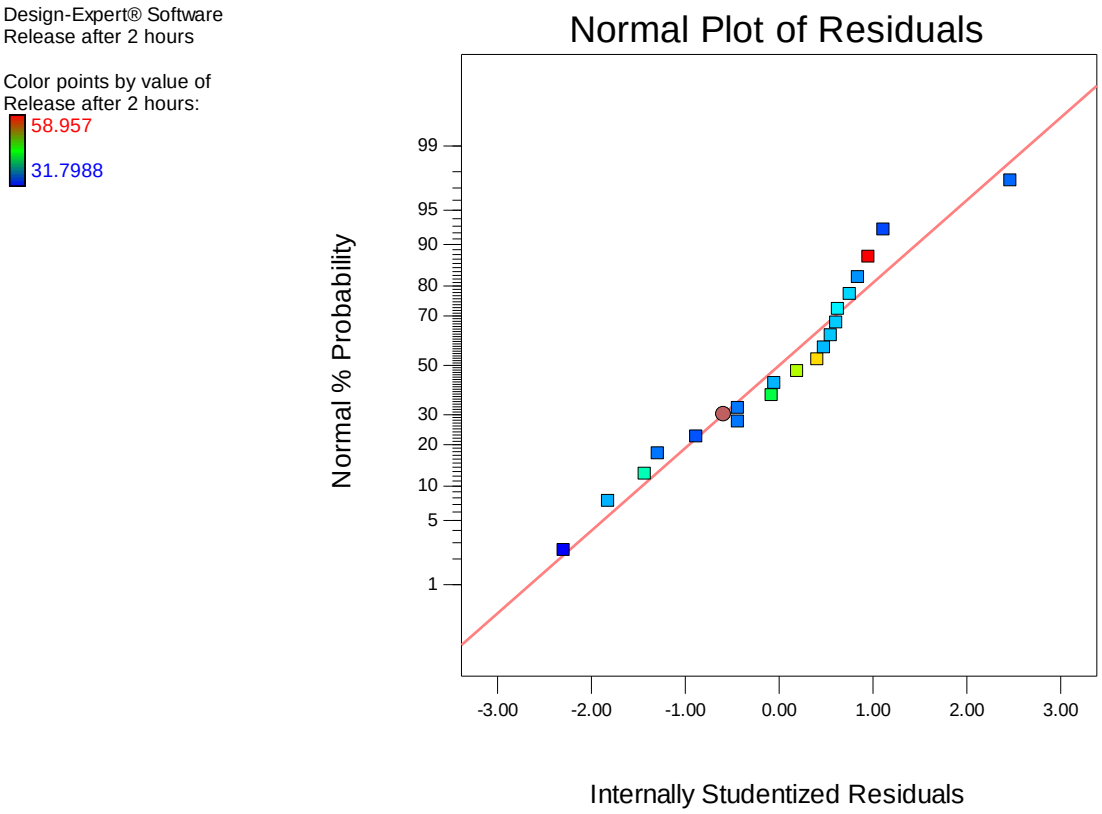

Figure Ap. 3.10 Normal plot of residuals for response Y_2

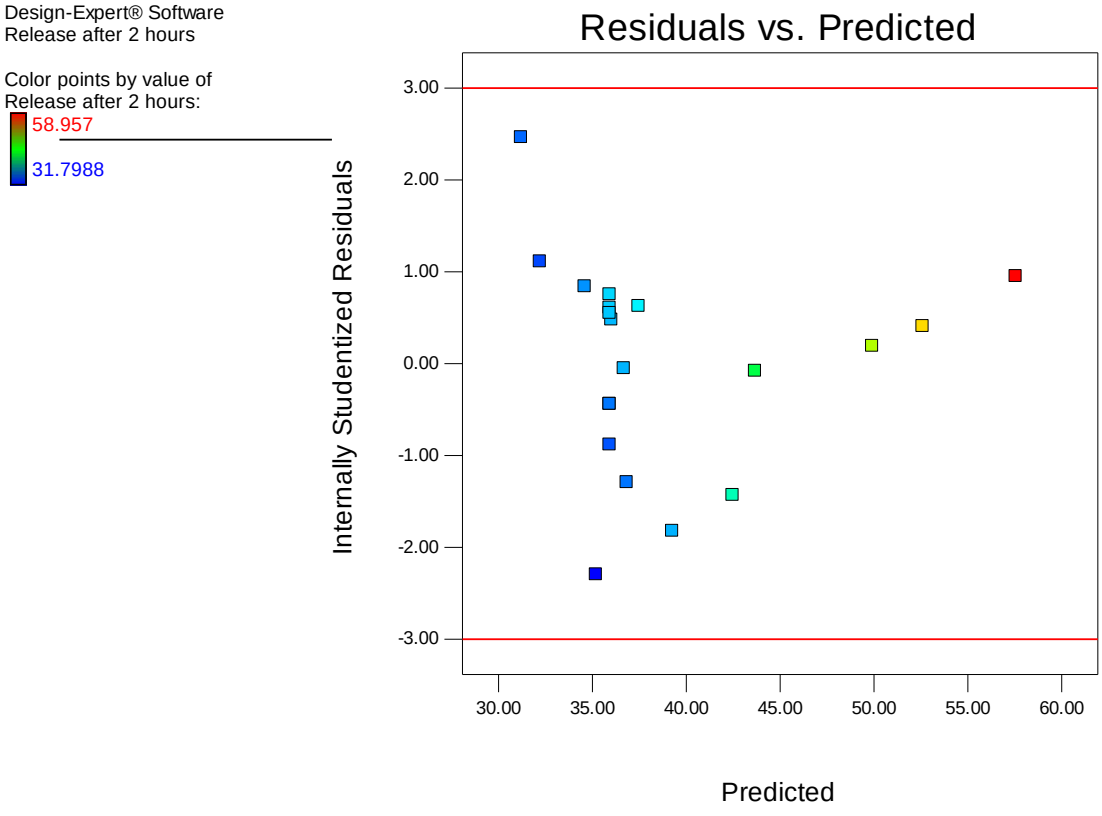

Figure Ap. 3.11 Plot of residuals vs. predicted for response Y_2

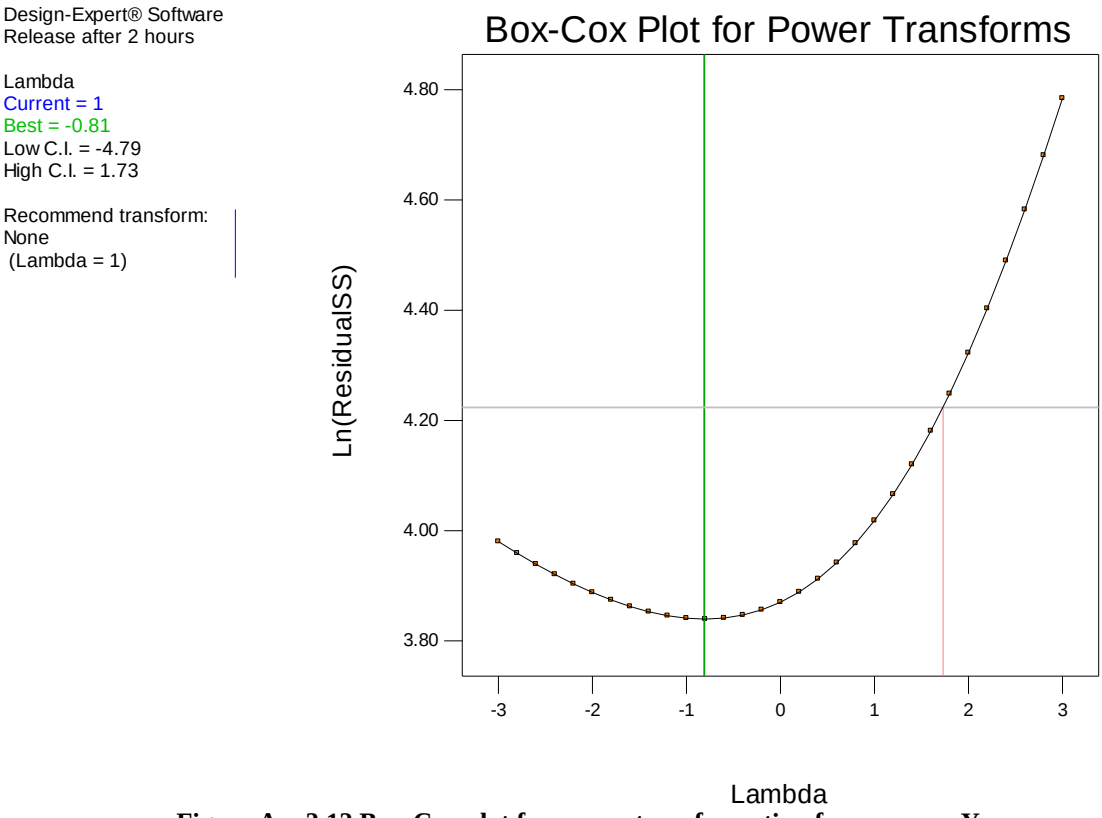

Figure Ap. 3.12 Box-Cox plot for power transformation for response Y_2

3. Response surface plots for response Y_2

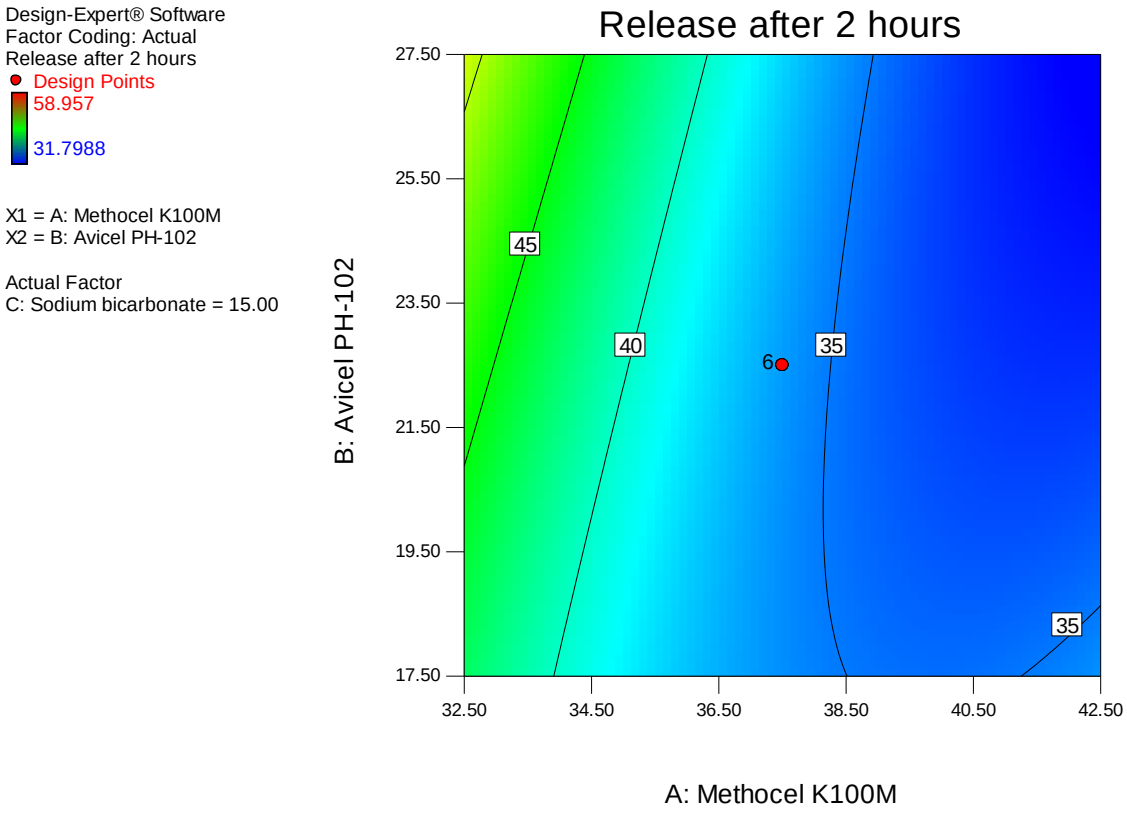

Figure Ap. 3.13 Two-dimensional contour plot of the effect of Avicel® PH-102 and Methocel® K100M on response Y_2

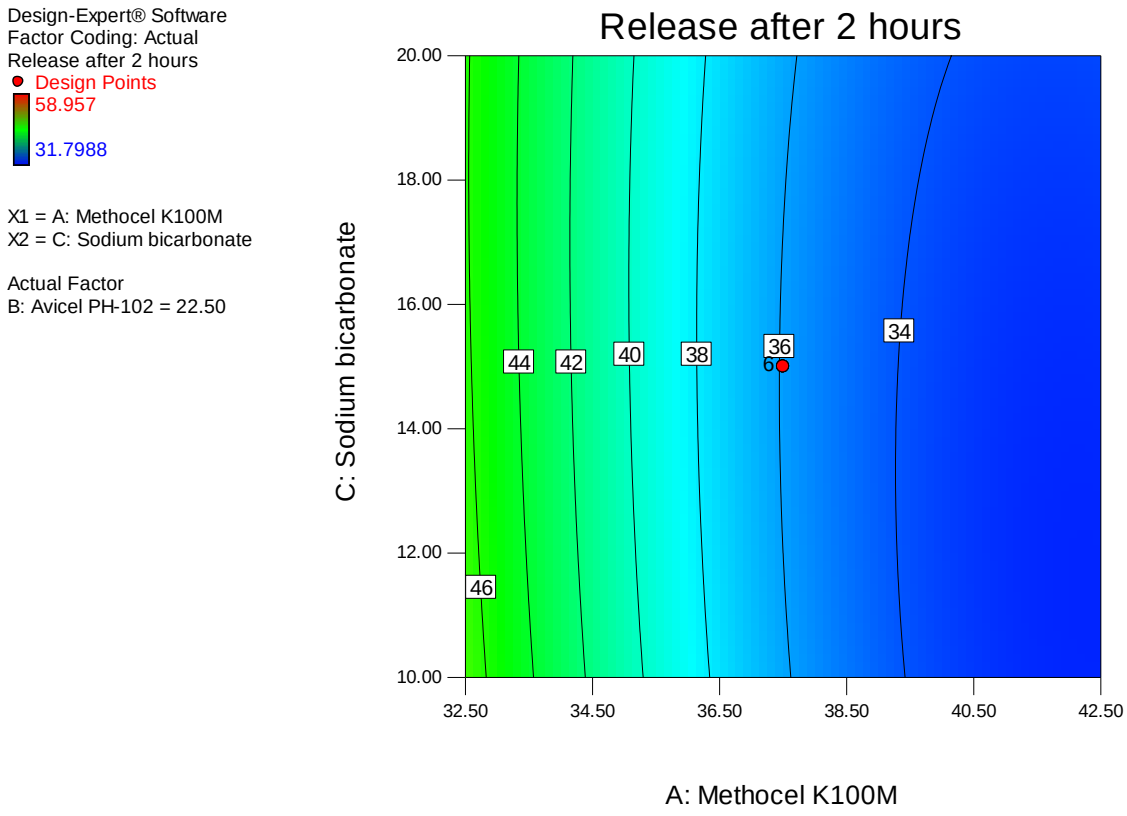

Figure Ap. 3.14 Two-dimensional contour plot of the effect of sodium bicarbonate and Methocel® K100M on response Y_2

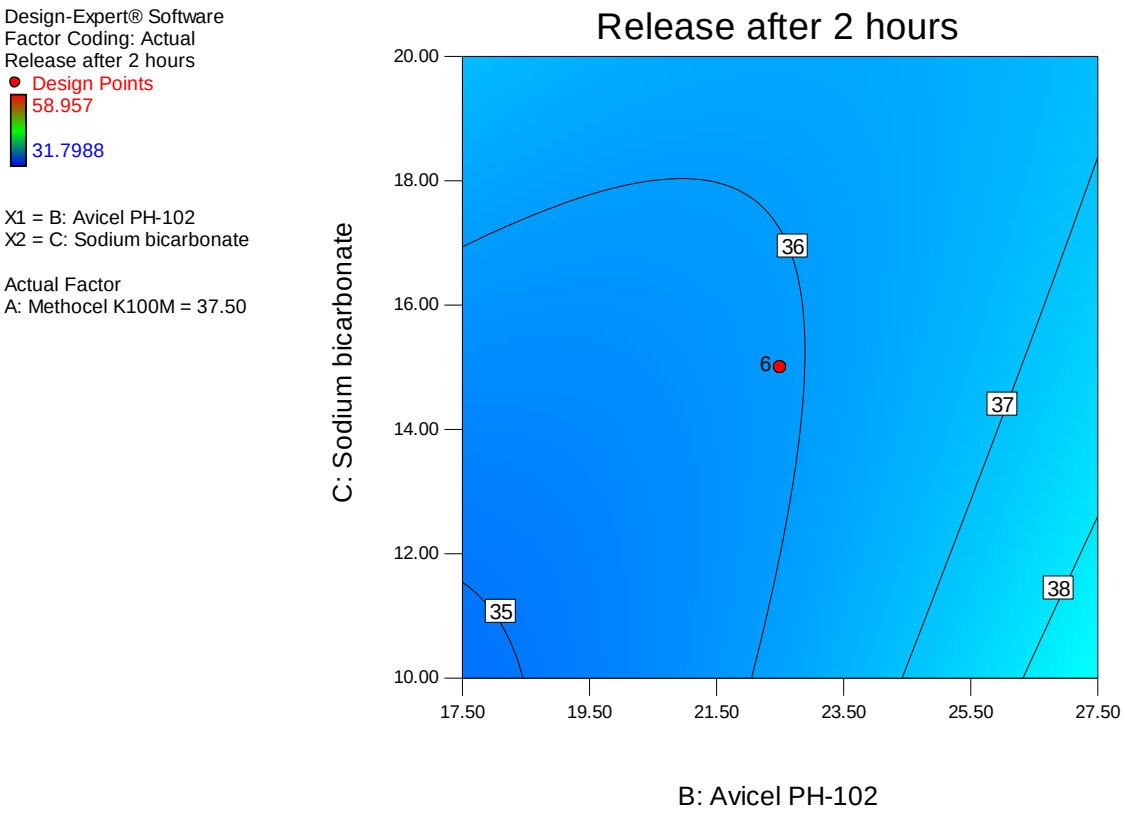

Figure Ap. 3.15 Two-dimensional contour plot of the effect of Avicel® PH-102 sodium bicarbonate on response Y_2

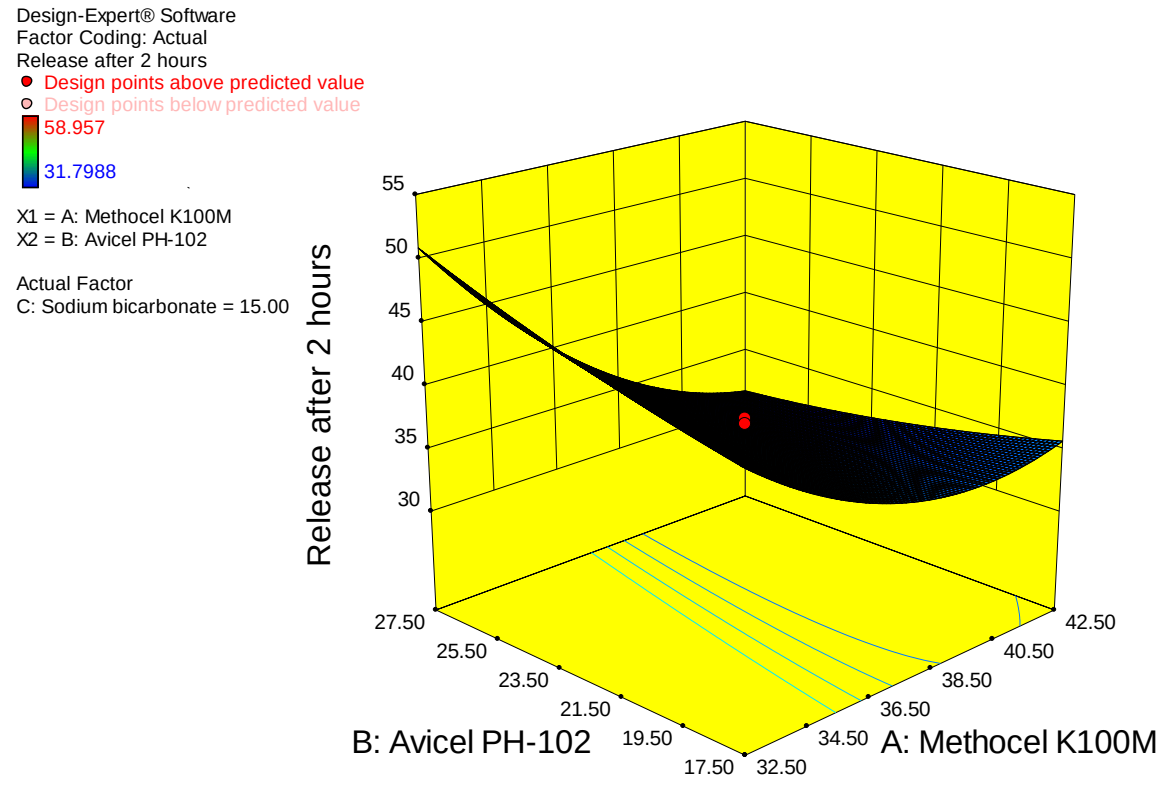

Figure Ap. 3.16 Three-dimensional contour plot of the effect of Avicel® PH-102 and Methocel® K100M on response Y_2

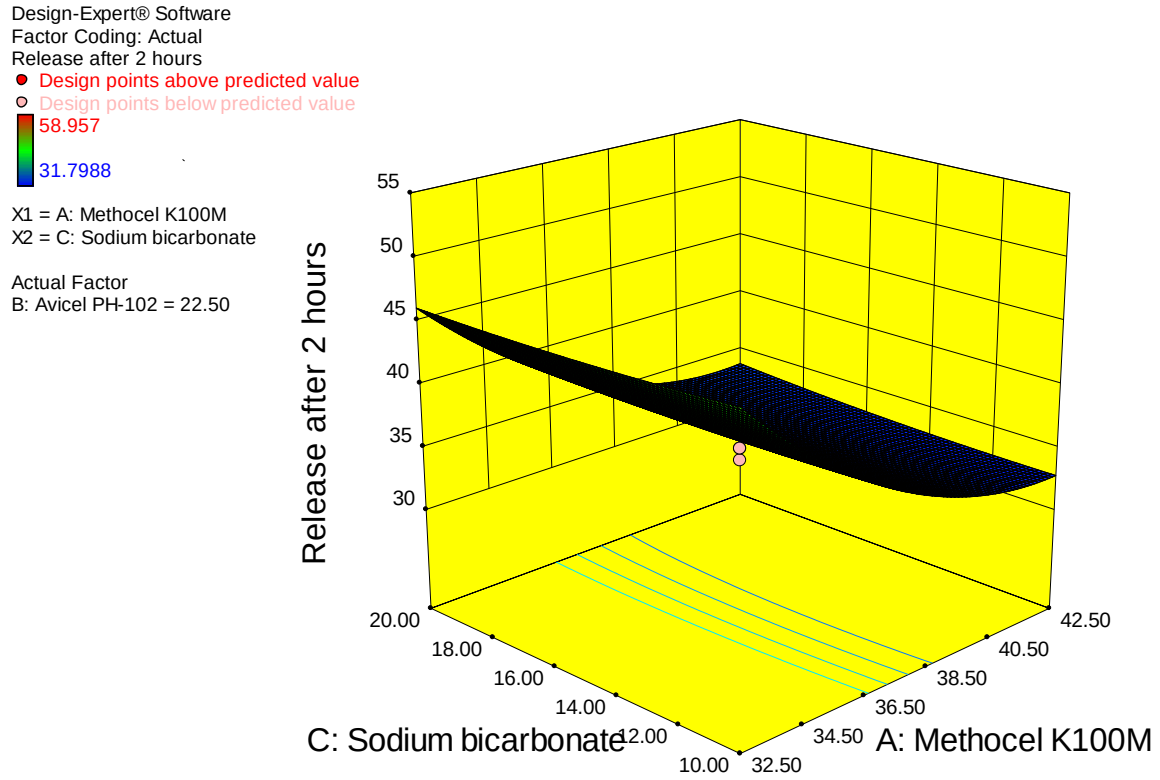

Figure Ap. 3.17 Three-dimensional contour plot of the effect of sodium bicarbonate and Methocel® K100M on response Y_3

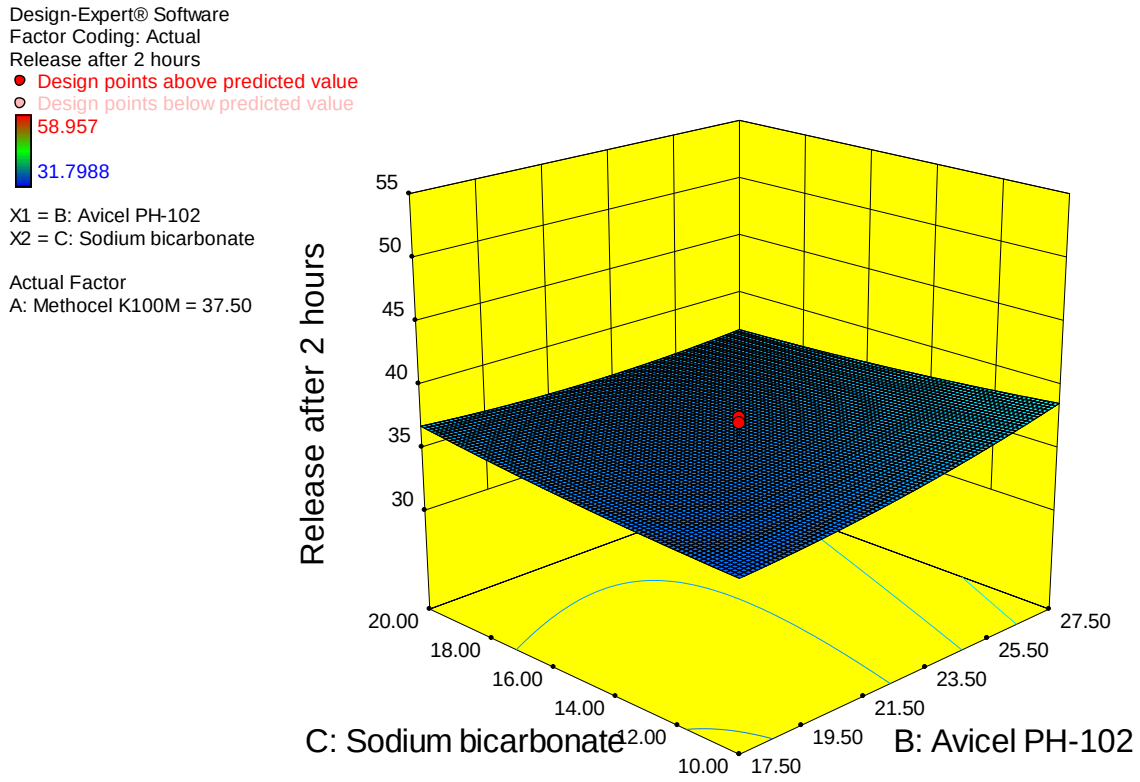

Figure Ap. 3.18 Three-dimensional contour plot of the effect of Avicel® PH-102 sodium bicarbonate on response Y_3

Diagnostic plots for response Y_4: CPT release after 12 hours – Linear model

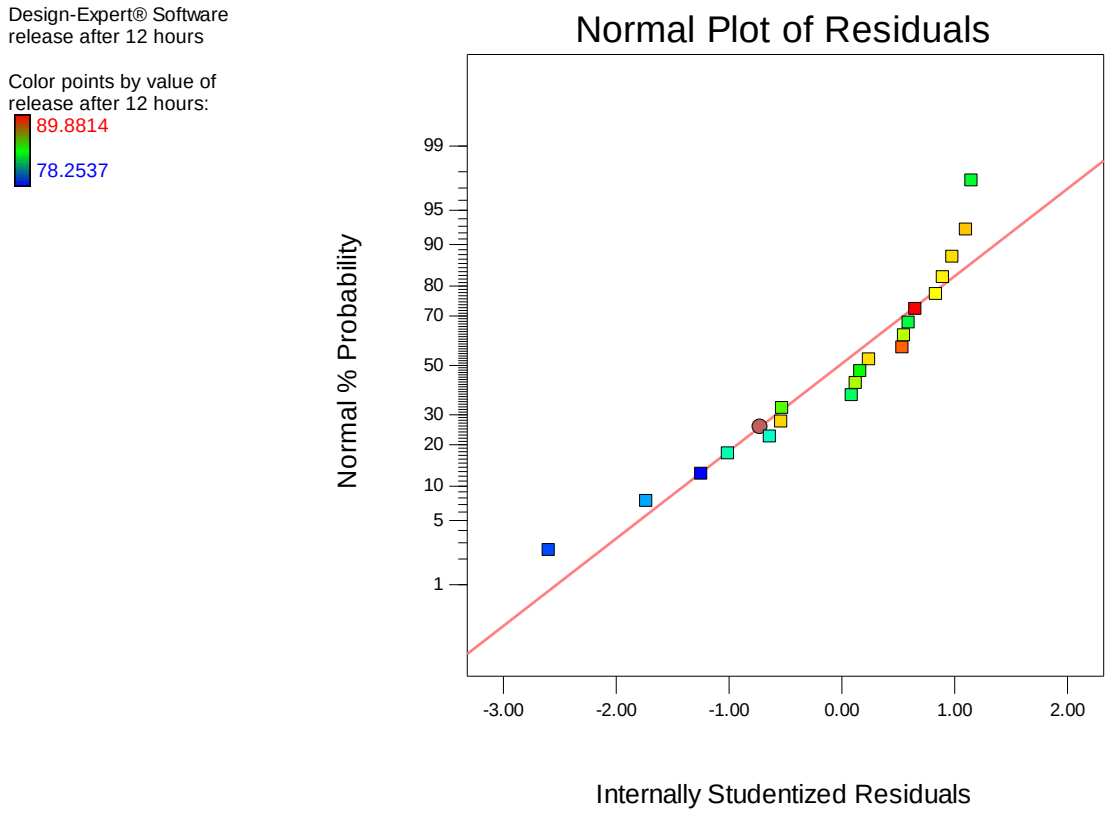

Figure Ap. 3.19 Normal plot of residuals for response Y_4

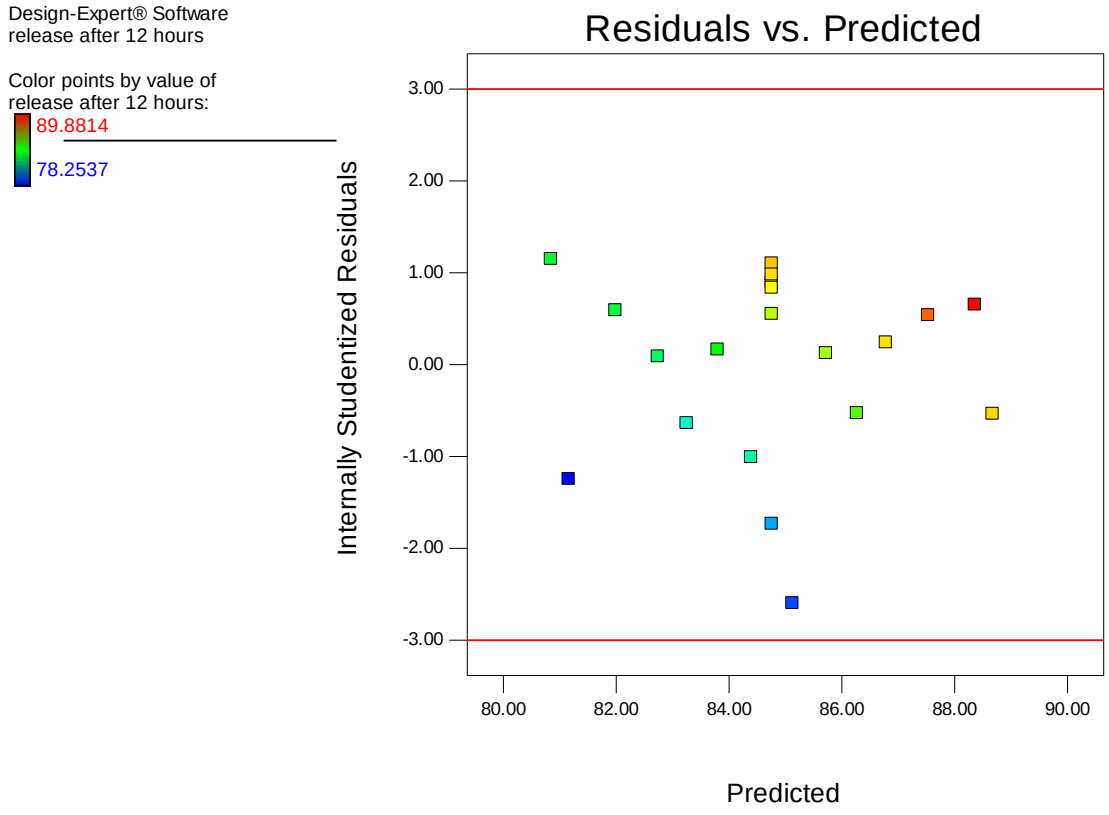

Figure Ap. 3.20 Plot of residuals vs. predicted for response Y_4

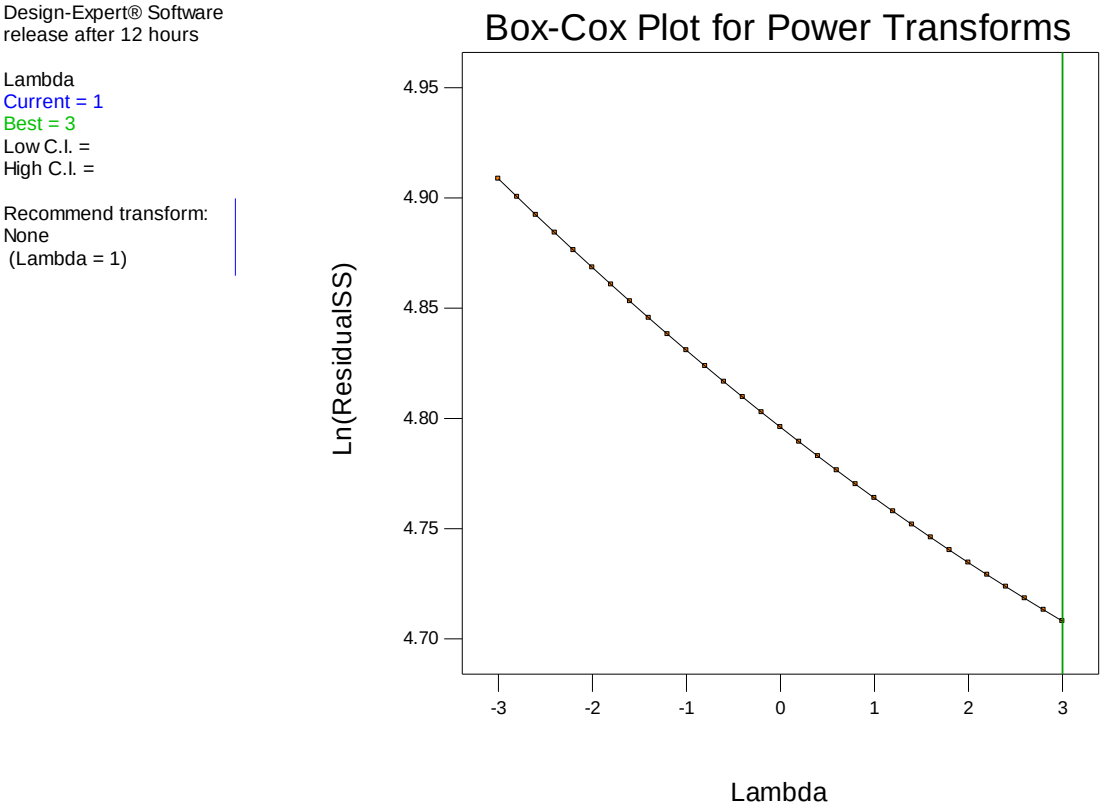

Figure Ap. 3.21 Box-Cox plot for power transformation for response Y_4

4. Response surface plots for response Y_4

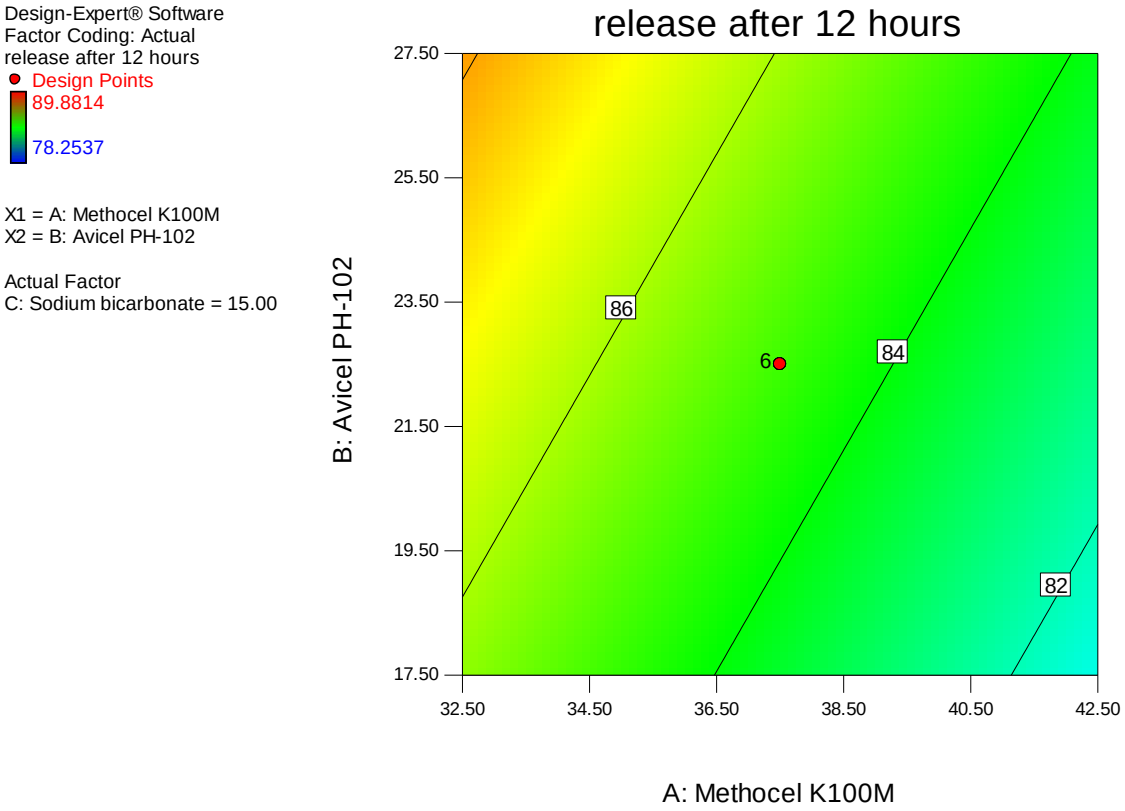

Figure Ap. 3.22 Two-dimensional contour plot of the effect of Avicel® PH-102 and Methocel® K100M on response Y_4

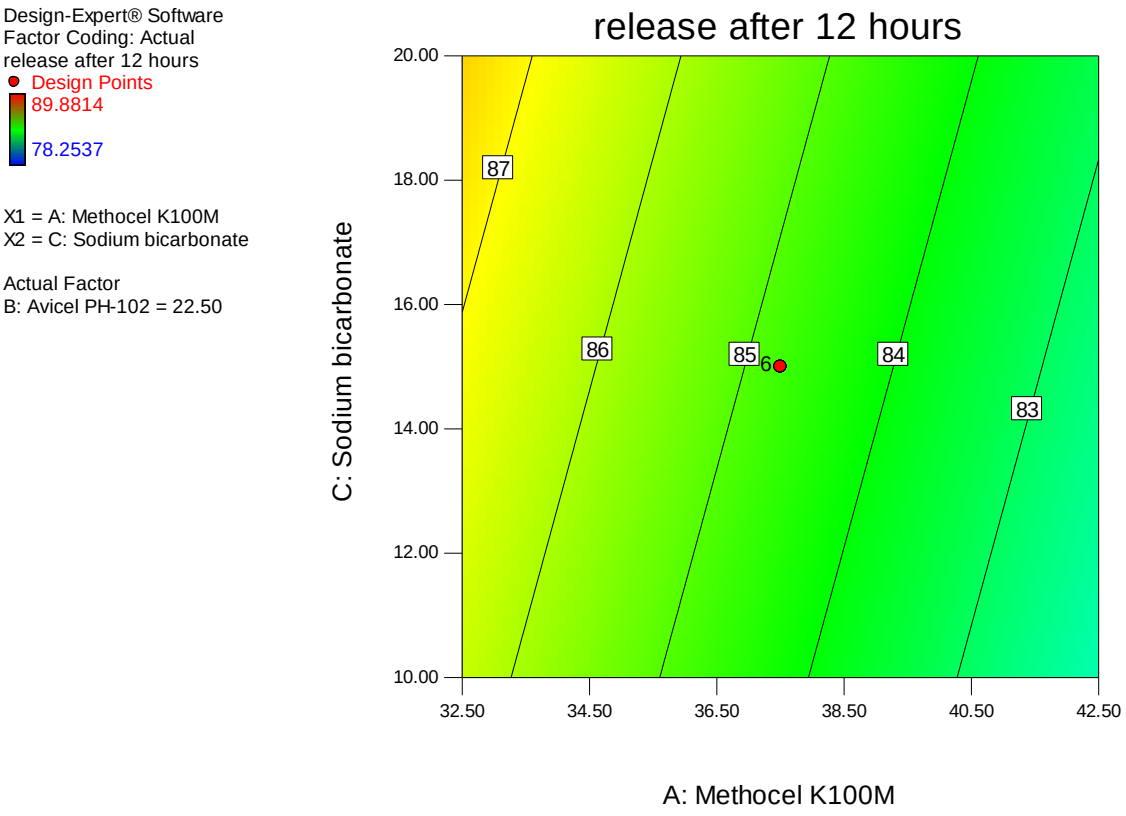

Figure Ap. 3.23 Two-dimensional contour plot of the effect of sodium bicarbonate and Methocel® K100M on response Y_4

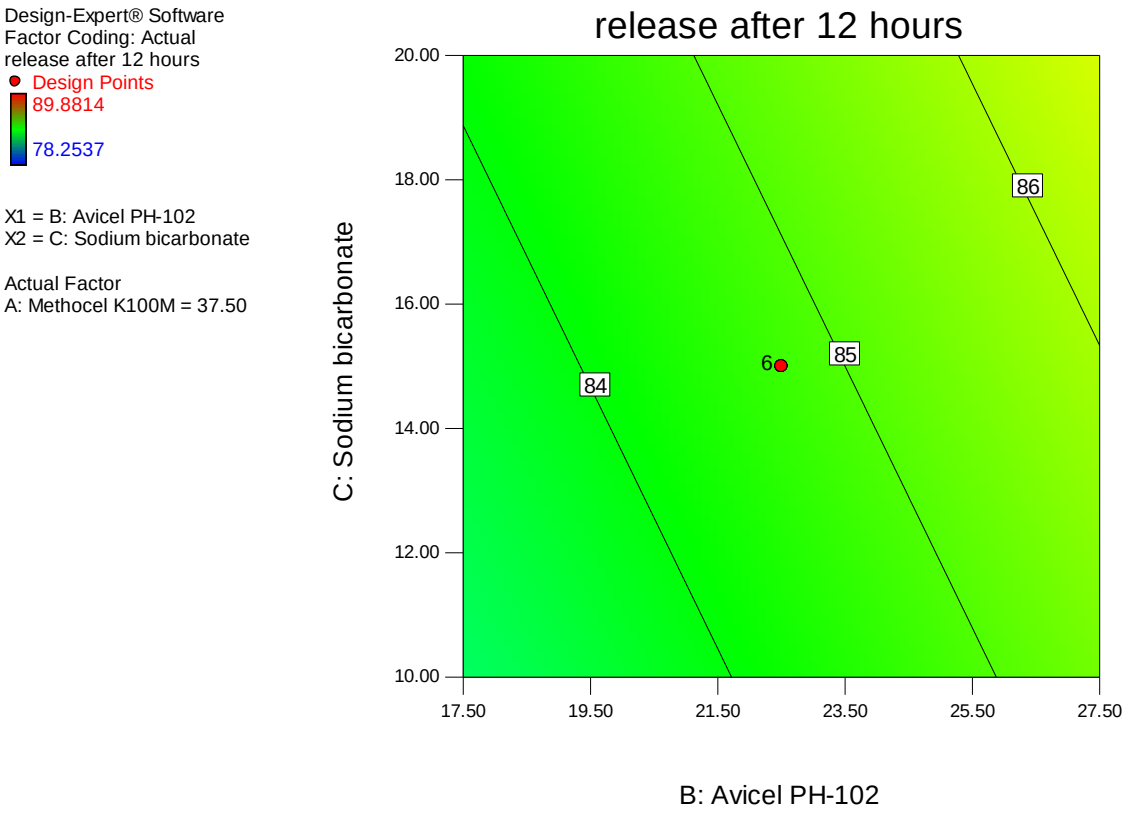

Figure Ap. 3.24 Two-dimensional contour plot of the effect of Avicel® PH-102 sodium bicarbonate on response Y_4

5. Diagnostic plots for response Y_5 – Linear model

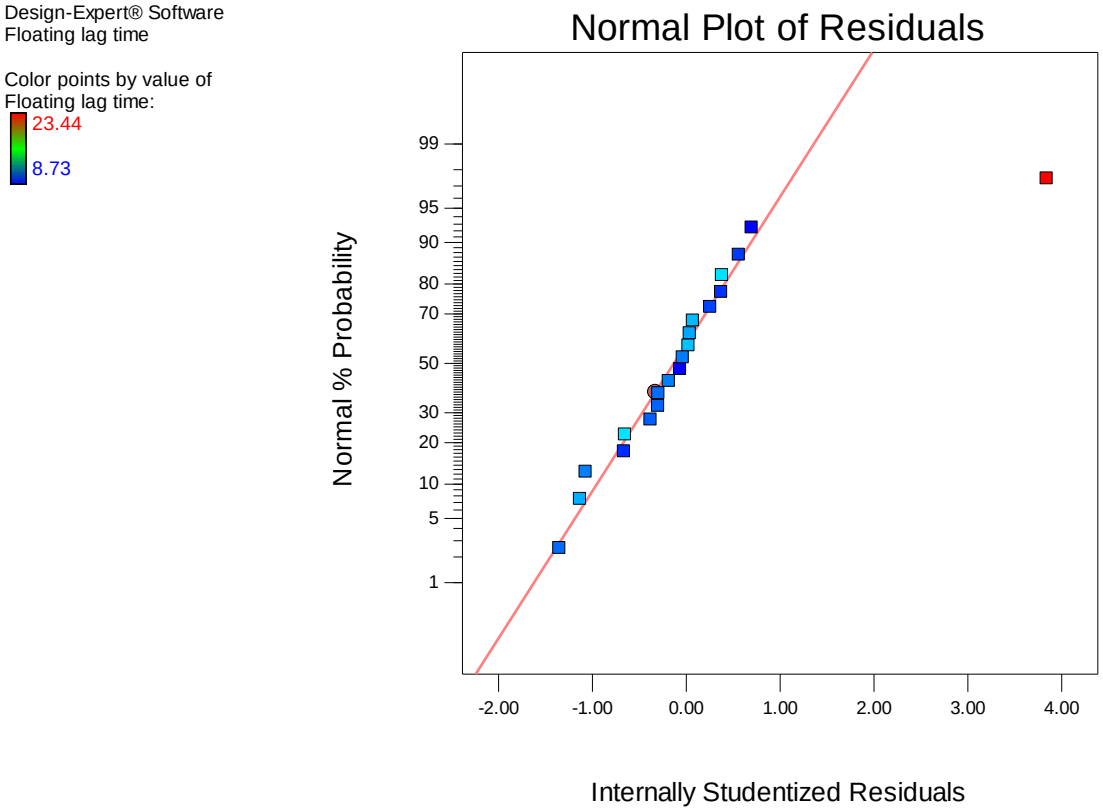

Figure Ap. 3.25 Normal plot of residuals for response Y_5

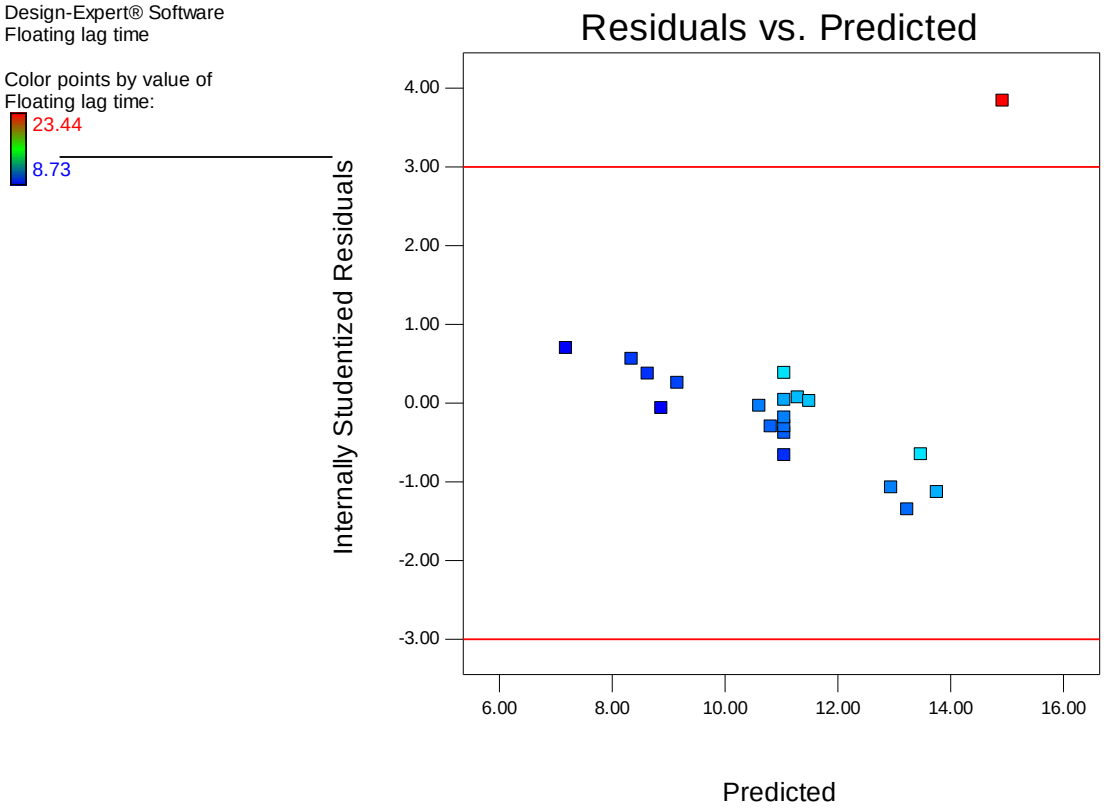

Figure Ap. 3.26 Plot of residuals vs. predicted for response Y_5

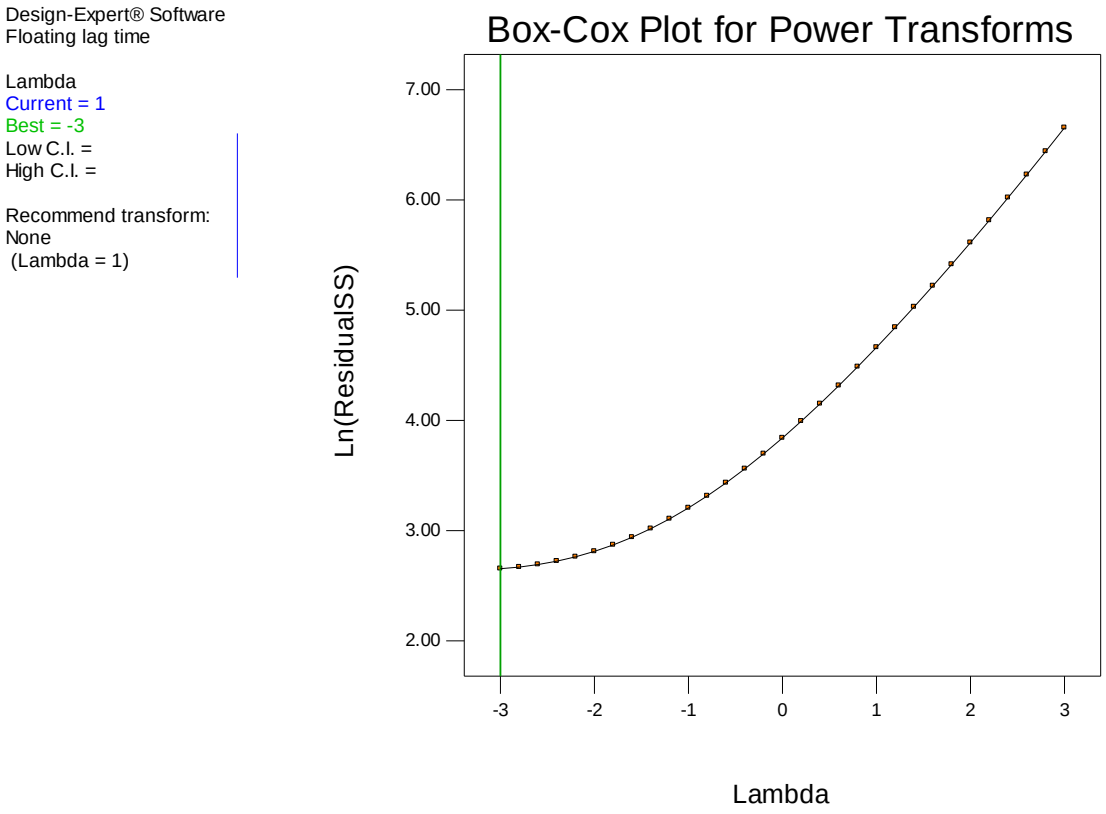

Figure Ap. 3.27 Box-Cox plot for power transformation for response Y_5

6. Response surface plots for response Y_5

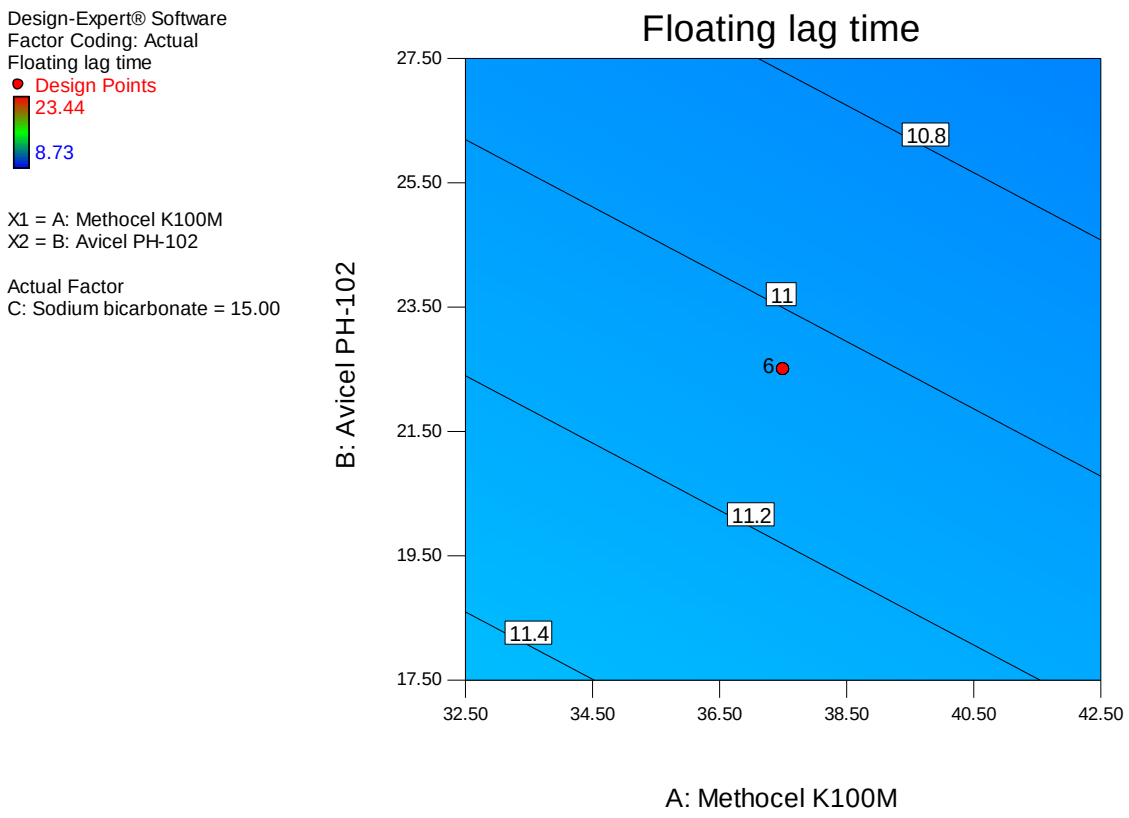

Figure Ap. 3.28 Two-dimensional contour plot of the effect of Avicel® PH-102 and Methocel® K100M on response Y_5

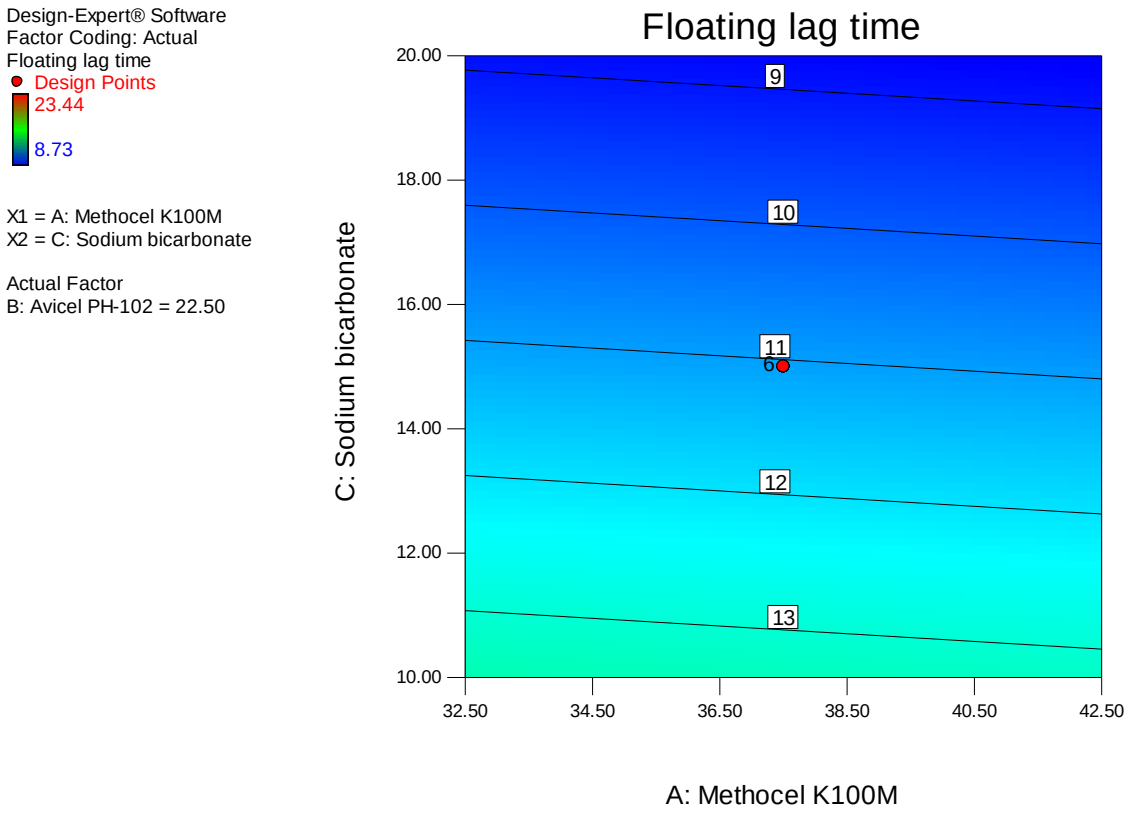

Figure Ap. 3.29 Two-dimensional contour plot of the effect of sodium bicarbonate and Methocel® K100M on response Y_5

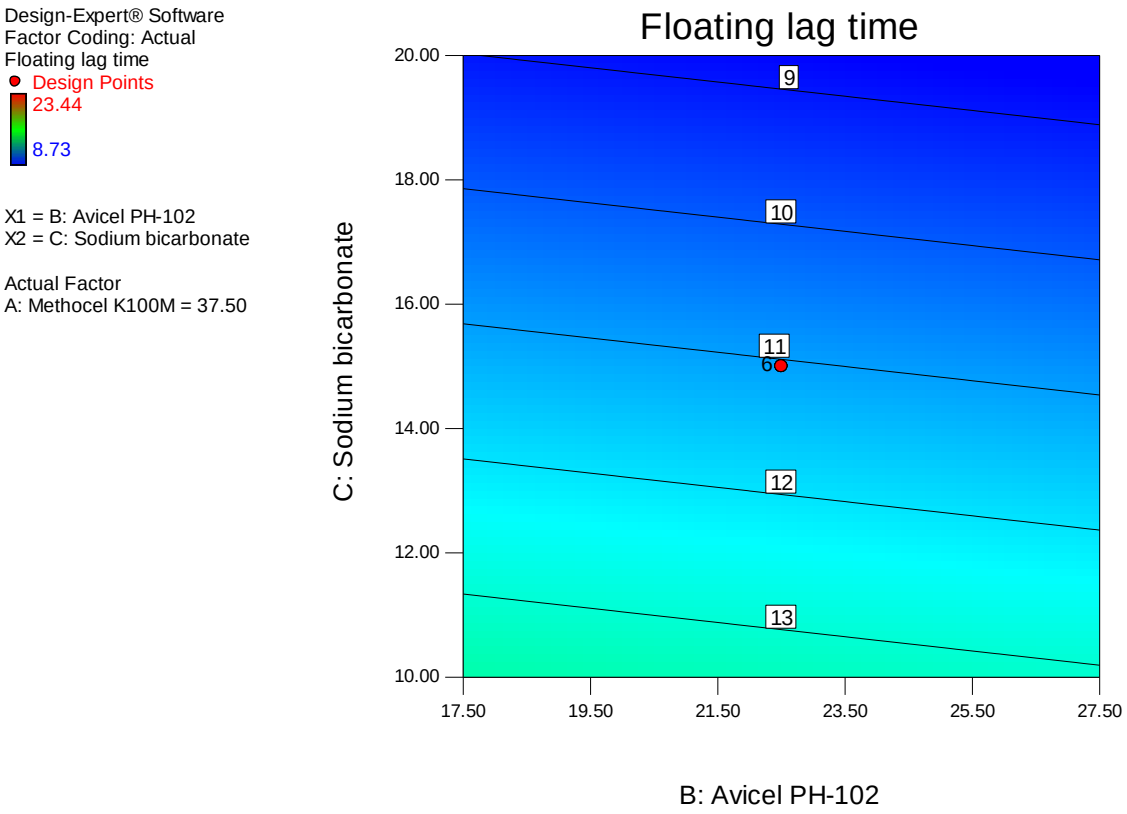

Figure Ap. 3.30 Two-dimensional contour plot of the effect of Avicel® PH-102 sodium bicarbonate on response Y_5